Vol. 60 AUGUST, 1956 No. 8

THE JOURNAL OF PHYSICAL CHEMISTRY

(Registered in U. S. Patent Office)

CONTENTS

THE JOURNAL OF PHYSICAL CHEMISTRY

(Registered in U. S. Patent Office)

Published monthly by the American Chemical Society at 20th and Northampton Sts., Easton, Pa.

Entered as second-class matter at the Post Office at Easton, Pennsylvania.

The *Journal of Physical Chemistry* is devoted to the publication of selected symposia in the broad field of physical chemistry and to other contributed papers.

Manuscripts originating in the British Isles, Europe and Africa should be sent to F. C. Tompkins, The Faraday Society, 6 Gray's Inn Square, London W. C. 1, England.

Manuscripts originating elsewhere should be sent to W. Albert Noyes, Jr., Department of Chemistry, University of Rochester, Rochester 20, N. Y.

Correspondence regarding accepted copy, proofs and reprints should be directed to Assistant Editor, Allen D. Bliss, Department of Chemistry, Simmons College, 300 The Fenway, Boston 15, Mass.

Business Office: Alden H. Emery, Executive Secretary, American Chemical Society, 1155 Sixteenth St., N. W., Washington 6, D. C.

Advertising Office: Reinhold Publishing Corporation, 430 Park Avenue, New York 22, N. Y.

Articles must be submitted in duplicate, typed and double spaced. They should have at the beginning a brief Abstract, in no case exceeding 300 words. Original drawings should accompany the manuscript. Lettering at the sides of graphs (black on white or blue) may be pencilled in and will be typeset. Figures and tables should be held to a minimum consistent with adequate presentation of information. Photographs will not be printed on glossy paper except by special arrangement. All footnotes and references to the literature should be numbered consecutively and placed in the manuscript at the proper places. Initials of authors referred to in citations should be given. Nomenclature should conform to that used in *Chemical Abstracts*, mathematical characters marked for italic, Greek letters carefully made or annotated, and subscripts and superscripts clearly shown. Articles should be written as briefly as possible consistent with clarity and should avoid historical background unnecessary for specialists.

Notes describe fragmentary or less complete studies but do not otherwise differ fundamentally from articles. They are subjected to the same editorial appraisal as are Articles. In their preparation particular attention should be paid to brevity and conciseness.

Communications to the Editor are designed to afford prompt preliminary publication of observations or discoveries whose value to science is so great that immediate publication is imperative. The appearance of related work from other laboratories is in itself not considered sufficient justification for the publication of a Communication, which must in addition meet special requirements of timeliness and significance. Their total length may in no case exceed 500 words or their equivalent. They differ from Articles and Notes in that their subject matter may be republished.

Symposium papers should be sent in all cases to Secretaries of Divisions sponsoring the symposium, who will be responsible for their transmittal to the Editor. The Secretary of the Division by agreement with the Editor will specify a time after which symposium papers cannot be accepted. The Editor reserves the right to refuse to publish symposium articles, for valid scientific reasons. Each symposium paper may not exceed four printed pages (about sixteen double spaced typewritten pages) in length except by prior arrangement with the Editor.

Remittances and orders for subscriptions and for single copies, notices of changes of address and new professional connections, and claims for missing numbers should be sent to the American Chemical Society, 1155 Sixteenth St., N. W., Washington 6, D. C. Changes of address for the *Journal of Physical Chemistry* must be received on or before the 30th of the preceding month.

Claims for missing numbers will not be allowed (1) if received more than sixty days from date of issue (because of delivery hazards, no claims can be honored from subscribers in Central Europe, Asia, or Pacific Islands other than Hawaii), (2) if loss was due to failure of notice of change of address to be received before the date specified in the preceding paragraph, or (3) if the reason for the claim is "missing from files."

Subscription Rates (1956): members of American Chemical Society, $8.00 for 1 year; to non-members, $16.00 for 1 year. Postage free to countries in the Pan American Union; Canada, $0.40; all other countries, $1.20. $12.50 per volume, foreign postage $1.20, Canadian postage $0.40; special rates for A.C.S. members supplied on request. Single copies, current volume, $1.35; foreign postage, $0.15; Canadian postage $0.05. Back issue rates (starting with Vol. 56): $15.00 per volume, foreign postage $1.20, Canadian, $0.40; $1.50 per issue, foreign postage $0.15, Canadian postage $0.05.

The American Chemical Society and the Editors of the *Journal of Physical Chemistry* assume no responsibility for the statements and opinions advanced by contributors to THIS JOURNAL.

The American Chemical Society also publishes *Journal of the American Chemical Society, Chemical Abstracts, Industrial and Engineering Chemistry, Chemical and Engineering News, Analytical Chemistry, Journal of Agricultural and Food Chemistry* and *Journal of Organic Chemistry*. Rates on request.

(*Continued from first page of cover*)

THE JOURNAL OF
PHYSICAL CHEMISTRY

(Registered in U. S. Patent Office) (© Copyright, 1956, by the American Chemical Society)

VOLUME 60 AUGUST 18, 1956 NUMBER 8

LIQUID VISCOSITIES AT ELEVATED TEMPERATURES AND PRESSURES: VISCOSITY OF BENZENE FROM 90° TO ITS CRITICAL TEMPERATURE

BY JOHN R. HEIKS[1a] AND EDWARD ORBAN[1b]

Mound Laboratory, Monsanto Chemical Company,[2] Miamisburg, Ohio

Received December 6, 1954

A viscometer suitable for measurement of viscosities of fluids at elevated temperatures and pressures is described. The time of fall of a radioactive plummet is determined by means of two sets of coincident ionization chambers and an electronic timer. The viscosity of benzene was measured from 90° to its critical temperature. From 90° to about 180° the variation of the logarithm of the viscosity of benzene with the reciprocal of the temperature is a straight line, but above this temperature the rate of change increases with increasing temperature.

Introduction

Viscosity measurements at elevated temperatures and pressures present a problem in construction of apparatus, particularly if a versatile apparatus is required which may be used for measurement of solutions of a conductive or corrosive nature and over a wide range of viscosities. A type of viscometer, originally developed by Lawaczeck,[3] appeared to be more adaptable to this work than others because: (1) it could be enclosed in a pressure vessel; (2) by a simple change of a plummet it could cover wide range of viscosities; (3) it and the containing pressure vessel could be constructed of non-corrosive materials; and (4) it could be constructed without a complicated internal device for timing the fall of the plummet.

Bridgman[4] employed a modification of such a viscometer for determining the viscosity of liquids at very high pressures but at low temperatures. Hawkins, Solberg and Potter[5] used this type of instrument for their work on the viscosity of water and superheated steam. Versluys, Michels and Gerver[6] used a falling-plummet viscometer for determining the viscosity of saturated methane–oil solutions at elevated temperatures and pressures. Mason[7] also used a similar instrument for measuring the viscosity of liquids at high pressures.

The viscometer consists essentially of a tube which is closed at its lower end and which has a diameter slightly greater than that of a plummet contained therein. As the plummet falls from the top to the bottom of the tube liquid moves by streamline flow through the annular space between the plummet and the wall of the tube. The rate of fall of the plummet can be controlled by proper selection of weight and diameter of the plummet.

According to Lawaczeck,[3] there are three distinct resistances to the fall of the plummet through the liquid. These are the result of: (1) the resistance which results from the liquid flowing through the annular space between the plummet and the fall tube; (2) a viscous drag resulting from the relative moment of the two cylindrical walls; and (3) a head resistance caused by the formation of streamlines. The head resistance can be minimized by using a long plummet and a small clearance between the plummet and the fall tube. Neglecting the head resistance, the equation proposed by Lawaczeck for calculating the absolute viscosity is

$$\eta = \left[\frac{t(\sigma - \rho)}{e}\right]\left[\frac{\delta^3 d}{3(d - 2\delta)^2 + 2(\delta)^2}\right] \quad (1)$$

where η is the absolute viscosity; t is the fall time; l is the distance the plummet falls in time t; σ is the density of the plummet; ρ is the density of the liquid; d is the diameter of the plummet; and δ

(1) (a) E. I. du Pont de Nemours and Company, Wilmington, Del. (b) Monsanto Chemical Company, St. Louis, Missouri.

(2) Mound Laboratory is operated by Monsanto Chemical Company for the United States Atomic Energy Commission under Contract Number AT-33-1-GEN-53.

(3) F. Lawaczeck, *Z. Ver. Deut. Ing.*, **63**, 677 (1919).

(4) P. W. Bridgman, *Proc. Nat. Acad. Sci.*, **11**, 603 (1925).

(5) G. A. Hawkins, H. L. Solberg, and A. A. Potter, *Trans. Am. Soc. Mech. Engrs.*, **57**, 395 (1935).

(6) J. Versluys, A. Michels and J. Gerver, *Physica*, **3**, 1093 (1936).

(7) C. C. Mason, *Proc. Phys. Soc.*, **47**, 519 (1935).

is the annular space between the fall body and the fall tube.

Although this type of viscometer has been used by some previous investigators[3] for the absolute measurement of viscosity, it is not recommended for use as an absolute instrument since the effect of the head resistance on the above equation has not been evaluated. However, when a reference liquid with a kinematic viscosity similar to the liquid under investigation is used, the instrument can be used satisfactorily for relative measurements. The relative viscosity is calculated by use of the equation

$$\frac{\eta}{\eta_0} = \frac{(\sigma - \rho)t}{(\sigma_0 - \rho_0)t_0} \qquad (2)$$

where η and η_0 are the absolute viscosities of the solution and the reference liquid; σ and σ_0 are the densities of the plummet filled with the solution and the reference liquid; ρ and ρ_0 are the densities of the solution and reference liquid; and t and t_0 are the fall times of the plummet in the solution and in the reference liquid, respectively.

An important innovation in the measurement of the fall times was the development of a timer whereby the time of fall of a plummet containing a radioactive source could be measured by means of two sets of coincident ionization chambers. The complete timing device, except the cobalt-60 source, was external to the viscometer system. Problems involved in using a window in a pressure vessel to observe the time of flow of a liquid or fall of a ball or plummet were avoided. Also, problems caused by introduction of an electrical circuit into a pressure vessel, which might contain an ionic or corrosive liquid at 300°, were eliminated. Only one other reference to the use of a radioactive source for measuring viscosities appears in the literature.[8]

The viscometer has been used to measure the viscosity of heavy water to 250°[9] and is presently measuring the viscosity of uranyl sulfate in water at elevated temperatures to 3,000 pounds per square inch pressure. Plans are being made to measure the viscosities of some aqueous suspensions and some fused salts and metals.

The viscosity of benzene to 185.7° has been reported in the literature,[10] but no data in the vicinity of the critical temperature are available. It is of interest to observe the behavior of benzene as the critical temperature is approached.

Viscometer

The measuring apparatus consists of the viscometer, pressure vessel, heating mantle and timing device.

The viscometer consists of a type 304 stainless steel fall tube through which the plummet of slightly smaller diameter is allowed to fall under the influence of gravity. The fall tube, 35 inches long and 0.020 inch wall thickness, has an inside diameter of 0.4992 ± 0.002 inch, throughout the length of the fall path, as measured by a Sheffield Precisionaire Gage. A funnel shaped plug, having a hole 0.03 inch in diameter through it, is inserted in the top of the tube. This plug provides a stop for the plummet when the plummet is returned to the top of the tube, and prevents gas bubbles from entering the fall tube.

The plummet, constructed of stainless steel (type 304), is a 2-5/8 inches long hollow cylinder with rounded ends. The cylinder is threaded at one end so that it can be opened to insert a radioactive cobalt-60 source and be filled with the liquid under investigation. The vapor pressure of the liquid inside prevents collapse of the plummet under most circumstances, but where the over-pressure is considerably greater than the vapor pressure, only a small air space is left inside for expansion.

The amount of clearance between the plummet and the fall tube and the weight of the plummet are determined by the range of viscosities being investigated. For viscosities between 0.06 and 1.0 centipoise, a plummet-fall tube combination having a clearance of 0.008 inch is used. The weight of this plummet is 19.834 g. For more viscous media, slightly larger clearances and slightly heavier plummets were used. The weight used in equation 2 as the density of the plummet, however, must include the weight of liquid in the hollow portion of the plummet. The Reynolds number of the liquid flowing between the plummet and fall tube for the above set of conditions never exceeded 500, and in most measurements it was near 100. Three centering projections were positioned on the plummet at each end to prevent the plummet from wobbling during its fall. The diameter around the centering projections is 0.001 inch less than the inside diameter of the fall tube. Inside of the plummet at its lower end is a screw containing a radioactive cobalt-60 source which is used for timing the fall of the plummet.

The fall tube is positioned concentrically within a stainless steel (type 347) pressure vessel which is capable of safely holding a pressure of 3,000 pounds per square inch at temperatures to 300°.

The vessel itself is a 36" long pressure cylinder with a blank head at the bottom threaded in a manner to hold the fall tube rigidly vertical, and an extended head at the top drilled for a pressure inlet and a thermocouple well which extends into the body of the liquid. Screw caps tighten the heads to the vessel with seals being accomplished with stainless steel gaskets.

The entire pressure vessel is surrounded with an electric heating mantle.

Temperature measurements are made to the nearest 0.2° with a single-junction copper constantan thermocouple enclosed in a copper slug which is positioned next to the fall tube in the middle of the fall path.

The whole unit is supported by a trunnion about which the apparatus can be rotated through an angle of 180° so that the plummet can be returned to the top of the fall tube for succeeding determinations. Temperatures are controlled manually by means of a Variac transformer.

Three 250-ml. pressure vessels are connected to the viscometer with high-pressure tubing to provide for expansion of the liquid at elevated temperatures. This design permits the viscometer to be filled completely with liquid at all temperatures, minimizing the formation of gas bubbles on the plummet. Nitrogen is introduced into the system through an expansion chamber to obtain the desired pressure. An over-pressure of approximately one atmosphere greater than the vapor pressure of benzene was used for the viscosity determination of benzene. Pressures are read to the nearest 5 pounds per square inch by means of an Ashcroft Duragauge of the proper range.

The timing assembly chosen for this work,[11] consists of a 12-millicurie cobalt-60 source placed within the plummet, three separate electronic units; and shielding for two pairs of coincidence Geiger–Mueller tubes placed outside of the heating mantle opposite the starting and finishing points of the fall path. The three electronic units are a low-voltage regulated power supply; a four-channel high-voltage regulated power supply; and a coincidence timer. The shielding assembly, constructed of lead and steel, completely encases the two pairs of Geiger–Mueller tubes except for narrow collimating slits opening in the direction of the viscometer.

The top pair of Geiger–Mueller tubes detect the position of the plummet (cobalt-60) at the start of the fall path and activate a timing clock. Pulses from the Geiger–Mueller

(8) J. Gueron, "Proceedings of the Isotope Techniques Conference, Oxford, July, 1951," Her Majesty's Stationery Office, Vol. II, 1952, p. 11.

(9) J. R. Heiks, M. K. Barnett, L. V. Jones and E. Orban, THIS JOURNAL, **58**, 488 (1954).

(10) "Landolt-Bornstein Physical-Chemical Tables," 5th Edition, Vol. I, Julius Springer, Berlin, 1923, p. 128.

(11) A. J. Rogers, J. W. Heyd, W. L. Hood and J. A. Williamson, *Nucleonics*, **12**, No. 6, 62 (1954); MLM-805, February 27, 1952.

tubes are injected into one channel of the coincidence time where they are amplified, equalized, and then applied to a coincidence mixer. This coincidence mixer generates an output pulse when pulses in the two Geiger–Mueller tubes occur within approximately 90 microseconds of each other. A conventional scaler totals the mixer output pulses. When the number of scaled mixer pulses exceeds a preset value, a clock-timer is activated. To prevent activation of the timer before the plummet is opposite the collimating slit, a resetting pulse is fed into all of the resetting grids of both scalers at a rate which prevents the totaling of sufficient counts to activate the timer until the plummet (cobalt-60 source) is directly opposite the Geiger–Mueller tubes. The resetting pulse is obtained from a line-voltage-synchronized multivibrator.

When the plummet reaches the bottom of the fall path, the timing clock is stopped by an analogous electronic assembly. The timing clock may be read to 0.1 second.

Procedure

The two sets of coincident counting tubes are placed 20 inches apart so that the central part of the fall tube may be used as the fall path of the plummet. A sufficient length of fall tube at both ends of the fall path allows time for acceleration of the plummet and reduces resistance effects caused by the closed ends of the tube. The times required for the plummet to fall 20 inches at various temperatures and pressures are measured, first, with the viscometer filled with an appropriate reference liquid, and then with the viscometer filled with the solution under investigation. The average of five unidirectional fall times is taken at each predetermined temperature and pressure over the range being investigated. The viscosity can then be calculated by means of equation 2, since the fall times of the plummet in the reference liquid and in the solution are known, as are the densities of the plummet, solution and reference liquid over the entire temperature and pressure range.

The standard deviation of a single determination, based on duplicate runs of an aqueous uranyl sulfate solution at ten different temperatures between 30 and 200° was calculated to be 0.00213 centipoise over a viscosity range of about 0.15 to 1.0 centipoise.

Viscosity of Benzene

The viscosity of benzene (Mallinckrodt Analytical Reagent grade) was determined at twelve temperatures between 90 and 288.5°. The literature values of the density of benzene[12] and the absolute viscosity of water[13] were used for calculations. The data are given in Table I and are plotted in Fig. 1. Inspection of the curve shows that the exponential equation for the general relationship between temperature and viscosity for undissociated liquids developed by Andrade,[14] but first suggested by Reynolds,[15] holds only to a temperature of 180°. This relationship is

$$\eta = Ae^{B/T} \qquad (3)$$

where η is the absolute viscosity and A and B are constants. Above 180° the rate of change of the logarithm of viscosity with the reciprocal of the temperature is no longer constant, but increases with increasing temperature.

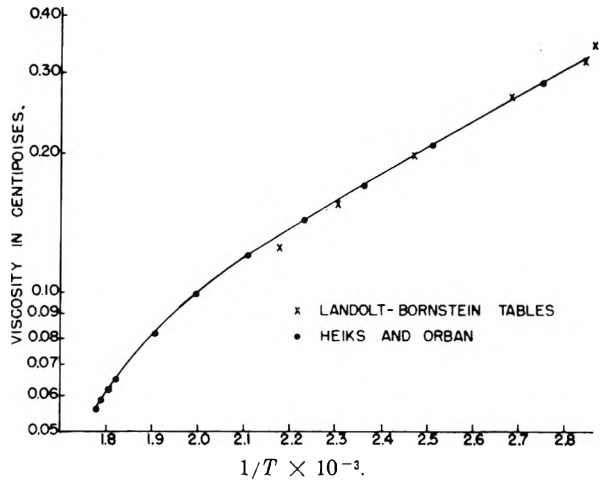

Fig. 1.—Viscosity of benzene in centipoises *vs.* reciprocal of absolute temperature, 90–288.5°.

TABLE I

VISCOSITY OF BENZENE (IN CENTIPOISES)

Temp., °C.	Pressure, p.s.i.	$\frac{\eta}{\eta\ E_{20}}$	$\eta^{a}{}_{H_2O}$	η Benzene
90	35	0.901	0.317	0.286
100	40	.922	.283	.261
125	60	.941	.223	.210
150	100	.921	.186	.171
175	150	.910	.158	.144
200	225	.886	.136	.121
225	315	.810	.123	.100
250	445	.723	.113	.082
275	635	.629	.104	.065
280	650	.610	.102	.062
285	700	.590	.100	.059
288.5[b]	720	.568	.099	.056

[a] A. Jaumotte, *Rev. Universelle Mine*, **17**, 213 (1951). [b] Critical temperature.

Acknowledgment.—The authors express their gratitude to Mr. T. G. Moore for the design of the pressure vessel and heating mantle used in this work.

(12) Ref. 10, 0.273.

(13) A. Jaumotte, *Rev. Universelle Mine*, **17**, 213 (1951).

(14) E. N. Andrade, *Phil. Mag.*, **17**, 497, 698 (1926); "Viscosity and Plasticity," Chemical Publishing Co., New York, N. Y., 1951, p. 22.

(15) O. Reynolds, *Phil. Trans.*, **177**, 157 (1886).

THE POLAROGRAPHIC REDUCTION OF N-NITROSAMINES

BY R. BRUCE MARTIN AND MARY O. TASHDJIAN

Department of Chemistry, American University, Beirut, Lebanon

Received September 12, 1955

The irreversible reduction of dimethyl-, piperidine- and diphenyl-N-nitrosamines has been studied over a range of *p*H and concentration in well buffered solutions. One step symmetrical curves are obtained. The diffusion current i_d varies directly with the concentration. The ratio of i_d/c varied with no definite trend. Temperature and height experiments indicate diffusion control. $E_{1/2}$ varied linearly with *p*H. Plots of $E_{d.e.}$ *versus* log $(i_d - i)/i$ yield straight lines with values of $n\alpha$ less than one. A correlation between $E_{1/2}$ and absorption spectra is described.

The polarographic reduction of N-nitrosamines has received little study. English[1] investigated the reduction of dimethyl-N-nitrosamine incidental to determining dimethylamine.[2]

In general nitroso compounds are more easily reduced (*ca.* 0.4 volt) than the corresponding nitro compounds[3] and have been shown to be a reduction product of the nitro group.[4] The ammonium salt of N-nitrosophenylhydroxylamine has been studied over a range of *p*H values.[5] At *p*H 1 a six electron wave is observed corresponding to the reduction to phenylhydrazine. At *p*H 7 to 9 the reduction involves 4 electrons. Two waves occur, of which the first is *p*H dependent.

In this paper the polarographic reduction of an aliphatic, heterocyclic and aromatic N-nitrosamine is reported. They are, respectively, dimethyl-, piperidine- and diphenyl-N-nitrosamine.

Experimental

Reagents.—The N-nitrosamines were prepared according to the procedures described by Hickinbottom.[6] The dried liquid nitrosamines were distilled twice and the physical constants determined: N-nitrosodimethylamine, b.p. 153°, $n^{18}D$ 1.4373; N-nitrosopiperidine, b.p. 215–217°, $n^{18}D$ 1.4932; N-nitrosodiphenylamine, m.p. 66–67°.

Commercial ethyl alcohol was distilled after the addition of MnO_2. The middle portion of the distillate was used to prepare a 50% by volume solution with water.

Pro Analysi potassium chloride was used as a supporting electrolyte.

Reagent grade hydrochloric acid, sodium acetate, acetic acid, sodium monobasic phosphate and citric acid were used in preparing buffer solutions.

Hydrogen was produced in a Kipp generator from C.P. hydrochloric acid and C.P. mossy zinc passed through a 30% potassium hydroxide solution and a sample of test solution before being passed through the sample. All rubber connections were soaked in concd. potassium hydroxide, rinsed with distilled water and dried.

Solutions.—Water solutions of the dimethyl and piperidine-N-nitrosamines were prepared. It was necessary to use a 50% by volume of ethanol solution for the diphenyl-N-nitrosamine.

All solutions were 0.1 *N* in potassium chloride.

All solutions were buffered. The concentration of the buffer mixture was usually 0.2 *N*.

Hydrogen gas was passed through the prepared solutions for 15 minutes. With alcoholic solutions the time and rate of flow was set at optimum for efficient oxygen removal, with the least change in concentration due to evaporation. In the case of alcoholic solutions small oxygen waves were observed, but their presence did not interfere with the interpretation of the polarogram.

Instruments.—A Sargent Model XII Polarograph was used with a Heyrovsky type cell. The mercury height was kept constant at 67 cm. The drop time (t) and weight in mg. of each drop (m) were measured at an applied potential of 1 volt (*versus* the saturated calomel electrode). m = 3.21 mg. and t = 2.32 sec., therefore $m^{2/3}t^{1/6}$ = 2.504. The cell resistance was about 200 ohms, so no correction for IR drop was necessary. Temperature was controlled to ±0.01°.

All *p*H measurements were made on a Cambridge glass electrode *p*H meter. In the case of alcoholic solutions no correction was made for the change in activity coefficients.

Spectra were determined on a Beckman Model DU spectrophotometer using matched one centimeter silica cells.

Results

In general, single well defined polarograms were obtained. In all cases the diffusion current (i_d) varied directly with the concentration (c). The ratio i_d/c is expressed in μ ampere/mole.

$E_{1/2}$ varied slightly with concentration. Average values *versus* the saturated calomel electrode are reported. The deviation was less than 0.03 volt.

Plots of $E_{d.e.}$ *versus* log $(i_d - i)/i$ yield straight lines, where $E_{d.e.}$ is the potential for current i. On the assumption that the equation

$$E_{d.e.} = E_{1/2} - \frac{0.0590}{n\alpha} \log (i_d - i)/i$$

was applicable, $n\alpha$ was determined.

The upper limit of *p*H was restricted in all cases by the hydrogen wave. Higher concentrations than those reported gave irregular maxima.

TABLE I

N-NITROSODIMETHYLAMINE

Concn. = 3.35 to 14.87 × 10^{-4} mole/l., temp. = 30.0°.

*p*H	i_d/c, μ amperes/mole	$E_{1/2}$ (volts)	$n\alpha$
1.41	23.4	0.90	0.77
1.41	22.3	0.90	.76
2.69	17.4	1.01	.72
2.80	17.1	1.04	.71
3.03	19.2	1.07	.69
3.37	22.2	1.09	.67
3.62	20.5	1.11	.64
3.71	21.5	1.12	.60
3.74	15.1	1.12	.60
4.00	22.6	1.15	.47
4.22	19.6	1.19	.47
4.34	17.5	1.23	.43

A plot of $E_{1/2}$ *versus* *p*H yields a straight line to *p*H 4.0. The slope is 0.096 volt/*p*H.

The temperature coefficient of $E_{1/2}$ is +1 mv./degree. The temperature coefficient for i_d, $1/i \times di/dT \times 100 = 0.80\%$.

(1) F. L. English, *Anal. Chem.*, **23**, 344 (1951).

(2) A referee mentions two references which duplicate in part this work. M. Lechercq, *Mem. Poudre*, **35**, 365 (1953), and G. Sifre, *ibid.*, **35**, 373 (1953). We do not have access to these papers or their abstracts.

(3) H. J. Gardner and L. E. Lyons, *Rev. Pure Appl. Chem.*, 134 (1953).

(4) I. M. Kolthoff and J. J. Lingane, "Polarography," Interscience Publishers, Inc., New York, N. Y., 1952, p. 746.

(5) Ref. 4, page 765.

(6) J. W. Hickinbottom, "Reactions of Organic Compounds," Longmans, Green and Co., London, 1945, p. 286.

TABLE II

N-NITROSOPIPERIDINE

Concn. = 3.55 to 8.87 × 10^{-4} mole/l., temp. = 25.0°.

pH[a]	i_d/c	$E_{1/2}$	$n\alpha$
1.89	17.5	0.83	0.79
2.24	23.8	0.86	.80
3.97	..	0.96	.75
4.50	18.0	1.02	.58
4.96	17.6	1.09	.56

[a] Below pH 1.89 a maximum was observed.

A plot of $E_{1/2}$ *versus* pH yields a straight line to pH 4.0. The slope is 0.053 volt/pH.

The temperature coefficient of $E_{1/2}$ is + 1 mv./degree. The temperature coefficient for i_d, $1/i \times di/dT = 1.5\%$ at 25.0°.

The diffusion current was found to vary as the square root of the height of the mercury. $E_{1/2}$ was found to be independent of the height.

TABLE III

N-NITROSODIPHENYLAMINE

Concn. = 4.77 60 24.70 × 10^{-4} mole/l. in 50% by volume of 95% ethyl alcohol; temp. = 25.0°.

pH	i_d/c	$E_{1/2}$	$n\alpha$
1.15	13.0	0.56	1.03
2.51	10.2	.69	1.03
3.93	13.4	.83	0.78
4.66	10.1	.88	.92
5.27	12.3	.92	.89

Below pH 1.15 the first wave of oxygen made the interpretation of the polarogram difficult. A study at a higher pH than those reported was limited by interference with the second wave of oxygen.

A plot of $E_{1/2}$ *versus* pH yields a straight line over the entire range studied. The slope is 0.090 volt/pH.

The temperature coefficient of $E_{1/2}$ is random and of the order of 7 mv./degree. The temperature coefficient for i_d, $1/i\ di/dT \times 100 = 2.3\%$.

Since N-nitrosodiphenylamine had to be studied in the 50% by volume solution of alcohol, a run was made on the other two compounds in the same solvent at similar pH for comparison.

TABLE IV

N-NITROSO COMPOUNDS AT 25.0° IN 50% ALCOHOL SOLVENT

N-Nitroso-	pH	i_d/c	$E_{1/2}$	$n\alpha$
Dimethylamine	4.06	11.5	1.23	0.44
Dipiperidine	4.06	11.9	1.08	0.69
Diphenylamine	3.93	13.4	0.83	0.78

Discussion

In all cases i_d varied directly as the concentration. Plots of i_d *versus* concentration gave straight lines. The irregularity in the values of i_d/c is difficult to explain. Different buffer components gave the same results. Solutions run immediately after mixing and a week later gave the same value, ruling out a time factor. The only conclusion seems to be that some variable(s) has not been sufficiently isolated.

The results of the temperature and height experiments seem to indicate a diffusion controlled process with the possible exception of N-nitrosodiphenylamine where a mixed process may be taking place.

Since the values of $n\alpha$ in Tables I, II, III and IV are less than one the process is irreversible. The curves obtained are all symmetrical and $E_{1/2}$ varies linearly with pH. These facts tend to indicate that there is a direct transfer of electrons from the electrode to the organic compound, but that either the product reacts further or the final equilibrium is attained slowly. Assuming the validity of the Ilkovic equation values of n were calculated assuming the following diffusion coefficients.[8]

N-nitrosodimethylamine	$D = 8.5 \times 10^{-6}$ cm.^{2} sec.$^{-1}$
N-nitrosopiperidine	$D = 8.0 \times 10^{-6}$ cm.^{2} sec.$^{-1}$
N-nitrosodiphenylamine	$D = 3.3 \times 10^{-6}$ cm.^{2} sec.$^{-1}$

The values of n vary from about 3.7 to 5.3. This would indicate a 4 or 5 electron process. A four electron process would yield the corresponding hydrazine plus a molecule of water. A five electron process would probably yield the corresponding amine plus one-half molecule of hydrazine.

Attempts to determine n directly proved unsuccessful. Micro-coulometric methods which depend on an external coulometer for the evaluation of the current passed require an increase in voltage.[9] This is sufficient to cause the reduction of hydrogen ions and vitiate the results.

Studies of the absorption of N-nitrosamines gave evidence for the mesomeric system[10]

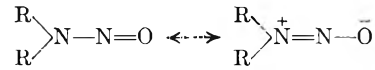

Bands due to a resonating system have relatively high molar extinction coefficients. Influences increasing the polarity facilitate the electron migration and displace the band to longer wave lengths.

The molar extinction coefficient (ϵ) for ethanol solutions of N-nitrosodimethylamine is 7,000 at 231 mμ and for N-nitrosopiperidine ϵ = 8,100 at 238 mμ.[10] The value for N-nitrosodiphenylamine as determined in this study is ϵ = 5,720 at 293 mμ. The diphenyl compound has therefore by far the greatest tendency to be polarized as indicated by its maximum at 293 mμ followed by the piperidine compound with a maximum at 238 mμ and finally by the dimethyl compounds with a maximum at 231 mμ.

It was shown above that in all probability there is a direct exchange of electrons between the electrode and the organic compound. It is likely that this exchange takes place with the polarized form of the molecule, with the practically simultaneous addition of an electron from the electrode to the plus nitrogen and the addition of a proton to the negative oxygen. If this is the case the compound most easily polarized should be most easily reduced.

Therefore, a correspondence should be observed between ease of reduction and wave length of light absorbed. The most easily reduced compound should have the longest wave length absorption, etc.

(7) J. E. Page, *Quart. Rev. Chem. Soc.*, **VI**, 262 (1952).
(8) Private communication from Dr. J. Heyrovsky.
(9) T. De Vries and J. L. Kroon, *J. Am. Chem. Soc.*, **75**, 2484 (1953).
(10) R. N. Haszeldine and J. Jander, *J. Chem. Soc.*, 691 (1954).

That this is in fact the case may be seen from Table IV where the $E_{1/2}$ values are compared under identical solvent conditions. The diphenyl compound is seen to be much the easiest to reduce followed by the piperidine and dimethyl compounds. Thus there is a correspondence between the absorption due to the resonating system and the polarographic reduction potential.

Comparing the absorption in alcohol with the reduction potential in 50% alcohol does not alter the conclusions, as the shift caused by a change of solvent would be about the same absolute value for each compound and hence the relative positions would not be affected.

Acknowledgment.—The authors greatly appreciate the support of the Research Corporation and wish to thank Dr. Robert H. Linnell for aid in initiating the study.

EFFECT OF CROSS-LINKING ON THE PROPERTIES OF CARBOXYLIC POLYMERS. I. APPARENT DISSOCIATION CONSTANTS OF ACRYLIC AND METHACRYLIC ACID POLYMERS[1]

BY SALLIE FISHER AND ROBERT KUNIN

Rohm & Haas Co., Philadelphia, Pa.

Received September 26, 1955

The apparent dissociation constants of cross-linked polyacrylic and polymethacrylic acids in contact with an aqueous phase 1 *M* in KCl have been determined. Polymers cross-linked with divinylbenzene and three other vinyl compounds have been studied. The determined values of pK_a increase with increasing degrees of cross-linking in both acrylate systems. The magnitude of the change is dependent on the mole percentage of acrylate in the polymer. Limiting values of pK_a as the cross-linking is decreased to zero are equal to the dissociation constants of the linear polymers of the corresponding acids.

Introduction

A number of studies have been made of the effect of the degree of polymerization on the apparent dissociation constant of linear polymers of acrylic and methacrylic acids.[2-4] Although Katchalsky and Michaeli[3] have proposed an equation to fit the case of the cross-linked polymers of these acids, few experimental data were published concerning these systems until recently when Gregor[5] has reported that the apparent dissociation constants of these materials decrease with increasing degrees of cross-linking with divinylbenzene. In the present work the effect of cross-linking has been studied over a wide range of cross-linking concentrations and the materials cross-linked with divinylbenzene have been compared with those prepared using other vinyl monomers.

Experimental

The comparison of the apparent dissociation constants of polymers of different degrees of cross-linking was made under arbitrarily chosen experimental conditions in which all variables except polymer composition were held constant. In particular, the system in which the hydrogen form of the polymer is neutralized with KOH has been chosen for study. Since all of the polymers included in the investigation are insoluble in water, the direct titration method wherein the *p*H is followed as known increments of KOH are added to the sample was not used because of the slow rate of establishment of equilibrium in such two-phase systems. This difficulty has been circumvented by weighing out a series of samples of each polymer and adding to each sample a known fraction of the KOH needed to neutralize it. The mixture of polymer and alkali was then allowed to stand until equilibrium, as shown by a constant *p*H in the aqueous phase, was reached. All measurements were made with the resin in contact with an aqueous phase 1 *M* in KCl to minimize the contribution to the equilibrium arising from changes in the ionic strength of the aqueous phase. This relatively high salt concentration also minimized the polymer swelling at low degrees of cross-linking and hence reduced the error arising from the imbibition of water by the polymer with a resultant shift of the Donnan concentrations. A constant ratio between milliequivalents of functional groups in the polymer phase and the volume of the aqueous phase was also maintained.

A series of methacrylic acid and acrylic acid samples copolymerized with known amounts of divinylbenzene and with other vinyl cross-linking agents were prepared for this study. All of the samples were in the form of 20–40 mesh beads. The size of the polymer particles was not reduced by grinding lest some change in functionality or structure be introduced thereby. The finished polymers were leached with a thousand-fold excess of 1 *M* HCl and then rinsed free of excess acid with deionized water until the effluent was neutral to methyl orange prior to the determination of the dissociation constants.

No attempt was made to define the entire titration curve of the polymers studied since several weeks are sometimes required for the establishment of equilibrium in the region of the equivalence point. Instead, the number of milliequivalents per dry gram of each polymer was determined by equilibrating a known dry weight of it with a known excess of standardized KOH solution that was also 1 *M* in KCl. The milliequivalents of the hydroxide reacting with the carboxyl groups of the polymer were determined by back titration of the supernatant liquid after the slurry had been shaken for 16 hours according to the method of Fisher and Kunin,[6] for the determination of total cation exchange capacity of ion exchange polymers. Once the total capacity of each polymer was known, the constants in the Henderson–Hasselbalch equation were determined by measuring the *p*H of a series of partially neutralized samples in the following manner.

Procedure.—To four dry samples of the hydrogen form of each polymer containing 10 meq. of carboxylic groups amounts of the standardized 0.1 *M* KOH solution containing 2.0, 4.0, 6.0 and 8.0 meq. of hydroxide ion were added. This solution was also 1 *M* in KCl. The volume of the aqueous phase was adjusted to 100 ml. by the addition of 1 *M* KCl solution. The samples were stoppered and sealed

(1) Presented before the 128th Meeting of the American Chemical Society, Minneapolis, Minn., September 11–16, 1955.

(2) R. M. Fuoss, *Ann. Rev. Phys. Chem.*, **3**, 81 (1952).

(3) A. Katchalsky and I. Michaeli, *Bull. Research Council Israel*, **2**, No. 3 (1952).

(4) A. Katchalsky and P. Spitnik, *J. Polymer Sci.*, **2**, 432 (1947).

(5) H. P. Gregor, M. J. Hamilton, J. Becker and F. Bernstein, THIS JOURNAL **59**, 874 (1955).

(6) S. Fisher and R. Kunin, *Anal. Chem.*, **27**, 1191 (1955).

and allowed to shake slowly for 48 hours. At the end of that time the *p*H of the polymer–alkali slurry was measured using a Leeds and Northrup Universal *p*H Meter. The constants of the Henderson–Hasselbach equation

$$pH = pK_a - n \log \frac{1 - \alpha}{\alpha} \qquad (1)$$

were determined by plotting *p*H as a function of the logarithm fraction of the polymer neutralized, assuming that all of the base added had reacted with the carboxyl groups of the polymer.

The validity of using the values for pK_a and n obtained by the investigation of a few equilibrium points for each polymer between the points of 20 and 80% neutralization rather than those obtained from the complete titration curve of the sample as described by Kunin and Myers[7] was tested by a comparison of the data of the two methods. Although eight weeks was required for the complete establishment of equilibrium for some of the points on the titration curves the two methods gave an identical line.

Results and Conclusions

From the data for the variation of *p*H with degree of neutralization of the series of methacrylic acid–divinylbenzene and acrylic acid–divinylbenzene polymers in Figs. 1 and 2 it may be seen that as the mole percentage of divinylbenzene increases the degree of dissociation of the polymeric acid decreases. Values of the constant for the Henderson–Hasselbalch equation for the two systems are given in Tables I and II.

TABLE I

APPARENT DISSOCIATION CONSTANTS OF METHACRYLIC ACID POLYMERS

Mole % acrylate	99.5	99.7	93.6	77.8
pK_a	5.6[5]	5.8[5]	6.0	6.8
n	1.3	1.7	1.7	1.8

TABLE II

APPARENT DISSOCIATION CONSTANTS OF ACRYLIC ACID POLYMERS

Mole % acrylate	pK_a	n	Cross-linking agent
99.2	4.9	1.3	DVB
97.3	5.0	1.8[5]	B
96.2	5.0	1.8[5]	DVB
93.1	5.2	1.7	A
92.8	5.2	1.9	DVB
90.6	5.3	2.0	B
89.2	5.6	1.6	A
86.5	5.2	2.0	C
84.0	5.6	1.8[5]	DVB
76.5	5.8[5]	1.9	DVB[a]
75.8	6.0	1.8	DVB
72.7	5.4	2.0	C
69.0	6.0	1.8	DVB[a]

[a] Polymer contains an inert diluent in addition to the divinylbenzene.

If the values of the apparent dissociation constants, pK_a, obtained experimentally are plotted as a function of the mole per cent. acrylate in the polymers (Fig. 3) a straight line function is obtained in both cases. Empirical inspection of these lines shows that they both are of the form

$$pK_a = pK_{a(m=1)}[2 - m] \qquad (2)$$

where pK_a is the apparent dissociation constant when the mole fraction of acrylate in the polymer is equal to m.

The values of $pK_{a(m=1)}$ obtained by extrapolating the lines for the two polymer types are 5.6 for methacrylic acid and 4.8 for acrylic acid polymers.

(7) R. Kunin and R. Myers, "Ion Exchange Resins," John Wiley & Sons, New York, N. Y., 1949.

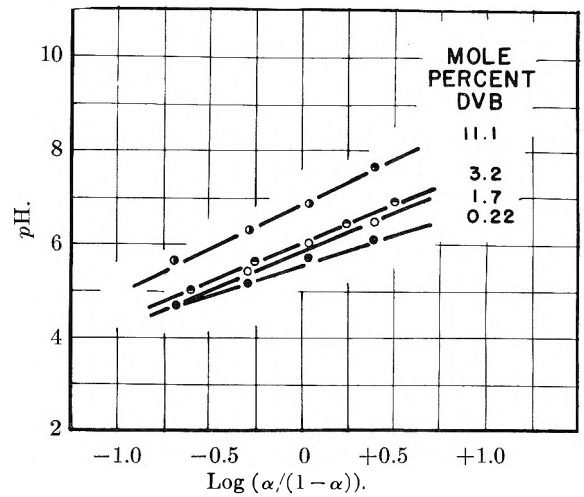

Fig. 1.—Henderson–Hasselbalch curves for methacrylic acid–divinylbenzene copolymers of varying mole percentage divinylbenzene.

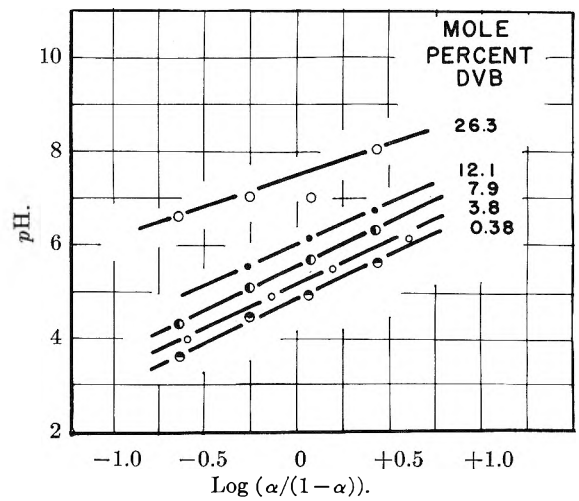

Fig. 2.—Henderson-Hasselbalch curves for acrylic acid-divinylbenzene copolymers of varying mole percentage divinylbenzene.

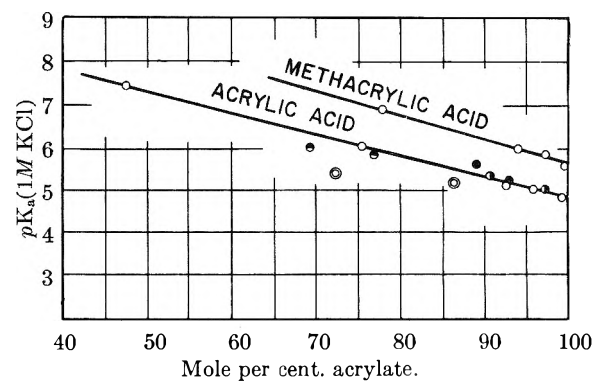

Fig. 3.—Effect of the nature of the cross-linking agent on the variation of pK_a with mole % acrylic acid: ○, DVB; ◓ = DVB + diluent; ● = cross-linking agent A; ◑, cross-linking agent B; ◎ = cross-linking agent C.

These values are in good agreement with the values of 5.65[8] and 4.75[5] reported for the linear polymers of these two acids in 1 *M* KCl. It is, of course, to be expected that the limiting value of the cross-linked polymer, which is at zero per cent. cross-linking or 100% acrylate, should be identical with the value for the linear polymers. Reported values for the dissociation constants of the two monomeric acids at room temperature in water are 4.86[9] for methacrylic acid and 4.24[10] for acrylic acid, showing a similar difference in acidity with the substitution of a methyl group on the alpha carbon.

The dependence of the apparent value of pK_a on the mole percentage of acrylate in the polymer is also not unexpected. In the case of linear polymers of these acids a number of equations have been derived to express the apparent dissociation constant in terms of a pK_0 value representing the dissociation of the monomeric acid.[2] Two of these equations[9,11] include a parameter representing the frequency of occurrence of functional groups in the polymer chain and hence might be expected to bear some resemblance to the present case where acrylate is diluted with cross-linking agent. The first of these, for coiled polyacids,[11] is probably not a suitable approximation to the present case where coiling is restricted by the three dimensional structure. The second, by Katchalsky, Shavit and Eisenberg,[9] is derived for linear, stretched polymers of the polycarboxylic type. Since cross-linked polymers swell most rapidly in the first 20% of the neutralization,[5,12] it is more logical to picture the polymer in the degree of neutralization where the present measurements were made as being stretched. This equation of Katchalsky, *et al.*,[9] has the form

$$pK = pK_0 - \frac{\epsilon^2}{Djbk'T}\left[1 - \frac{6}{\kappa' sb}\right] \qquad (3)$$

In it, pK_0 is the dissociation constant of the monomeric acid and all of the other parameters except j are concerned with a description of the degree of polymerization and of the solution properties of the polymer. As the polymers studied in this work are high molecular weight, insoluble materials, the variables concerned with the degree of polymerization and with the solution properties may be considered constant over the range of formulations studied. Thus, at constant temperature, the value of pK for similar cross-linked polymers compared under similar conditions should, by this equation, vary primarily as $1/j$. Further, since j in this equation is the distance between adjacent carboxyl groups on the linear chains, $1/j$ would be directly proportional to m, the mole percentage of acrylate monomers in the polymers. This variation is found experimentally (equation 2).

In the case of the acrylic acid polymers the validity of the dependence of pK on m was further checked by preparing polymers with cross-linking agents other than divinylbenzene, and by diluting the acrylate monomer with a non-functional vinyl monomer. Three cross-linking agents other than divinylbenzene were used and the apparent dissociation constants of the resultant polymers were studied by the method already outlined. The constants for the Henderson–Hasselbalch equation of these materials are included in Table II. When these constants are included on the plot of pK_a as a function of the mole percentage of acrylic acid in the polymer (Fig. 3) the data from two of the cross-linking agents and from the diluted copolymer follow the same straight line as the data from the divinylbenzene cross-linked polymers. Thus, it would appear that the nature of the monomeric acid and its concentration in the finished polymer are the primary factors determining the degree of dissociation of the polymeric acid. The third cross-linking agent, C, gave polymers of apparent dissociation markedly higher than the other formulations at equivalent mole percentage of acrylate. An examination of the other properties of the polymers made from it showed that the porosity and the swelling characteristics of the samples were similar to polymers of very much lower degrees of cross-linking. It is therefore presumed that this cross-linking agent does not enter into the polymerization with the acrylate in monomeric form and hence that the effective mole percentage of acrylate in its polymer is higher than that calculated from the polymer composition.

No direct correlation has been found between the determined values of n and the polymer composition. It would appear from the data in Table I and II that this constant is dependent on both the nature and the concentration of the cross-linking agent. In the divinylbenzene series, where more polymer compositions have been investigated, there is evidence that n increases with increasing cross-linking, reaches a maximum value close to 2, and then decreases again at high concentrations of cross-linking agent. This same behavior is to be observed in the work of Gregor, *et al.*[5] Further work with cross-linking agents other than divinylbenzene is required for a more complete understanding of the relationship between the cross-linking agent and the observed n values.

Acknowledgment.—The authors wish to thank Drs. Jesse C. H. Hwa, William Lyman and Erich Meitzner of the Rohm & Haas Company for their coöperation in the preparation of the polymers studied. They are also indebted to Diana Kenny and Robert Topoleski for assistance with the measurements reported herein.

(8) A. Arnold and J. Th. G. Overbeek, *Rec. trav. chim.*, **69**, 191 (1950).

(9) A. Katchalsky, N. Shavit and H. Eisenberg, *J. Polymer Sci.*, **13**, 69 (1954).

(10) Beilstein's "Handbuch der Organische Chemie," Julius Springer, Berlin.

(11) A. Katchalsky and J. Gillis, *Rev. trav. chim.*, **68**, 879 (1949).

(12) A. Katchalsky, *Experientia*, **8**, 314 (1949).

POWER RATE LAW IN HETEROGENEOUS CATALYSIS

BY TAKAO KWAN[1]

Frick Chemical Laboratory, Princeton University, Princeton, New Jersey

Received December 17, 1955

It is emphasized that a number of chemisorption data can suitably be represented by a power rate law and the Freundlich type of chemisorption isotherm. The formulation of heterogeneous kinetics is developed on this basis with reference to some fundamental heterogeneous reactions such as ammonia synthesis, water gas shift, parahydrogen conversion, etc. The conformity with experimental kinetics is attained generally in a simple way. An added feature is that kinetic constants can be calculated from chemisorption data.

Introduction

The formulation of heterogeneous kinetics has been achieved in many cases by use of the Langmuir–Hinshelwood treatment.[2] This treatment is essentially based on an ideal picture as if a *homogeneous* reaction occurs on an energetically *uniform* surface. Numerous experimental data on chemisorption rates and equilibria, notably by H. S. Taylor and his school, however, indicate that surfaces are probably not uniform; the heat of chemisorption decreases and the activation energy for chemisorption increases with increasing coverage. Thus, Temkin and Pyzhev[3] advanced an adsorption rate expression, given in the second line of Table I, based on the assumption that the heat of chemisorption and the activation energy are linear functions of surface coverage. If chemisorption and desorption are rate-determining steps of a surface reaction, this expression represents fairly satisfactorily the reaction kinetics as in ammonia synthesis.

As pointed out by Temkin and Pyzhev and by Brunauer, *et al.*,[4] the Temkin–Pyzhev equation is valid only for a middle range of coverage. Furthermore it fails to account for certain chemisorption rate data, *e.g.*, for the adsorption of hydrogen on zinc oxide.[5] Thus, de Bruijn[6] introduced a factor to take into consideration the inhomogeneous nature of the surface, arriving at the same expression as Temkin–Pyzhev's with the exception of this factor. Boudart[7] recalled that experimental kinetics in a restricted range of coverage can be fitted by both Langmuir and Freundlich functions equally well, and derived the kinetic law of ammonia synthesis on the basis of the Langmuir kinetics.

On the other hand, reference should be made to the fact that a number of chemisorption rate data have been shown to obey the power rate law[8] (see Table I). Moreover many experimental data[9–13] have been found to be most suitably expressed by the Freundlich equation over a very wide range of pressure. So it seems justified to develop the kinetics of heterogeneous reactions on the basis of the power rate law and the corresponding Freundlich isotherm equation.

Power Rate Law.—Some basic characteristics of the power rate law will be reviewed here in order to prepare the ground for its application to reaction kinetics. This law was originally deduced to fit the rate of chemisorption of nitrogen on a promoted iron catalyst, and was expressed as

$$-\frac{dp}{dt} = kp\theta^{-\alpha} - k'\theta^{\beta} \qquad (1)$$

where k, α, k' and β are constants except for a low coverage. At equilibrium, it gives the Freundlich equation in the form

$$\ln \theta = \frac{1}{n} \ln \frac{p}{p_s} \qquad (2)$$

where $n = \alpha + \beta$ and $p_s = k'/k$. It shows that when p reaches p_s, θ becomes unity. In the case of the nitrogen–iron catalyst system, p_s was found to be approximately independent of temperature; in other words, all isotherms in the log–log plot have a common intersection if extrapolated linearly to higher equilibrium pressures. A similar trend has been shown in other gas–solid systems.[9–13]

The validity of the power rate law may be examined by evaluating $-dp/dt$ graphically from the chemisorption rate curve in the plot of p *vs.* time, and plotting $\log(-1/p\ (dp/dt)/1 - (p_e/p))$ *vs.* $\log\theta$. Here, p_e is the pressure of gas which would be in equilibrium with chemisorbed amounts at time t, and is obtainable from the isotherm. If the reverse rate is negligible, *i.e.*, $p_e << p$, it is sufficient to plot $\log(-1/p(dp/dt))$ *vs.* $\log\theta$.

In general chemisorption rate data may be adequate for testing the power rate law in the form $-dp/dt = kp\theta^{-\alpha}$, if the measurements are made at coverages sufficiently below equilibrium. It should be noted that this rate equation was proposed earlier by Ghosh, Sastri and Kini[14] to interpret the chemisorption rate of hydrogen on a cobalt Fischer–Tropsch catalyst. They also found that this equation fits a number of chemisorption rate data of other systems. Table II shows α, the slope of the straight line, when $\log(-1/p(dp/dt))$ or $\log(-1/p\text{-}(dp/dt)/1 - (p_e/p))$ are plotted against $\log\theta$ for the chemisorption rate data reported in the literature.

As reported previously,[8] the investigation of the chemisorption rate of nitrogen on a sparsely covered surface of iron shows that α changes discontinu-

(1) 1954–1955 Fulbright/Smith–Mundt scholar, on leave of absence from Hokkaido Univ., Sapporo, Japan.

(2) C. N. Hinshelwood, "Kinetics of Chemical Change," Oxford Univ. Press, London, 1940, p. 218.

(3) M. Temkin and V. Pyzhev, *Acta Physicochim.* **12**, 327 (1940).

(4) S. Brunauer, K. S. Love and R. G. Keenan, *J. Am. Chem. Soc.*, **64**, 751 (1942).

(5) H. S. Taylor and D. V. Sickman, *ibid.*, **54**, 602 (1936).

(6) H. de Bruijn, *Faraday Soc. Disc.*, **8**, 69 (1950).

(7) M. Boudart, *Ind. Chim. Belge*, **19**, 489 (1953).

(8) T. Kwan, *J. Res. Inst. Catalysis*, **3**, 16 (1953).

(9) W. G. Frankenburg, *J. Am. Chem. Soc.*, **66**, 1827 (9144); (b) R. T. Davis, *ibid.*, **68**, 1395 (1946).

(10) E. Cremer, *Z. Elektrochem.*, **56**, 439 (1952).

(11) B. M. W. Trapnell, *Proc. Roy. Soc.* (*London*), **206A**, 39 (1951).

(12) G. C. A. Schuit, *Rec. trav. chim.*, **72**, 909 (1953).

(13) T. Kwan, *J. Res. Inst. Catalysis*, **9**, 109 (1955).

(14) J. C. Ghosh, M. V. C. Sastri and K. A. Kini, *Curr. Sci. India*, **15**, 282 (1946); *Ind. Eng. Chem.*, **44**, 2463 (1952).

TABLE I

	Adsorption rate equation	Isotherm equation
Langmuir kinetics	$-dp/dt = kp(1-\theta) - k'\theta$	$\theta = bp/1 + bp,\ b = k/k'$
Temkin kinetics	$-dp/dt = kpe^{-\alpha\theta} - k'e^{\beta\theta}$	$\theta = \frac{1}{f}\ln ap,\quad f = \alpha + \beta,\quad a = k/k'$
Power rate law	$-dp/dt = kp\,\theta^{-\alpha} - k'\theta^{\beta}$	$\theta = (p/p_s)^{1/n},\quad n = \alpha + \beta,\quad p_s = k'/k$

TABLE II

Adsorbent	Gas	Temp., °C.	α	Ref.
Ni	H_2	−78	5.2	15
C	H_2	482	1.2	16
ZnO	H_2	184	3.4	5
Cr_2O_3	H_2	154	0.8	17
$CuCr_2O_4$	O_2	200	2.4	18
Fe promoted	N_2	397	5.2	19
W	N_2	500	15.0	9
Co Fischer	H_2	51	5.5	14
Co Fischer	CO	178	2.0	14

ously, becoming smaller with decreasing coverage. A similar discontinuity also takes place in the value of n of the corresponding isotherm. The slope of the straight line, α, in the plot of $\log(-1/p(dp/dt))$ against $\log\theta$ determined at 400° will be given in Table III.

TABLE III

θ	$\theta < 0.025$	$0.025 < \theta < 0.08$	$0.08 < \theta$
α	0	1.4	3.0

If we assume that $n = 1$ (Henry's law) or $n = 2$ at a low coverage and $\alpha = 0$ and hence $\beta = 1$ or 2, the power rate law assumes a special form as

$$-\frac{dp}{dt} = kp - k'\theta \tag{3}$$

or

$$-\frac{dp}{dt} = kp - k'\theta^2 \tag{3}'$$

which, however, will be valid only for a sparsely covered surface.

Now, except for a sparsely covered surface, the temperature dependence of α and n has been expressed by

$$\alpha = \frac{g}{RT} - \frac{g}{RT_\alpha} \tag{4}$$

$$n = \frac{\gamma}{RT} - \frac{\gamma}{RT_n} \tag{5}$$

where g, γ, T_α and T_n are constants over the temperature range 300 ~500° and R is the gas constant. Incidentally, eq. 5 is the same expression as that suggested by Halsey[20] to take into account the possible variation of the entropy of chemisorption with θ.

From eq. 1, 2, 4 and 5 we obtain thermodynamic and kinetic quantities of chemisorbed nitrogen as a function of surface coverage.[21] The result is listed in Table IV.

The power rate law may now be expressed alternatively as

$$-\frac{dp}{dt} = \frac{kT}{h}pe^{-\Delta F_s^*/RT}e^{-g\left(1-\frac{T}{T_\alpha}\right)\ln\theta/RT} - \frac{kT}{h}p_s e^{-\Delta F_s^*/RT}e^{h\left(1-\frac{T}{T_\beta}\right)\ln\theta/RT} \tag{6}$$

where $h = \gamma - g$ and as T_α is found[21] to be equal to T_n, T_β must also have the same value.

TABLE IV

Energy of activation E	Entropy of activation ΔS^*	Free Energy of activation ΔF^*
$g\ln\theta + E_s$	$\frac{g\ln\theta}{T_\alpha} + \Delta S_s^*$	$g\left(1-\frac{T}{T_\alpha}\right)\ln\theta + \Delta F_s^*$
Heat of chemisorption q	**Entropy of chemisorption** ΔS°	**Free Energy of chemisorption** ΔF°
$-\gamma\ln\theta$	$\frac{\gamma\ln\theta}{T_n} - \ln p_s$	$\gamma\left(1-\frac{T}{T_n}\right)\ln\theta + RT\ln p_s$

As shown in Table IV, the *logarithmic* change[22] of the thermodynamic quantities of chemisorbed species against θ is a basic feature of the power rate law.

Suppose, for simplicity, a monomolecular catalyzed reaction A → B, occurring on a given catalyst, where A is chemisorbed much stronger than B. If the rate of chemisorption of A is the slowest step, the rate of the over-all reaction may be expressed as $kp_A\theta_A^{-\alpha} = k(p_sK)^{\alpha/n}(p_A/p_B^{\alpha/n})$, where K is the equilibrium constant of the reaction.

Let us consider now the reverse reaction in which the desorption of A is the slowest step. The rate of reaction is given by $k'\theta_A^\beta$; θ_A in turn being given by $(1/p_sK)^{1/n}p_B^{1/n}$. If, on the other hand, the surface reaction is the rate-controlling step, the over-all reaction may perhaps be given in the form: $k\theta^{\beta'} = k'p^{\beta'/n}$. In the following sections this approach will be illustrated in several catalytic reactions.

(15) S. Iijima, *Rev. Phys. Chem. Japan*, **12**, 1 (1938).
(16) F. E. T. Kingman, *Trans. Faraday Soc.*, **28**, 269 (1932).
(17) R. L. Burwell and H. S. Taylor, *J. Am. Chem. Soc.*, **58**, 697 (1936).
(18) J. C. W. Frazer and L. Heard, THIS JOURNAL, **42**, 855 (1938).
(19) S. Brunauer and P. H. Emmett, *J. Am. Chem. Soc.*, **56**, 35 (1935).
(20) G. D. Halsey, *Advances in Catalysis*, vol. 4, Academic Press Inc., New York, N. Y., 1952, p. 259.
(21) T. Kwan, THIS JOURNAL, **59**, 285 (1955).
(22) It may be noted that the heat-coverage relationship is formally identical with that given by Halsey and Taylor[23] and others. In contrast with their view, however, a different physical picture of heterogeneity has been suggested on the basis of the band theory of crystals, *e.g.*, by Eley[24a] and by Mignolet.[24b] The *induction* theory in catalysis proposed by Boudart[25] depends also on such an idea. Developing Boudart's idea more quantitatively, Higuchi, Ree and Eyring[26] have recently explained why the activation energy for the desorption of Cs from tungsten decreases with increasing coverage monotonically in accordance with the experiments of Taylor and Langmuir[27] rather than linearly. As we are not yet in a position to understand fully the cause for the fall in heat, we shall apply for the present the power rate law to heterogeneous kinetics purely on empirical grounds.
(23) G. D. Halsey and H. S. Taylor, *J. Chem. Phys.*, **15**, 624 (1947).
(24) (a) D. D. Eley, THIS JOURNAL, **55**, 1017 (1951); (b) J. C. P. Mignolet, *J. Chem. Phys.*, **23**, 753 (1955).
(25) M. Boudart, *J. Am. Chem. Soc.*, **74**, 3556 (1952).
(26) I. Higuchi, T. Ree and H. Eyring, *ibid.*, **77** 4969 (1955).
(27) J. B. Taylor and I. Langmuir, *Phys. Rev.*, **44**, 432 (1933).

Ammonia Synthesis.—Suppose that the synthesis of ammonia occurs according to the scheme

$$N_2 \xrightarrow{A} 2N(a) \quad (i)$$

$$2N(a) + 3H_2 \rightleftarrows 2NH_3 \quad (ii)$$

where (a) denotes the chemisorbed state and $\xrightarrow{A}$ the slowest step. Let us assume that gases other than nitrogen chemisorb weakly on the catalyst surface. The rate of ammonia synthesis is now given by

$$\frac{d[NH_3]}{dt} = k p_{N_2} \theta^{-\alpha} \quad (6)$$

where p_{N_2} is the partial pressure of nitrogen and θ the fraction of surface covered by nitrogen during the steady state of synthesis. Let p_e be the pressure of nitrogen which would be in equilibrium with the chemisorbed nitrogen so that p_e is given by

$$p_e = K \frac{p_{NH_3}^2}{p_{H_2}^3} \quad (7)$$

Remembering that $\theta = (p_e/p_s)^{1/n}$, we have from (6) and (7).

$$\frac{d[NH_3]}{dt} = k p_s^{\alpha/n} K^{-\alpha/n} p_{N_2} \left(\frac{p_{H_2}^3}{p_{NH_3}^2}\right)^{\alpha/n} = k_1 p_{N_2} \left(\frac{p_{H_2}^3}{p_{NH_3}^2}\right)^{\alpha/n} \quad (8)$$

where k_1 is a new constant equal to $k p_s^{\alpha/n} K^{-\alpha/n}$. For the chemisorption of nitrogen on a promoted iron, we have shown[13] that

$$\frac{\alpha}{n} = \frac{\frac{g}{RT} - \frac{g}{RT_\alpha}}{\frac{\gamma}{RT} - \frac{\gamma}{RT_n}} = \frac{g}{\gamma} = 0.65$$

so that the rate of ammonia synthesis should obey the law

$$\frac{d[NH_3]}{dt} = k_1 p_{N_2} \frac{p_{H_2}^{1.95}}{p_{NH_3}^{1.30}} \quad (9)$$

The Arrhenius activation energy of ammonia synthesis, $E = RT^2 (d \ln k_1/dT)$, is given by

$$E = E_s - \frac{\alpha}{n} Q = 38 - 0.65 \times 23 = 23 \text{ kcal./mole} \quad (10)$$

where Q is the heat of reaction of $3H_2 + N_2 = 2NH_3$, E_s being $RT^2 (d \ln k/dT)$. The agreement between the calculated and the experimental value 23 kcal./mole, obtained by Kiperman[28] might be fortuitous, considering the experimental error, 2 kcal., involved in the estimation of E_S.

Turning now to the decomposition of ammonia, we have the rate expression

$$-\frac{d[NH_3]}{dt} = k' \theta^\beta = k' p_s^{-\beta/n} K^{\beta/n} \left(\frac{p_{NH_3}^2}{p_{H_2}^3}\right)^{\beta/n} = k_{-1} \left(\frac{p_{NH_3}^2}{p_{H_2}^3}\right)^{0.35} = k_{-1} \frac{p_{NH_3}^{0.70}}{p_{H_2}^{1.05}} \quad (11)$$

The activation energy for decomposition is

$$E' = E_s + \frac{\beta}{n} Q = 38 + 0.35 \times 23 = 46 \text{ kcal/mole} \quad (12)$$

Emmett and Love[29] found a kinetic law over a doubly promoted iron catalyst to be

$$-\frac{d[NH_3]}{dt} = k \left(\frac{p_{NH_3}^{0.6}}{p_{H_2}^{0.85}}\right) \quad (13)$$

the activation energy being 45.6 ± 2.0 kcal./mole in agreement with the above estimated value.

According to Love and Emmett, the order of ammonia decomposition does not change appreciably over a temperature range from 347 to 430°. The present treatment is consistent with this fact because $\beta/n = (\gamma - g)/\gamma$ is essentially independent of temperature. If we assume that $\alpha/n = \beta/n = 0.5$ as in Temkin and Pyzhev's treatment, the kinetic law becomes

$$\frac{d[NH_3]}{dt} = k_1 p_{N_2} \frac{p_{H_2}^{1.5}}{p_{NH_3}} - k_{-1} \frac{p_{NH_3}}{p_{H_2}^{1.5}} \quad (14)$$

Studying ammonia synthesis by use of the Temkin–Pyzhev expression (12), Brill[30] pointed out, however, that equation 14 is not correct. It should be noted that the improved equation of Brill on a doubly promoted iron catalyst is identical with (9) and (11). At lower coverage of chemisorbed nitrogen which might be realizable at high temperature or on a poor catalyst, the kinetic expression may be given by

$$\frac{d[NH_3]}{dt} = k_1 p_{N_2} - k_{-1} \frac{p_{NH_3}^2}{p_{H_2}^3} \quad (15)$$

because $\alpha = 0$, and $\beta = n$. The first term of the right of eq. 15 has been obtained by Kiperman, *et al.*,[28] on a less active catalyst.

Ammonia Synthesis on a Poisoned Surface.—Brunauer and Emmett[31] studied the synthesis of ammonia in the presence of water vapor, finding that the poisoning of catalyst is almost entirely reversible. If we assume that the reaction $H_2O = O(a) + H_2$ proceeds rapidly compared with the slowest step of ammonia synthesis, we may also formulate the synthesis reaction in a similar way to that in the foregoing section. The net rate of ammonia synthesis may be given by

$$k p \theta_N^{-\alpha} \theta_O^{-\alpha'} - k' \theta_N^{\beta} \theta_O^{-\beta'} \quad (16)$$

provided that the water vapor *poisons* both forward and backward reactions in proportion to the power of the concentration of chemisorbed oxygen. The $\theta_0^{-\alpha'}$, etc., are expressed by

$$\theta_0^{-\alpha'} = \left(\frac{p_{O_2}}{p'}\right)^{-\alpha'/n'} = \left(\frac{p_s'}{K'}\right)^{\alpha'/n'} \left(\frac{p_{H_2}^2}{p_{H_2O}^2}\right)^{\alpha'/n'} \quad (17)$$

$$\theta_0^{-\beta'} = \left(\frac{p_{O_2}}{p_s'}\right)^{-\beta'/n'} = \left(\frac{p'}{K'}\right)^{\beta'/n'} \left(\frac{p_{H_2}^2}{p_{H_2O}^2}\right)^{\beta'/n'} \quad (18)$$

where K' is the equilibrium constant of the reaction $2H_2 + O_2 = 2H_2O$. Assuming for simplicity that $\alpha'/n' = \beta'/n' = 0.5$, we have the expression

$$\frac{d[NH_3]}{dt} = k_1 p_{N_2} \frac{p_{H_2}^{2.5}}{p_{H_2O} p_{NH_3}} - k_{-1} \frac{p_{NH_3}}{p_{H_2}^{0.5} p_{H_2O}} \quad (19)$$

which has been shown by Kiperman[32] to represent the experimental data at low and high pressures.

(28) S. L. Kiperman and V. Sh. Granovskaya, *J. Phys. Chem., U.S.S.R.*, **26**, 1619 (1952).

(29) K. S. Love and P. H. Emmett, *J. Am. Chem. Soc.*, **63**, 3297 (1941).

(30) R. Brill, *J. Chem. Phys.*, **19** 1047 (1951).

(31) S. Brunauer and P. H. Emmett, *J. Am. Chem. Soc.*, **52**, 2682 (1930).

(32) S. L. Kiperman, *J. Phys. Chem., U.S.S.R.*, **28**, 389 (1954).

Water Gas Reaction.—Temkin and Kul'kova[33] found a kinetic law for the water gas reaction, $H_2O + CO = H_2 + CO_2$, over an iron oxide catalyst as given by

$$-\frac{d[H_2O]}{dt} \propto p_{CO}\left(\frac{p_{H_2O}}{p_{H_2}}\right)^{1/2} \quad (20)$$

Parravano,[34] on the other hand, found the expression

$$-\frac{d[H_2O]}{dt} \propto p_{H_2O}\left(\frac{p_{CO}}{p_{CO_2}}\right) \quad (21)$$

on a ruthenium catalyst. Let us assume that the reaction takes place according to the scheme

$$H_2O \longrightarrow O(a) + H_2 \quad (i)$$
$$O(a) + CO \longrightarrow CO_2 \quad (ii)$$

By assuming that (ii) is the slowest step on the iron oxide while (i) on the ruthenium catalyst, one can find the kinetic law, respectively, as

$$-\frac{d[H_2O]}{dt} \propto p_{CO}\theta_0^{\beta/2} \propto p_{CO}\left(\frac{p_{H_2O}^2}{p_{H_2}^2}\right)^{\beta/2n} \propto p_{CO}\left(\frac{p_{H_2O}}{p_{H_2}}\right)^{\beta/n} \quad (22)$$

$$-\frac{d[H_2O]}{dt} \propto p_{H_2O}\theta_0^{-\alpha/2} \propto p_{H_2O}\left(\frac{p_{CO_2}^2}{p_{CO}^2}\right)^{-\alpha/2n} \propto p_{H_2O}\left(\frac{p_{CO}}{p_{CO_2}}\right)^{\alpha/n} \quad (23)$$

The rate of reaction of oxygen *atom* with carbon monoxide molecule to form carbon dioxide at the surface should be proportional to $\theta_0^{\beta/2}$, because the desorption rate of two chemisorbed oxygen atoms has been expressed as $k'\theta_0^{\beta/2}\theta_0^{\beta/2} = k'\theta_0^{\beta}$ in the power rate law.

Expression (23) is however not in agreement with Parravano's finding, if $\alpha/n = 0.5$. To account for the experimental facts, we have to assume that the rate is proportional to $\theta_0^{-\alpha}$ instead of $\theta_0^{-\alpha/2}$; in other words, the chemisorption of a water molecule to form a chemisorbed oxygen atom and a chemisorbed hydrogen molecule would presumably be the rate-controlling step.

Parahydrogen Conversion.—Laidler[35] interpreted the low order of the conversion of parahydrogen into orthohydrogen on tungsten on the basis of the Bonhoeffer–Farkas mechanism, in which the rate of conversion is assumed to be governed by the chemisorption or desorption of hydrogen from the surface. Accordingly, the rate can be expressed by $kp(1 - \theta)^2$.

By using the chemisorption data obtained by Frankenburg and Rideal and Trapnell, Laidler estimated the pressure dependency of both k and $(1 - \theta)^2$ which are equal, respectively, to $p^{-0.4}$ and $p^{-0.6}$, hence finally zero-order kinetics was obtained.

Now according to the power rate law, the conversion rate should be given on the basis of the same mechanism as

$$kp\,\theta^{-\alpha} = kp_s^{\alpha/n}p^{1-\alpha/n} = k'p^{\beta/n} \quad (24)$$

the order of the conversion being given simply by β/n.

The Freundlich type of isotherm has been obtained by Trapnell[11] for hydrogen on tungsten. Accordingly, n ranges from 17 to 25 at temperatures between 0 and −183°. However, we have no knowledge about β, as the rate of chemisorption of hydrogen is so fast. It is noted, however, that the analysis of the chemisorption of nitrogen on tungsten due to Davis[9] yields $\beta/n = 3/17 = 0.17$. The low order of the parahydrogen conversion on tungsten is probably associated with a much smaller value of β compared with n. An alternative mechanism which assumes the reaction of chemisorbed hydrogen atom with gaseous hydrogen, on the other hand, gives

$$kp_{H_2}\theta_H^{\beta/2} = k'p_{H_2}^{1+\beta/2n} \quad (25)$$

which undoubtedly fails to account for the observed kinetics.

Ethane Hydrocracking on an Iron Catalyst.—In studying the ethane hydrocracking on a promoted iron catalyst, Cimino, Boudart and Taylor[36] obtained a kinetic law

$$-\frac{d[C_2H_6]}{dt} = kp_{C_2H_6}^n p_{H_2}^{1-n(6-x/2)} \quad (26)$$

Assuming the following mechanism

$$C_2H_6 \longrightarrow C_2H_x(a) + \frac{6-x}{2}H_2 \quad (i)$$
$$C_2H_x(a) + H_2 \xrightarrow{A} \text{products} \quad (ii)$$

where the C–C bond breaking by reaction with molecular hydrogen on the surface is the slowest step of the over-all reaction, they could satisfactorily interpret the reaction order of hydrogen as a function of that of ethane, n, and x which, in turn, is dependent of the amount of potash in the catalyst. Following the same mechanism, the kinetic law, according to the power rate law, may be written

$$-\frac{d[C_2H_6]}{dt} \propto p_{H_2}\theta_{C_2H_x}^{\beta} \propto p_{H_2}\left(\frac{p_{C_2H_6}}{p_{H_2}^{6-x/2}}\right)^{\beta/n} \propto p_{C_2H_6}^{\beta/n}\,p_{H_2}^{1-[\beta/n(6-x/2)]} \quad (27)$$

Carbon Monoxide Oxidation on NiO.—Parravano[37] found the following kinetic law for the oxidation of carbon monoxide on nickel oxide

$$\frac{d[CO_2]}{dt} = kp_{O_2}^{0.5}p_{CO}^{0.5} \quad (106\text{–}174°) \quad (28)$$

$$\frac{d[CO_2]}{dt} = kp_{O_2}^{0.2}p_{CO} \quad (205\text{–}222°) \quad (29)$$

Let us assume that the reaction takes place according to the scheme

$$O_2 \longrightarrow 2\,O(a) \quad (i)$$
$$O(a) + CO \longrightarrow CO_2 \quad (ii)$$

if (ii) is the slowest step, the rate of reaction may be expressed as

$$\frac{d[CO_2]}{dt} = kp_{CO}\theta_0^{\beta/2} = k'p_{CO}(p_{O_2})^{\beta/2n} \quad (30)$$

which is in agreement with the observed kinetics at higher temperatures provided that $\beta/n = 0.5$. If, on the other hand, (i) is the slowest step, the rate may be

$$\frac{d[CO_2]}{dt} = kp_{O_2}\theta_0^{-\alpha} = k'p_{O_2}\left(\frac{p_{CO_2}^2}{p_{CO}^2}\right)^{-\alpha/n} = k'p_{O_2}\left(\frac{p_{CO}}{p_{CO_2}}\right) \quad (31)$$

(33) M. Temkin and N. V. Kul'kova, *J. Phys. Chem., U.S.S.R.* **23**, 695 (1949).
(34) G. Parravano, private communication.
(35) K. J. Laidler, THIS JOURNAL, **57**, 320 (1953).
(36) A. Cimino, M. Boudart and H. S. Taylor, *ibid.*, **58**, 769 (1954).
(37) G. Parravano, *J. Am. Chem. Soc.*, **75**, 1448 (1953).

The experimental result is, however, that the reaction is approximately first order[37,38] with respect to the total pressure over the temperature range investigated, and carbon dioxide has no effect[39,40] on the rate at temperatures above 160–200°. So eq. 31 cannot describe the observed kinetics. It seems likely that the reaction between O(a) and CO(a) is the rate-controlling step so that the kinetics can be expressed by

$$\frac{d[CO_2]}{dt} \propto \left(\frac{p_{CO}}{p_s}\right)^{\beta/n}\left(\frac{p_{O_2}}{p_s'}\right)^{\beta'/2n'} \propto p_{CO}^{\beta/n} p_{O_2}^{\beta'/2n'} \quad (32)$$

With rising temperature, we may expect the order of the reaction, $(\beta/n + \beta'/2n')$, to increase from 0.75 to 1.50 if β/n, etc., are assumed to be 0.5 throughout.

Conclusion

The formulation of surface kinetics has been developed on the basis of a generally acceptable empirical law for chemisorption. Two parameters involved in surface kinetics, *i.e.*, *reaction order* and *activation energy* were taken into consideration and found to be correlated with kinetic constants of chemisorption. The Freundlich isotherm equation implies some disadvantages in its original form such that there is no saturation value for chemisorption at high equilibrium pressures and heats of chemisorption becomes infinity as θ approaches zero. These difficulties are avoided in the present treatment. The θ scale may be a matter of convenience; if one takes $\theta = 1$ at a definite coverage smaller than that defined in this paper, p_s, equilibrium pressure at $\theta = 1$, will then become dependent on temperature. There is, however, no difference between the two cases so far as reaction order and activation energy are concerned. Thus it may be concluded that the present method may help to clarify the mechanism of heterogeneous kinetics in a simple and straightforward way, especially when chemisorption data are available.

Acknowledgments.—The author wishes to thank Dean Hugh Taylor and Dr. Boudart for their kind comments on this work.

(38) W. A. Bone and G. W. Andrews, *Proc. Roy. Soc.* (*London*), **110A**, 16 (1926).

(39) S. Roginsky and T. Tselinskaya, *J. Phys. Chem., U. S. S. R.*, **21**, 919 (1947).

(40) R. M. Dell and F. S. Stone, *Trans. Faraday Soc.*, **50**, 501 (1954).

THE MECHANISM OF THE INHIBITION OF CORROSION BY THE PERTECHNETATE ION IV. COMPARISON WITH OTHER XO_4^{n-} INHIBITORS

BY R. F. SYMPSON[1] AND G. H. CARTLEDGE

Chemistry Division, Oak Ridge National Laboratory, Oak Ridge, Tennessee[2]

Received January 5, 1956

The effect of the addition of electrolytes on the potential of iron electrodes immersed in solutions of four inhibitors—$CrO_4^{=}$, TcO_4^{-}, $MoO_4^{=}$, $WO_4^{=}$—has been determined at 57.5°. The behavior of the electrode potentials confirms the previous conclusion that a labile state exists at the metal–solution interface, and that the mechanism of corrosion inhibition is reversible with respect to addition or removal of electrolyte. All four inhibitors maintained the iron electrodes at potentials more noble than the Flade potential in the presence of dissolved air, but only the pertechnetate ion did so in deaerated solutions. In deaerated solutions of $MoO_4^{=}$ and $WO_4^{=}$, the iron electrode potentials were essentially the same as in sodium sulfate. The potentials in deaerated $CrO_4^{=}$ solution were 200 mv. or more less noble than in TcO_4^{-}, but still considerably more positive than the potentials in solutions of $MoO_4^{=}$ or $WO_4^{=}$. Addition of chloride or thiocyanate ions initially produced an ennobling of the potentials, up to the concentration at which final debasing set in. The bearing of the results on the theory of inhibition and electrode potentials is discussed.

A previous paper[3] presented results on measurements of the electrode potential of electrolytic iron in a corrosion-inhibiting solution of potassium pertechnetate. It was shown that the noble potential was debased and the inhibition weakened by addition of sufficient sodium sulfate. Potassium perrhenate was shown to be much less effective than sodium sulfate in this action. These measurements, together with other evidence, were interpreted as indicating that inhibition by the pertechnetate ion depends upon a labile state of adsorption at the interface that is subject to competition among the various ions or molecules present in the solution.

As a possible means of deciding by what mechanism other ions of the XO_4^{n-} type act as inhibitors it seemed desirable to make similar measurements on chromates, molybdates and tungstates. The Evans school of thought[4,5] has considered the chromate ion to act because of its oxidizing power, whereas Uhlig[6] has ascribed its action to effects associated with adsorption of the unreduced ions. The action of molybdate and tungstate ions[7] has been interpreted by Pryor and Cohen[5] as arising also from film repair, in spite of the fact that these ions in approximately neutral solution are much weaker oxidizing agents than the chromate ion. It was hoped that comparative studies of the susceptibility of the electrode potentials to foreign electrolytes might give an indication whether there were any differences in the action of the four inhibitors, since their effectiveness as oxidizing agents

(1) Summer Research Participant from Ohio University, Athens, Ohio.

(2) Operated by Union Carbide Nuclear Company for the U. S. Atomic Energy Commission.

(3) G. H. Cartledge, THIS JOURNAL, **60**, 28 (1956).

(4) T. P. Hoar and U. R. Evans, *J. Electrochem. Soc.*, **99**, 212 (1952).

(5) M. J. Pryor and M. Cohen, *ibid.*, **100**, 203 (1953).

(6) H. H. Uhlig, "Metal Interfaces," A Symposium, Am. Soc. Metals, Cleveland, Ohio, 1951, pp. 312–335.

(7) W. D. Robertson, *J. Electrochem. Soc.*, **98**, 94 (1951).

should be unaffected by the low concentrations of electrolytes added, whereas adsorption under the influence of weak electrostatic forces should be affected.[8]

The present work covers measurements with the pertechnetate, chromate, molybdate and tungstate ions as inhibitors, and with the chloride, thiocyanate, sulfate and perrhenate ions as non-inhibiting competing ions. In order to obtain stable potentials more quickly and reliably, the experiments were conducted at 57.5° in well-agitated solutions. Both aerated and deaerated solutions were used.

Experimental

The electrolytic iron, potassium pertechnetate and potassium perrhenate were from the supply used in previous work.[3,8-10] Solutions of the other salts were prepared by direct weighing of chemicals of analytical grade. The *p*H values were determined with a Beckman Model G *p*H meter by withdrawing small portions of solutions from the cell at various points in each experiment. The inhibitors were used at low concentrations (10^{-3} to 10^{-4} *f*) which previous work[5,7] had shown to be inhibitive at 25°.

The iron electrodes were in the form of strips about 5 mm. wide. The electrodes were abraded with 2/0 emery paper, degreased and coated with an insulating lacquer except for a section about 1 to 2 cm. long near the end of the electrode. The tips of the electrodes were lacquered to minimize effects due to strains produced in the end of the electrodes by cutting. The lacquer was dried for three hours or longer at 110°. Immediately before use the exposed portions of the electrodes were lightly emeried again. Two electrodes designated as No. 1 and No. 2 were used in each experiment. The potential was measured alternately between each iron electrode and the saturated calomel electrode.

The cell consisted of the experimental half-cell immersed in a constant-temperature oil-bath and bridged to a 0.1 *N* potassium chloride solution outside the bath. A commercial Beckman saturated calomel electrode was dipped into the 0.1 *N* potassium chloride solution. Electrical contact between the inhibitor solution and the potassium chloride solution was made through a stopcock coated with a bentonite paste[5] and kept in the closed position during the entire experiment. The temperature of the oil bath was controlled at 57.5 ± 0.5°. Although the temperature gradient in the salt bridge introduced a small but unknown e.m.f., both this and the liquid-junction potential are unimportant, since only large changes of potential are of interest. Potentials were measured either manually with a Beckman Model G *p*H meter or recorded continuously with a modified Leeds and Northrup line-operated *p*H meter the output of which was connected to a Brown recorder. The magnitude of the current drawn by either instrument is small enough so that no appreciable polarization occurs. During the experiments conducted in aerated solutions, a stream of air, saturated with water vapor at 57.5°, was bubbled continuously through the solution. In the experiments conducted in deaerated solutions, nitrogen was continuously bubbled through the solution after being freed of oxygen by passage over copper filings heated to 450° and saturated with water vapor at 57.5°. The bubbling of gas through the solution provided stirring to minimize any concentration polarization in addition to keeping the solution saturated with the desired gas.

In all experiments, the electrodes were allowed to stand in the inhibiting solution at 57.5° from 4 to 16 hours to attain a steady initial potential before addition of the foreign electrolyte. After addition of each portion of the electrolyte, at least 20 min., and usually about 60 min., elapsed before the next addition. The potentials given in the tables are the essentially stable values attained at each concentration before the next addition of electrolyte. In the experiments in which chloride ions or thiocyanate ions were added, there was always an initial ennobling that does not necessarily appear in the tabulated data, since the ennobling was not always maintained in its entirety (*cf.* Fig. 1). The temporary ennobling by these ions will be shown in Table XI in connection with the discussion.

Results in Aerated Solutions.—Four of the experiments that were performed with the iron electrodes immersed in Na_2MoO_4 solutions of two concentrations are summarized in Tables I and II.

TABLE I

ELECTRODE POTENTIALS OF IRON IN 1.0×10^{-3} *f* Na_2MoO_4 (Experiments 1, 2)

Concn. of added electrolyte, *f*		Electrode potential[a] (mv. *vs.* S.C.E.)		
Na_2SO_4	NaCl	No. 1	No. 2	*p*H
0	...	+103	+100	6.54
3.1×10^{-4}	...	+103	+101	
6.2×10^{-4}	...	− 82	− 21	6.45[b]
...	0	+ 97	+ 93	6.50
...	3.1×10^{-4}	+100	+ 99	
...	6.2×10^{-4}	+ 60 to +80	+ 70 to +90[c]	
...	9.4×10^{-4}	+ 35 to +40	+ 40 to +50	6.32[c]
...	1.2×10^{-3}	−190	−144[d]	

[a] The European sign convention for electrode potentials is used throughout this paper. [b] Potential became unstable in 20 min. and dropped to the values indicated overnight. Both electrodes were pitted. [c] Potentials unstable. [d] Both electrodes showed corrosion spots.

TABLE II

ELECTRODE POTENTIALS OF IRON IN 1.0×10^{-4} *f* Na_2MoO_4 (Experiments 3, 4)

Concn. of added electrolyte, *f*		Electrode potential (mv. *vs.* S.C.E.)		
Na_2SO_4	NaCl	No. 1	No. 2	*p*H
0	...	+126	+133	6.52
1.6×10^{-4}	...	−108 to −118	−103 to −113	6.37[a]
...	0	+ 88	+ 90	6.53
...	6.2×10^{-4}	+ 24	+ 29[b]	
...	1.2×10^{-3}	−344	−419	7.1[c]

[a] Corrosion spots visible after 35 min. [b] Potential unstable. [c] Potential reached after 16.5 hr. Slight corrosion occurred in 1 hr. General corrosion and turbidity in solution. The acidity shortly after addition of NaCl was 6.50; *p*H increased to 7.1 after general corrosion occurred on standing overnight.

In one experiment (4a), the thiocyanate ion was added to aerated 1×10^{-3} *f* Na_2MoO_4. It was shown that the thiocyanate ion alone at 1×10^{-4} *f* and 5×10^{-3} *f* failed to inhibit at 57.5°. When added to the molybdate solution, it caused additional prompt ennobling at 6.2×10^{-5} *f*, at 3.1×10^{-4} *f* and, initially, on one electrode at 9.4×10^{-4} *f*. At the last concentration, electrode no. 1 quickly became unstable and debased 450 mv. within 48 min., whereas no. 2 ennobled by 29 mv. and remained noble for 20 min. after the addition before beginning to debase. One hour after the addition it also had debased by 440 mv. and was lightly pitted.

It was found necessary to immerse the iron electrodes in the aerated Na_2MoO_4 inhibitor solution at room temperature for 30 minutes to one hour before immersing the cell in the oil-bath. When the electrodes were immersed directly in the solution at 57.5°, slight corrosion occurred immediately.

Experiments 5–10 were conducted with iron specimens inhibited by Na_2WO_4. Experiments 5 and 6 measured the effect of adding Na_2SO_4 to a 1×10^{-2} *f* solution. In experiment 5, the Na_2SO_4 was added from a 0.5 *f* stock solution until the concentration of sulfate was 0.05 *f*. Further sulfate was added from a 2.0 *f* stock solution. Due to the high concentration of sulfate needed to debase the potential of the iron electrodes, the Na_2WO_4 solution was appreciably diluted by the volume of Na_2SO_4 solution added. Experiment 6 was a repetition of experiment 5 in which the required Na_2SO_4 was added entirely from a 2.0 *f* stock solution. In

(8) G. H. Cartledge, THIS JOURNAL, **60**, 32 (1956).
(9) G. H. Cartledge, *Corrosion*, **11**, 335t (1955).
(10) G. H. Cartledge, THIS JOURNAL, **59**, 979 (1955).

experiments 7 and 8 the effect of adding NaCl to 1.0×10^{-2} *f* Na_2WO_4 was measured. The results of experiments 5, 6, 7 and 8 are given in Table III, and the potential–time curve for electrode no. 1 of experiment 8 is shown in Fig. 1. Experiments 9 and 10 determined the effect on the potential of the iron of adding Na_2SO_4 and NaCl to a 1.0×10^{-3}*f* Na_2WO_4 solution. The results of experiments 9 and 10 are given in Table IV. Two additional experiments which are not shown in Table IV were done with 1.0×10^{-3} *f* tungstate. With addition of sulfate ion, both electrodes debased severely at 5.0×10^{-3} *f;* with chloride ion, debasing occurred at 2.5×10^{-3}*f*.

TABLE III

ELECTRODE POTENTIALS OF IRON IN 1.0×10^{-2} *f* $NaWO_4$

Concn. of added electrolyte, *f*		Electrode potential (mv. *vs.* S.C.E.)		
Na_2SO_4	NaCl	No. 1	No. 2	pH
0	...	+ 71	+ 69	7.29
5×10^{-3}	...	+ 69	+ 69	
7.5×10^{-3}	...	+ 79	+ 70	7.20
1×10^{-2}	...	+ 79	+ 70	
2×10^{-2}	...	+ 82	+ 71	7.20
4×10^{-2}	...	+ 79	+ 70	
8×10^{-2}	...	+ 72	−270	7.12
1.2×10^{-1}	...	+ 70	−301	7.15[a]
0	...	+ 53	+ 54	7.20
2×10^{-2}	...	+ 59	+ 56	
4×10^{-2}	...	− 45 to −60	+ 35	7.07[b]
6×10^{-2}	...	− 12 to −30	+ 28[b]	
8×10^{-2}	...	− 10	+ 28	7.08[b,c]
...	0	+ 70	+ 69	7.17
...	3.1×10^{-4}	+ 72	+ 71	
...	6.2×10^{-4}	+ 78	+ 76	7.18
...	9.4×10^{-4}	+ 80	+ 75	
...	1.2×10^{-3}	+ 83	+ 80	7.13
...	2.5×10^{-3}	+ 73	+ 86[d]	
...	3.8×10^{-3}	+ 85	+ 55[e]	
...	5×10^{-3}	+ 96	+ 71	7.10
...	7.5×10^{-3}	+ 96	+ 87	
...	1.0×10^{-2}	+ 81	+100	
...	2.0×10^{-2}	−271	−270	7.40[f]
...	0	+ 53	+ 38	7.18
...	5×10^{-3}	+ 65	+ 65	
...	7.5×10^{-3}	+ 84	+ 73	
...	1×10^{-2}	+ 98	+ 84	7.18[g]
...	2×10^{-2}	− 58 to −97	+ 90 to +101[h]	
...	3×10^{-2}	−276	−225 to −229[i]	

[a] Visible corrosion on no. 2. [b] Corrosion visible on no. 1 and potential very unstable. Potential of no. 2 somewhat unstable. [c] Potential and *p*H measurements made 35 min. after adding Na_2SO_4; 64 hr. after addition of Na_2SO_4 both electrodes were deeply pitted and solution was quite turbid. Potential was not measured at that time, however. [d] Potential of no. 1 dropped to 59 initially but was slowly increasing. [e] No. 2 became unstable temporarily and dropped to −30 at one point. [f] Both electrodes corroded. [g] No. 2 became unstable at one point but slowly recovered. [h] No. 1 very unstable. No. 2 slightly unstable. [i] Pitting type corrosion occurred.

One experiment, no. 11, was performed to determine the degree of reversibility in the potential changes of the iron electrodes inhibited by Na_2WO_4 upon addition and removal of sulfate. In this experiment, Na_2SO_4 was added to a 1.0×10^{-2} *f* Na_2WO_4 solution until the potentials of the iron electrodes became unstable and debased to a fairly negative potential. Before any extensive corrosion could occur, the Na_2WO_4–Na_2SO_4 solution was removed and 35 ml. of sulfate-free 1.0×10^{-2} *f* Na_2WO_4 solution was added. The results of this experiment are summarized in Table V. The potentials remained fairly steady until the concentration of sulfate became 0.2 *f;* the potentials then debased to the values indicated in Table V in 45 minutes. After removal of the Na_2WO_4–Na_2SO_4 solution and addition of sulfate-free Na_2WO_4 solution, the potential of electrode no. 1 increased about 200 mv. in 6 minutes and increased further to the value indicated in Table V upon standing overnight. The potential of electrode no. 2 increased approximately 130 mv. in 6 minutes and reached the value indicated in Table V after standing overnight. One small corrosion spot developed on electrode no. 1 while the iron electrodes were in the 0.2 *f* sulfate solution, but no further corrosion occurred in sulfate-free Na_2WO_4 solution. No corrosion was visible on electrode no. 2 at any time.

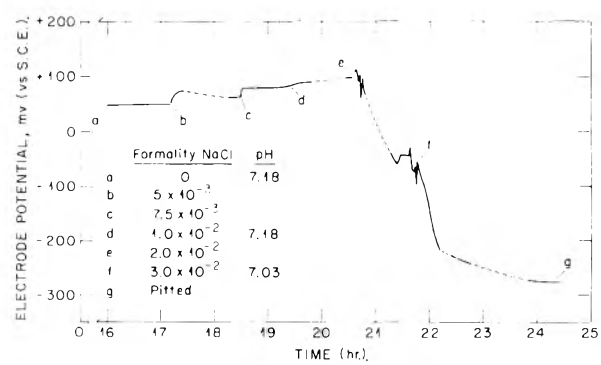

Fig. 1.—Electrode potentials of iron in aerated 1×10^{-2} *f* Na_2WO_4 with addition of NaCl (experiment 8, electrode no. 1).

TABLE IV

ELECTRODE POTENTIALS OF IRON IN 1.0×10^{-3} *f* Na_2WO_4 (Experiments 9, 10)

Concn. of added electrolyte, *f*		Electrode potential (mv. *vs.* S.C.E.)		
Na_2SO_4	NaCl	No. 1	No. 2	pH
0	...	+118	+130	6.64
1.2×10^{-3}	...	+115	+125	
2.5×10^{-3}	...	+108	+118	
5.0×10^{-3}	...	+106	+116	6.53
7.5×10^{-3}	...	−341	−323	6.78[a]
...	0	+ 42	+ 93	6.70
...	2.5×10^{-3}	+ 61	+ 55 to +100[b]	
...	5.0×10^{-3}	− 25 to +3	−213	6.69[c]
...	7.5×10^{-3}	−180	−226[d]	

[a] Both electrodes corroding. [b] No. 2 unstable. [c] Corrosion pits visible on No. 2; No. 1 quite unstable. [d] Corrosion pits starting on no. 1; no. 2 heavily pitted.

TABLE V

REVERSIBILITY OF THE POTENTIAL CHANGES IN INHIBITION BY Na_2WO_4 (Experiment 11)

Concn. of Na_2SO_4, *f*	Electrode potentials (mv. *vs.* S.C.E.) No. 1	No. 2	pH
0	+ 70	+ 67	7.15
5×10^{-3}	+ 69	+ 65	
1×10^{-2}	+ 60	+ 67	
2×10^{-2}	+ 60	+ 70	
4×10^{-2}	+ 65	+ 64	7.14[a]
6×10^{-2}	+ 68	+ 65	
8×10^{-2}	+ 46	+ 71[b]	
1.0×10^{-1}	+ 46	+ 71	
2.0×10^{-1}	−282 to −302	−117 to −142	7.09[c]
0	− 7	+ 68	7.15

[a] No. 1 dropped to 40 mv. at one point but slowly recovered. [b] No. 1 slightly unstable. [c] Both electrodes very unstable.

Experiments using a 4.7×10^{-4} *f* $KTcO_4$ solution as the inhibitor were conducted and the effect on the potential of the iron electrodes caused by the addition of NaCl, Na_2SO_4 and $KReO_4$ was observed. The results of experiments 12 and 13 are summarized in Table VI. The data are in substantial agreement with those of two exploratory experiments of the same type. It is to be noted that the technetium concentration is lower and the temperature higher than in the experiments previously reported.[3] Potassium pertechnetate was also used at a concentration of 1.0×10^{-3} *f*, with chloride, sulfate and thiocyanate ions as additives. The additions of thiocyanate ions produced initial ennobling exactly as shown in Fig. 1 for chloride ions.

TABLE VI

ELECTRODE POTENTIALS OF IRON IN 4.7×10^{-4} *f* $KTcO_4$

(Experiments 12, 13)

Concn. of added electrolyte, *f* Na_2SO_4	NaCl	Electrode potential (mv. *vs.* S.C.E.) No. 1	No. 2	*p*H
0	...	+175	+183	
2.1×10^{-4}	...	+168	+180	
4.2×10^{-4}	...	+161	−173[a]	
6.2×10^{-4}	...	−225	−235	6.52[b]
...	0	+125	+126	6.39
...	4.2×10^{-4}	+133	+130	
...	8.3×10^{-4}	+138	+134	
...	1.2×10^{-3}	+148	+142	
...	1.7×10^{-3}	− 5 to −18	+130	6.31[c]
...	2.5×10^{-3}	−421	−131 to −142[d]	

[a] No. 2 broke sharply in 10 min. and corroded. [b] Visible corrosion on no. 1. [c] No. 2 dropped to +110 at one point but recovered. No. 1 unstable. [d] No. 2 became unstable in 10 min. Several large pits on both electrodes.

In previous work,[8] it was found that the perrhenate ion, which is identical to the TcO_4^- ion in charge and configuration and similar in size, does not inhibit the corrosion of iron. The ReO_4^- ion also did not produce the pronounced debasing of the potential of iron electrodes inhibited by TcO_4^- at room temperature that the sulfate ion did.[3] In experiments 14 and 15, $KReO_4$ was added to 4.7×10^{-4} *f* $KTcO_4$ inhibitor and the changes in electrode potential were measured. The results of these two experiments are given in Table VII. In experiment 14, the $KReO_4$ was added from a 0.01 *f* stock solution. When the concentration of added ReO_4^- was approximately 2×10^{-3} *f*, dilution of the TcO_4^- solution had become appreciable. No further ReO_4^- was added but, instead, sufficient 0.5 *f* Na_2SO_4 was added to make the sulfate concentration 1.6×10^{-3} *f*. The sulfate produced a rapid debasing of potential to the value indicated in Table VII. In experiment 15, the $KReO_4$ was added from a solution containing both 0.05 *f* $KReO_4$ and 4.7×10^{-4} $KTcO_4$. No significant changes in potential were produced even when the concentration of ReO_4^- was raised to 0.01 *f*. Sufficient sulfate was then added to make the sulfate concentration 1×10^{-3} *f*. This produced the rapid debasing indicated in Table VII.

Two experiments, 16 and 17, were conducted using a potassium chromate–potassium dichromate solution (1×10^{-3} *f* in Cr) as an inhibitor, the mixture being in such proportions as to give a *p*H value of approximately 6.5. In experiment 16, Na_2SO_4 was added to the chromate solution until the potential of the iron became unstable and debased. The chromate–sulfate solution was then removed and 40 ml. of the sulfate-free chromate inhibitor solution was added to the cell. The potential slowly ennobled by approximately 300 mv. at each electrode. Experiment 17 measured the effect of the addition of NaCl on the potential of the iron electrodes. The results of these two experiments are summarized in Table VIII and the potential–time curve for electrode no. 1 of experiment 16 is shown in Fig. 2.

Results in Deaerated Solutions.—In order to determine to what extent dissolved oxygen affects the potential of iron electrodes immersed in an aerated inhibitor solution, experiments were performed in which the potentials of iron electrodes were measured in deaerated solutions of the same inhibitors.

TABLE VII

EFFECT OF $KReO_4$ ON ELECTRODE POTENTIALS OF IRON INHIBITED BY $KTcO_4$

(Experiments 14, 15)

Concn. of added electrolyte, *f* $KReO_4$	Na_2SO_4	Electrode potentials (mv. *vs.* S.C.E.) No. 1	No. 2	*p*H
0	0	+151	+150	6.46
1×10^{-4}	0	+150	+148	
2×10^{-4}	0	+146	+145	
4×10^{-4}	0	+145	+143	
6×10^{-4}	0	+145	+148	6.28
8×10^{-4}	0	+150	+152	
1×10^{-3}	0	+146	+145	
2×10^{-3}	0	+144	+146	6.20
2×10^{-3}	8×10^{-4}	+141	+145	
2×10^{-3}	1.6×10^{-3}	−337	−323	6.26[a]
0	0	+175	+172	6.03
5×10^{-4}	0	+175	+173	
1×10^{-3}	0	+179	+176	
2×10^{-3}	0	+170	+166	
5×10^{-3}	0	+167	+169	
7.5×10^{-3}	0	+161	+162	
1×10^{-2}	0	+159	+160	6.00[b]
1×10^{-2}	1×10^{-3}	−247	−265[c]	

[a] Potentials dropped very sharply and visible corrosion occurred in 30 min. [b] No. 2 dropped to +120 at one point but recovered. [c] Potential dropped immediately and visible corrosion occurred on both electrodes in 30 min.

TABLE VIII

ELECTRODE POTENTIALS OF IRON IN POTASSIUM CHROMATE SOLUTION

(Experiments 16, 17)

Concn. of added electrolyte, *f* Na_2SO_4	NaCl	Electrode potential (mv. *vs.* S.C.E.) No. 1	No. 2	*p*H
0	...	+189	+173	6.52
3.1×10^{-4}	...	+192	+169	
6.2×10^{-4}	...	+191	+165	
1.2×10^{-3}	...	+190	−257	
1.9×10^{-3}	...	+185	−307[a]	
2.5×10^{-3}	...	+185	...	6.49
3.1×10^{-3}	...	−346	−393[b]	
0	...	− 16	−111	6.56[c]
...	0	+119	+167	6.48
...	6.2×10^{-4}	+121	+169	
...	1.2×10^{-3}	+122	+170	
...	2.5×10^{-3}	+126	−110 to −136	6.45[d]
...	3.8×10^{-3}	−306	−317[e]	

[a] Corrosion spot visible on no. 2. [b] Corrosion spot visible on no. 1. [c] No further corrosion on either electrode. [d] No. 2 unstable and debasing. No. 1 dropped at one point but recovered. [e] One deep pit present on each electrode.

Experiment 18 was performed with 1.0×10^{-3} *f* Na_2MoO_4 as the inhibitor. Nitrogen was started bubbling through the solution as soon as the electrodes were immersed. The potentials of the iron electrodes debased rapidly at first and then more slowly, and eventually reached a steady potential after six hours. The final potentials were −712 and −714 mv., respectively. A blue-black film was present on both electrodes. The *p*H of the solution was 6.80. Electrode no. 1 was removed for closer observation. Air was then bubbled through the cell and the potential of electrode no. 2 was measured. The potential increased rapidly during the first 15 minutes and reached a maximum at −435 mv. The potential then decreased slowly as corrosion occurred. The final potential attained after

standing overnight was −531 mv. This result and experiments 1–4 make it clear that use of 1×10^{-3} *f* $MoO_4^=$ necessitates the presence of oxygen prior to exposure to a temperature of 57.5° if inhibition is to be established. Previous work in this Laboratory[11] demonstrated that inhibition by the molybdate ion is soon lost at temperatures approaching 100°, even at concentrations much higher than 10^{-3} *f*.

Experiments 19 and 20 were conducted using deaerated 1.0×10^{-2} *f* Na_2WO_4 solution. In experiment 19, air was first bubbled through the solution for 55 minutes and the potentials of the electrodes were measured during this time. Electrode no. 1 attained a potential of +80 mv., and no. 2 +69 mv. The air line was then disconnected and oxygen-free nitrogen was bubbled through the solution. The potentials of the electrodes slowly debased, and eight hours after starting nitrogen through the cell the potential of electrode no. 1 was −40 mv. and that of no. 2 was −79 mv. After nitrogen had been passed for 72 hours, the potential of electrode no. 1 was about −750 mv. and the potential of electrode no. 2 −757 mv. A visible, brassy film covered the surface of both electrodes. The *p*H of the air-saturated solution was 7.18.

In experiment 20, nitrogen was started bubbling through the solution as soon as the electrodes were immersed in the Na_2WO_4 solution. Electrode no. 1 attained a potential of −448 mv. and electrode no. 2 reached a potential of −756 mv. No explanation can be given for the large difference in the potential of electrode no. 1 from the potential of electrode no. 2 and the values obtained in experiment 19. A brassy film was again visible on both electrodes. Electrode no. 1 was then removed and the potential of electrode no. 2 measured as the solution was saturated with air. The potential increased rapidly to about −208 mv. in 14 minutes. After air had been passed through the solution overnight, the potential had increased to −118 mv. Approximately one third to one-half of the surface was corroded. The *p*H of the solution was 7.21 shortly after air had been started through the solution. Tungstate solutions of 1×10^{-3} *f*, like the molybdate solutions, failed to inhibit completely at 57.5° unless they were first fully aerated at room temperature for a half hour.

Two experiments, 21 and 22, were performed in deaerated $K_2Cr_2O_7$–K_2CrO_4 (1×10^{-3} *f* in Cr) as inhibitor. In experiment 21, the potentials of the two iron electrodes were measured as nitrogen was passed through the solution. The potentials of both electrodes debased quite slowly and after 26.5 hours the potential of no. 1 was −263 mv. The potential of electrode no. 2 was −86 mv., but it was still slowly drifting to a more negative potential. The *p*H of the solution was 6.55.

In experiment 22, nitrogen was initially bubbled through the solution and the potentials of the two electrodes were measured. After 17.5 hours the potentials were −171 and −145 mv., respectively. The potentials of both electrodes were still very slowly drifting to more negative values. Sufficient 0.5 *f* Na_2SO_4 solution was then added to make the concentration of sulfate 1.4×10^{-3} *f*. The potential of electrode no. 1 became −174 mv. and that of electrode no. 2 −151 mv. The sulfate concentration was then increased to 2.8×10^{-3} *f*. Electrode no. 1 debased rapidly to −308 mv. Electrode no. 2 maintained a potential of −160 mv. The sulfate concentration was again increased to 4.8×10^{-3} *f*. The potential of electrode no. 1 became −345 mv.; the potential of electrode no. 2 was −163 mv. The sulfate concentration was finally increased to 1.2×10^{-2} *f*. The potential of electrode no. 2 became quite unstable and debased rapidly. One hour after the last addition of sulfate the potential of electrode no. 1 was −415 mv. and that of no. 2 was −445 to −456 mv. Air was then passed through the solution, and after an initial ennobling the potentials continued to debase. Two and a half hours later the potentials of electrodes no. 1 and 2 were −521 and −586 mv., respectively. One corrosion spot had appeared on each electrode. The *p*H of the solution was 6.45.

One experiment, no. 23, was performed with deaerated 4.7×10^{-4} *f* $KTcO_4$ solution. The potentials of electrodes no. 1 and 2 were +88 and +87 mv., respectively. Sufficient Na_2SO_4 was then added to make the sulfate concentration 2.1×10^{-4} *f*. The potentials of both electrodes became quite unstable and in 1.75 hr. numerous pits were visible on both electrodes. After 2 hr. the potential of electrode no. 1 was −278 mv. and that of no. 2 was −268 mv.

(11) Unpublished results by Ruth P. Yaffe and one of us.

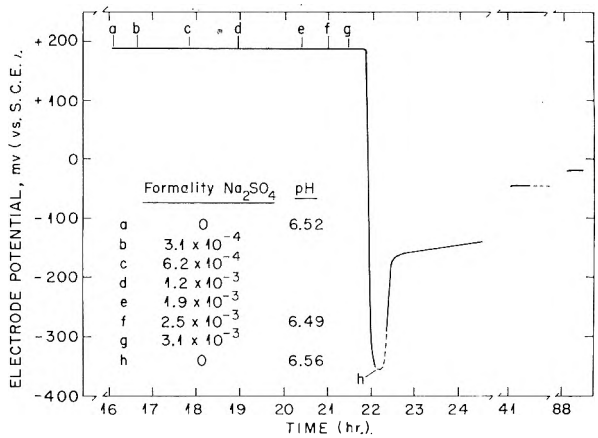

Fig. 2.—Electrode potentials of iron in aerated 1×10^{-3} *f* chromate solution with addition and removal of Na_2SO_4 (experiment 16, electrode no. 1).

Discussion

The comparative effects of the individual inhibitors upon the electrode potentials may be seen in Table IX. While the preceding tables gave only typical examples of the experiments done, Table IX includes all experiments, the indicated values being the average of the measurements and the average deviation for the number of electrodes shown in parentheses. The potentials shown are the stable values attained before addition of foreign electrolyte.

TABLE IX

STABLE INITIAL ELECTRODE POTENTIALS

Inhibitor	Formality	*p*H	Initial potential (mv. *vs.* S.C.E.) Aerated	Deaerated
TcO_4^-	1.0×10^{-3}	6.58	+141 ± 19 (6)	....
	4.7×10^{-4}	6.4	+157 ± 17 (12)	+ 88 ± 1 (2)
$MoO_4^=$	1.0×10^{-3}	6.62	+ 89 ± 10 (13)	−713 ± 1 (2)
	1.0×10^{-4}	6.52	+109 ± 23 (4)	....
$WO_4^=$	1.0×10^{-2}	7.18	+ 64 ± 9 (10)	−754 ± 3 (3)[a]
	1.0×10^{-3}	6.74	+ 87 ± 20 (8)	....
$CrO_4^=$	1.0×10^{-3}	6.54	+162 ± 22 (4)	< −164 variable

[a] Omitting electrode no. 1 of experiment 20, which was entirely at variance with three other closely agreeing electrodes.

In agreement with Pryor and Cohen,[5] it is seen that noble potentials were produced by molybdate and tungstate ions only in the presence of air. Even the chromate ion mixture induced only moderate (and very erratic) ennobling in the absence of air, whereas the pertechnetate ion showed the least dependence upon oxygen. Flade[12] found that anodically passivated iron rapidly becomes active in sulfuric acid at potentials that are reasonably definite for specified concentrations and temperatures. The *p*H dependence has been shown[13,14] to be given by the relation $e_H = 0.58 - 0.058pH$ at 20°. Although Flade was unable to determine the value above room temperature, he observed an ennobling of approximately 50 mv. on going from 0 to 15°. If one assumes a similar

(12) F. Flade, *Z. physik. Chem.*, **76**, 513 (1911).
(13) U. F. Franck, *Z. Naturforschg.*, **4a**, 383 (1949).
(14) K. J. Vetter, *Z. physik. Chem.*, **202**, 1 (1953).

rate of increase up to 60° and applies the *p*H values appropriate to the present experiments, the activating potential come out to be ≈ −10 mv. *vs.* S.C.E. for the $10^{-2}f WO_4^=$ and ≈44 mv. for the other inhibitors. It is evident that all the initial potentials were in the passive region under aeration, whereas only the pertechnetate ion gave such a potential in the absence of air. The blue and brassy film colorations seen in the tests in deaerated molybdate and tungstate solutions, coupled with the sharp rise in anodic polarization observed by Pryor and Cohen[5] when the polarization curves in a tungstate solution were determined repeatedly in absence of air, suggest that in these cases an insoluble ferrous salt may have been forming gradually at the anodes. The difference of 41 mv. between the base potentials in deaerated molybdate and tungstate solutions compares with 26 mv., as calculated from the difference in *p*H and the known *p*H dependence of the iron potential.[15]

The data showed that all four inhibitors were sensitive to added electrolytes, though there were significant differences both in degree and in the order of response to the chloride and sulfate ions. It may be recalled that the sulfate ion was chosen in the previous work[3] because of its bivalence and flocculating (rather than dispersing) action on iron oxide. It was consistently observed that incipient debasing of the potential was indicated by irregular oscillations of the potential. Typical potential–time curves are shown in Figs. 1 and 2. The comparative sensitivities to electrolytes in aerated solutions are shown in Table X.

TABLE X

CONCENTRATIONS OF ADDED IONS THAT INDUCED DEBASING ($f \times 10^4$)

Inhibitor		Cl^-	SCN^-	$SO_4^=$	ReO_4^-
TcO_4^-,	$1 \times 10^{-3} f$	24–32	22–>42	4	...
	$4.7 \times 10^{-4} f$	17–25	...	4.2–6.2	>100
$MoO_4^=$,	$1 \times 10^{-3} f$	6.2–9.4	<9.4	6.2	...
	$1 \times 10^{-4} f$	<6.2	...	<1.6	...
$WO_4^=$,	$1 \times 10^{-2} f$	200–300	...	400–2000	...
	$1 \times 10^{-3} f$	25–50	...	50–75	...
$CrO_4^=$,	$1 \times 10^{-3} f$	25–38	...	12–31	...

By comparing the results at inhibitor concentrations of $1 \times 10^{-3} f$ it will be noted that all the inhibitors were sensitive to the added ions, but in varying degrees. In all cases excepting the tungstate solutions the sulfate ion debased the potential at lower concentrations than were required by the univalent ions. As shown in experiment 11, for the tungstate ion, in experiment 16 for the chromate ion and, in the previous paper,[3] for the pertechnetate ion, removal of the foreign electrolyte led to prompt ennobling and more or less complete recovery from the debased potential. Use of two concentrations of molybdate and tungstate ions showed, especially for the tungstates, the greater susceptibility at the lower inhibitor concentration. Working in a higher concentration range, Pryor and Cohen[5] observed a similar result for chromate, nitrite and tribasic phosphate ions. Although these authors showed the molybdate ion to exceed the tungstate ion in effectiveness at 25° in the absence of added ions, the present work demonstrated that the molybdate is more susceptible to electrolytes than is the tungstate, and that its effectiveness diminishes more rapidly with rise of temperature. In other experiments,[11] it was found that $10^{-2} f$ sodium tungstate maintained the inhibition of a specimen of S.A.E. 1010 carbon steel at temperatures alternating between 24 and 96° with exposure to air over a period of four months. The radically different resistance of the tungstate ion toward the sulfate ion in comparison with the other inhibitors is probably sufficient to indicate that its action is unique among the four inhibitors and may depend in part upon formation of an insoluble anodic product without reduction of the ion.

The high sensitivity of the other three inhibitors to ions, the decreasing order of sensitivity to sulfate, chloride and perrhenate ions, and the prompt reversals of potential observed upon removing the added ion are all in harmony with the hypothesis of competitive adsorption discussed in the earlier paper.[3]

The Specific Effect of Chloride and Thiocyanate Ions.—In Fig. 1 it may be noted that each addition of chloride ions, up to the point of instability, produced a definite ennobling of the potential. This was observed with all four inhibitors, although the effect was small with the chromate ion. Only small increments could be observed also with chloride additions to the molybdate inhibitor, owing to the fact that the potential debased with quite low concentrations of added ions. Exactly similar ennobling to even a greater extent was observed with the thiocyanate additions to pertechnetate and molybdate inhibitors. In no case was such a conspicuous result observed with additions of sulfate or perrhenate ions (see Fig. 2). The observation clearly demonstrates that the chloride and thiocyanate ions affect the electrode potentials by two mechanisms, one of which is lacking with the sulfate and perrhenate ions. Table XI shows the ennobling observed for the different inhibitors. The $\Sigma(\Delta E)$'s are the sums of the increments in potential after additions up to the indicated concentration. In similar experiments with stainless steel electrodes, ennobling was observed upon addition of both chloride and thiocyanate ions, but not with sulfate ions. The result was shown to be independent of added inhibitor by repeating the experiment with type 347 stainless steel in aerated $5 \times 10^{-4} f$ K_2SO_4 to which thiocyanate ions were progressively added. The ennobling was observed just as before.[16]

The unique action of the chloride and thiocyanate ions here demonstrated is doubtless to be associated with electrochemical effects that have been reported by other investigators. Thus, Gerischer[17] has shown that, in the electrode reaction (Pt) $Fe^{++} \rightleftarrows Fe^{+++}$, the exchange current increases upon addition of chloride ions, the relative increase being related to the concentration ac-

(15) K. F. Bonhoeffer, *Z. Elektrochem.*, **55**, 151 (1951).

(16) NOTE ADDED IN PROOF.—Subsequent measurement of this ennobling effect has shown that the results may be expressed by an equation of the Freundlich type; that is, $\Sigma(\Delta E) = k\alpha_i{}^{\rho}$, in which α_i is the activity of the chloride or thiocyanate ion that produces the total ennobling $\Sigma(\Delta E)$.

(17) H. Gerischer, *Z. Elektrochem.*, **54**, 366 (1950).

TABLE XI

TRANSIENT ENNOBLING BY CHLORIDE OR THIOCYANATE IONS

Inhibitor	Total increments $\Sigma(\Delta E)$, mv.	Concn., f
TcO_4^-, $1 \times 10^{-3} f$	12[a]	$2.4 \times 10^{-3} f$ Cl^-
	35[a,d]	$4.2 \times 10^{-3} f$ SCN^-
	68[b]	$2.2 \times 10^{-3} f$ SCN^-
TcO_4^-, $4.7 \times 10^{-4} f$	23, 28	$1.2 \times 10^{-3} f$ Cl^-
	25, 15	$1.6 \times 10^{-3} f$ Cl^-
$MoO_4^=$, $10^{-3} f$	3, 6	$3.1 \times 10^{-4} f$ Cl^-
	4, 10	$8.0 \times 10^{-4} f$ Cl^-
	44	$3.1 \times 10^{-4} f$ SCN^-
	76	$9.4 \times 10^{-4} f$ SCN^-
$MoO_4^=$, $10^{-4} f$	15[c]	$6.2 \times 10^{-4} f$ Cl^-
$WO_4^=$, $10^{-2} f$	22[a]	$1.0 \times 10^{-2} f$ Cl^-
	53, 50, 60	$2.0 \times 10^{-2} f$ Cl^-
$WO_4^=$, $10^{-3} f$	20, 11, 19	$2.5 \times 10^{-3} f$ Cl^-
	29	$5.0 \times 10^{-3} f$ Cl^-
$CrO_4^=$, $10^{-3} f$	4, 6	$2.5 \times 10^{-3} f$ Cl^-

[a] Electrode pre-stabilized overnight. [b] Electrode not entirely stabilized. [c] Subsequently debased. [d] Potential fell at one point but recovered.

cording to an adsorption isotherm. This effect was attributed to a decrease in the activation energy for the transfer of electrons between the ions as a result of adsorption of chloride ions. In the case of iron passivated by nitric acid, Vetter[18] showed that the corrosion-equivalent current increases approximately linearly upon addition of chloride ions in concentrations of 1 to $5 \times 10^{-3} f$. It was also shown by Heyrovsky[19] that a number of cathodic reductions at the mercury electrode that are "oscillographically irreversible" in solutions of sulfates, perchlorates, nitrates or hydroxides become reversible in chloride solutions. The chloride ion was assumed to provide a favorable bridge for transfer of electrons by virtue of its polarizability.

It was suggested[8] previously that, according to the hypothesis of electrostatic polarization by inhibitors, adsorption of chloride ions should lead to activation of electrons at the interface so that cathodic processes would be stimulated. This effect will be considered in more detail in a subsequent paper, but it may be pointed out that the ennobling observed is in complete accordance with the hypothesis. Since both the chloride and thiocyanate ions accelerate corrosion, the ennobling cannot arise from an increase in anodic polarization. Without needing to known specifically which of several possible interfacial processes determines the observed potential, it may be seen that preferential stimulation of any cathodic process would be associated with a rise of potential.

That the observed ennobling is associated with readily reversible effects was shown by the rapid loss of excess nobility when the electrolyte was removed and replaced by solution containing no chloride or thiocyanate. Thus, both the inhibitor ions and the chloride or thiocyanate ions are involved in labile adsorption processes by which the corrosion rate and potential are altered. The results indicate that all four of the inhibitors investigated act at least in large part by an adsorption mechanism, under conditions of aeration. The possibility of blocking of anodes by precipitation of insoluble salts may be significant with the tungstate and molybdate inhibitors in absence of air.

(18) K. J. Vetter, *Z. Elektrochem.*, **55**, 274 (1951).
(19) J. Heyrovsky, *Far. Soc. Disc.*, **1**, 212 (1947).

ISOTOPIC EXCHANGE BETWEEN DEUTERIUM AND HYDROCARBONS ON NICKEL–SILICA CATALYSTS

BY ROBERT L. BURWELL, JR., AND RICHARD H. TUXWORTH

Contribution from the Department of Chemistry, Northwestern University, Evanston, Illinois

Received January 20, 1956

The effect of temperature, of the ratio of deuterium to hydrocarbon, and of nickel crystallite size upon the isotopic exchange reaction between hydrocarbon and deuterium is reported for nickel–silica catalysts which have been characterized by the magnetic method of Selwood. Cyclohexane and, to a lesser extent, heptane, cyclopentane and (+)3-methylhexane have been employed as test hydrocarbons. Increasing multiple exchange of the hydrocarbon results from increased temperature, decreased ratio of deuterium to hydrocarbon, and increased crystallite size. In large measure, the increased multiple exchange probably results from increased availability of the free surface sites which are required for the propagation reaction leading to multiple exchange. At 60–150°, the concentrations of the exchanged species of cyclohexane exhibit a discontinuity between $C_6H_6D_6$ and $C_6H_5D_7$. At higher temperatures no such discontinuity is apparent. The propagation reaction does not pass readily from one set of six hydrogen atoms to the other at lower temperatures. Cyclopentane behaves similarly. In the hydrogenation of 1-hexene with deuterium at about 100°, decrease in partial pressure of olefin results in increasing multiple introduction of deuterium, presumably owing to the increased availability of free sites with the decreased partial pressure of the strongly adsorbed olefin.

In a study of the mechanism of interaction of hydrogen and hydrocarbons, we investigated the isotopic exchange between alkanes and deuterium on a nickel–kieselguhr catalyst,[1] on reduced nickel oxide[2] and on evaporated nickel films.[2] The latter two catalysts exhibited rather similar behavior in the temperature range investigated, 160–200°. The nickel–kieselguhr catalyst, which was studied at temperatures in the vicinity of 100°, diverged in certain details from this behavior. It appeared desirable to determine whether the origin of these differences lay in differences in temperature or in differences in catalytic characteristics or in both.

We have also investigated the effect of variation

(1) R. L. Burwell, Jr., and W. S. Briggs, *J. Am. Chem. Soc.*, **74**, 5096 (1952).
(2) H. C. Rowlinson, R. L. Burwell, Jr., and R. H. Tuxworth, THIS JOURNAL, **59**, 225 (1955).

in the ratio of the partial pressures of deuterium and hydrocarbon since, in our previous work, this ratio had always been about 2.

Selwood, Phillips and Adler[3] have recently developed a magnetic method for the determination of particle size distributions of the crystallites in nickel catalysts. We have used the opportunity provided by this work to determine how variation in particle size of the nickel in nickel catalysts affects the exchange reaction. Variation in isotopic distribution patterns of a variety of hydrocarbons is likely to be of greater utility in studying variations among catalysts than mere determination of the relative rates of some particular reaction.

Experimental Procedure

Analytical procedures and hydrocarbon preparation have been described.[2] We are indebted to S. F. Adler for the nickel–silica catalysts which were prepared by mixing solutions of sodium silicate and high purity nickel nitrate.[4,5] The resulting gel was dried at 105°, powdered, pelletted and crushed. Material of 20–40 mesh was used. The material contained about 42% nickel.

Reduction regimens were chosen to yield catalysts of known characteristics.[5] Reduction was in hydrogen for 48 hours at 350° save where otherwise stated. When indicated, the catalyst was then sintered in helium for one hour at 600°. Catalytic activity would sometimes decline with use. It was usually possible to restore original behavior by retreating the catalyst with hydrogen at 350°.

The feed unit of the apparatus, shown in Fig. 1, permits the immediate establishment of any desired feed rates of deuterium and hydrocarbon, it insures the feeding of an oxygen-free hydrocarbon and it permits changing the type of hydrocarbon being fed without the danger of oxygen introduction.

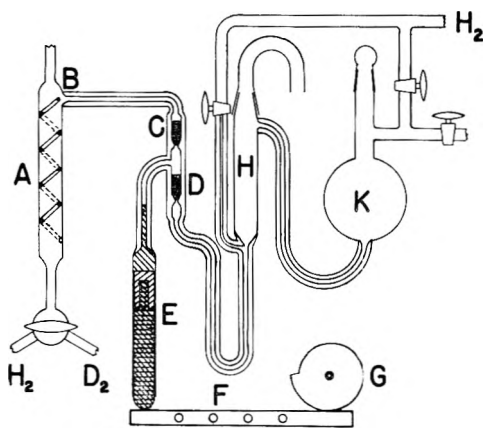

Fig. 1.—Schematic diagram of the feed apparatus.

The liquid hydrocarbon feed rate is determined by the stroke and by the reciprocation frequency of the piston at E which operates in a cylinder of 1/4 inch precision bore tubing. The lower portion of the piston is of stainless steel and of a diameter slightly smaller than that of the cylinder. This portion is surmounted by a portion of reduced diameter over which was forced a piece of Kel-F (polytrifluorochloroethylene) which was then machined to a close fit to the cylinder. Enough mercury was placed above the piston to extend into the 1 mm. capillary joined to the top of the precision bore tubing. The piston moved readily in the cylinder yet would hold pressures in excess of 1/4 atmosphere without mercury being forced into the annular space between piston and cylinder. The stroke of the piston is determined by the hole in the lever arm F into which the pivot bearing bolt is inserted. The lever arm is actuated by the cam G (an Archimedean spiral) rotated by a 3 r.p.m. motor through a Metron variable ratio speed changer (4 to 1 to 1 to 4).

Valves C and D were made by constricting a section of 3 mm. capillary to somewhat less than 1 mm. A section of drill rod machined at one end into a 60° cone was ground into the constricted portion with the use of aqueous suspensions of abrasives. This operation was repeated with three new sections of drill rod and the grinding was terminated with the use of polishing alumina. The drill rod was then cut off about 6 mm. above the ground cone.

The rate of liquid feed is measured by volume decrement in the buret H which is made of precision bore tubing of a cross-sectional area of 0.3195 sq. cm.

Hydrocarbon in the storage bulb K and that in H are deaerated by a stream of hydrogen introduced at the upper right.

In operation, as the piston E moves up, mercury rises in the capillary tube over the cylinder. Displaced hydrocarbon flows out through valve C and enters the evaporator tube A at B. The evaporator tube, of 10 mm. inside diameter, encloses a closely fitting Nichrome helix, one section of which touches the entrance at B. The hydrocarbon flows down along the interface between helix and tubing. The evaporator tube is warmed by a winding of Nichrome ribbon. Deuterium gas is fed to the bottom of the evaporator tube through a flow meter. The current in the Nichrome ribbon is adjusted so that the hydrocarbon thread penetrates about five turns of the helix. Very smooth evaporation results.

When the cam G comes to the step, the lever arm F falls back abruptly about 4 mm. closing valve C, opening D and sucking in a unit of hydrocarbon from H. Disturbance to the composition of the mixture of deuterium and hydrocarbon vapor issuing from the top of the evaporator is small. The hydrocarbon thread retreats slightly momentarily and then resumes it usual position. The vapor mixture leaving the evaporator is passed over the catalyst and then through a Dry Ice trap in which the hydrocarbon is recovered for analysis.

Results

The experimental conditions, the % of the hydrocarbon molecules which suffer isotopic exchange and the % of the total hydrogen in the hydrocarbon which undergoes isotopic exchange are shown in Table I. The original data for these and other runs are available in the doctoral thesis of R. H. Tuxworth, Northwestern University, 1955.

To avoid smearing the distribution pattern as a result of isotopic dilution of the deuterium we have worked at low total conversions. This results in low accuracy for the singly exchanged species since the correction for the species $C_5{}^{12}C^{13}H_{12}$ is large compared to the contribution of $C_5{}^{12}H_{11}D$.

The effect of temperature upon isotopic exchange between cyclohexane and deuterium is shown in Fig. 2. Arbitrary multiplying factors have been used to facilitate presentation. Cyclopentane also exhibits a discontinuity at half-deuteration at lower temperatures. For example, at 68° (run E), the concentrations of the exchanged species in per cent. are: D_1, 0.59; D_2, 0.97; D_3, 0.62; D_4, 0.37; D_5, 0.27; D_6, 0.09; D_7, 0.07; D_8, 0.04; D_9, 0.03 and D_{10}, 0.02. At 150° and at 200° on evaporated nickel film[2] and at 172° on a sintered and rather inactive nickel–silica catalyst, the isotopic distribution patterns of cyclopentane exhibit a minimum between D_4 and D_6 and a maximum at D_{10}. Multiple exchange also increases with temperature with heptane, but, with the one catalyst investigated, sintered nickel–silica, the effect is less marked than with cyclohexane.

(3) P. W. Selwood, T. R. Phillips and S. Adler, *J. Am. Chem. Soc.*, **76**, 2281 (1954).

(4) J. J. B. van Eijk van Voorthuijsen and P. Franzen, *Rec. trav. chim.*, **70**, 793 (1951), catalyst CLA-5421.

(5) P. W. Selwood, S. Adler and T. R. Phillips, *J. Am. Chem. Soc.*, **77**, 1462 (1955).

TABLE I

ISOTOPIC EXCHANGE RUNS

Run	Cat.,[a] cc.	Hydrocarbon[b]	Temp., °C.	$L_{HC} \times 10^2$, mole/hr.	$L_{D_2} \times 10^2$, mole/hr.	Exchange,[c] %	D_1[d] %
A	0.5A	cH	60	1.75	1.77	4.0	1.05
B	2.5B	cH	100	1.72	1.77	1.6	0.46
C	0.5B	cH	159	1.82	1.77	1.8	0.77
D	2.0B	cH	187	1.44	2.62	4.3	2.78
E	.2A	cP	68	2.10	4.66	3.0	0.83
F	.5B	S	145	2.59	1.31	2.7	1.32
G	.5B	S	145	0.69	4.66	2.7	1.19
H	.5B	cH	159	3.57	1.77	1.6	0.66
I	.5B	cH	159	0.89	4.66	1.8	0.47
J	2.0E	S	156	2.32	2.66	3.0	2.12
K	0.5B	cH	139	1.80	4.68	1.2	0.52
L	1.0B	cH	124	1.74	4.66	2.7	1.21
M	0.5A	cH	131	2.44	3.93	3.3	1.37
N	2.0F	S	96	2.08	2.80	5.8	2.56
O	2.0G	S	86	0.75	2.68	6.1	2.38
P	2.5B	S	99	0.71	4.64	2.7	0.99
Q	0.5D	S	96	1.06	1.74	4.0	0.89
R	2.0A	3MH	93	1.43	2.62	5.4	2.12
S	0.5C	3MH	141	2.75	4.35	11.8	5.01

[a] A is nickel–silica reduced at 350° for 48 hr. B is A sintered in helium for 1 hr. at 600°. C is like A but with reduction at 250°. D is like C but with reduction for 15 hr. E is nickel oxide reduced at 300° (ref. 2). F is Harshaw nickel–kieselguhr reduced at 325–350°. G is Universal Oil Products Co. nickel–kieselguhr reduced at 300°. Run O is from ref. 1. [b] cH is cyclohexane, cP is cyclopentane, S is heptane, 3MH is (+)3-methylhexane. [c] % of total hydrocarbon molecules which have suffered isotopic exchange. [d] % of total hydrogen atoms in hydrocarbon which have been replaced by D.

At 307° with inactive nickel catalyst prepared by impregnation, cyclohexane desorbed as deuterated benzenes. There was little if any deuterated cyclohexane. Such a result would have been thermodynamically impossible at the lower temperatures of the reactions on the other catalysts. At 277°, cyclopentane yielded deuterocyclopentanes characterized by a continuous increase in concentration from D_1 to D_{10}.

At about 150°, increase in p_{D_2}/p_{HC} (the ratio of the partial pressures of deuterium and hydrocarbon) at a total pressure of one atmosphere changes the shape of the exchange distribution pattern so as to favor a somewhat larger proportion of the very extensively exchanged species. At lower temperatures, the effect of change in p_{D_2}/p_{HC} is smaller.

Curves F ($p_{D_2}/p_{HC} = 0.5$) and G (6.8) in Fig. 3 exhibit this effect for heptane at 145°. An intermediate pattern results for $p_{D_2}/p_{HC} = 1.0$ (run C). At 99°, the exchange pattern of heptane is nearly independent of p_{D_2}/p_{HC}.

Curves H and I (0.5 and 5.2) exhibit the effect for cyclohexane at 159°. Curve B in Fig. 2 for cyclohexane was obtained at 100° with $p_{D_2}/p_{HC} = 1.0$. Proceeding from a ratio of 5.0 to 0.5, relative increases in D_{11} and D_{12} and relative losses in D_2 to D_4 resulted. A similar but smaller effect was observed at 60°; p_{D_2}/p_{HC} also affects $\%D_6/\%D_7$. At 100°, as p_{D_2}/p_{HC} exceeds 0.7, $\%D_6/\%D_7$ is progressively greater than unity and *vice versa* as the ratio falls below 0.7.

Figures 4 and 5 exhibit exchange distribution patterns on several catalysts which have been characterized magnetically[3] as to size of nickel crystallites. Reproducibility in rates with different samples of catalyst prepared by reduction at 250° or by sintering operations was only fair.

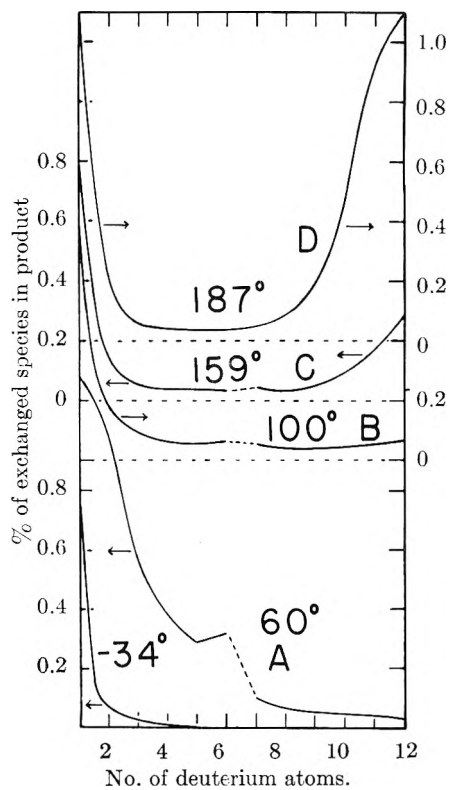

Fig. 2.—The effect of temperature on exchange of cyclohexane. The curve at −34° is on evaporated nickel film from ref. 6.

The sintered catalyst (catalyst B) gives rates of exchange of cyclohexane which are 0.14 to 0.4 those of the unsintered (catalyst A). Sintering reduces the activity for the exchange reaction much less than for the hydrogenation of benzene.[5] Catalyst reduced at 250° is 2 to 4 times more active than

TABLE II

HYDROGENATION OF 1-HEXENE WITH DEUTERIUM

Run	T[a]	U[a]	V[a]	W[b]
Hydrocarbon[c]	1-C_6H_{12}	1-C_6H_{12} + 5 cH	1-C_6H_{12} + 30 cH	n-C_6H_{14}
Temp., °C.	105	104	105	95
$L_{C_6H_{12}}$, moles/hr.[d]	0.0123	0.00234	0.00058	0.028
L_{D_2}, moles/hr.	0.0425	0.0422	0.0422	0.0431
% D in product[e]	22	28	33	2.8
% D in exit hydrogen[f]	78	94.3	98.2	87.3
% D_0	4.9	1.4	1.8	91.2
% D_1	15.2	6.1	2.8	1.42
% D_2	23.2	16.3	9.4	1.91
% D_3	22.0	21.3	15.7	1.16
% D_4	15.7	21.0	19.6	0.86
% D_5	9.3	16.8	21.4	.68
% D_6	4.9	8.0	12.1	.55
% D_7	2.3	4.5	8.7	.45
% D_8	1.2	2.2	3.8	.38
% D_9	0.6	1.1	2.5	.32
% D_{10}	.4	0.9	1.4	.29
% D_{11}	.2	.4	0.7	.25
% D_{12}	.1	...	...	.21
% D_{13}	...	...	...	.18
% D_{14}	...	...	...	.09

[a] Catalyst: 2 cc. of sintered nickel–silica. [b] Catalyst: 0.5 cc. unsintered nickel–silica. [c] 1-C_6H_{12} is 1-hexene, cH is cyclohexane. [d] Actual net flow rate of olefin or, in run W, of hexane. [e] % deuterium in product hexane. [f] Computed from flow rates and analysis of hydrocarbon product. In run T, the exit hydrogen was analyzed mass spectrographically, % D = 74.

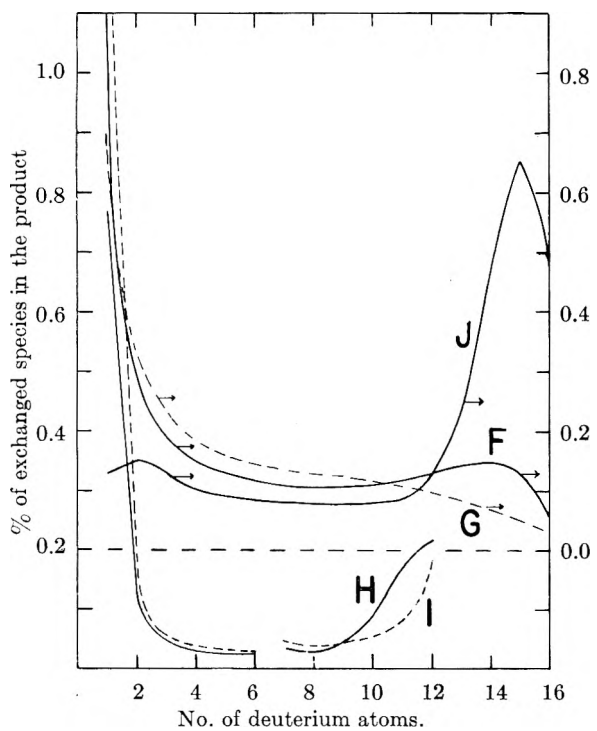

Fig. 3.—The effect of the ratio of the partial pressures of hydrocarbon and deuterium. The observed concentrations of F and I are multiplied by 1.07 and 1.28, respectively. In I, D_1 is 1.47. H and I are cyclohexane, F, G and J are heptane.

that reduced at 350° in contrast to nickel–kieselguhr in which reduction at the lower temperatures led to a much less active catalyst.[1]

For comparison with isotopic exchange patterns, we examined the product of the addition of deuterium to 1-hexene on a nickel–silica catalyst as shown in Table II. The deuterium–olefin ratio was increased by diluting the olefin with 5 and 30 parts of cyclohexane. Since the diluent is of lower molecular weight yet of higher boiling point than hexane, hexane could be concentrated for mass spectroscopy by distillative topping, yet residual cyclohexane would not interfere with the parent peak of hexane. As shown by the absence of any C–D band at 4.6 μ in the still pot residue from the distillation of run V, cyclohexane was negligibly exchanged although olefin was fully hydrogenated.

Isotopic exchange of (+)3-methylhexane on the nickel–silica catalyst gives results similar to those on catalysts studied previously. For comparison, the following data should be added to Table II of ref. 2. In run R at 93°, the ratio of exchange to racemization was 2.0 ± 0.4, the fraction $D_1 + D_2 + D_3$ was 0.36. In run S at 141°, on a catalyst reduced at 250°, the ratio was 2.1 ± 0.2 and the fraction, 0.33.

Discussion

Anderson and Kemball[6] have reported that isotopic exchange between cyclohexane and deuterium on films of evaporated palladium (18.5 and 44°) and evaporated rhodium (−48 and −28°) leads to exchanged cyclohexanes in which marked discontinuities separate the concentrations of $C_6H_6D_6$ and $C_6H_5D_7$. Similar discontinuities separate $C_5H_5D_5$ and $C_5H_4D_6$ when cyclopentane is used. At 160–200° no such discontinuities appear when evaporated nickel films or reduced nickel oxide are used as the catalyst.[2] Under these conditions, the perdeuterohydrocarbon is the most abundant species. On the other hand, at −34° on evaporated nickel films,[6] the decline in concentration with increasing deuterium content is so rapid that species beyond $C_6H_8D_4$ have negligible concentrations. Thus the possibility of a discontinuity could not be examined.

(6) J. R. Anderson and C. Kemball, *Proc. Roy. Soc.* (*London*), **226**, 472 (1954).

The effect of temperature upon the distribution patterns in the isotopic exchange of cyclohexane on nickel catalysts in the temperature zone between the two ranges previously reported is, therefore, of particular interest.

Actually, as shown in Fig. 2, two different effects of temperature are evident. Although one can observe no discontinuity between $C_6H_6D_6$ and $C_6H_5D_7$ at $-34°$ (from Anderson and Kemball[6]) a distinct discontinuity appears at 60° (run A). However, above 100°, the discontinuity largely disappears into the experimental error. Run D at 187° closely resembles those reported earlier[2] for reduced nickel oxide and evaporated nickel films at these temperatures. The other effect is that increased temperature results in a very marked increase in extensive multiple exchange. Comparison of the relative numbers of species D_7 to D_{12} in curves A to D shows this particularly clearly. The effect of temperature upon the exchange of cyclopentane resembles that of cyclohexane both in regard to discontinuity and to extensive multiple exchange.

The production of multiply exchanged species must involve steps equivalent to the following

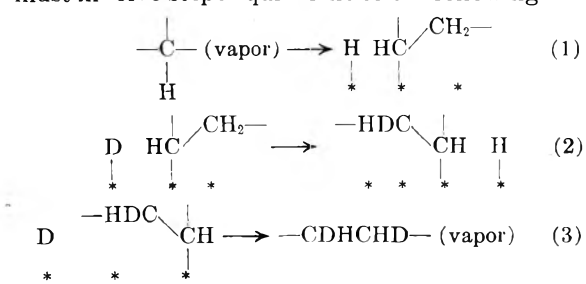

Step (2) can be multiply repeated. In this formulation the exact details of the processes and the method of binding to the surface are left open. Rapidly established equilibrium is assumed to exist between gaseous and adsorbed hydrogen (H + D). The average % deuterium in the desorbed hydrocarbon is determined by the relative probabilities of the propagation step (2) and the desorption step (3). From the increasing predominance with increasing temperature of multiply exchanged species, the propagation step is increasingly favored and must possess a higher net activation energy than the desorption step.

In cyclohexane, the hydrogen atoms exist in two sets of six atoms each. As shown in curve A, step (2) cannot easily lead from one set to the other at lower temperatures. With increasing temperature, the probability of passing from one set to the other increases markedly.

The Effect of Pressure.—As exhibited in Fig. 3 and elaborated in the Experimental section, the ratio of the partial pressures of deuterium and hydrocarbon at a total pressure of one atmosphere affects the shape of the exchange distribution pattern, but to no large degree. An increased ratio leads to relative decreases in the most extensively exchanged species. The effect of the ratio is more pronounced at 150° than at 60 to 100°. The change in over-all rate is large and is consistent with the kinetics which obtain in the racemization of (+)3-methylhexane[1]

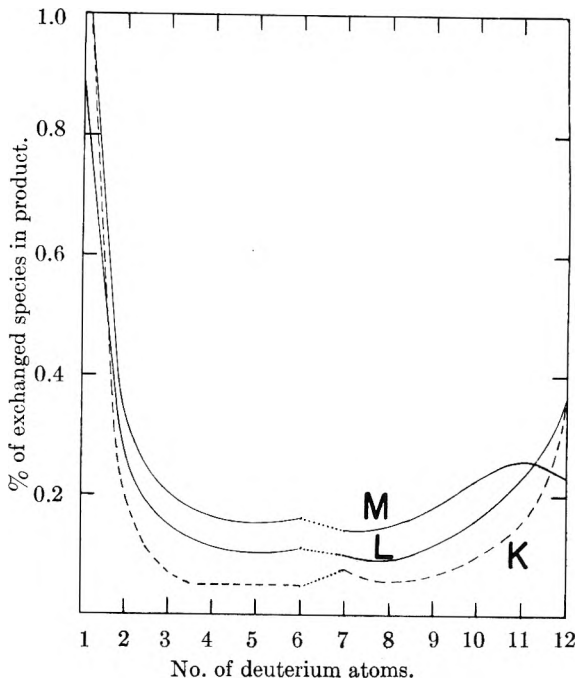

Fig. 4.—The effect of sintering on the exchange patterns of cyclohexane as determined at about 130°. The observed concentrations in K are multiplied by 2.00. In K and M, D_1 is 1.20 and 1.11.

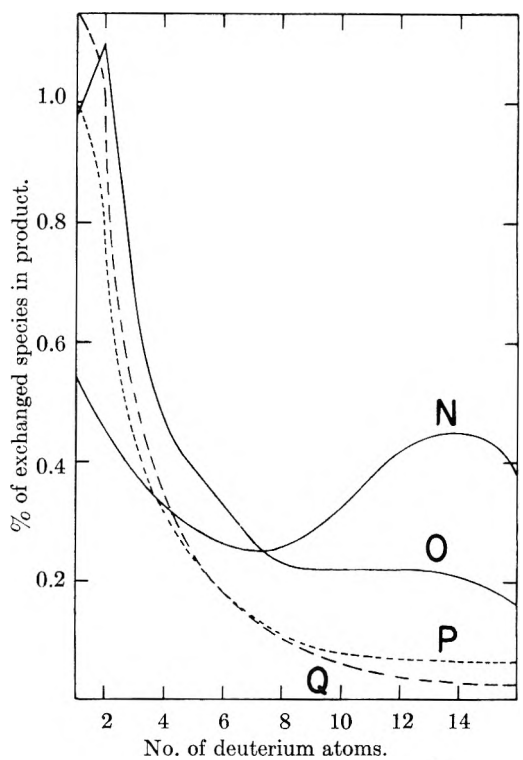

Fig. 5.—Exchange of heptane on various catalysts. The observed concentrations in P are multiplied by 1.41.

$$L \ln (\alpha_0/\alpha) \propto p_{H_2}^{-0.6} p_{HC}^{0.33}$$

where L is the liquid flow rate. One replaces the term at the left by $L \ln(1/Z)$ where Z is the fraction of molecules without deuterium substitution. A relation of similar form was found in the first study of alkane exchange and, in particular, for the ex-

change of propane on a nickel-kieselguhr catalyst.[7]

Effect of Crystallite Size.—Before reduction, the coprecipitated nickel–silica catalyst forms a layer lattice with sheets of a silicon–oxygen network separated by nickel ions.[4] Nickel–kieselguhr catalysts are prepared by adding a solution of sodium carbonate to a slurry of kieselguhr in a solution of nickel salt. Chemical reaction of the kieselguhr occurs and a material rather similar to coprecipitated nickel–silica results.[8]

During reduction of any of these materials, nickel atoms agglomerate into small cubic close-packed crystallites.[4,5] The adsorption of hydrogen on catalysts of both types is similar.[9] The silica skeleton of the reduced catalysts retards sintering.[9]

The particle size distributions of both types of catalysts have been characterized by Selwood and co-workers by magnetic means[5,10]: Catalyst A (Table I), nickel–silica reduced at 350°, consists mainly of very small crystallites. The average diameter is probably less than 10 Å. although there are some with diameters as large as 50 Å. Catalyst B, like A but then sintered at 600°, shows a large loss of the very small crystallites and a marked gain in crystallites of 50+ Å. Catalysts C and D, nickel–silica reduced at 250° for 48 and 15 hr., respectively, exhibit an increasing preponderance of very small crystallites. Reduction is probably incomplete. Catalyst E, nickel oxide reduced at 300°, is magnetically massive nickel.[2,5] The magnetically very similar catalysts F and G are nickel–kieselguhr, Harshaw (68% Ni) and Universal Oil Products (53%). Upon reduction at 350°, a much larger fraction of the nickel crystallites are relatively large than is the case with nickel–silica.

As shown in Fig. 4, sintering (runs K and L) a nickel–silica catalyst reduced at 350° (run M) leads to increased multiple exchange. Reduction at 250° leads to less multiple exchange, and reduction for 15 hr. to less multiple exchange than reduction for 48 hr. It was previously observed[1] with Universal Oil Products Company nickel–kieselguhr catalyst that reduction at 250° as compared with 300° resulted in much less multiple exchange of 3-methylhexane. The difference was much more drastic than that observed with nickel–silica because the higher temperature reduction leads to much more extensive multiple exchange with nickel–kieselguhr than with nickel–silica (runs N and O *vs.* P) whereas the patterns obtained with reduction at 250° are relatively similar for both catalysts (run Q). Nickel oxide reduced at 300° gives much more multiple exchange than does sintered nickel–silica (run J *vs.* runs F and G in Fig. 3). Evaporated nickel film which is also massive magnetically[5] results in a curve of the type of J^2 at 130°. By and large, multiple exchange is favored by large crystallites. Thus, increase in crystallite size seems relatively to favor the propagation step, equation 2, over the desorption step, equation 3. Sintered nickel–silica gives less multiple exchange than might be expected from its particle size alone, but, in catalysts in which various crystal faces are exposed in unknown degree, one could hardly expect the isotopic exchange distribution patterns to correlate perfectly with but one variable.

Variation in these patterns is larger for heptane (see Fig. 5) than for cyclohexane as might be expected since compact molecules such as cyclohexane and 2,3-dimethylbutane exhibit more extensive multiple exchange than do extended molecules such as heptane and 3-methylhexane.[2]

At identical temperatures, palladium catalysts favor the formation of relatively more of the extensively exchanged species than do nickel catalysts.[11] At 183° a Fischer–Tropsch catalyst (cobalt, thoria, magnesia and kieselguhr) even more heavily favors extensively exchanged species; butane forms perdeuterobutane nearly exclusively.[12]

Mechanism.—One would expect the propagation step to require a free site adjacent to the site or sites by which a hydrocarbon molecule is bound to the surface. Reduction in crystallite size should reduce the number of neighboring free sites particularly with crystallites as small as 10 Å.; thus, the relative extent of the propagation reaction would be decreased.

The increased surface coverage by hydrogen which accompanies increase in its partial pressure would relatively depress multiple exchange both by augmenting the rate of the desorption reaction and by reducing the number of free sites. A substantial part of the increasing multiple exchange with increasing temperature may result from decreased coverage by hydrogen. However, this simple geometric explanation may be oversimplified. Adsorption of hydrogen on nickel increases the number of electrons in the d-band[5,13] and the changing electronic states of the nickel may affect the isotopic distribution patterns.

At lower temperatures, in view of the discontinuity between $C_5H_5D_5$ and $C_5H_4D_6$, the propagation reaction (step 2) with cyclopentane must proceed preferably to an adjacent *cis*-position. The process which proceeds to a *trans*-position and permits exchange of more than 5 deuterium atoms is very probably closely related to that which leads to racemization of (+)3-methylhexane. The species A which we earlier proposed as a possible one for racemization[1,2] may not be satisfactory for *trans*-migration in cyclopentane. (Here, R_2 = H.) Species B, proposed by Anderson and Kemball[6] for *trans*-migration cannot accommodate racemization. Species C seems to be the simplest of this general type which can accommodate both reactions.

What one needs for either reaction is a carbon atom in threefold coördination symmetrically located with respect to surface hydrogen atoms. A radical adsorbed perpendicularly to the surface or in other symmetrical ways[2] would also accommodate both reactions.

(7) K. Morikawa, N. R. Trenner and H. S. Taylor, *J. Am. Chem. Soc.*, **59**, 1103 (1937).

(8) J. J. de Lange and G. H. Visser, *De Ingenieur*, **58**, 0.25 (1946).

(9) G. C. A. Schuit and N. H. de Boer, *Rec. trav. chim.*, **70**, 1067 (1951).

(10) J. A. Sabatka and P. W. Selwood, *J. Am. Chem. Soc.*, **77**, 5799 (1955).

(11) R. L. Burwell, Jr., and B. Shim, unpublished results.

(12) S. O. Thompson, J. Turkevich and A. P. Irsa, *J. Am. Chem. Soc.*, **73**, 5213 (1951).

(13) L. E. Moore and P. W. Selwood, *ibid.*, **78**, 697 (1956).

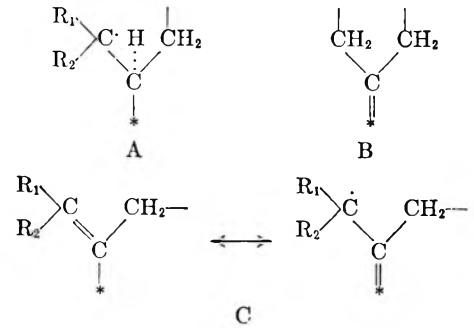

Addition of Deuterium to 1-Hexene.—We have assumed that isotopic exchange involves partial reversal of olefin hydrogenation.[1,2] Accordingly, one might expect that hydrogenation of the optically active olefin, C—C—C—C=C—C, would
C
result in racemization since identical intermediates would arise in the hydrogenation of the olefin and in exchange of (+)3-methylhexane. However, hydrogenation with nickel–kieselguhr at 70° and 120 atm. or at 45° and 1 atm. leads to (+)3-methylhexane which is hardly racemized at all.[1] It appeared desirable to determine the isotopic distribution pattern resulting from addition of deuterium to an olefin under conditions more closely approaching those of exchange between deuterium and alkanes. We chose 1-hexene for this purpose with the results shown in Table II.

With increasing deuterium–olefin ratio, the most abundant species moved from D_2 (run T) to D_3 (run U) to D_5 (run V), the amount of multiple exchange increased and the total deuterium content of the product hexane increased. In run T with undiluted olefin, correction for isotopic dilution of deuterium would shift the isotopic distribution pattern to higher deuterium content. Such correction would be small in runs U and V.

We suggest that the increase in deuterium content which results from decrease in the partial pressure of olefin is consequent to the strong adsorption of olefin. At high partial pressures of olefin, migration of the point of attachment is inhibited by the paucity of free sites. At low partial pressures, more free sites are available and more multiple exchange occurs. In run W with hexane, the virtual pressure of olefin resulting from hexane = hexene + hydrogen is about 10^{-10} atm. Here, multiple exchange is more abundant and would be even more abundant if correction to the conditions of run V was made for: (a) a 10° lower temperature, (b) replacement by sintered catalyst of the unsintered catalyst which was used to get adequate activity, (c) isotopic dilution of the deuterium.

Similarly, in the hydrogenation of (+)C—C—C—C=C—C, one would expect the propaga-
C
tion reaction to be depressed and therefore racemization to be reduced. The propagation reaction would also be relatively reduced by reduction in temperatures from those of exchange of alkanes to those employed in hydrogenation.

Results generally similar to run T with undiluted hexene were reported[14] for hydrogenation of *cis*-2-butene on a nickel–kieselguhr catalyst.

Acknowledgment.—This research was supported in part by the Office of Naval Research. One of us (R. H. Tuxworth) was the Visking Company Fellow, 1953–54. We are indebted to Professor P. W. Selwood and Dr. S. Adler for their kind coöperation in the supply of catalysts and of information on their characterization.

(14) C. D. Wagner, J. N. Wilson, J. W. Otvos and D. P. Stevenson, *J. Chem. Phys.*, **20**, 338 (1952).

MEASUREMENT OF THE AMOUNT OF BOUND WATER BY ULTRASONIC INTERFEROMETER.
II. POLYVINYL ALCOHOL AND ITS PARTIALLY SUBSTITUTED ACETATES

BY HAZIME SHIIO AND HIROSHI YOSHIHASHI

Chemical Institute, Faculty of Science, Nagoya University, Nagoya, Japan

Received February 7, 1956

Ultrasonic velocities in ethanol–water solutions of polyvinyl alcohol and its partially substituted acetates have been measured by an ultrasonic interferometer and, thence, the amount of bound water and compressibility of the solute molecule determined, with the following results: the amounts of bound water of polyvinyl acetates of 99.8, 96, 90.6 and 70.9% saponification degree are 0.45, 0.43, 0.48 and 0.29 cc./g., respectively. The compressibility of the solute molecule of many OH radicals is decreased by the increasing ethanol ratio, but with the solute of saponification degree 70.9%, the compressibility has a smaller value in water, and increases with the addition of ethanol to solvent. These results suggest that the materials of saponification value 99.8% or 96% are swollen to large extent in water owing to their OH radicals, but that the one of saponification 70.9% is in a compressed state in water, through the hydrophobic acetyl radical.

Introduction

A series of investigations concerning ultrasonic velocities through aqueous solution has been carried out in our laboratory[1,2] and elsewhere.[3–6] In the previous report[7] we deduced a general formula which enables us to evaluate the amount of bound water of non-electrolyte, and applied it to the solutions of saccharides.

(1) Y. Miyahara and H. Shiio, *J. Chem. Soc. Japan*, **72**, 876 (1951).
(2) Y. Miyahara and H. Shiio, *ibid.*, **73**, 1 (1952).
(3) T. Sasaki, T. Yasunaga and H. Fujiwara, *ibid.*, **73**, 181 (1952).
(4) A. Passynsky, *Acta Physicochim. U.R.S.S.* **22**, 263 (1947).
(5) B. Jacobson, *Arkiv För Kemi*, **2**, 117 (1950).
(6) F. T. Tucker, F. W. Lamb, G. A. Marsh and R. M. Haag, *J. Am. Chem. Soc.*, **72**, 310 (1950).
(7) H. Shiio, T. Ogawa, and H. Yoshihashi, *J. Am. Chem. Soc.*, **77** 4980 (1955).

The present study was undertaken to determine the amounts of bound water of polyvinyl alcohol and its partially substituted acetates, and to further investigate the compressibilities of these molecules in solutions.

Experimental

The ultrasonic velocities in solutions were measured by an ultrasonic interferometer. The frequency of ultrasonics used was 1090 kc. Materials were prepared by saponification of polyvinyl acetate, and dried in a vacuum desiccator for one week, and subsequently made into solution; their properties are shown in Table I. Mean polymerization degrees of the materials were measured by the viscosity method.

Results and Discussion

According to the previous report,[7] it follows that

$$K \equiv (\beta/\beta_0 - V_0)\,\beta_0/\beta\omega = (\beta_1/\beta\omega)\,(1/d_1) - (v_0\,\beta_0/\beta\omega - v_2\,\beta_2/\beta\omega)/c \qquad (1)$$

The notations used are as follows:

- β = adiabatic compressibility of soln. $1/\{d(\text{sonic velocity})^2\}$
- β_0 = adiabatic compressibility of solvent
- β_1 = adiabatic compressibility of solute molecule
- β_2 = adiabatic compressibility of bound water
- $\beta\omega$ = adiabatic compressibility of water
- v_0 = apparent specific vol. fraction of the bound water, the density being assumed normal
- v_2 = specific vol. fraction of bound water
- V_0 = apparent specific vol. fraction of total solvent used, *i.e.*, $V_0 = (d - c)/d_0$
- c = concentration of solute in grams per cc. of solution
- d_0 = density of solvent
- d_1 = density of solute in soln.
- d = density of soln.

TABLE I

Sample	Saponification, degree mole %	Mean polymerization, degree
I	99.8	1490
II	96.0	2000
III	90.6	1400
IV	70.9	1300

From measurements of concentration, density and sonic velocity of solution and solvent, we can calculate the values of β, β_0, $\beta\omega$ and V_0, and thus the K values. On the other hand, the first term of the right side of equation 1 is due to the compressibility of solute β_1, and the second due to the hydration effect. By addition of ethanol to the aqueous solution, the bound water should be dehydrated, and the second term becomes negligible. Therefore, we obtain the amount of bound water and compressibility of the solute molecule from measurements of K values in solutions of varying ethanol content. The results are shown in Table II and Fig. 1.

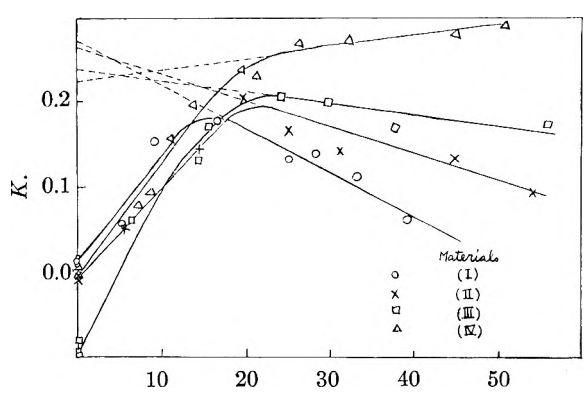

Ethanol concn. in solvents, %.

Fig. 1.—Ethanol concn.-K curves.

TABLE II

THE SAMPLE (I)

Ethanol, %	c, (g./cc.)	d_0	d	V_0	β/β_0	K
0	0.0352	0.9971	1.0054	0.9732	0.9736	0.012
0	.0329	.9971	1.0051	.9750	.9753	.009
0	.0383	.9971	1.0090	.9706	.9712	.016
5.4	.0303	.9906	0.9983	.9772	.9790	.056
9.1	.0316	.9852	.9936	.9756	.9808	.152
16.8	.0304	.9732	.9811	.9768	.9828	.178
25.1	.0276	.9633	.9723	.9804	.9838	.132
28.3	.0272	.9583	.9657	.9794	.9838	.142
33.3	.0306	.9497	.9584	.9770	.9811	.112
39.2	.0359	.9384	.9492	.9732	.9755	.061

In the figure the values of K are initially found to increase with ethanol concentration. However, after the concentration of ethanol in the solvent has passed 15% K value shows a different behavior in each case. In solutions of material I and II, the curve reaches the maximum point and then decreases linearly, but in the solution of III, the curve becomes almost horizontal, and with IV the curve displays a tendency to increase.

Consideration of these results with reference to equation 1 shows that the effect of hydration, *i.e.*, the second term of the right side, may be predominant in the initial increasing part. In the neighborhood of 15% ethanol concentration, the amounts of bound water might have been almost dehydrated, and so the second term would be very small, nearly zero.

Beyond 15% ethanol concentration each figure shows that the K values vary almost linearly with the weight percentage of ethanol in solution.

Then we might well assume, as in the previous report, that the above-mentioned effect of β_1 is linear with respect to the ethanol concentration from the beginning. We can calculate β_1 from the dotted portion of the figure, where the density of solute, d_1, is calculated by eq. 2.

$$(1 - V_0)/c = 1/d_1 \qquad (2)$$

The results are shown in Table III.

TABLE III

Ethanol, %	0	0	15	30
Sample	Amount of bound water, cc./g.	Adiabatic compressibility of solute ($\beta \times 10^{-12}$ barye^{-1})		
I	0.45	16.8	12.0	7.2
II	.43	15.6	12.6	9.6
III	.48	12.0	11.4	10.8
IV	.29	9.0	12.0	14.4

From Table III we derive the following results. The samples I and II which involve many OH radicals have large values of β_1 in aqueous solutions, but with increasing ethanol concentration β_1 assumes smaller values gradually. In the sample III, only a little change occurs in β_1 with the addition of ethanol. In the sample IV, however, β_1 becomes larger as ethanol is added.

Flory[8] concluded from light scattering measurements that the root-mean-square end-to-end di-

(8) A. R. Shultz and P. J. Flory, *J. Polymer Sci.*, **15**, 231 (1955).

mension of flexible linear polymers decreased in going from a good to a poor solvent. Thus our results might be explained as follows: for sample I and II water is a good solvent, owing to their many OH radicals, but with the addition of ethanol the solutions turn into poor solvents, and solute molecules are compressed gradually, and β_1 goes to smaller values. OH radicals being decreased, water mixed with ethanol behaves as fairly good solvent (as in sample III), and for sample IV, ethanol is a good solvent as compared with water. For this reason β_1 increases with the increase of ethanol concentration.

By substituting the value for K and β_1 in aqueous solution in equation 1, assigning 45×10^{-12}, 18×10^{-12} barye^{-1} to $\beta\omega$, β_2 respectively, and putting $v_0 = v_2$, the amounts of bound water in pure aqueous solutions are calculated. These values are shown in Table III. The amount of bound water of sample III is larger than that of I and II in spite of the fewer OH radicals. This result is in line with the fact that the material of about 90% saponification degree has remarkable swelling property, and has been made use of as commercial paste.

The effect of ethanol solvation must be next considered, particularly with respect to sample IV. The compressibility of the bound water of an ion, in general, may be assigned a zero value, by reason of its powerful electrostriction. For the bound water of a non-electrolyte, mainly attracted through a hydrogen bond, we may take the value of ice (18×10^{-12}). By such assignment, we have obtained, as reported in the previous paper, reasonable values of the amounts of bound water for saccharides. The solvation layer of ethanol molecules would be made up by weaker hydrogen bonds, or London–van der Waals forces. Then the force attraction between the ethanol molecule and the solute molecule might be considered not so different from that between solvent ethanol molecules themselves. If the ethanol molecules in the solvation layer are as much compressed as the water in the bound state, the K curve beyond about 15% of ethanol should have a considerable downward tendency with increasing acetyl radicals. This is, however, contrary to the experimental results. In sample IV, which concerns the material containing the large number of hydrophobic acetyl groups among our samples, K curve exhibits no tendency to decrease, notwithstanding the addition of ethanol to the solution; thus, compressibility of solvation layer of ethanol is not so changed from the normal ethanol value. The effect of ethanol solvation on the K value seems to be smaller in comparison to the change of the amount of bound water or the compressibility of solute molecule. However, the question of whether or not the effect of ethanol solvation can be negligible will be answered only by further research.

The authors wish to express their heartfelt thanks to Prof. Isamu Sano and Assist. Prof. Yutaka Miyahara, Nagoya University, for their kind advice and encouragements.

FILM DRAINAGE TRANSITION TEMPERATURES—SALT EFFECT

BY M. B. EPSTEIN, A. WILSON, J. GERSHMAN AND J. ROSS

Colgate Palmolive Co., Jersey City, N. J.

Received February 7, 1956

For the system sodium lauryl sulfate, lauryl alcohol and water data on the film drainage transition temperatures are extended to include the effects of sodium chloride, a typical strong electrolyte. Over the micellar region, the temperatures are related quantitatively to the micelle composition. The relation is treated as a temperature–solubility function between two assumed quasi-phases, the micelles and the surface. Heats of transition are calculated conventionally.

An earlier paper reported the film drainage transition temperatures and the phase relations for the system sodium lauryl sulfate, lauryl alcohol and water.[1] As an extension of this work the influence of sodium chloride upon the system has been studied. The results serve in part as a means of examining certain of the considerations previously offered on the relation between film drainage transition temperatures and the composition of the solution.

Experimental

For a description of the materials, the observation of film drainage transition temperatures, and the method of analysis of adducts, see the previous paper.

Results and Discussion

Film Drainage Transition Temperatures.—These temperatures for solutions 0.02 and 0.10 N in sodium chloride (Tables I and II) may be plotted against concentration of lauryl alcohol at a series of fixed concentrations of sodium lauryl sulfate. The resulting figures are similar to that given for the absence of salt (Fig. 1, ref. 1), the transition temperature rising with increasing concentration of lauryl alcohol and falling with increasing concentration of sodium lauryl sulfate.

When the curves with added salt are compared to those obtained without added salt, it is found that the transition temperatures fall with increasing salt concentration. This effect has been found also with sodium sulfate.

From these data isotherms may be constructed at selected temperatures, and in Fig. 1 isotherms are given for 25°, the curve for no salt being taken from the previous paper. As before a sharp break occurs near the critical micelle concentration (CMC). The estimated values for the CMC com-

(1) M. B. Epstein, A. Wilson, C. W. Jakob, L. E. Conroy and J. Ross, THIS JOURNAL, **58**, 860 (1954).

TABLE I

FILM DRAINAGE TRANSITION TEMPERATURES IN 0.02 *N* SODIUM CHLORIDE

Sodium lauryl sulfate, g./100 g. soln.	Lauryl alcohol, g./100 g. soln. × 10²	Transition temp. of film, °C.
0.800	7.36	27.1
	3.64	21.5
	1.86	16.6
	0.932	11.0
0.398	7.60	31.2
	4.94	30.4
	3.39	27.9
	1.98	24.3
	1.64	22.4
	1.60	22.5
0.399	0.60	13.9
0.251	7.88	31.3
	5.14	31.3
	3.49	31.1
	1.75	28.8
	0.864	23.6
	0.434	18.2
0.170	5.00	32.0
	3.48	32.0
	2.05	31.6
	1.04	30.2
	0.48	25.8
	0.24	20.2
0.100	8.28	37.9
	6.43	36.6
	4.14	35.7
	3.63	35.7
	2.01	33.8
	1.85	33.9
	0.904	32.1
	.462	31.8
	.213	30.8
	.085	27.5
	.080	28.9
	.063	26.4
	.046	25.8
	.04	23.5
	.02	21.2
0.050	1.009	37.6
	0.053	34.6
	.033	34.6
	.022	29.2
	.014	27.1
	.0055	21.6

TABLE II

FILM DRAINAGE TRANSITION TEMPERATURES IN 0.10 *N* SODIUM CHLORIDE

Sodium lauryl sulfate, g./100 g. soln.	Lauryl alcohol, g./100 g. soln. × 10²	Transition temp. of film, °C.
0.801	20.31	28.7
0.800	10.06	26.2
	8.02	24.8
	3.99	19.0
	2.76	16.4
	0.848	4–7
0.398	7.33	28.5
	5.19	28.1
0.397	3.30	24.7
	3.22	24.4
	2.99	23.8
	1.85	21.1
0.251	8.26	28.6
0.250	6.01	28.9
	3.71	27.6
	1.98	25.2
	1.019	20.6
	0.391	15.5
0.170	5.02	30.2
	3.58	29.8
	2.00	28.3
	0.996	24.2
	.482	19.5
0.0499	0.566	29.7
	.180	27.7
	.136	26.4
	.092	24.8
	.069	22.6
	.046	19.6
	.023	17.2

TABLE III

CRITICAL MICELLE CONCENTRATIONS

NaCl, mole/l.	CMC, NaLS (Fig. 1), g./100 g. soln.	CMC, NaLS (ref. 2) g./100 cc. soln.
nil	0.226	0.234
0.02	.112	.1125
0.10	.0390	.0422

pare rather well with the values obtained by several methods[2] as shown in Table III.

For concentrations above the CMC, an attempt was made to relate the film drainage transition temperatures to the micelle composition.[1] A quantity, Z, was defined as the mole fraction of alcohol computed from the moles of alcohol in the system and from the moles of alcohol sulfate diminished by the CMC. This quantity is an approximation, on a mole fraction basis, of the relative amounts of alcohol and alcohol sulfate in the micelles, being uncorrected for non-micellar alcohol and variation of non-micellar alcohol sulfate. With this approach, it was found from an empirical plot of the transition temperatures against the logarithm of Z that above the CMC the film drainage transition temperature of the system is fixed by the composition of the micelles and quite closely is independent of their number.

Corresponding plots may be constructed for the data obtained with added sodium chloride. In Fig. 2, for each experimental point in the micellar regions, the transition temperatures are plotted against log Z. The values of the CMC used in the calculations are those selected from the 25° isotherm and given in Table III. The calculated points scatter about two lines which are for 0.02 and 0.10 N sodium chloride. The curve for no added salt, taken from the previous paper, is also presented. At each sodium chloride concentration solutions which have the same calculated micelle compositions have similar transition temperatures. Quite definitely, however, these temperatures are lowered with increasing salt concentration at constant mi-

(2) R. J. Williams, J. N. Phillips and K. J. Mysels, *Trans. Faraday Soc.*, **51**, 728 (1955).

celle composition (fixed Z). This effect is in addition to the marked lowering of the CMC brought about by the sodium chloride and the accompanying effect upon the transition temperatures.

The temperature of the upper, level section of the curves in Fig. 2 decreases with increase of salt concentration.

Heats of Transition.—It is interesting to consider the possible meaning of the slopes appearing on Fig. 2. These curves relate a transition temperature to composition for a system in equilibrium, suggesting a thermodynamic interpretation. We treat the system arbitrarily as consisting, below the transition temperature, of three quasi-phases in equilibrium, namely, a surface layer of a condensed type, the aqueous medium, and the micelles. Above the transition temperature the surface layer undoubtedly is of the expanded or gaseous type, and to treat it as a quasi-phase probably is unjustified. The heats of transition between the quasi-surface phase and the micelles would be given by the relation

$$\frac{d \ln Z}{dt} = \frac{\Delta H}{RT^2}$$

The calculated heats are as follows: no added NaCl, 17.2 kcal./mole; 0.02 N NaCl, 20.2 kcal./mole; 0.10 N NaCl, 24.2 kcal./mole.

It is appreciated that it would be desirable to calculate the heat corresponding to the change in entropy that must accompany the disruption of the ordered structure that confers such high viscosity upon the surface below the transition temperature. This calculation cannot be made with the present data.

The history and the validity of considering solutions of colloidal electrolytes as a system of quasi-phases has been discussed critically by McBain and Hutchinson.[3]

Adducts.—A limited examination of the phases which may be observed with sodium chloride present in the system was carried out but is not reported here. Of some interest however are the adducts which were obtained and are set forth in Table IV. The adducts reported in the previous paper were prepared by cooling after removal of a first crop by filtration. The materials described in Table IV were prepared without such a rejection.

TABLE IV

COMPOSITION OF ADDUCTS

NaCl, moles/l.	Initial solution NaLS, g./100 g. soln.	Alcohol, g./100 g. soln.	Alcohol in adduct % by wt.
nil	0.40	0.032	25.80
	.80	.070	36.07
	.80	.126	23.84
	.80	.151	24.47
	.81	.191	38.71
0.02	.80	0.057	23.15
	.80	.087	23.65[a]
	.81	.206	35.95[a]
	.81	.418	38.64
	.80	.539	38.95

[a] Examined for chloride.

(3) M. E. L. McBain and E. Hutchinson, "Solubilization," Academic Press Inc., New York, N. Y., 1955, pp. 139, *et. seq.*

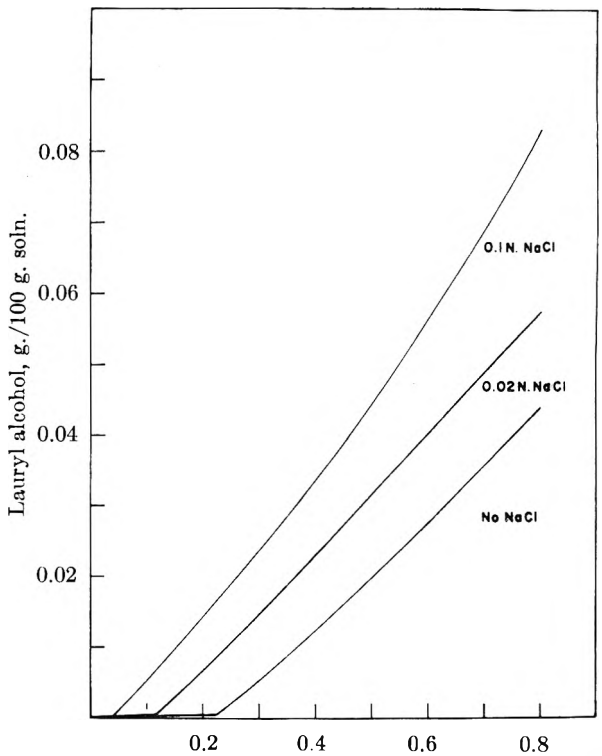

Fig. 1.—25° Isotherms of film drainage transition temperatures.

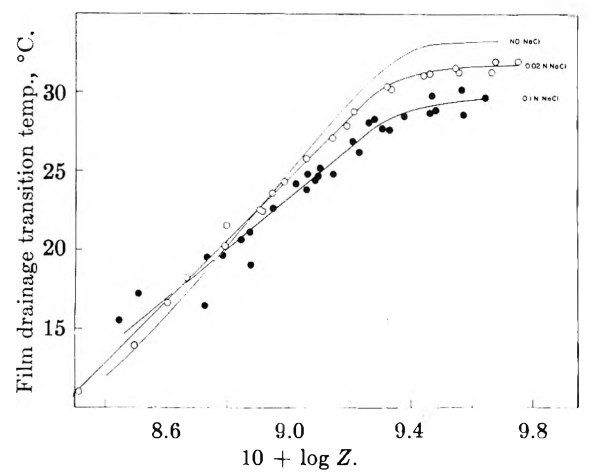

Fig. 2.—Film drainage transition temperatures *vs.* log Z.[4]

The analytical values for the latter materials approached two compositions, a mole ratio of sodium lauryl sulfate to lauryl alcohol of 1:1 (39.3% alcohol) and a mole ratio of 2:1 (24.5% alcohol).

Evidence of a continuum of adduct compositions was not obtained. Examination of the starred adducts (Table IV) showed at most only traces of chloride.

The finding that the film drainage transition temperatures are similar, excepting the salt effect, for solutions of the same calculated micelle composition may be expressed in somewhat different language, namely, that the micelles act as reservoirs of material which buffer the transition temperatures. We suggest that over the micellar region (but not at

(4) In Fig. 3 of ref. 1, the numbers giving the scale of log Z should be moved 0.2 unit to the right, for correction.

lower concentrations) constant transition temperatures mean essentially constant adsorption of alcohol sulfate and alcohol corresponding to an essentially constant composition of the non-micellar or aqueous medium. This constant surface composition is reached when the bulk solution has the composition given by the break of each corresponding isotherm in Fig. 1 and in Fig. 2 of the previous paper. The view taken differs from that of others, that for solutions of one surface active component the surface adsorption continues to rise at concentrations above the CMC, allegedly in contradiction to the Gibbs Adsorption Theorem.[5]

(5) J. K. Dixon, C. M. Judson and A. J. Salley in "Monomolecular Layers," H. Sobotka, Editor, Am. Assoc. for Advancement of Science, 1954, pp. 63, *et seq.*

In this connection, it should be recorded that although we have examined many systems, we have never found slow draining films for systems which contained only one surface active component. Apparent exceptions are those for which hydrolysis in the bulk occurs, such as salts of long chain carboxylic acids and of long chain amines. We conclude that surface hydrolysis[6] has not been observed in the absence of hydrolysis in the bulk, in particular not with pure sodium lauryl sulfate, which does not give slow draining films at a *p*H as low as 3. The same conclusion may be reached from the absence of minima in the surface tension curves for rigorously purified materials.

(6) M. A. Cook and E. L. Talbot, THIS JOURNAL, **56**, 412 (1952).

THE INFRARED SPECTRUM OF BIPHOSPHINE[1,2]

BY EUGENE R. NIXON

Department of Chemistry, University of Pennsylvania, Philadelphia, Pennsylvania

Received February 20, 1956

The infrared spectra of the gas at 28° and of the crystalline solid at −180° have been recorded for biphosphine and deuterated biphosphine. A preliminary powder X-ray study at −136° has also been made. The gas spectra are most readily interpreted in terms of a molecule of C_2 symmetry although do not prove it. The X-ray and infrared data are consistent with a monoclinic crystal of C^1_2 or C^1_s space group and two molecules per unit cell.

Introduction

Biphosphine has been known for many years. A few of its chemical and physical properties have been reported by Royen,[3] by Royen and Hill[4] and more recently by Dr. E. C. Evers and his students[5] but nothing concerning its structure has appeared in the literature. Because of the interest in the related hydrazine molecule and because biphosphine is one of the few simple molecules containing a P–P bond, a study of the infrared spectrum was undertaken.

Depending upon the orientation of one PH_2 group with respect to the other about the P–P bond, P_2H_4 has three possible structures: the *cis*-model (C_{2v} symmetry), the *gauche*-model (C_2) or the *trans*-model (C_{2h}). If the potential barriers to internal rotation were sufficiently small, the substance would consist of a mixture of two or more of these rotational isomers and for very low barriers, the essentially free rotation would reduce the effective symmetry to C_2.

Experimental

Biphosphine is a colorless compound with a m.p. of −99° and a b.p. (obtained by extrapolation of the vapor pressure curve) of about 52°. It is characterized by flammability and instability. Heat, light and contact with impurities of various sorts cause decomposition, in which the products are PH_3 and a yellow solid with an empirical formula of approximately P_2H.[3,5] After considerable experimentation it was found that liquid biphosphine can be stored for months with only negligible decomposition if it is kept in a high vacuum system of clean glass, if strong light is excluded and if the temperature of the liquid is maintained sufficiently low (say, Dry Ice temperature). Despite all precautions, however, the vapor at room temperature always undergoes slow decomposition.

Our samples of P_2H_4 were prepared by the action of water on calcium phosphide in an all glass vacuum system. The calcium phosphide, 200 to 400 g. of Fisher Scientific technical lump, was placed in an ice-cooled reaction vessel and the system evacuated. Water, about 25 ml. for each 100 g. of phosphide, was then admitted dropwise through a dropping funnel over a period of 20 to 30 minutes. Throughout the course of the reaction the pumping was continued. The reaction products, PH_3, P_2H_4, H_2 and unreacted H_2O, were passed through a series of cold traps (1–4). The H_2O condensed in trap (1) at −33°; relatively pure P_2H_4 collected in trap (2) at −78° and a mixture of P_2H_4 and PH_3 in trap (3) at −180°. The remainder of the PH_3 condensed in trap (4), also at −180°. The H_2, of course, was discharged through the pump. After the addition of the water, the reaction and fractionation were allowed to continue for 2.5 to 4 hours. At the end of this period the pumping was discontinued and both traps (3) and (4) were permitted to stand for a short time at −78° so that most of the PH_3 escaped through a mercury blow-off. Finally by means of liquid ammonia and liquid air baths the P_2H_4 in traps (2) and (3) was distilled through P_2O_5 into a final collection trap (5). The entire preparation required 10 to 12 hours. Yields of about 12 ml. of liquid P_2H_4 were recovered from 200 g. of calcium phosphide and 50 ml. of water, 25 ml. of which was collected as unreacted water.

Deuterated biphosphine was prepared in the same manner except for the substitution of 99.8% deuterium oxide, obtained from the Stuart Oxygen Co.

Only a moderate amount of decomposition occurred during these preparations. At the finish the walls of the system were coated with a thin film of the yellow solid hydride. The final product in trap (5) contained no trace of the yellow material. The biphosphine was next subjected to a fractional distillation by sealing trap (5) into another all glass system consisting of four cold traps (1′–4′). Trap (5) was cooled in a frozen chloroform-bath and after a two-hour

(1) This research was supported by the Office of Naval Research under Contract Nonr-294(00).

(2) Presented before the First Delaware Valley Regional Meeting of the American Chemical Society at Philadelphia, February 16, 1956.

(3) P. Royen, *Z. anorg. allgem. Chem.*, **229**, 112 (1936).

(4) P. Royen and K. Hill, *ibid.*, **228**, 97 (1936).

(5) E. H. Street, Jr., Ph.D. thesis, University of Pennsylvania, 1955.

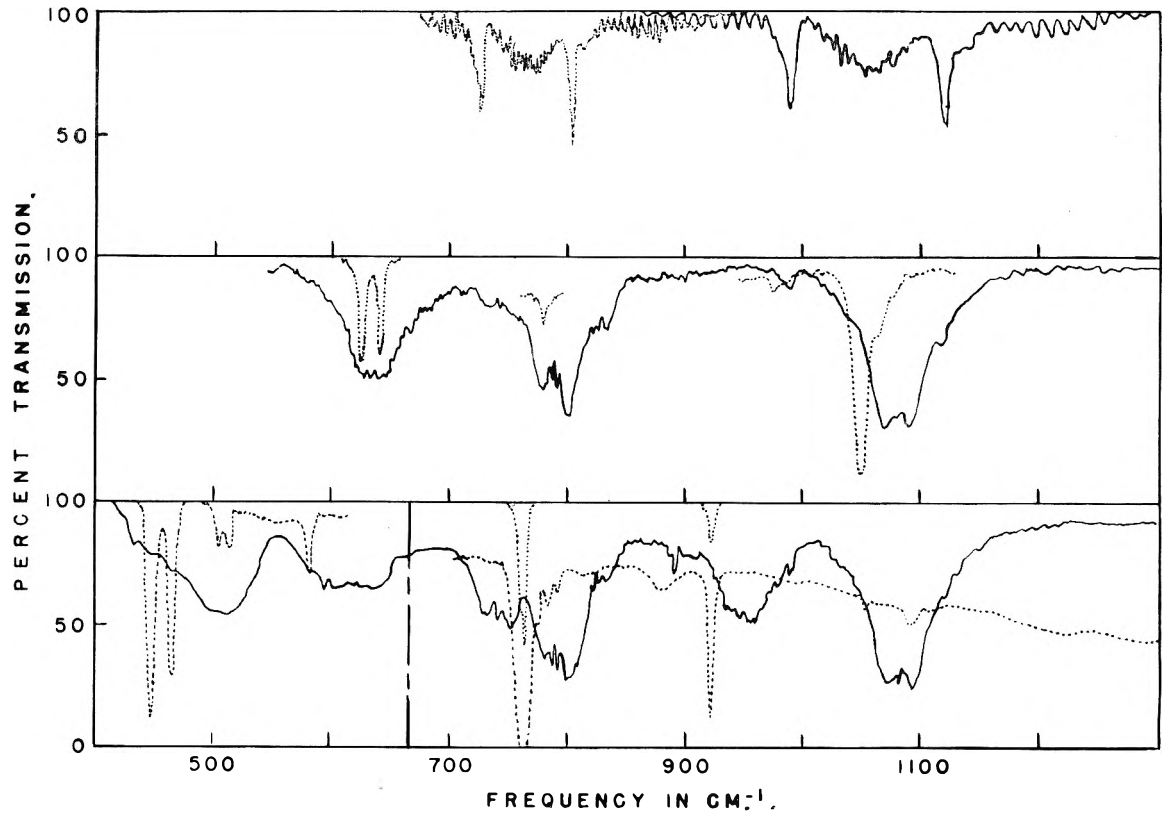

Fig. 1.—Infrared spectra of phosphine and biphosphine. Region A: solid line, 51 mm. press. PH_3 in 10 cm. cell at 28°; dotted line, 41 mm. press. PD_3 in 10 cm. cell at 28°. Region B: solid line, 7.5 mm. press. P_2H_4 in 100 cm. cell at 28°; dotted line, medium thick film P_2H_4 at −180°. Region C: solid line, 12 mm. press. deuterated P_2H_4 in 100 cm. cell at 28°; dotted line, medium thick film deuterated P_2H_4 at −180°. Region C′: solid line, 12 mm. press. deuterated P_2H_4 in 100 cm. cell at 28°; dotted line, thin and thick films deuterated P_2H_4 at −180°.

distillation, the material was distributed as shown in Table I. All traps were then isolated and the coolants replaced by Dry Ice for storage.

TABLE I

FRACTIONATION OF BIPHOSPHINE

Trap	Trap temp., °C.	Vol. P_2H_4 (ml.)
5	− 63	8
1′	− 78	2.5
2′	− 95	1
3′	−126	0.5
4′	−180	trace

In the course of the preparation of P_2H_4, traces of a white solid were encountered but the substance was never satisfactorily identified.[5]

The samples of PH_3 and PD_3 used in the infrared work described below were collected as by-products during the biphosphine preparations.

Biphosphine for the infrared spectra was withdrawn from traps (2′) and (3′) of the fractionation train. Since PH_3 is formed when P_2H_4 decomposes, the usual practice was to bring the trap to liquid ammonia temperature and to discard a number of small portions of the vapor until the vapor pressure was constant at 7 to 8 mm. Pressures for the gas spectra were limited to a maximum of about 10 mm. since liquid P_2H_4 decomposes rather rapidly much above −33°.

Spectra were recorded on a Perkin-Elmer Model 12C spectrometer. In each case a background was recorded with the empty cell, the cell filled as quickly as possible and the sample run. For the solids we used a low temperature cell of the type described by Wagner and Hornig.[6] The region from 3500 to 300 cm.$^{-1}$ was covered with LiF, NaCl, KBr and CsBr prisms and the absorption bands in this region are plotted in Fig. 1 and 2.

(6) E. L. Wagner and D. F. Hornig, *J. Chem. Phys.*, **18**, 296 (1950).

In order to estimate the amount of decomposition of the biphosphine samples, we have included in Fig. 1 and 2 the spectra of PH_3 and PD_3. We have also examined the spectrum of the solid hydride P_2H but neither Nujol mulls, dilute solutions in CS_2 nor films prepared by evaporation of solutions or by decomposition of biphosphine vapor gave any measurable absorption bands. (The solid hydride also proved to be amorphous to X-rays.)

Models for Biphosphine.—In order to describe the vibrational models of the P_2H_4 molecule one can set up the appropriate symmetry coördinates for the three possible configurations in terms of the internal coördinates shown in Fig. 3. The symmetry coördinates are listed in Table II, in which the numbering of the internal coördinates is maintained as one PH_2 group is rotated with respect to the other to obtain the different configurations. As an approximation the symmetry coördinates will also represent the normal coördinates of the molecule and Table II lists the species of each normal mode. For the infrared-active normal modes the band type is also given when it is assumed that the molecule is a symmetric top. Also included in Table II are the frequency ranges in which, partially by comparison with PH_3[7], PH_2D[7] and N_2H_4[8], the normal modes might reasonably be expected to fall. The P–P stretching frequency was approximated by Badger's rule.[9]

(7) R. E. Weston, Jr., and M. H. Sirvetz, *J. Chem. Phys.*, **20**, 1821 (1952).

(8) P. A. Giguère and I. D. Liu, *ibid.*, **20**, 136 (1952).

(9) R. M. Badger, *ibid.*, **2**, 218 (1934).

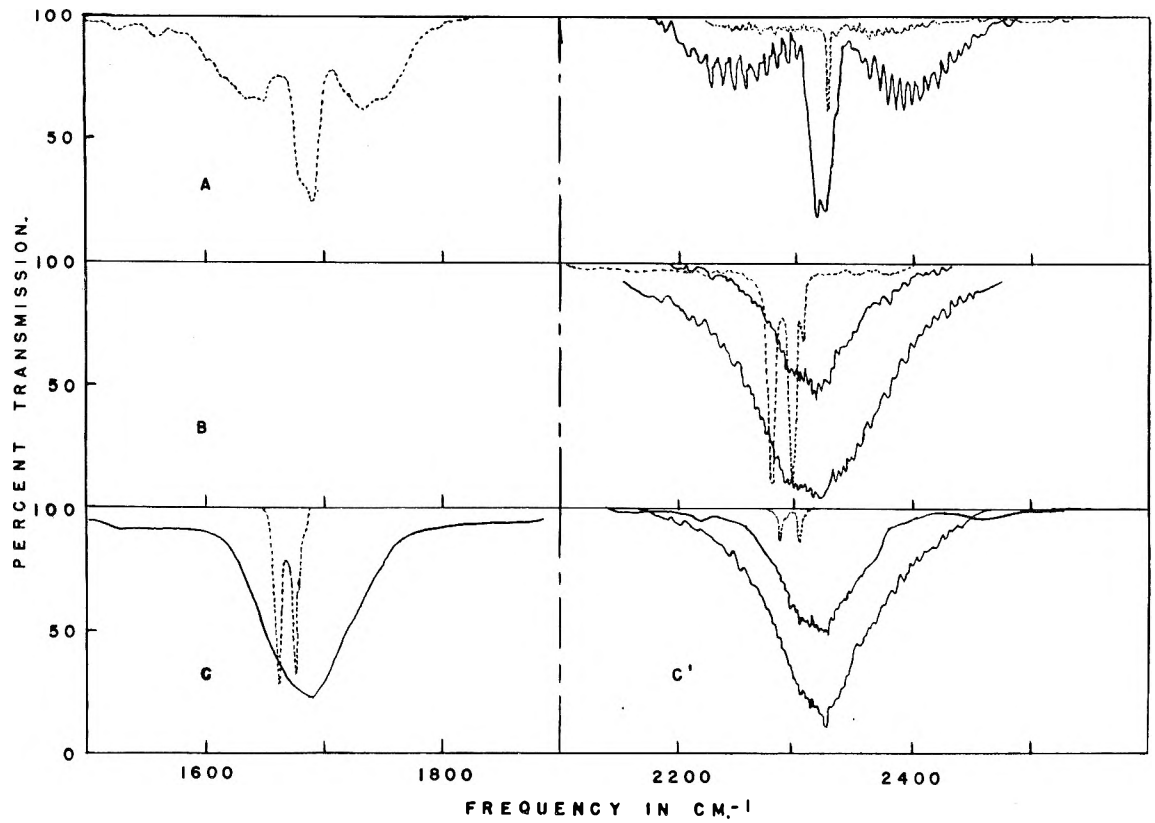

Fig. 2.—Infrared spectra of phosphine and biphosphine. Region A: solid line, 45 mm. press. PH_3 in 10 cm. cell at 28°; dotted line, 41 mm. press. PD_3 in 10 cm. cell at 28°. Region B: solid line, 7.5 mm. press. P_2H_4 in 10 cm. cell, 5 mm. press. P_2H_4 in 100 cm. cell at 28°; dotted line, medium thick film P_2H_4 at −180°. Region C: solid line, 12 mm. press. deuterated P_2H_4 in 100 cm. cell at 28°; dotted line, thin film deuterated P_2H_4 at −180°. Region C′: solid line, 2 mm. and 5 mm. press. deuterated P_2H_4 in 100 cm. cell at 28°; dotted line, medium thick film deuterated P_2H_4 at −180°.

TABLE II

VIBRATIONAL MODES OF P_2H_4

Symmetry coörd.	Normal vib.	Range (cm.$^{-1}$)	C_2 species	C_{2v} species	C_{2h} species
$^1/_2(r_1 + r_2 + r_3 + r_4)$	ν_2		A ⊥	A_1 ⊥	A_g
$^1/_2(r_1 + r_2 - r_3 - r_4)$	ν_1	2300	A ⊥	A_2	A_u ⊥
$^1/_2(r_1 - r_2 + r_3 - r_4)$	ν_8	to	B hyb.	B_2 ⊥	B_g
$^1/_2(r_1 - r_2 - r_3 + r_4)$	ν_9	2400	B hyb.	B_1 ∥	B_u hyb.
R	ν_6	460	A ⊥	A_1 ⊥	A_g
$^1/_2(\alpha_1 + \alpha_2)$	ν_3	1000	A ⊥	A_1 ⊥	A_g
		to			
$^1/_2(\alpha_1 - \alpha_2)$	ν_{10}	1100	B hyb.	B_1 ∥	B_u hyb.
$^1/_2(\beta_1 + \beta_2 + \beta_3 + \beta_4)$	ν_5		A ⊥	A_1 ⊥	A_g
$^1/_2(\beta_1 + \beta_2 - \beta_3 - \beta_4)$	ν_4	700	A ⊥	A_2	A_u ⊥
$^1/_2(\beta_1 - \beta_2 + \beta_3 - \beta_4)$	ν_{11}	to	B hyb.	B_2 ⊥	B_g
$^1/_2(\beta_1 - \beta_2 - \beta_3 + \beta_4)$	ν_{12}	900	B hyb.	B_1 ∥	B_u hyb.
torsion	ν_7	150	A ⊥	A_2	A_u ⊥

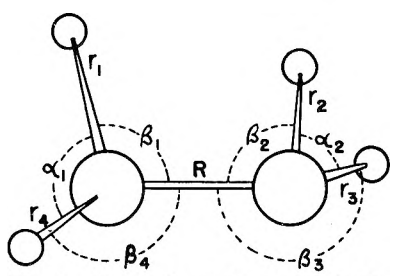

Fig. 3.—Internal coördinates for P_2H_4.

For PH_3 Nielsen[10] has reported the values of 93°50′ and 1.424 Å. for the HPH angle and PH distance. The electron diffraction value for the P–P distance in P_4 vapor[11] is 2.21 Å. If we assume that these values apply to P_2H_4 and also take the PPH angle as 93°50′, the calculated moments of inertia are as shown in Table III. I_C is the moment about the C_2 symmetry axis and δ is the angle between the P–P bond and the axis of least moment.

It can be seen that our assumed geometry makes P_2H_4 very nearly a symmetric top and that the moments are quite insensitive to the torsion angle. From the results of Gerhard and Dennison[12] one would expect the parallel type bands of P_2H_4 to

(10) H. H. Nielsen, *J. Chem. Phys.*, **20**, 759 (1952).

(11) Maxwell, Hendricks and Mosley, *ibid.*, **3**, 699 (1935).

(12) S. L. Gerhard and D. M. Dennison, *Phys. Rev.*, **43**, 197 (1933)

TABLE III

CALCULATED MOMENTS OF INERTIA OF P_2H_4(g.cm.^{2} × 10^{40})

Torsion angle	δ	I_A	I_B	I_C
0° (*cis*)	0°	13.13	141.12	142.48
90°	2°26.8′	13.09	142.03	142.00
180° (*trans*)	3°26.3′	13.05	142.94	141.52

exhibit dominant P and R branches whose maxima have a room temperature separation of 19.7 cm.$^{-1}$ and a weak central Q branch with an intensity of about 10% of that of the total band. Perpendicular bands should have a single maximum forming the background for a series of Q branches whose spacing is 2(A-B) = 3.88 cm.$^{-1}$

Infrared Spectra of Biphosphine and Deuterated Biphosphine.—In the gas spectrum of P_2H_4 (middle sections of Fig. 1 and 2) an intense perpendicular type band is observed in the P–H stretch region. The band, centered at about 2312 cm.$^{-1}$, is underlaid by a weaker band due to PH_3. Judging from the band intensities, we estimate that this particular sample of P_2H_4 contains as much as 25 to 50 mole % of PH_3. The fine structure lines on the outer shoulders of the band are spaced at 8 to 10 cm.$^{-1}$ and are doubtless due to PH_3. In the region of the band center, however, 16 or more lines with an average spacing of 3.8 cm.$^{-1}$ can be distinguished. These lines are listed in Table IV, which also gives their probable assignments.

TABLE IV

ROTATIONAL ANALYSIS OF THE 2312 CM.$^{-1}$ BAND OF P_2H_4

K	P_{Q_K}	R_{Q_K}	$(R_{Q_K} - P_{Q_K})/4K$
0		2314.0	
1	2310.0	2317.5	1.88
2	2306.0	2321.0	1.88
3	2303.0		
4	2298.5	2328.0	1.88
5	2294.5	2332.0	1.88
6	2291.0	2336.0	1.88
7	2287.0	2339.5	1.88
8	2283.5	2343.5	1.88

Table IV shows the satisfactory agreement with our calculated value of 1.94 cm.$^{-1}$ for A-B = $({}^RQ_K - {}^PQ_K)/4K$.

In the PH_2 bending region of the gas there is a strong parallel band with a weak Q branch at 1081 cm.$^{-1}$ and a P–R spacing of 20 cm.$^{-1}$ (our calculated value 19.7 cm.$^{-1}$). On the sides of the band there are peaks at 990 and 1120 cm.$^{-1}$ due to the underlying PH_3 band.

The absorption of P_2H_4 gas in the PH_2 wagging and rocking range is somewhat more complicated, there being two regions of strong absorption. The first, centered at about 790 cm.$^{-1}$, has four prominent peaks; the central weaker pair separated by 4 cm.$^{-1}$ and the outer pair by 21 cm.$^{-1}$. This 790 cm.$^{-1}$ band is overlapped on the high frequency side by a much weaker band at 825 cm.$^{-1}$, which also appears to have four peaks with the same type of spacings. Now type B bands of asymmetric top molecules may exhibit four maxima, but such bands would not be expected here because of the slight asymmetry of P_2H_4. Moreover, the separations of the peaks suggest hybrid bands with both perpendicular and parallel components. The second strong band in this region is at 633 cm.$^{-1}$, with a large perpendicular component. Although the lines in the band form a rather irregular pattern, there are a number with spacing close to 4 cm.$^{-1}$. Between 700 and 750 cm.$^{-1}$ and between 850 and 950 cm.$^{-1}$ there is a very irregular background absorption. A weak band that appears to be of the parallel type with its Q branch at 743 cm.$^{-1}$ is discernible but the 850–950 cm.$^{-1}$ absorption is difficult to characterize. At least some of this weak absorption is doubtless due to PH_3. The gas frequencies are listed in Table V.

Crystalline biphosphine at liquid air temperature shows several very sharp absorption bands falling near the gas frequencies. These are also given in Table V.

It is quite evident from the spectrum of gaseous deuterated biphosphine (lower portions of Fig. 1 and 2) that the sample contained a considerable amount of hydrogenated biphosphine. The hydrogen content is probably due to moisture in the original technical calcium phosphide, although exchange with hydrogen-containing materials (stopcock grease, traces of moisture, etc.) in our fractionation system and absorption cells must also have occurred. It seems only safe to conclude that the deuterated compound probably contained all of the various isotopic forms. Indeed the spectra of both the gas and solid are much richer than the spectra of P_2H_4 itself.

TABLE V

TENTATIVE VIBRATIONAL ASSIGNMENTS FOR BIPHOSPHINE

P_2H_4 (gas)	C_{2h} assign.	C_2 assign.	P_2H_4 (crystal)	P_2D_4 (crystal)
			2305	
2312 ⊥ vs	$\nu_1(A_u)$, $\nu_9(B_u)$	P–H	2297	1674
		stretch	2280	1660
1091 R				
1081 Q ∥, s	$\nu_{10}(B)$	$\nu_{10}(B)$	1066	765
1071 P			1051	
			975	
835				
827 hyb.?, w	$\nu_5 + \nu_7(A_u)$	$\nu_{11}(B)$		
823				
...				
801				
792 hyb., s	$\nu_{12}(B_u)$	$\nu_{12}(B)$	780	582
788				
780				
...				
743 Q ?, w	$\nu_6 + \nu_7(A_u)$	$\nu_4(A)$?		
735				
633 ⊥, s	$\nu_4(A_u)$	$\nu_5(A)$	642	466
			626	448

With the crystalline deuterated biphosphine, however, one can see from the 2280 and 2297 cm.$^{-1}$ bands that the P_2H_4 content is very small. Contamination by hydrogen-deuterium exchange was kept at a minimum in taking the solid samples since liquid biphosphine was distilled from the storage trap (at −78°) at its low vapor pressure directly on the cold plate of the cell.

With the same geometry as assumed for P_2H_4, it follows that P_2D_4 should exhibit parallel bands with dominant P and R branches separated at

300°K. by 20.5 cm.$^{-1}$. Perpendicular bands should have a single maximum overlaid by a series of Q branches with a spacing of 1.86 cm.$^{-1}$.

In the gas spectrum of the deuterated biphosphine, a strong perpendicular band appears at 1685 cm.$^{-1}$ in the P–D stretch region but since the band falls in the water vapor range only its envelope could be determined. Throughout the rest of the gas spectrum there are a number of bands, some of which coincide with those of P_2H_4. Overlapping of the bands makes it difficult to make assignments for P_2D_4.

In the solid spectrum overlapping is much less serious and in Table V we list those frequencies we believe belong to P_2D_4.

Interpretation of the Gas Spectrum.—Several general considerations concerning the P_2H_4 molecule seem pertinent.

1. Regardless of the relative orientation of the PH_2 groups, the four P–H stretching modes should all be essentially perpendicular and should separate into the nearly coincident pairs ν_1, ν_8 and ν_2, ν_9. The PH_2 bendings, ν_3 and ν_{10}, should lie relatively close together and be either largely perpendicular or rather weak. The rocking and wagging modes should group into the pairs ν_4, ν_{11} and ν_5, ν_{12}, with both ν_4 and ν_{11} very weak perpendicular vibrations and ν_{12} largely parallel and probably strong. The P–P stretching vibration ν_6 should be very weak.

2. Of the three distinct rotational isomers, the *cis*-form (C_{2v}) is expected to be the least likely because of the eclipsed positions of the hydrogen atoms. Furthermore, in the symmetric top approximation the C_{2v} model does not permit bands of hybrid character such as has been ascribed to the 790 cm.$^{-1}$ band.

If we first assume C_{2h} symmetry, the most reasonable set of band assignments, listed in Table V, involve several anomalies. The weak bands at 825 and 743 cm.$^{-1}$ appear, as has been stated, to be a hybrid and a parallel band, respectively. The only apparent way in which they can be assigned are as the combinations $\nu_5 + \nu_7$ and $\nu_6 + \nu_7$, both of which should be perpendicular bands of A_u species. Secondly, while ν_{10} is a hybrid of B_u species, our assumed geometry would make it essentially perpendicular whereas the assigned band at 1081 cm.$^{-1}$ is actually largely parallel.

In view of the fact that the barriers to internal rotation are unquestionably small and the torsional oscillation has a large amplitude, P_2H_4 is most likely to follow the selection rules of point group C_2. A tentative set of assignments based on C_2 symmetry is given in Table V. These assignments violate some of the general premises stated at the beginning of this section, notably that ν_{10} has too great a parallel component and ν_5 is rather stronger than expected. It is entirely possible that a number of the allowed fundamentals are either overlapped or too weak to be observed in our work. Our maximum gas path without prohibitive decomposition was about 5 cm. atm.

Solid Biphosphine.—In crystalline P_2H_4 the P–H stretching region shows two strong, sharp bands and one much weaker one, all three falling within a 25 cm.$^{-1}$ interval. In place of the 633 cm.$^{-1}$ gas band, the solid has two strong bands, this time separated by only 16 cm.$^{-1}$. Either these bands may be interpreted as each due to a different vibration or else they constitute components into which the gas bands are split in the crystalline field. According to Giguère and Liu,[8] the four N–H stretching frequencies in solid hydrazine have a spread of at least 110 cm.$^{-1}$ and the four NH_2 rocking and wagging modes occur over an interval of 500 cm.$^{-1}$, the closest two being separated by 70 cm.$^{-1}$. In analogy, then, the close spacings of the bands in P_2H_4 would suggest the splitting of the gas frequencies.

Before we discuss the infrared spectrum further, we shall describe briefly a preliminary X-ray investigation of P_2H_4 powder at −136°. In this work we encountered two difficulties: the tendency of P_2H_4 to form a single crystal in the capillary and the condensation of moisture on the X-ray trap located midway between the capillary and the film. The X-ray film showed that the biphosphine was in the form of fairly large single crystals (*i.e.*, 0.05 to 0.2 mm.) rather than a homogeneous powder. Instead of the usual powder rings, the pattern consisted of single crystal reflections arrayed in rings about the origin. There were at least eleven reasonably well formed such circles of spots. It was clear from the spots which fell at impossibly low angles that the ice on the trap was also contributing to the observed reflections. In spite of the fact that it was not possible to separate unambiguously the ice spectrum from that of the P_2H_4, it was found that a monoclinic unit cell with a = 3.6, b = 6.6, c = 5.2 Å. and β = 104° was fairly consistent with our eleven defined rings. We feel that we cannot definitely exclude a related orthorhombic cell. We have overcome the above-mentioned experimental difficulties and intend to check our X-ray data more carefully.

It may be of interest to point out that our parameters seem sensible when compared with the values for hydrazine[13]; a = 3.56, b = 5.78, c = 4.53 Å. and β = 109.5°. If, as with hydrazine, P_2H_4 has two molecules per unit cell, then our tentative cell dimensions lead to a calculated density of 0.9. It has been observed that liquid biphosphine, at least, is a little less dense than water.

We have assigned the 633 cm.$^{-1}$ gas band for P_2H_4 either as $\nu_4(A_u)$ for C_{2h} symmetry or as $\nu_5(A)$ for the C_2 form. Restricted to an orthorhombic or monoclinic cell, the only situation[14] in which a vibration of A_u or A species can give rise to two infrared active components is for the molecule to occupy a site of C_1 symmetry in a monoclinic crystal. With two molecules per unit cell (or per lattice point), the only suitable crystal space groups are the following: C_2^1, C_2^2, C_s^1, C_s^2, C_s^3 or C_s^4. The reflection extinctions in our preliminary X-ray work would seem to eliminate all groups except C_2^1 or C_s^1.

With these tentative conclusions regarding the crystal structure, it follows that each molecular vibration should have two infrared active components. The 2312 and 633 cm.$^{-1}$ do indeed have

(13) R. L. Collin and W. N. Lipscomb, *Acta Cryst.*, **4**, 10 (1951).
(14) See for example D. F. Hornig, *J. Chem. Phys.*, **16**, 1063 (1948).

two strong components in the crystal. The 1051 cm.$^{-1}$ band has a definite shoulder at 1066 cm.$^{-1}$, while the 780 cm.$^{-1}$ band is too weak to be certain of the number of components. This would leave the weak band at 2305 cm.$^{-1}$ as perhaps a combination involving a lattice mode.

In summary, it is clear that our data do not establish the structure of biphosphine. A detailed examination of the fine structure obtained under high resolution is needed to settle the problem. Other information, such as dipole moment and Raman spectrum, would be most helpful but this is likely to be difficult to obtain because of the instability of the compound. Biphosphine decomposes in light and various attempts to prepare solutions showed that biphosphine decomposes completely in benzene and in carbon tetrachloride.

Acknowledgments.—The author wishes to acknowledge the assistance of Dr. Walter O. Freitag in recording the infrared spectra and the advice and aid of Dr. Robert E. Hughes in the X-ray investigation.

STUDIES OF DIFFUSION FLAMES. II. DIFFUSION FLAMES OF SOME SIMPLE ALCOHOLS

BY S. RUVEN SMITH AND ALVIN S. GORDON

Contribution from Chemistry Division, Research Department U. S. Naval Ordnance Test Station, China Lake, California

Received February 27, 1956

Using a quartz probe technique, samples of precombustion products have been removed from the diffusion flames of methyl, ethyl, normal and isopropyl alcohols and analyzed with a mass spectrometer. Analyses of these products for all the flames are self consistent, and indicate that the mechanism of burning involves a pyrolysis of the alcohol followed by an oxidation of the pyrolysis products. The mechanisms of these pyrolyses are discussed.

Introduction

Previous spectroscopic work[1] has shown that the pyrolysis of the hydrocarbon must play a role in hydrocarbon diffusion flames. Other workers probed a methane diffusion flame[2] with mass spectrometric analysis of the samples. They showed in detail that the hydrocarbon diffusion flame mechanism was a pyrolysis of the hydrocarbon followed by oxidation of hydrogen and very small carbonaceous particles.

The present work is an extension of the work to simple alcohol diffusion flames. It will be shown that the burning mechanism is a pyrolysis of the alcohol, followed by oxidation of the pyrolysis products, as in the hydrocarbon flames. In the alcohol flames, aldehydes and ketones as well as hydrocarbons are formed by pyrolysis, and these oxygenates break down to give CO, so that CO, H_2 and carbon particles are the ultimate species oxidized.

Fletcher[3] studied the pyrolysis of methanol in a static system at pressures less than atmospheric and temperatures between 626 and 730°. He proposed that the pyrolysis occurs in two stages; the first stage gives formaldehyde and hydrogen, and the formaldehyde is pyrolyzed in the second stage to CO and H_2.

Someno[4] studied the thermal decomposition and slow combustion of monohydric alcohols. He worked in quartz vessels at subatmospheric pressure at temperatures up to 650°. Identification of products was made spectrographically. Ketones, aldehydes, ketenes and unsaturated hydrocarbons were found in the products. Formaldehyde was found only in the products from the slow oxidation.

(1) H. G. Wolfhard and W. J. Parker, *J. Chem. Soc.*, 2058 (1950).
(2) S. R. Smith and A. S. Gordon, THIS JOURNAL, **60**, 759 (1956).
(3) J. C. N. Fletcher, *Proc. Roy. Soc. (London)*, **A147**, 119 (1934).
(4) Fujiko Someno, *Bull. Ins. Phys. Chem. Research (Tokyo)*, **21**, 277 (1942).

The pyrolysis reactions in the diffusion flame give information on the homogeneous mechanism of the reactions, but none on the kinetics of the processes.

Experimental

The apparatus and procedures are similar to those described previously.[2] An alcohol burner with a Pyrex glass wool wick was set up on a micromanipulator in a Plexiglas hood to eliminate the effects of air currents on the flame. A quartz probe with a ground diaphragm opening was sealed into position above the burner, and the samples probed from the flame were expanded into previously evacuated flasks. Samples have been probed at the central axis near the wick and in the neighborhood of the tip of the inner cone of the flame in all cases.

The probed samples were analyzed with a Consolidated Analytical mass spectrometer. Analyses were carried out in triplicate after proper equilibration and conditioning of the sample system. The procedure gives reproducible results for the water and alcohol components. Identification of the components was aided by thermal fractionation of the samples from a series of temperatures from liquid nitrogen to room temperature and the use of high mass resolution. The summation of the partial pressures of the components of the sample always checked within 1% of the total pressure reading of the sample introduced into the mass spectrometer. The partial pressures were used to calculate the reported mole percentages.

The temperature profiles of the inner pyrolysis zone have been determined with a hairpin shaped 1 mil quartz coated Pt–Pt 10% Rh thermocouple. This type of thermocouple eliminates errors due to catalysis on the surface of the platinum. An accurate correction for conductivity errors is not possible; however, with low temperature gradients near the central axis of the flame any error in temperature measurement in this zone is probably small. The temperatures measured in the flames varied from about 200° at the wick to about 1400° at the tip and the edge of the flame. The temperature profile of these flames corresponds closely to that of the methane flame.

Discussion

The following alcohol diffusion flames were studied: methanol, ethanol, *n*-propyl and isopropyl alcohol. We believe that the pyrolysis is free radical induced, probably by the small percentage of O_2 which diffuses in near the base of the

burner. In part, the O_2 may react with H_2 and the resulting H and OH radicals can also induce pyrolysis of the alcohol. The heat for the pyrolysis is supplied by hot CO, CO_2, N_2 and H_2O molecules which diffuse from the edge of the flame where H_2, CO and carbon particles burn.

Methanol Diffusion Flame.—The analysis of samples probed from various regions of a methanol flame are reported in Table I. Samples no. 1 and 2 were probed from the zone near the wick of the flame, while the successive samples were probed along the central axis of the flame toward the tip.

Table I

Samples Probed from Methanol Flame

Sample no.	1	2	3	4	5
Carbon dioxide	7.56	6.98	8.17	9.04	11.21
Argon	0.55	0.51	0.55	0.61	0.63
Methyl alcohol	16.29	14.76	6.03	3.04	0.04
Oxygen		0.03	0.04		0.06
Formaldehyde	0.51	0.52	0.27	0.27	0.02
Ethylene	0.05	0.02	0.03	0.03	0.03
Acetylene	0.04	0.03	0.02	0.03	
Water	14.08	19.61	25.09	21.18	26.59
Methane	0.28	0.24	0.21	0.06	0.01
Carbon monoxide	8.58	7.93	7.51	9.19	4.61
Nitrogen	46.09	43.41	47.23	51.33	54.71
Hydrogen	5.97	5.94	4.83	5.23	2.07
	100.00	100.00	100.00	100.00	100.00
T, °C.	350	375	980	1150	1300

The primary attack on methanol is *via*

$$R + CH_3OH \rightarrow RH + CH_2OH \quad (1)$$

$$R + CH_3OH \rightarrow RH + CH_3O \quad (1a)$$

where R is a free radical including H atoms and O_2. Reaction (1) has an energy of activation of about 10 kcal. and reaction (1a) has an energy of activation of about 25 kcal. In addition, there is an *a priori* factor of about 3 in favor of reaction (1). These reactions are followed by

$$CH_2OH \rightarrow CH_2O + H \quad (2)$$

$$CH_3O \rightarrow CH_2O + H \quad (2a)$$

The heat of reaction of (2) may be estimated; the strength of the bond between H and oxygen is not over 115 kcal., and the heat of formation of the doubly bonded C and O from singly bonded C and O in an alcohol is about 85 kcal. The heat of reaction is thus about 30 kcal. From similar reasoning reaction (2a) has a heat of reaction of about 15 kcal. Some of the formaldehyde may also result from a radical attack on the CH_2OH

$$CH_2OH + R \rightarrow CH_2O + RH \quad (3)$$

The presence of methane in the reaction products shows that CH_3 radicals are present in this flame. Thus a small percentage of the methanol decomposes *via*

$$H + CH_3OH \rightarrow CH_3 + H_2O \quad (4)$$

The strength of the H_3C–OH bond is too great to permit a split into CH_3 and OH at the temperatures inside the flame cone where CH_3OH is present in reasonably high concentrations.

Ethylene and acetylene probably result from the pyrolysis of ethane which in turn may result from methyl radical combinations. Ethylene, which is more stable than ethane, is present in quite small concentrations, so that the ethane concentrations are below the limit of mass spectrometer identification.

It should be noted that methane is present in much smaller concentration than formaldehyde, even though methane is much more stable to pyrolysis than is formaldehyde. This shows that formaldehyde production is the most favorable path for methanol pyrolysis. The importance of the formaldehyde production reaction is also shown by the high steady-state concentration of its pyrolysis products CO and H_2 compared to the concentration of these materials in the methane diffusion flame.[2]

Ethanol Diffusion Flame.—The samples probed from an ethanol diffusion flame are shown in Table II. Both samples were taken on the flame axis. Sample I was probed from just above the wick and sample II from just inside the luminous cone. The products formed indicate that ethanol decomposes *via* four primary processes.

Table II

Samples Probed from Ethanol Flames

Sample no.	1	2
Ethyl alcohol	9.47	2.95
Benzene	0.02	0.02
1,3-Butadiene	0.02	0.02
Vinylacetylene	0.04	0.04
Diacetylene	0.01	0.02
Acetaldehyde	0.55	0.51
Propylene	0.04	0.04
Carbon dioxide	7.84	8.49
Argon	0.59	0.63
Oxygen	0.05	0.04
Propyne	0.04	0.04
Formaldehyde	0.03	0.03
Ethane	0.29	0.27
Ethylene	1.70	1.54
Acetylene	1.16	1.23
Water	14.49	16.17
Methane	1.29	1.52
Carbon monoxide	7.41	7.55
Nitrogen	51.24	55.13
Hydrogen	3.72	3.76
	100.00	100.00
T, °C.	350	1050

$$CH_3CH_2OH + R \rightarrow CH_3CHOH + RH \quad (5)$$

$$CH_3CH_2OH + R \rightarrow CH_2CH_2OH + RH \quad (6)$$

$$CH_3CH_2OH + R \rightarrow CH_3CH_2O + RH \quad (7)$$

$$CH_3CH_2OH + H \rightarrow CH_3CH_2 + H_2C \quad (8)$$

when R may be a free radical including H and O_2.

These reactions are followed by reactions of the free radicals formed in the primary processes.

$$CH_3CHOH \rightarrow CH_3\overset{H}{\overset{|}{C}}{=}O + H \quad (9)$$

$$CH_3CH_2O \rightarrow CH_3\overset{H}{\overset{|}{C}}{=}O + H \quad (9a)$$

$$CH_3CH_2O \rightarrow CH_3 + CH_2O \quad (9b)$$

$$CH_2CH_2OH \rightarrow C_2H_4 + OH \quad (10)$$

$$CH_3CH_2 \rightarrow C_2H + H \quad (11)$$

$$CH_3CH_2 + CH_3CH_2OH \rightarrow C_2H_6 + CH_3CH\,OH \quad (12)$$

Reactions (5) and (6) are low energy of activation reactions compared with reactions (7) and (8). Reactions (9) and (10) should be the preferred stabilization reaction for each of the primary free radicals since a sizable portion of the necessary energy to split the C–H or C–OH bonds is simultaneously available from the formation of the C=O or C=C bond.

The formation of the ethyl free radical is *via* an unfavorable path. The radical stabilizes itself by reaction (11) or (12). At room temperature recombination of ethyl radicals and disproportionation of ethyl radicals are the predominating reactions but as the temperature is increased abstraction of hydrogen becomes increasingly important.[5] At still higher temperatures there is evidence that the ethyl radical can pyrolyze[6] to ethylene and H.

Since ethylene is considerably more stable than acetaldehyde, the fact that ethylene/acetaldehyde ratios are about 3 must mean that both reactions (5) and (6) are important pyrolysis paths at flame temperatures. The ethoxy radical will stabilize itself as acetaldehyde in part (9a), but mostly as formaldehyde (9b). The steady-state concentration of formaldehyde is quite low and less than 10% of the acetaldehyde. Thus reaction (7) does not form an important reaction path. Acetaldehyde in the diffusion flame will rapidly pyrolyze to CH_4 + CO *via* its well known free radical chain mechanism.

The possible reactions which could lead to ethane formation are

$$CH_3 + CH_3 \rightarrow C_2H_6 \quad (13)$$

$$C_2H_5 + R \rightarrow C_2H_6 + R \quad (14)$$

Both reactions (13) and (14) are important paths for ethane production. With increasing temperature, abstraction processes are favored over recombination. However, the CH_3 concentration is so high in these flames that reaction (13) is an important process.

Ethane pyrolysis gives rise successively to ethylene, acetylene, and the reactions of acetylene. The reaction products of acetylene with itself and with ethylene form the vinylacetylene, diacetylene, 1,3-butadiene and benzene found in the product gas. A 4-carbon compound such as vinylacetylene is a reasonable intermediate for benzene formation.

The methane in the ethanol flame is the result of the extremely fast pyrolysis of acetaldehyde formed in reaction (9). Methyl radicals from this pyrolysis stabilize themselves by abstracting hydrogen and by recombination.

A small percentage of propylene and propyne are formed in the ethanol pyrolysis. These species are probably *via* radical–radical reactions.

$$CH_3 + HC{=}CH_2 \rightarrow CH_3CH{=}CH_2 \quad (15)$$

$$CH_3 + C{\equiv}CH \rightarrow CH_3C{\equiv}CH \quad (16)$$

We feel that the formation of propyne by propylene pyrolysis is not an important reaction because McNesby, *et al.*,[7] found no evidence of propyne when propylene was pyrolyzed in the presence of methyl radicals at *ca.* 500°. The $CH_2CH{=}CH_2$ radicals formed diallyl instead of propyne or allene.

n-Propyl and Isopropyl Alcohol Flames.—The analysis of the samples probed from the normal and isopropyl alcohol flames are reported in Tables III and IV. *n*-Propanol may decompose along four main primary paths

$$R + CH_3CH_2CH_2OH \rightarrow RH + CH_3{-}\underset{\displaystyle H}{\underset{|}{C}}{-}CH_2OH \quad (17)$$

$$R + CH_3CH_2CH_2OH \rightarrow RH + CH_2{-}CH_2{-}CH_2OH \quad (18)$$

$$R + CH_3CH_2CH_2OH \rightarrow RH + CH_3CH_2\dot{C}HOH \quad (19)$$

$$R + CH_3CH_2CH_2OH \rightarrow RH + CH_3CH_2CH_2O \quad (20)$$

followed by

$$CH_3{-}\underset{\displaystyle H}{\underset{|}{C}}{-}CH_2OH \rightarrow CH_3CH{=}CH_2 + OH \quad (21)$$

$$CH_2CH_2CH_2OH \rightarrow C_2H_4 + CH_2OH \quad (22)$$

$$CH_3CH_2CHOH \rightarrow CH_3 + CH_2{=}CHOH \quad (23)$$

$$CH_3CH_2CH_2O \rightarrow CH_3CH_2 + CH_2O \quad (24)$$

The CH_2OH decomposes to CH_2O + H and the vinyl alcohol appears as acetaldehyde, presumably by rearrangement on the wall of the sample flask.

TABLE III

SAMPLES PROBED FROM *n*-PROPANOL FLAMES

Sample no.	1	2
Benzene	0.04	0.10
n-Propyl alcohol	13.50	0.69
Toluene	0.01	0.01
2,3-Cyclohexadiene	0.01	0.01
Cyclopentadiene	0.02	...
Butene-1	0.06	0.05
1,3-Butadiene	0.06	0.07
Vinylacetylene	0.06	0.09
Diacetylene	0.02	0.03
Acetaldehyde	0.41	0.35
Carbon dioxide	7.31	8.49
Propylene	0.60	0.44
Propyne	0.06	0.12
Ethyl alcohol	...	0.09
Argon	0.57	0.64
Oxygen	0.04	0.06
Ethane	0.32	0.22
Ethylene	2.10	2.25
Acetylene	1.36	1.85
Formaldehyde	0.16	0.15
Water	11.93	12.49
Methane	1.88	2.31
Carbon monoxide	6.24	7.78
Nitrogen	49.65	58.02
Hydrogen	3.59	3.75
	100.00	100.00
T, °C.	320	925

Isopropyl alcohol decomposes along three main primary paths

$$R + CH_3\underset{\displaystyle HO}{\underset{|}{C}}H{-}CH_3 \rightarrow RH + CH_2\dot{C}H\underset{\displaystyle OH}{\underset{|}{C}}H_3 \quad (25)$$

(5) M. H. J. Wijnen and E. W. R. Steacie, *Can. J. Chem.*, **29**, 1092 (1951).

(6) J. R. McNesby and A. S. Gordon, *J. Am. Chem. Soc.*, **77**, 4719 (1955).

(7) J. R. McNesby, T. W. Davis and A. S. Gordon, *ibid.*, **76**, 823 (1954).

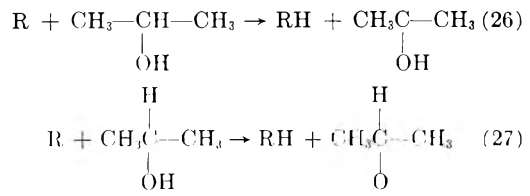

(26)

(27)

followed by

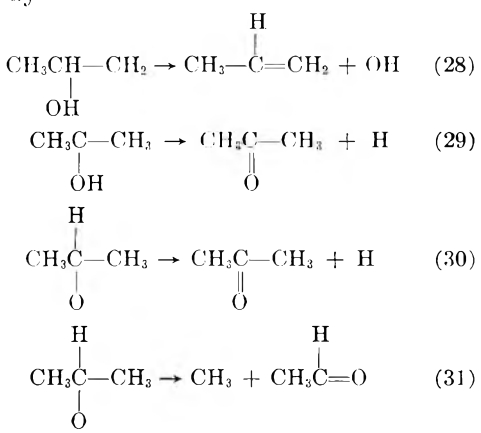

(28)

(29)

(30)

(31)

It is probable that reactions (20) and (27) have the slowest rates, and that reactions (19) and (26) have the fastest rates for *n*-propyl and isopropyl alcohol, respectively.

Table IV

Samples Probed from Isopropyl Alcohol Flames

Sample no.	1	2
Isopropyl alcohol	17.63	4.06
Benzene	0.05	0.09
Toluene	0.01	
Cyclohexadiene	0.01	0.01
Cyclopentadiene	0.02	0.03
Acetone	0.34	0.58
Ethyl alcohol	0.06	0.09
Isobutylene	0.08	0.10
1,3-butadiene	0.09	0.12
Vinylacetylene	0.07	0.09
Diacetylene	0.03	0.04
Acetaldehyde	0.41	0.42
Carbon dioxide	7.04	8.02
Propylene	1.09	1.34
Propyne	0.16	0.18
Argon	0.47	0.56
Oxygen	0.04	0.03
Ethane	0.30	0.33
Ethylene	1.08	1.47
Acetylene	1.05	1.33
Water	15.75	18.31
Methane	1.78	2.63
Carbon monoxide	4.78	5.88
Nitrogen	45.37	51.36
Hydrogen	2.31	2.95
	100.00	100.00
T, °C.	300	825

We note that propionaldehyde is not present in detectable amounts in the products from *n*-propyl alcohol. This indicates that the CH_3CH_2C-OH and the CH_3CH_2CO radicals decompose exclusively via reactions (23) and (24).

In both the *n*-propyl and the isopropyl alcohol flames, methane is formed via hydrogen abstraction by CH_3 and ethane is formed via $CH_3 + CH_3$. In the *n*-propyl alcohol flame ethane is formed in addition by C_2H_5 abstracting H.

In the isopropyl alcohol flame the formation of ethylene is probably exclusively via the dehydrogenation of ethane. Acetylene is formed from the dehydrogenation of ethylene. The usual hydrocarbons which result from reactions involving acetylene, including 1,3-butadiene, vinylacetylene, diacetylene and benzene are also present

Ethylene is roughly twice as large in the *n*-propyl alcohol flame as in the isopropyl alcohol flame, even though the ethane concentration is quite close in the two flames. The higher concentration of ethylene in the *n*-propyl alcohol flame is probably caused by reactions (22) and (24). Reaction (22) generates ethylene while reaction (24) generates ethyl radicals which stabilize themselves both by H abstraction to form ethane and by loss of H to form ethylene. There are no analogous sources of ethylene in the isopropyl alcohol flame.

A small concentration of formaldehyde results from reactions (22) and (24) in the *n*-propyl alcohol flame. As would be predicted, no formaldehyde is found in the isopropyl alcohol flame. A small concentration of ethyl alcohol has been found in both the *n*-propyl and isopropyl alcohol flames.

Carbon Formation.—Observation of the flames studied indicated an increasing amount of carbon production as one proceeds from C_1 to C_3 alcohol. The methanol flame produces no carbon, the ethanol flame a small amount of yellow tipping, and the propanol flames produce relatively large amounts of carbon. Analysis shows no benzene and less than 0.004% acetylene in the methanol flame, but the amounts of these precombustion products in the ethanol and *n*- and isopropyl alcohol flames are very similar—benzene 0.1%, and acetylene (1–2%). The temperature profiles of these flames are quite similar so that this lack of correlation indicates that the tendency toward carbon formation does not depend only on the steady state concentration of these constituents in the flame.

Acknowledgment.—We wish to acknowledge the coöperation of Mr. Maynard H. Hunt, who helped in carrying out the temperature measurements. We wish also to acknowledge the assistance of Mr. Andreas V. Jensen for the operation of the mass spectrometer, and Mrs. Helen R. Young, for assistance in the reduction of the mass spectral data.

THE ANOMALOUS ADSORPTIVE PROPERTIES OF NITRIC OXIDE[1]

BY R. NELSON SMITH, DAVID LESNINI AND JOHN MOOI

Pomona College, Claremont, Calif.

Received March 12, 1956

Nitric oxide reacts readily with carbon surfaces at 0 and −78° to form gaseous nitrogen and carbon–oxygen surface complexes. Thus, adsorption isotherms determined at these temperatures with carbon are fictitious; likewise, previous calorimetric measurements are heats of reactions, not heats of adsorption, for unknown amounts of nitric oxide. Nitric oxide does not react with a carbon surface at −154° and adsorption appears to be normal, though the adsorbed state is probably N_2O_2. NO also adsorbs normally on both porous and non-porous SiO_2 at 0° and −78°, though there is some reversible chemisorption in each case (NO can be removed intact by heating) and it appears that the NO interacts to some extent at −78° with the water bound in the silica gel.

The original objective of this study was utilization of the free radical properties of NO as a means of characterizing the "free-valence" nature of surfaces. It was thought that the odd electron in NO would pair off with an odd electron in the surface, and that the amount of NO thus chemisorbed would be a measure of this type of surface activity. This phenomenon does not occur, and the reasons therefor are the subject of this paper.

Experimental

Two types of carbon and two types of silica were used in this study.

Graphon.—A partially graphitized carbon black (lot #328) furnished through the courtesy of the Godfrey L. Cabot Co., Boston, Mass. The surface area is 82.8 m.^{2} per gram and the ash content is about 0.02%. Before each series of measurements the Graphon was given three 15-minute treatments with H_2 gas at 1000°. The H_2 was pumped out between each treatment and after the last treatment the sample was cooled slowly with continuous pumping. About 1.9-g. samples were used for measurements.

Su-60.—An activated sugar charcoal of extremely low ash content (less than 0.005%) prepared from Confectioners AA sugar furnished by the California and Hawaiian Sugar Refining Corporation, San Francisco, Calif. The activation method is described elsewhere.[2] The BET nitrogen surface area is 1060 m.^{2} per gram. It was H_2-treated in the same way as for Graphon before each series of measurements. About 0.8-g. samples were used for measurements.

XC-54.—A non-porous "hyperfine silica" furnished through the courtesy of Dr. Mark Olson, Pigments Dept., E. I. du Pont de Nemours & Co. Electron micrographs show most of the particles to be discrete spheres of the order of 10–40 millimicrons diameter. The nitrogen surface area is 20.5 m.^{2} per gram. Before making adsorption measurements the samples were heated to 850° *in vacuo* for about 1 hour, then cooled with continuous pumping. Heating to higher temperature caused partial sintering of the silica. Approximately 0.45-g. samples were used.

D-3707.—A commercial silica gel furnished through the courtesy of the Davison Chemical Corp., Baltimore, Md. The BET ethyl chloride surface area is 838 m.^{2} per gram. Translucent particles of approximately 0.5–1.0 mm. diameter were used in the measurements. Approximately 0.49-g. samples were used and outgassed for several hours at 300° before making measurements.

Nitric oxide was prepared by the method of Marqueyrol and Florentin.[3] Twenty g. of diphenylnitrosoamine (Eastman #759) was put into a 200-ml. round-bottom flask and sealed to the high-vacuum system which included a 2-liter evacuated Pyrex reservoir and a Dry Ice trap between the reservoir and diphenylnitrosoamine. The diphenylnitrosoamine was outgassed with continuous pumping and its temperature raised to about 150° with a Glas-col heater. At this temperature the gas generating system was closed off from the pumping system and opened to the 2-liter reservoir. The heating was then continued to about 250° until decomposition was complete, as evidenced by no more gentle bubbling of the liquid. The remaining tetraphenylhydrazine and the Dry Ice trap were then closed off from the rest of the system and cooled. The gas analytical methods used in this study showed this gas to be pure NO.

A conventional volumetric adsorption apparatus was used for determination of the isotherms. The dead space in the system was kept as small as possible; it was determined volumetrically with helium at each temperature for each sample. The Graphon, Su-60 and XC-54 samples were sealed in quartz tubes and connected to the system with Pyrex-to-quartz graded seals so that these samples could be treated at temperatures up to 1000° directly in the system prior to adsorption measurements. The D-3707 was sealed in a Pyrex tube since it was not possible to heat it above 300°. Provision was made for removal of small amounts of gas by a Toepler pump and for its analysis by the micro methods of Blacet and Leighton. Two types of gas samples were involved; mixtures of CO, CO_2 and N_2 and mixtures of CO_2, NO and N_2. Both types were analyzed by the same method. CO_2 was removed by a KOH bead[4]; CO or NO was removed by a dry Ag_2O bead[5] held to the platinum wire with Kronig cement (NO has not heretofore been determined by this method); N_2 was determined by difference. For samples containing a high percentage of CO or NO, it was found expedient to dilute the samples with pure N_2 before analysis. To achieve the constant temperatures used for the various adsorption measurements the following materials were used in Dewar flasks: ice and water for 0°; Dry Ice for −78°; and a solid–liquid mixture of 2-methylpentane (99 mole % minimum purity, Phillips Petroleum Co.) for −154°. 2-Methylpentane is convenient in that it supplies the desired temperature at its freezing point and yet is easily stored at room temperature (b.p. 60°). It is inconvenient in that its ice must be made with the adsorption bulb *in situ* by carefully adding liquid nitrogen and stirring well. A good large Dewar flask, well-insulated from the surroundings and initially filled almost solid with the ice, will keep about 7 to 8 hours before re-preparation of ice is necessary. The temperature obtained with 2-methylpentane mush was probably not controlled very precisely in this manner, but for the purpose of these experiments it was satisfactory, and will be referred to as −154°.

Results

Figure 1 shows characteristic adsorption and desorption isotherms for NO on Su-60. The adsorption at 0 and −78° is not large, but judging from the unusual hysteresis loop the adsorbed NO is unquestionably chemisorbed. If one then endeavors to desorb this tightly-bound NO by vigorous heating, he finds that the volume of gas thus evolved plus the small bit desorbed before heating is only a little more than half of the gas which was originally introduced to the charcoal. Analysis of the gas desorbed on heating shows it to be al-

(1) Progress report of work done under contract N8onr54700 with the Office of Naval Research. Reproduction in whole or in part is permitted for any purpose of the United States Government.

(2) R. N. Smith and J. Mooi, THIS JOURNAL, **59**, 814 (1955).

(3) M. Marqueyrol and D. Florentin, *Bull. soc. chim. France*, [4] **11**, 804 (1912).

(4) F. E. Blacet and P. A. Leighton, *Ind. Eng. Chem., Anal. Ed.*, **3**, 266 (1931).

(5) F. E. Blacet, G. D. McDonald and P. A. Leighton, *ibid.*, **5**, 272 (1933).

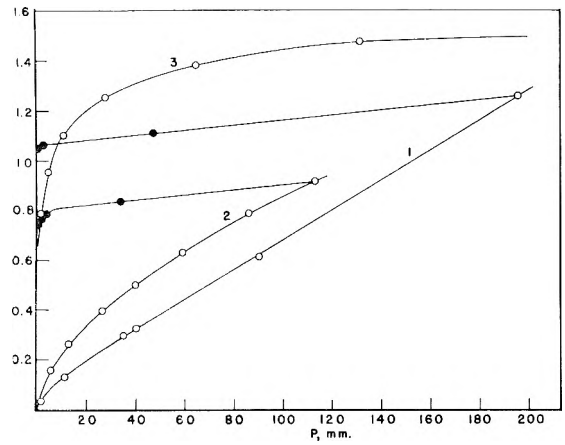

Fig. 1.—Adsorption (○) and desorption (●) isotherms for NO on charcoal, Su-60: curve 1 for 0°; multiply ordinate by 10^{-3} for moles/g.; curve 2 for −78°; multiply ordinate by 4×10^{-3} for moles/g.; curve 3 for −154°; multiply ordinate by 10^{-2} for moles/g.; curve 3 is the only true isotherm.

most entirely CO_2 and CO, and in relative amounts typical of the thermal decomposition of carbon–oxygen surface complexes (preponderance of CO_2 at the lower temperatures; CO at the higher). One cannot escape the fact that the NO has reacted rapidly with the carbon surface to form N_2 and carbon–oxygen surface complexes, and that the gas pressure measured for the isotherm is essentially N_2, not NO. This is easily verified by analysis, and for an "equilibrium pressure" of about 75 mm. at 0° one finds a typical analysis to be 92.9% N_2, 6.2% NO and 0.9% CO_2 after standing 1 hour, and after 24 hours the analysis becomes 99.0% N_2, 0.5% NO and 0.5% CO_2. With higher pressures one finds increasing amounts of NO in the gas phase. At −78° "equilibrium" is also rapidly achieved, and at a pressure of 113 mm. the gas was found to be 96.2% N_2, 3.1% NO and 0.7% CO_2. With Graphon (Fig. 2) the apparent effect is not so pronounced as with Su-60 simply because of the smaller specific surface area. Thus, with a larger

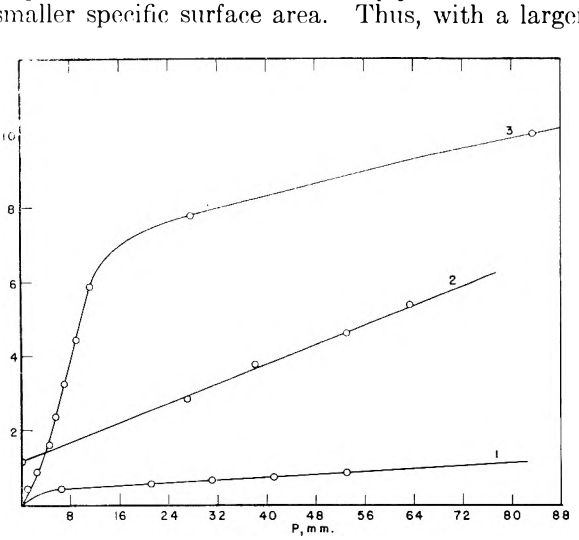

Fig. 2.—Adsorption isotherms for NO on Graphon, a carbon black: curve 1 for 0°; multiply ordinate by 10^{-5} for moles/g.; curve 2 for −78°; multiply ordinate by 10^{-5} for moles/g.; curve 3 for −154°; multiply ordinate by 10^{-4} for moles/g.; curve 3 is the only true isotherm.

sample at 0° and at a pressure of 50 mm., the "equilibrium gas" was 14.0% N_2 and 86.0% NO; at −78° and 60 mm. pressure, the gas was 38% N_2 and 62% NO.

Another experimental difficulty involved with "adsorption" of NO at these temperatures is the slow rate of attainment of equilibrium after the initial adsorption. This difficulty is caused by NO having to diffuse through N_2 in order to reach the surface, and it can be eliminated by occasionally withdrawing and mixing the gases with a gas buret and returning them to the carbon sample. Perreu[6] had the same difficulty with slow attainment of equilibrium in his calorimetric studies.

At −154° (in the narrow liquid range of NO, −151.8 to −163.5°) the situation is quite different. Here the adsorption is some 10 times greater than the apparent adsorption observed at −78 and 0°, and furthermore analysis shows the equilibrium gas to contain only a trace of N_2. One also finds that equilibrium is rapidly attained. In other words in the temperature range where NO is normally a liquid, true adsorption occurs and not reaction. However, even this true adsorption is complicated for all evidence indicates that liquid nitric oxide is a dimer.[7] This dimerization also probably accounts for its unreactivity toward the carbon surface.

A BET plot of the adsorption of NO on Graphon at −154° gives a V_m value of 8.75×10^{-4} mole of NO per gram; this in turn corresponds to the reasonable cross-sectional area of 15.7 Å.^{2} per molecule of NO (or 31.4 Å.^{2} per molecule of N_2O_2). Calculations using gas analyses and the apparent adsorptions show that at 0° and 200 mm. pressure 2% of the surface carbon atoms of Su-60 are oxidized by NO (assuming 1 oxygen atom per carbon atom), whereas under the same conditions O_2 oxidized 1.5%. At −78°, 1% of the surface is oxidized by NO. In the case of Graphon, similar calculations show 1.1% oxidized at 0° and 0.3% at −78%.

These results are significant in connection with the heats of adsorption ($-\Delta H_{ads}$) which have been measured for nitric oxide on charcoal. These heats have in reality been heats for the reaction

$$NO + C = (CO) + {}^1/_2N_2 \qquad (1)$$

where (CO) is the solid carbon–oxygen surface complex. In these calorimetric measurements the amounts of NO assumed to have been adsorbed are in error, for in correcting for the amount of gas unadsorbed the assumption was made that the residual gas was NO, not N_2. In reality, then, more moles of NO had reacted with the surface than had been assumed to be adsorbed, and thus the integral heats of *reaction* (cal./mole) would be lower than those published erroneously as integral heats of adsorption. A plot of integral heats *vs.* gas pressure is meaningless since the gas (N_2 + NO) pressures are in reality functions of the dead space in the calorimeter.

It is also not reasonable to compare directly the heats of adsorption of NO with those for O_2 as has

(6) J. Perreu, *Bull. soc. chim. France*, [5] **16**, 919 (1949).

(7) A. L. Smith, W. E. Keller and H. L. Johnston, *J. Chem. Phys.*, **19**, 189 (1951).

been done previously. However, one might look at the "adsorption" of each of these gases as the production of a carbon–oxygen surface complex. For oxygen, the "heat of adsorption" is identical with the "heat of formation" of this surface complex. For NO, the heat of formation of the surface complex may be calculated assuming $\Delta H = 0$ for the formation of C and N_2 and $\Delta H = +21.6$ kcal./mole for NO. Thus, from (1)

$$\Delta H_{complex} = \Delta H_{ads} - 21.6$$

where $-\Delta H_{ads}$ = the observed heat of reaction. Using Perreu's[6] values for the adsorption of NO at 0° on an activated coconut charcoal one may calculate that the heat of formation of the complex, $-\Delta H_{complex}$, for the first amount added is 48.6 kcal. per g. atom of oxygen and that this drops to about 45 kcal. per g. atom of oxygen at a pressure of about 100 mm. If *all* the unadsorbed gas in the calorimetric measurements was nitrogen, then these values should be cut in half for the number of moles of NO which had reacted would be twice the number believed to have been adsorbed. Actually, the unadsorbed gas will be a mixture of N_2 and NO (being almost entirely NO in the leads) and these heats of formation must lie somewhere between 25 and 50 kcal. per g. atom of oxygen. In another paper, Perreu[8] also determined the heat of adsorption of oxygen (the heat of formation of surface complex) on this charcoal at 0° and found a value of 78.9 kcal. per mole of O_2; this is equivalent to 39.5 kcal. per g. atom of oxygen, a value of the same order as that obtained with NO. In other ways too (from the composition as a function of temperature of the gases evolved on heating) it appears that the carbon–oxygen complexes formed by NO and O_2 are much the same. The mechanism by which these two dissimilar molecules give the same complex is of some interest. Each is paramagnetic and it may be that the first step in each case is the pairing of electrons by oxygen atoms with the surface.

Bull and Garner[9] have published for an activated charcoal graphs of differential heats of adsorption of NO and O_2 *vs.* the amount absorbed, and these values too must be in error for NO since the curve (of integral heats *vs.* concentration) from which the differential heats were taken must be in error for the reasons given above.

The adsorption studies using NO and SiO_2 were undertaken to see whether NO would be chemisorbed on this type of surface, and to check on the very unusual adsorption isotherm found at −78° for NO on silica gel by Briner and Sguaitamatti.[10] The results are summarized in Figs. 3 and 4.

The same amount (about 36 μmoles per g.) of NO is very strongly adsorbed on the non-porous silica at both −78 and 0°; at 0° this is about all of the NO which is adsorbed even at the higher pressures. There is a great difference between the amount of NO very strongly held by the silica gel at the two temperatures; at 0° the amount is about 7 μmoles per gram and at −78° it is about

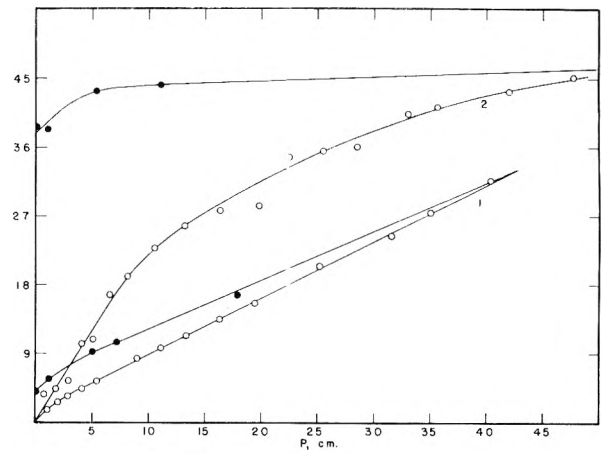

Fig. 3.—Adsorption (○) and desorption (●) isotherms for NO on NC-54, a non-porous silica: curve 1 for −78°; multiply ordinate by 10^{-5} for moles/g.; curve 2 for 0°; multiply ordinate by 10^{-6} for moles/g.

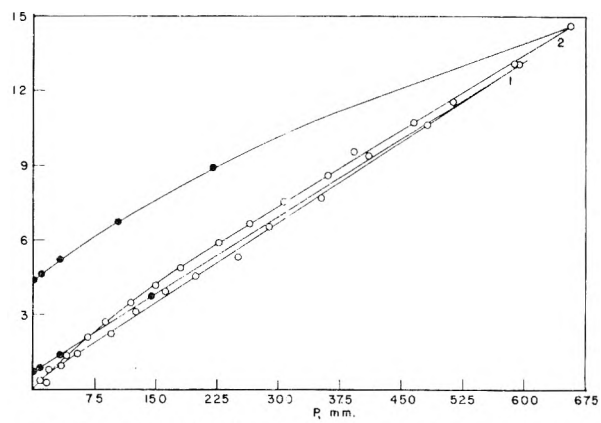

Fig. 4.—Adsorption (○) and desorption (●) isotherms for NO on D-3707, a silica gel: curve 1 for 0°; multiply ordinate by 10^{-5} for moles/g.; curve 2 for −78°; multiply ordinate by 10^{-4} for moles/g.

440 μmoles per g. For both the non-porous silica and the silica gel it was found that the tightly-held NO could be removed intact by heating and in amounts corresponding to that expected from the hysteresis loop of the isotherm. It is interesting to note that some NO is "chemisorbed" on these samples of SiO_2, but the amount does not seem to be related in any simple way to the nature of the surface. The adsorption isotherms appear to be normal and the one published by Briner and Sguaitamatti showing an enormous increase in adsorption at a pressure of 300–400 mm. at −78° seems very improbable. Their isotherm was based on only 4 points determined by a gravimetric method, and no points are given for pressures below 300 mm.

It was observed under certain conditions, in agreement with Briner and Sguaitamatti, that silica gel with its adsorbed NO is brick-red in color at −78°. If, starting at a pressure of 600 mm., the temperature is allowed to rise and the NO to escape, the color weakens, changes to an olive green and then to colorless. If one starts at −78° and a pressure of 1 mm. the color is initially a pale olive green which changes to colorless as the temperature rises. At a pressure of 600 mm. the silica

(8) J. Perreu, *Compt. rend.*, **226**, 907 (1948).

(9) H. E. Bull and W. E. Garner *Nature*, **124**, 409 (1929).

(10) E. Briner and B. Sguaitamatti, *Helv. Chim. Acta*, **23**, 1216 (1940).

gel contains 1.25 mmoles per gram, while at a pressure of 1 mm. it contains 0.035 mmole per gram. The non-porous SiO_2 holds 0.35 mmole per gram at 500 mm. pressure and is absolutely colorless (white) just as it is at 1 mm. pressure where it holds 0.01 mmole per gram. Briner and Sguaitamatti ascribe this coloration in the gel to the color of the dimer, but NO when at temperatures above its boiling point (and not adsorbed) is a monomer.[7] Thus, it seems unlikely that there will be any significant amount of N_2O_2 at a low pressure at $-78°$ (which is 72° higher than the boiling point and 16° above the critical temperature.) It is also difficult to explain why the NO would be adsorbed as N_2O_2 on the gel and yet only as NO on the non-porous SiO_2, with the amounts adsorbed being of the same order of magnitude. It seems more likely that the NO is in some way bound with some of the water which is present in the gel (and which is not present in the non-porous silica) and that it is this water-bound NO which is the cause of the color. After the usual outgassing (300° for 2 hours) a sample of silica gel still retains 3.7% water, as judged by weight loss after further outgassing for one half hour at 1000°. When exposed to a nitric oxide pressure of 640 mm. at $-78°$, this sample showed only a faintly reddish color. After the sample had been heated to about 1400° *in vacuo* it was exposed to a nitric oxide pressure of 550 mm. at $-78°$; its color was then only an olive green. These qualitative tests do not show conclusively that the red coloration is due to the presence of water, for at the same time the water was removed the gel was doubtless sintered to a considerable extent. It does seem more reasonable, however, to associate this phenomenon with the water than with the presence of pores.

GOUY DIFFUSION STUDIES OF BOVINE SERUM ALBUMIN[1]

BY MYRON L. WAGNER AND HAROLD A. SCHERAGA

Department of Chemistry, Cornell University, Ithaca, N. Y.

Received March 13, 1956

In conjunction with studies of the hydrodynamic properties of proteins, diffusion coefficients have been obtained by the Gouy method (making use of Rayleigh interference patterns to determine the total number of fringes). The satisfactory performance of the Spinco Model H apparatus for this purpose was established by the excellent precision, and good agreement with literature values, obtained in diffusion runs on sucrose at 1°. The use of the cylindrical lens to obtain a threefold magnification of the Gouy pattern, and the passage of the light beam twice through the diffusion cell, as well as other novel features of the instrument appear to be satisfactory. Accordingly, a study of bovine serum albumin in 0.5 *M* KCl at *p*H 5.14 has been carried out in the mean concentration range of 0.25 to 1.25% as part of a program to relate the hydrodynamic properties of albumin to its reactivity. Extrapolation to zero concentration yielded a value for the diffusion coefficient of 3.261 ± 0.004 Fick units (1 Fick unit = 10^{-7} cm.^{2}/sec.) at 1° in 0.5 *M* KCl at *p*H 5.14. The effect of heterogeneity on the diffusion coefficient has been discussed. It is concluded that the presence of 2 to 3% of a second component having a diffusion coefficient 1.5 times smaller than that of albumin is compatible with the diffusion data and also sedimentation data on the same samples.

Introduction

Recent considerations of the hydrodynamic properties of proteins[2] have indicated the need for high precision in order to be able to interpret data obtained from measurements of intrinsic viscosity, sedimentation, diffusion, flow birefringence, etc. Appropriate combinations of pairs of data, such as intrinsic viscosity and translational frictional coefficient provide a basis for computing the size and shape of an equivalent hydrodynamic ellipsoid for the protein molecule. Since good precision is obtainable in viscosity measurements, our attention is centered here on the determination of precise translational frictional coefficients of proteins from diffusion measurements in dilute solution. If the *solvent* consists of more than one component, it is preferable to obtain the frictional coefficient from diffusion, rather than from sedimentation measurements, since the former technique does not involve the partial specific volume problem present in sedimentation, as has been discussed recently.[3]

Bovine serum albumin has been chosen for this study because it appears that its configuration plays an important role in determining its reactivity (*e.g.*, binding of hydrogen and other small ions). At present, the reactivity of this molecule is known to be anomalous at low and high *p*H.[4,5] These anomalies could arise either from changes in molecular size and shape,[4] or from reversible formation and breakage of internal hydrogen bonds,[6] or from a combination of both of these effects. It appeared that this question could be resolved by an investigation of the effect of *p*H on the size and shape of the equivalent hydrodynamic ellipsoid of bovine serum albumin. Due to complications from heterogeneity[7] at low and high *p*H, and to

(1) This investigation was supported by grant NSF G-507 from the National Science Foundation and by Grant H-1662 from the National Heart Institute of the National Institutes of Health, Public Health Service.

(2) H. A. Scheraga and L. Mandelkern, *J. Am. Chem. Soc.*, **75**, 179 (1953).

(3) H. A. Scheraga, W. R. Carroll, L. F. Nims, E. Sutton, J. K. Backus and J. M. Saunders, *J. Polymer Sci.*, **14**, 427 (1954).

(4) C. Tanford, J. G. Buzzell, D. G. Rands and S. A. Swanson, *J. Am. Chem. Soc.*, **77**, 6421 (1955).

(5) I. M. Klotz and J. Ayers, *Disc. Faraday Soc.*, **13**, 189 (1953).

(6) M. Laskowski, Jr., and H. A. Scheraga, *J. Am. Chem. Soc.*, **76**, 6305 (1954).

(7) (a) H. A. Saroff, G. I. Loeb and H. A. Scheraga, *ibid.*, **77**, 2908 (1955); (b) P. Bro, S. J. Singer and J. M. Sturtevant, *ibid.*, **77**, 4924 (1955).

charge effects, this initial study has been confined to the isoionic protein.

Gosting, Kegeles, Longsworth and others have developed the theory and experimental techniques for Gouy diffusiometry and have shown that the diffusion coefficients of small molecules can be determined with a precision of the order of $\pm 0.1\%$.[8-15] Akeley and Gosting[16] have applied this method to systems containing two diffusing solutes and also to a solution of serum albumin at a single concentration with results of comparable precision.[17]

In the present work the Gouy optical system of the Spinco Model H electrophoresis-diffusion apparatus has been used to study first the well characterized sucrose diffusion at a single concentration and then the diffusion of isoionic bovine serum albumin over a range of concentrations. The results indicate that a precision of about $\pm 0.2\%$ is obtainable for both sucrose and protein diffusion coefficients.

Theory

The following aspects of the theory[8,9,14,16] underlying the study of diffusion by means of Gouy interferometry are required for interpretation of the data to be presented here.

For a system containing q diffusing solutes designated as $k = 1, 2, 3, \ldots, q$, the relative distance in the focal plane from the position of the undeviated slit image to each intensity zero of the Gouy fringe pattern is given by equation 6 of reference 16.

$$\frac{Y_j}{C_t} = \frac{\sum_{k=1}^{q} (\alpha_k/\sqrt{D_k})\, e^{-z^2_{jk}}}{\sum_{k=1}^{q} (\alpha_k/\sqrt{D_k})} \qquad (1)$$

where Y_j is the measured downward displacement at time t of the jth intensity zero ($j = 0, 1, 2 \ldots$) and α_k is the solute fraction expressed in terms of refractive index.[16] C_t is the maximum displacement of light at time t and is determinable by analytical or extrapolation procedures to be described below; D_k is the diffusion coefficient of the kth solute and z is the "reduced height" defined by[16]

$$z_{jk} = x_j/2\sqrt{D_k t} \qquad (2)$$

the cell coördinate, x, being taken as positive downward, with $x = 0$ being the position of the starting boundary.

The total number of fringes, j_m, is given by[10,16]

$$j_m = \frac{a \sum_{i=1}^{q} \Delta n_i}{\lambda} \qquad (3)$$

$$= I + F \qquad (3a)$$

where a is the path length of light through the solution in the cell (being twice the cell thickness in the Spinco apparatus because of the passage of the light beam through the cell twice), λ is the wave length of light used, Δn_i is the change in refractive index due to the difference in the concentrations of the ith solute across the initially sharp boundary, I is the integral number of intensity zeros and F is the fractional number of fringes as obtained by the fractional displacement of Rayleigh interference fringes across the boundary. In practice, j_m is obtained from equation 3a rather than from equation 3. Thus, the values of a and Δn_i need not be known.

The interference condition for intensity zeros is given by[16]

$$f(\zeta_j) = \sum_{k=1}^{q} \alpha_k f(z_{jk}) = \frac{(j + 3/4 + \ldots.)}{j_m} \sim \frac{Z_j}{j_m} \qquad (4)$$

where Z_j is the Airy integral approximation, valid for large j_m (>50), of the series expansion[20] $(j + {}^3/_4 + \ldots)$. The function $f(\zeta_j)$ is defined by the first equality, and $f(z_{jk})$ is defined by[16]

$$f(z_{jk}) = (2/\sqrt{\pi}) \left[\int_0^{z_{jk}} e^{-\beta^2}\, d\beta - z_{jk}\, e^{-z^2_{jk}} \right] \qquad (5)$$

The height–area average diffusion coefficient, D_A, is given by[16]

$$D_A = \left[\sum_{k=1}^{q} \alpha_k/\sqrt{D_k} \right]^{-2} \qquad (6)$$

which is obtained from

$$D_A = \frac{(j_m \lambda b)^2}{4\pi C_t^2 t} \qquad (7)$$

where b is, in the Spinco Model H apparatus, the distance from the Schlieren lens to the plane of the diaphragm (see Experimental section).

For single solute diffusion, where $\alpha_1 = 1$, equations 1, 3, 4, 6 and 7 reduce to

$$\frac{Y_j}{C_t} = e^{-z^2_j} \qquad (8)$$

$$j_m = \frac{a\Delta n}{\lambda} = I + F \qquad (9)$$

$$f(\zeta_j) = f(z_j) = \frac{(j + 3/4 + \cdots)}{j_m} \sim \frac{Z_j}{j_m} \qquad (10)$$

$$D_A = D = \frac{(j_m \lambda b)^2}{4\pi C_t^2 t} \qquad (11)$$

The Gouy pattern is created in the following manner in order to obtain the diffusion coefficient from the above equations. The "zero" intensity (*i.e.*, dark) fringes are indexed by $j = 0, 1, 2, \ldots$, the value of $j = 0$ being assigned to the most deviated dark fringe. Also, the distance Y_j of each fringe from the position of the image of the undeviated

(8) L. G. Longsworth, *J. Am. Chem. Soc.*, **69**, 2510 (1947).
(9) C. Kegeles and L. J. Gosting, *ibid.*, **69**, 2516 (1947).
(10) L. J. Gosting and M. S. Morris, *ibid.*, **71**, 1998 (1949).
(11) L. J. Gosting, *ibid.*, **72**, 4418 (1950).
(12) M. S. Lyons and J. V. Thomas, *ibid.*, **72**, 4506 (1950).
(13) L. J. Gosting and D. F. Akeley, *ibid.*, **74**, 2058 (1952).
(14) L. J. Gosting and L. Onsager, *ibid.*, **74**, 6066 (1952).
(15) P. J. Dunlop and L. J. Gosting, *ibid.*, **75**, 5073 (1953).
(16) D. F. Akeley and L. J. Gosting, *ibid.*, **75**, 5685 (1953).
(17) More recently, the theory of Gouy diffusiometry has been extended to systems of three or more components in which the flows interact.[18,19]
(18) R. L. Baldwin, P. J. Dunlop and L. J. Gosting, *J. Am. Chem. Soc.*, **77**, 5235 (1955).
(19) P. J. Dunlop and L. J. Gosting, *ibid.*, **77**, 5238 (1955).
(20) Gosting and Onsager[14] have obtained a refinement of the Airy integral approximation which they call the "saddle-point interference condition." This refinement has not been used here since, as has been pointed out by Gosting and Onsager, it is necessary that it be used only for values of j very near to j_m and is needed only in very precise work. It will be shown later that the precision obtained in the present work is not sufficient to warrant its use.

slit is measured. The values of Z_j corresponding to each j-value are obtained from Table I of reference 10. The value of j_m (constant during a given run) is determined from the Rayleigh interference pattern; the integral number of fringes I is obtained from a Rayleigh photograph taken at the end of a run where the Rayleigh fringes are resolved, while the fractional number of fringes F is obtained from a Rayleigh photograph taken at the start of a run, the procedure for determining F being described at the end of the Experimental section. Then, from equation 10, $f(z_j)$ is computed for each j-value. Values of $f(z_j)$ are converted to $e^{-z^2_j}$ using Table I of reference 9. Since linear interpolation in this table is not sufficiently precise we have computed a larger number of entries by means of equation 5. Measured values of Y_j, together with their corresponding $e^{-z^2_j}$ values, yield the value of C_t by means of equation 8. Ideally, C_t, for a single solute diffusion, should be constant for all j at any given time t. In practice, however, it is sufficient[10] to take the average value of C_t calculated from the fringes numbered $j = 1, 2 \ldots 0.25\, j_m$. This value of C_t, used in equation 11, leads to the value of D.

Since the initial boundary is not *ideally* sharp, the time intervals are designated as t' with $t' = 0$ being the time at which the run began. A small disturbance in the boundary at $t' = 0$ means essentially that diffusion has already taken place[8] for an increment of time Δt. The true time, t, of diffusion is therefore

$$t = t' + \Delta t \qquad (12)$$

and the diffusion coefficient, calculated from

$$D' = \frac{(j_m \lambda b)^2}{4\pi C_t^2 l'} \qquad (13)$$

is related to the true diffusion coefficient D by

$$D' = D\left(1 + \frac{\Delta t}{t'}\right) \qquad (14)$$

D and Δt can readily be obtained from a linear plot of D' *vs.* $1/t'$.

The diffusion coefficient at infinite dilution is obtained from the intercept of a plot of D *vs.* the average concentration $\bar{c}$, defined as $(c_A + c_B)/2$, where c_A and c_B are the solute concentrations at $t = 0$ on the upper and lower sides of the boundary, respectively.

For a system of more than one solute, Akeley and Gosting[16] have pointed out that equations 1 and 4 indicate that values of $e^{-\zeta_i^2}$ corresponding to $f(\zeta_j)$ are not equal to Y_j/C_t but represent relative fringe displacements from a single-solute diffusion with the same j_m. They have, therefore, defined the relative fringe deviation as an easily measurable quantity for studying the diffusion of mixtures.

$$\Omega_j = e^{-\zeta_i^2} - Y_j/C_t \qquad (15)$$

Ω_j is a measure of the departure of the boundary from Gaussian form due to the presence of additional solutes. Akeley and Gosting have shown that in multi-component systems equation 15 can be put in the limiting form

$$\frac{Y_j}{e^{-\zeta_i^2}} = C_t - mZ^{2/3} \qquad (16)$$

valid as $\zeta \to 0$ (*i.e.*, for the lower fringes) and for small Ω_j (*i.e.*, for a solute having only a small amount of impurity). The constant m need not be determined since the value of C_t is obtained as the intercept of a plot of $Y_j/e^{-\zeta^2_j}$ *vs.* $Z_j^{2/3}$. Using the value of C_t determined in this manner, equation 15 permits the construction of a plot of Ω_j *vs.* $f(\zeta_j)$ which is useful for the analysis of mixed-solute diffusion as shown below.

The theoretical dependence of Ω_j on $f(\zeta_j)$ for a system involving only two diffusing solutes with α_2 being small, has been expressed as[16]

$$\Omega_j = \alpha_2 F(\zeta_j, r_2) - \alpha_2^2 G(\zeta_j, r_2) + \ldots \qquad (17)$$

where $r_2 = D_1/D_2$ and $F(\zeta_j, r_2)$ and $G(\zeta_j, r_2)$ are defined in reference 16. Values of these latter functions have been calculated[16] for various $f(\zeta_j)$ and r_2. The validity of equation 17 has been very successfully demonstrated by Akeley and Gosting[16] and by Dunlop and Gosting[19] using systems in which known amounts of well characterized components were allowed to diffuse simultaneously. Where neither α_2 nor r_2 are known, as will usually be the case in protein diffusion, those values which will enable equation 17 to best fit the experimental Ω_j *vs.* $f(\zeta_j)$ curve are found by successive approximation. It may be mentioned that theory[16] and experiment[21] indicate that Ω_j approaches zero as r_2 approaches unity, regardless of the relative amounts of the two components present.

Experimental

Materials and Solutions.—Mallinckrodt analytical reagent sucrose was used without further purification. The sucrose solutions were aerated for 10 minutes at 1°, the temperature of diffusion, prior to being used.

Armour's Crystallized Bovine Plasma Albumin, lot N67009 was used in the protein diffusion. Protein solutions were prepared by dissolving sufficient albumin in 0.5 *M* KCl to give a concentration of about 2–3 g./100 cc. These solutions were then dialyzed against 0.5 *M* KCl in a rocking dialyzer at about 2–4°. The solutions outside the bag were changed after about 4 and 12 hours, and then allowed to equilibrate for 12–14 hours. Upon completion of the dialysis, a small amount of stock solution (*p*H 5.14) was brought to room temperature, pipetted into a tared weighing bottle, and placed in an oven (102–107°) to dry. After 24 hr., the weighing bottle was reweighed. The concentration calculated from this single 24 hr. weight was used in preparing solutions of the desired concentrations to be used in the diffusion runs. Subsequent heatings and weighings provided some small changes in the calculated concentrations,[22] but in most cases the 24 hr. drying period was sufficient to bring the residue to a constant weight. The protein solutions were, of course, not aerated but it is believed that they became sufficiently air-saturated during the course of the dialysis.

Mallinckrodt analytical reagent KCl was used without further purification. Conductivity water was used for all solutions.

The following density and viscosity data were used for reducing diffusion coefficients to standard conditions.

Diffusion Apparatus.—The diffusion experiments were carried out at 1.00 ± 0.005° with the Spinco Model H apparatus, which contains a rotatable turret on which the cell racks are mounted in the constant temperature bath enabling three runs to be made simultaneously. The cells are of the conventional Tiselius type with Rayleigh side arms, and each cell fits into its own cell rack with a clearance of not

(21) P. J. Dunlop, *J. Am. Chem. Soc.*, **77**, 2994 (1955).

(22) All protein concentrations were determined and are given at room temperature and, since the diffusion was carried out at 1°, are in error by about 0.3%. The dependence of the diffusion coefficient on concentration is, however, so small ($\Delta D/\Delta \bar{c} = 0.034 \times 10^{-7}$ for $\bar{c}$ in g./100 cc.) that the 0.3% error in $\bar{c}$ is negligible.

Temp., °C.	1	20	25
	0.5 *M* KCl		
Density,[a] g./cc.	1.0244	1.0216	1.0203
Viscosity coefficient,[b] poise	0.01655	0.00994	0.00888
	H_2O		
Viscosity coefficient,[c] poise	0.01726	0.01002	0.00891

[a] "International Critical Tables," Vol. 3, McGraw-Hill Book Co., New York, N. Y., 1933, p. 87. [b] Ref. *a*, Vol. 5, p. 17, 1933. [c] "Handbook of Chemistry and Physics," 36th ed., 1954–55, pp. 2001–2.

more than 0.002″ in any direction. The minimum speed of rotation of the turret is 0.04 to 0.05 r.p.m. in either direction.

The diffusion cells are constructed from Schott Heavy Crown glass (Schott and Genossen, Jenaer Glasswerke, Jena) and are sufficiently uniform so that the Rayleigh fringes are straight within 0.1 of the fringe separation or better over the whole length of the cell window.

The optical system has all the required components for use as either a Schlieren, Rayleigh or Gouy diffusiometer (see Fig. 1). The light source is an AH-4 mercury lamp and the green line of mercury (5460.7 Å. in air) is isolated by means of a Wratten G 15 filter used in combination with a three-step didymium filter. The slit assembly contains a vertical slit for use with Rayleigh optics and horizontal slits for use with Gouy or Schlieren optics. The desired slit may be positioned by sliding the slit assembly into either of two positions against metal stops.

Also located in the bath, on a stationary post which supports the turret, is a first surface bath mirror which is located directly behind the diffusion cell when the cell is in the optical path. The bath mirror reflects the light back through the cell, bath window and Schlieren lens to another first surface mirror located immediately in front of and slightly below the slit (see Fig. 1). From this latter mirror, the light is reflected to the Schlieren diaphragm. It is in the plane of this diaphragm that the Schlieren lens focuses the image of the slit. The distance in air between the exit principal plane of the Schlieren lens and the diaphragm is the "optical lever arm" b, which in our instrument is equal to 152.8 cm.

Below the diaphragm is a camera lens which focuses the image of the cell on the photographic film at unit magnification. The cylindrical lens, located below the camera lens, magnifies the diaphragm by a factor of about 3.2. This lens may be rotated through 90° between two metal stops for alternative use in Gouy or Rayleigh (plus Schlieren) optics.

To determine the magnification factor of the camera lens, a glass mm. scale is placed in a special scale mount on a cell rack on the turret. The axis of the cylindrical lens is set perpendicular to the scale lines. With this arrangement, the only magnification recorded at the camera is the magnification of the camera lens. The magnification of the cylindrical lens is obtained by placing the mm. scale in the plane of the diaphragm with the scale lines parallel to the axis of the cylindrical lens. Magnification photos were obtained before each run, the factor calculated for each run being used for that run alone. However, the average magnification factors were 3.2069 and 1.0002 for the cylindrical and camera lenses, respectively, with a variation of about ±0.06% over a period of several months. The magnification factor of the camera lens was the same for all 3 positions of the turret as judged by the distances 5.5900, 5.5900 and 5.5897 cm. obtained from photographs of a given pair of scale lines. These values are identical within the precision of the measurements (±0.001 cm.).

Boundary Stability.—The stability of the boundary during rotation of the turret was ascertained by rotation of the turret at various speeds during a sucrose diffusion run. Comparison of the values of $1/C_i^2t$ after each movement of the turret ($0.9636 \times 10^{-4} \pm 0.0014 \times 10^{-4}$ cm.$^{-2}$ sec.$^{-1}$) with values obtained before rotation ($0.9624 \times 10^{-4} \pm 0.0008 \times 10^{-4}$ cm.$^{-2}$ sec.$^{-1}$) indicates that *careful* rotation does not disturb the diffusion boundary. Subsequent experiments with albumin bore out the validity of this conclusion.

Cell Masking.—Masking of the cell is accomplished by means of two bath masks The first, which clips onto the cell proper, contains a pair of vertical slits for each limb of the cell. This mask, when used in conjunction with the vertical light source slit, produces the familiar Rayleigh double-slit interference pattern required for the determination of the total number of fringes. The second mask, shown in part in Fig. 2, is used both to locate the center of the optic axis for boundary sharpening purposes, and for Gouy photographs during the course of the run. This mask is suspended in position with the central, fixed, vertical slit of A in front of the solution chamber of the cell. The two pair of horizontal slits permit light to pass through either the right or left reference window of the cell, depending on which limb is being used. The sliding V-shaped jaws,[23] B, can be made to converge on the optic axis designated by the dashed line, and are used to reduce the amount of undeviated light passing through those portions of the cell above and below the boundary that contain homogeneous solution.

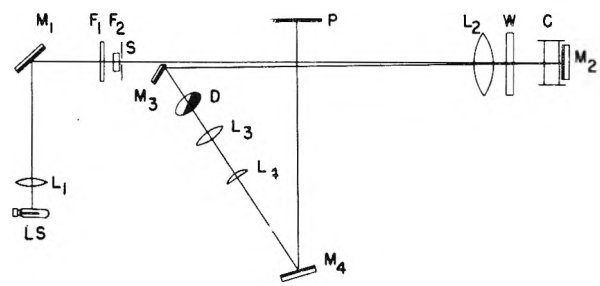

Fig. 1.—Sketch of optical path in Spinco Model H diffusion apparatus: LS, light source; L_1, condensing lens; M_1, first surface mirror; F_1, Wratten G15 filter; F_2, didymium filter; S, slit assembly; L_2, Schlieren lens; W, bath window; C, diffusion cell; M_2, first surface bath mirror; M_3, first surface mirror; D Schlieren diaphragm or analyzer; L_3, camera lens; L_4, cylindrical lens; M_4, first surface focusing mirror; P, plane of photographic film (camera). Sketch is not to scale.

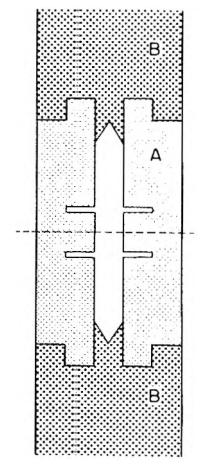

Fig. 2.—Portion of Gouy mask. The movable sections B lie over the fixed section A. The v-shaped jaws in sections B can be made to converge on the optic axis indicated by the dashed line. The horizontal slits in A enable one to obtain Gouy reference fringes through the bath water.

Comparator.—The comparator used for measuring the photographic film was a modification of that described by Longsworth[24] and was designed to project an enlarged image of the fringe pattern onto a flat white screen having a cross-hair ruled on it. The film was driven by a calibrated screw

(23) Gosting and Onsager[11] have calculated the effect of various geometrical shapes for the jaws of the Gouy mask. Ours is not the ideal shape for minimum interference of the Gouy pattern due to diffraction from the edges of the mask but, by keeping the jaws well separated and in a region where $dn/dx \sim 0$, this interference has been minimized. We have, in fact, kept the separation of the jaws ≧ twice the width of the boundary as estimated from the Schlieren pattern in accordance with the suggestion of Longsworth.[8]

(24) L. G. Longsworth, *J. Am. Chem. Soc.*, **74**, 4155 (1952).

so that the image passed over the fixed cross-hair. In this manner no error was introduced due to possible aberrations in the lens. For convenience in reading the photographic plates, magnifications of the order of 20× to 30× were used. It was found necessary to calibrate the precision screw of the comparator. This was done by reading the distance between the mm. lines on a 9 cm. glass scale both on our comparator and on another comparator[25] which was known to be accurate to 0.0001 cm. per centimeter of length. From these data, a calibration curve was constructed which allowed readings to be made with a precision of ±10 μ or less. This seems quite large but, remembering that all Gouy photographs are magnified by the 3.2 factor of the cylindrical lens, this corresponds to a precision of about 3 μ when reduced to dimensions in the plane of the diaphragm.

Procedure.—The cells were filled by adding enough of the more dense solution to bring the menisci to about the center of the two limbs of the center cell section. In order to avoid contamination, the first solution was added through the right limb, the boundary being formed subsequently in the left limb. The cell was then partially immersed in the constant temperature bath to bring the solution to the temperature of the diffusion run before closing the bottom section. With the bottom section closed, the less dense solution was then carefully layered on top of the meniscus in the left limb. Slow addition of the solution was continued until the left limb was filled up to the bottom of the top cell section. The right limb was similarly filled with the *more* dense solution. The top section was then closed and its right and left limbs filled to the same height with the more dense and less dense solutions, respectively. With this technique, the mixing at the boundary could be kept down to a centimeter or less (as judged by the Schlieren pattern) which reduced the need for extensive rinsing of the cell windows during the boundary sharpening procedure.[3] The double-slit Rayleigh mask was then positioned in front of the cell, the cell and rack were placed on the turret, and the top and bottom sections were opened.

In order to sharpen the boundary in the region of the optic axis, the Gouy mask was placed in position and the jaws were almost completely closed, thus allowing only a very narrow strip of light to pass through the cell. This narrow strip of light coincides with the optic axis of the instrument. A magnifying (7×) ocular was placed at the camera and the position of the narrow light strip was noted on the scale of the ocular. This scale is 2 cm. long and is graduated in 0.1 mm. Without moving the ocular, the Gouy mask was removed and the boundary sharpening needle (0.2 mm. inside diameter) was lowered slowly until its tip was in the same position as the Gouy mask slit had been previously. In this manner, the boundary was formed within a few tenths of a mm. of the optic axis, which is well within the 1 mm. limit suggested by Longsworth.[8]

The boundary sharpening needle is connected to a syringe whose plunger may be controlled automatically at variable speeds. In sharpening a protein boundary, 20 cc. was first withdrawn at a relatively fast rate, less than 10 cc. being sufficient to completely renew the solution in the limb being used. After 10–15 min., another 10 cc. was withdrawn at a slower rate (~0.5 cc./min.). After an additional wait of 10–15 min., a final 10 cc. was withdrawn at the slower rate; the syphoning was then stopped and the electric timer simultaneously started, initiating the run. The bottom section of the cell was then closed, the capillary was removed and the limbs of the top section were covered to prevent evaporation.

In the event that two or three runs were to proceed at the same time, the following procedure was employed. The first cell was filled and placed in position. Boundary sharpening in this first cell was allowed to proceed while the second cell was being filled and placed in the bath. The capillary was then removed from the first cell, rinsed and lowered into the second cell where sharpening proceeded while the third cell was filled and placed in the bath. After a preliminary sharpening of the third boundary, each boundary was sharpened a second time and then a third time after which the runs were initiated as previously described. This procedure eliminated having to place a cell rack on the turret when other runs were in progress.

(25) We are grateful to C. W. Gartlein of the Physics Dept. for making this comparator available to us.

Rayleigh photographs were taken within the first three to four minutes of the run, after which the optics and mask were arranged to give the Gouy interference pattern. Since the only means of controlling the intensity of the interference pattern were the step filters at the slit and the jaws on the mask, at no time was it possible to completely resolve the fringes adjacent to the *undeviated* image of the slit. For example, in a typical sucrose run 99 of the 101 fringes were resolvable. However, this presented no problem in establishing the exact number of fringes since this was easily obtained from a Rayleigh photograph taken after the run was completed. To obtain Y_j, however, the position of the undeviated slit image had to be known. It was noted that the intense light at the slit image formed a "spike" which was projected perpendicular to the interference pattern (see Fig. 3). It has been assumed in this work that the center of this spike represents the center of the undeviated slit. This appears justified since most of the intensity of light in this region is due to undeviated light. The fact that the deviated light is not symmetrical about this position but is displaced only in one direction may move the spike slightly off the center of the undeviated slit image. If this effect existed, one would expect the position of the "spike" relative to the reference slit, *i.e.*, δ, to vary with

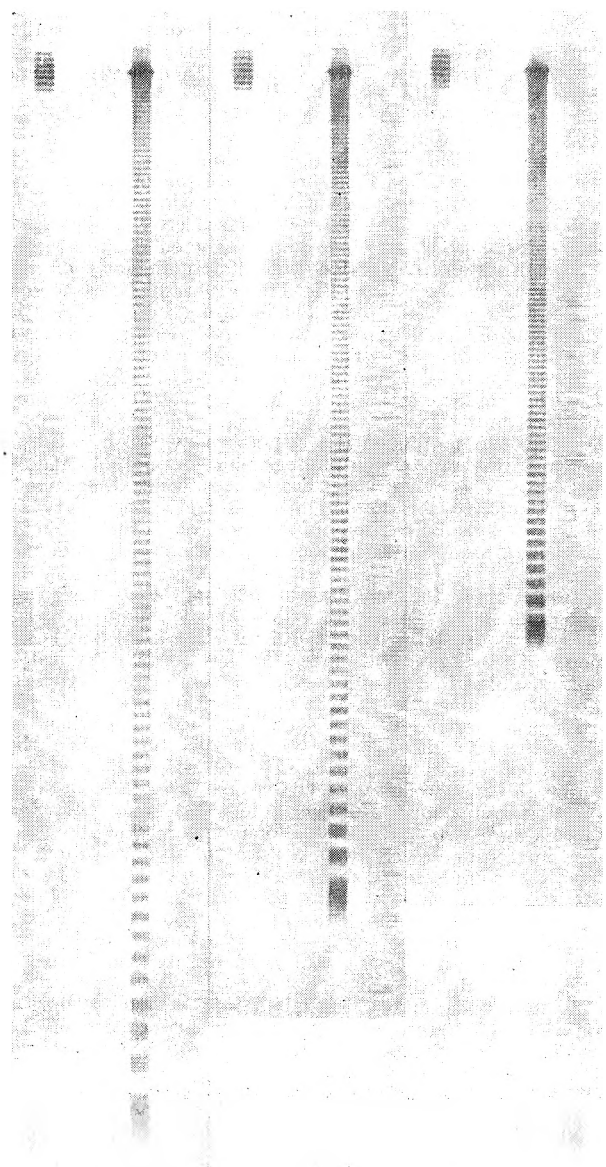

A B C

Fig. 3.—Typical photos of Gouy interference fringes from a sucrose run. These photos were taken, from left to right, at $t' = 4628$, 7458, and 16408 sec., respectively.

time, since an increasing amount of light is deviated from the position of the undeviated slit image as the run proceeds. In a typical sucrose run the value of δ was found to be 16 μ throughout the entire run with a random variation of only ± 2 μ which is within the error of reading the plates. Further evidence of the validity of using the spike as the center of the undeviated slit is shown in Fig. 4. Here, curve B was calculated with $\delta = 16$ μ, the experimentally determined value. Curves A and C were calculated with $\delta = 6$ and 26 μ, respectively. For high values of j, curve B drops off slightly which may be due to a small error in δ ($\sim$2–3 μ) or to a defect in the optics (to be discussed later). In the region of $j < 50$, however, the measured value of 16 μ for δ gives a constant value of $Y_j/e^{-z_j^2}$ as it should, while there is a definite slope at low j-values, in both curves A and C. It might also be mentioned that, by keeping the mask jaws well apart more undeviated light is admitted to the film which would again serve to minimize any deviation of the spike from the center of the slit image.

Photographs of the interference patterns were recorded on two types of film. Rayleigh fringes were photographed on Kodak contrast process type B panchromatic 4″ × 5″ sheet film which is a slow, high contrast film. Gouy patterns were recorded on Kodak Royal Pan 4″ × 5″ sheet film which is a fast, fine grain film of moderate contrast. At any given time three photos were taken using different time exposures for each. The photo with the best contrast and "readability" was used to calculate D'. Reproducibility of scale photos and the comparison of air-dried with fan-dried film provided sufficient evidence that either there was no shrinkage of the film or that the shrinkage was the same on all sheets.

The fractional number of fringes, F, was determined by measuring the displacement of the Rayleigh fringes across the initially sharp boundary. The readings of the fringe position at various heights above and below the boundary are plotted as in Fig. 5. The straight lines drawn through the points on either side of the boundary provide a convenient means of determining the displacement across the boundary to within 0.02–0.03 fringe. Additional advantages to this method are that accurate alignment of photographic plates in the comparator is not essential and the optical quality of the cell in the region of the optic axis can be observed.

Results

Sucrose.—Before evaluating the results of the protein diffusion experiments it is worthwhile first to compare the data obtained from the diffusion of sucrose with those reported in the literature. In a particular sucrose run at 1°, $c_A = 0.000$ g./100 cc. and $c_B = 0.750$ g./100 cc., giving $\bar{c} = 0.375$ g./100 cc. and $\Delta c = 0.750$ g./100 cc. The value of j_m was 101.07 ± 0.02. The measured values of Y_j (corrected by a factor of $\delta = 0.0016$ cm.) are listed in Table I for one photo near the beginning, one near the middle and one near the end of the run. The corresponding values of $Y_j/e^{-z_j^2}$ which, in single solute diffusion, should be constant for all j at any given time, are also shown in this table. Figure 6 shows a plot of $Y_j/e^{-z_j^2}$ *vs.* j for these three photos. It can be seen that there is a slight slope in the region of $j < 60$ and an appreciable decrease in $Y_j/e^{-z_j^2}$ for $j > 60$. The initial slope is very small, being positive near the beginning of the run, passing through zero and becoming slightly negative near the end of the run. The exact reason for this is not known but it has been observed elsewhere. For example, Riley and Lyons[26] have encountered a greater than normal shift in Y/c^{-z^2} near the beginning of diffusion runs and have attributed it primarily to a non-Gaussian boundary which remains for some time after boundary sharpening. Gosting and Morris[10] have given some data for a sucrose run where $\bar{c} = 3.7543$ g./100 cc., $\Delta c = 1.5018$ g./100 cc., and $j_m = 100.21$. Their values

(26) J. F. Riley and P. A. Lyons, *J. Am. Chem. Soc.*, **77**, 261 (1955).

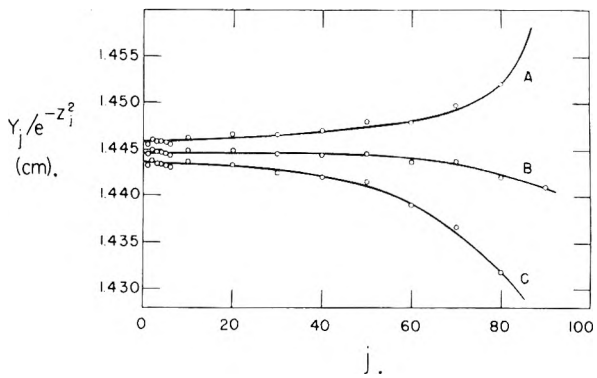

Fig. 4.—Effect of an error of ± 10 μ in δ on the value of $Y_j/e^{-z_j^2}$. Curve B was calculated with the measured value of $\delta = 16$ μ. Curves A and C were calculated with $\delta = 6$ and 26 μ, respectively.

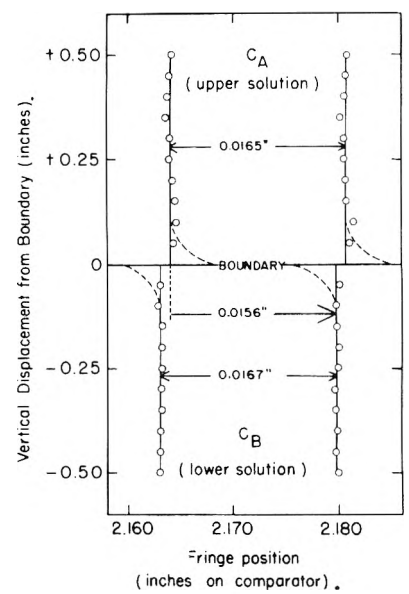

Fig. 5.—Plot for F determination in a typical albumin run. Average fringe separation, 0.0166″. Lateral displacement from c_A to c_B, 0.0156″. $F = 0.0156/0.0166 = 0.94$. The large arrow indicates the direction of the displacement. The dashed lines indicate the Rayleigh fringe position at a time subsequent to that indicated in the figure.

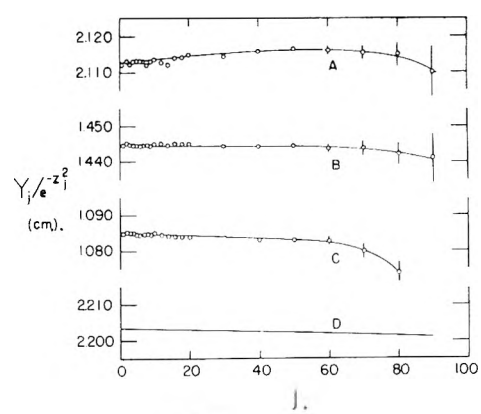

Fig. 6.—Values of $Y_j/e^{-z_j^2}$ for various j in a sucrose run: curve A, $t' = 5258$ sec.; curve B, $t' = 11298$ sec.; curve C, $t' = 20028$ sec.; curve D, data of Gosting and Morris[10] (see text).

TABLE I

GOUY DIFFUSION DATA FOR SUCROSE AT 1° ($\bar{c}$ = 0.375 g./100 cc., j_m = 101.07)

	Photo no. 2 t' = 5258 sec.; C_t = 2.1129 cm.[a]			Photo no. 6 t' = 11298 sec.; C_t = 1.4446 cm.[a]			Photo no. 8 t' = 20028 sec.; C_t = 1.0847 cm.[a]		
	Y_j (cm.)	$Y_j/e^{-z_j^2}$ (cm.)	$\Omega \times 10^4$	Y_j (cm.)	$Y_j/e^{-z_j^2}$ (cm.)	$\Omega \times 10^4$	Y_j (cm.)	$Y_j/e^{-z_j^2}$ (cm.)	$\Omega \times 10^4$
0	2.0165	2.1132	−2	1.3783	1.4445	+1	1.0349	1.0845	+1
1	1.9427	2.1120	+4	1.3286	1.4445	+1	0.9977	1.0847	0
2	1.8845	2.1131	−1	1.2886	1.4449	−2	.9676	1.0850	−2
3	1.8325	2.1124	+2	1.2532	1.4447	0	.9410	1.0848	0
4	1.7861	2.1132	−1	1.2210	1.4446	0	.9169	1.0848	−1
5	1.7422	2.1128	+1	1.1911	1.4445	+1	.8943	1.0845	+1
6	1.7016	2.1134	−1	1.1629	1.4443	+2	.8732	1.0845	+2
7	1.6624	2.1131	−1	1.1363	1.4444	+1	.8533	1.0847	0
8	1.6252	2.1124	+2	1.1114	1.4446	+1	.8346	1.0848	0
9	1.5904	2.1132	−1	1.0870	1.4443	+1	.8163	1.0846	0
10	1.5564	2.1136	−2	1.0640	1.4449	−1	.7989	1.0849	−1
12	1.4911	2.1127	+1	1.0198	1.4450	−1	.7653	1.0843	+3
14	1.4297	2.1120	+4	0.9779	1.4446	+1	.7337	1.0839	+6
16	1.3732	2.1139	−3	.9387	1.4450	−2	.7042	1.0841	+4
18	1.3182	2.1143	−4	.9009	1.4449	−1	.6759	1.0841	+4
20	1.2657	2.1149	−5	.8648	1.4449	−1	.6487	1.0839	+5
30	1.0284	2.1146	−4	.7025	1.4445	0	.5270	1.0836	+5
40	0.8249	2.1161	−6	.5631	1.4444	0	.4223	1.0831	+5
50	.6447	2.1166	−7	.4401	1.4446	−1	.3299	1.0831	+5
60	.4835	2.1162	−3	.3298	1.4437	+2	.2474	1.0828	+4
70	.3385	2.1156	−2	.2311	1.4438	0	.1727	1.080	+8
80	.2124	2.115	−4	.1425	1.442	+2	.1062	1.074	+9
90	.0948	2.11	+1	.0649	1.441	+1			

[a] Obtained from average values of $Y_j/e^{-z_j^2}$ for j = 1,2,3,4,5,6 and 10.

of $Y_j/e^{-z_j^2}$ *vs.* j at t' = 20280 sec. are shown by curve D in Fig. 6 and may be compared to our data at t' = 20020 sec. (curve C). Both are seen to have a slightly negative slope.

The value of C_t in this work has been taken as the average value of $Y_j/e^{-z_j^2}$ for j = 1 to 6 and 10. By averaging all the values in the region $j < 60$, this value of C_t would be changed by only 0.04% early in the run and by lesser amounts as time progressed. The use of 7 fringes to obtain C_t is therefore justified. The drop in $Y_j/e^{-z_j^2}$ in the region of $j > 60$ appears to be due to some small defect in the optics. The vertical lines through the points in Fig. 6 show how an error of ±0.0003 cm. affects the value of $Y_j/e^{-z_j^2}$ as j approaches j_m. Though this error becomes quite large, it is not large enough in itself to account for the existing curvature. If the value of j_m were too small, it could also account for some of this curvature, however, it would require an error of 2 to 4 times the precision of determination of j_m to straighten out the line. A combination of errors in Y_j, δ and j_m could satisfactorily account for all of this decrease in $Y_j/e^{-z_j^2}$, however it would appear that these errors would lead to a more random scattering of points than is indicated. This same type of curvature has been obtained in all experiments on both sucrose and albumin, so it appears that, as stated above, it is due to some small optical defect.

It should be mentioned here that the Airy integral approximation becomes less exact as j increases, and the "saddle-point interference condition" should be used[14] for fringes close to the undeviated slit. It can be shown that the use of this latter condition for j = 90 in the present run would produce a change of only 0.1% in e^{-z^2} while, for j = 80, there is essentially no difference in the value of $e^{-z_j^2}$ calculated by either method. The saddle-point refinement is thus needed only for values of $j \geqq 90$ where $j_m \cong 100$ and has not been used in the present work.

Using equation 13, values of D' for each t' were calculated (see Table II) with λ = 5460.7 Å. and b = 152.8 cm. The data are plotted in Fig. 7 as D' *vs.* $1/t'$; a zero time correction, Δt, of 35 seconds was calculated from the least squares line. Extrapolation to $1/t' = 0$ leads to a value[27] of

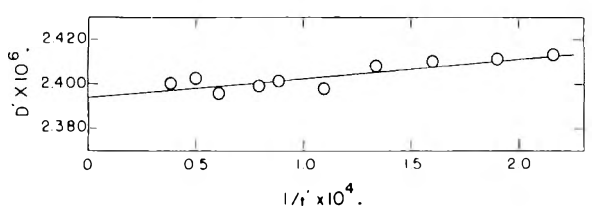

Fig. 7.—Determination of zero time correction in a typical sucrose run at 1°; Δt = 35 sec.

23.94 F for the diffusion coefficient of sucrose at this temperature and concentration. The values of t' were converted to t by addition of the 35 second zero time correction, and the value of D for each time interval calculated; these are shown in the last column of Table II, their average value being equal to the extrapolated value of D'. The average deviation in D is ±0.002 F, indicating a precision of about ±0.08%. This represents the precision in $1/C_t^2 t$. Other errors in D will be discussed in the following section.

(27) To avoid repetitious use of the exponential and units of diffusion coefficients, we propose the designation of 10^{-7} cm.²/sec. as one Fick unit F. This notation will be used throughout this paper.

TABLE II

VALUES OF C_t AT VARIOUS TIMES DURING A SUCROSE RUN AT 1°

t' (sec.)	C_t (cm.)	D', F	D,[a] F
4628	2.2514	24.13	23.95
5258	2.1129	24.11	23.95
6258	1.9374	24.10	23.96
7458	1.7755	24.08	23.96
9108	1.6097	23.98	23.89
11298	1.4446	24.01	23.93
12598	1.3686	23.99	23.92
16408	1.2000	23.96	23.91
20028	1.0847	24.02	23.98
25838	0.9554	24.00	23.97

Av. 23.94 ± 0.02

[a] Calculated with t' corrected to t by Δt = 35 sec.

In consideration of the problem of mixed solutes, the relative fringe deviation, Ω, was calculated for a large number of fringes from eight to ten photos taken during the course of the diffusion. A plot of Ω *vs.* $f(\zeta)$ is shown in Fig. 8. It can be seen that within the experimental error of ±0.0002 to 0.0003, the value of Ω remains equal to zero over most of the range of $f(\zeta)$. The slight increase in Ω in the region of $f(\zeta) > 0.6$ is a reflection of the drop in $Y_j/e^{-z_j^2}$ for high j previously referred to and will be shown later to be of little significance in the analysis of the protein diffusion results.

Bovine Serum Albumin.—Typical Y_j data for 3 photographs in a single serum albumin diffusion run are listed in Table III, δ being zero for all runs on serum albumin. In these runs, as with sucrose, the value of C_t was obtained from the first six or seven fringes but in albumin, where heterogeneity was expected, values of $Y_j/e^{-z_j^2}$ were plotted against $Z^{2/3}$ and C_t was taken as the value of $Y_j/e^{-z_j^2}$ where $Z^{2/3} = 0$. It was somewhat surprising to find that $Y_j/e^{-z_j^2}$ remained essentially constant and that C_t could just as well have been found by obtaining a numerical average over the lowest fringes. Figure 9 shows representative examples of the extrapolation procedure and indicates a rather high degree of homogeneity in the solutions (see Discussion). It is of interest to note that the extrapolated value of C_t seldom differed by more than 0.03% from the average value of $Y_j/e^{-z_j^2}$ over the range of $j = 0$ to $j = 0.25\ j_m$ which corresponds to the conventional height-area method.[10] For high values of j, $Y_j/e^{-z_j^2}$ again dropped off in the same manner as it did in the sucrose runs.

Values of D' were calculated according to equation 13 and plotted against $1/t'$ to obtain D_A and Δt. Figure 10 shows the D' *vs.* $1/t'$ graph for a particular run in which diffusion was allowed to proceed until the product of the diffusion coefficient and the time was about 0.1. Feeling certain from this run that the extrapolation to infinite time was valid, subsequent runs were stopped sooner ($Dt \sim 0.03$) to eliminate errors which might arise from misalignment of photographic films in the comparator when the fringe pattern was very short. From Fig. 10, a zero-time correction of 298 sec. was calculated, and in all subsequent runs Δt was in the range of 202 to 318 sec.

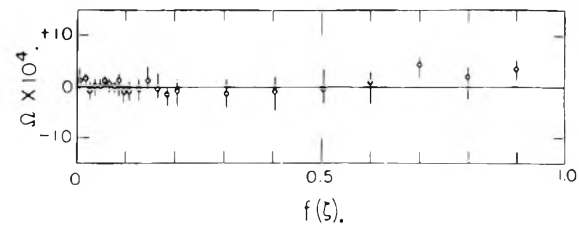

Fig. 8.—Relative fringe deviation for sucrose. Circles represent average values for eight to ten photos. Vertical lines represent the average deviation, either + or −, from the circled average values.

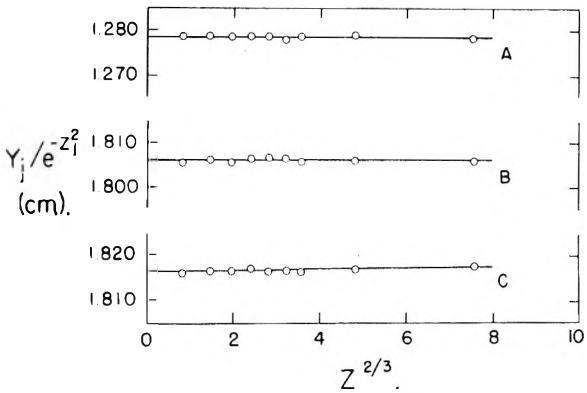

Fig. 9.—Extrapolation of $Y_j/e^{-z_j^2}$ to $Z^{2/3} = 0$ for determination of C_t in 3 serum albumin runs, A, B and C.

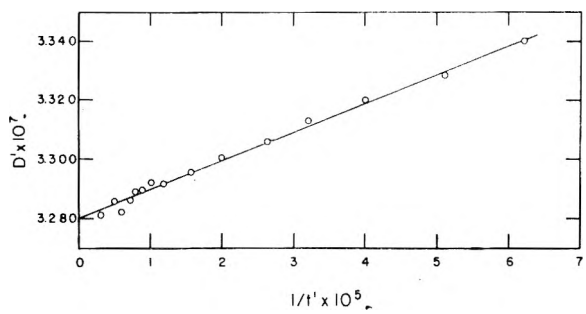

Fig. 10.—Determination of zero time correction for a particular albumin run; Δt = 298 sec.

Data from the albumin diffusion runs are given in Table IV. The temperature of diffusion was 1.00 ± 0.005° and for all runs, Δc was 0.50$_0$ g./100 cc. In each solution the solvent was 0.500 *M* KCl and the *p*H was 5.14 ± 0.02 at room temperature.[28]

According to equation 9, for a constant value of Δc (or Δn) one would expect j_m to be more nearly constant than is indicated in Table IV. The reason for this variation is due primarily to the uncertainty in Δc. For example, for the last line in Table IV the error in Δc is 5% if the error is 1% in c_A and c_B. A 5% variation in Δc corresponds to a variation of 4.2 in the tabulated value of j_m. It might also be mentioned that three different cells were used and they probably all have slightly different path lengths a. It is important to note that the values of j_m listed were *not* calculated from equation 9 but were obtained from Rayleigh

(28) At *p*H 5.14, essentially only carboxyl groups ionize and, since they have a heat of ionization very close to zero,[29] the *p*H at 1° would be almost identical to the *p*H at room temperature.

(29) C. Tanford, S. A. Swanson and W. S. Shore, *J. Am. Chem. Soc.*, **77**, 6414 (1955).

TABLE III

GOUY DIFFUSION DATA FOR SERUM ALBUMIN AT 1.0° ($\bar{c}$ = 0.492 g./100 cc., j_m = 87.96)

	Photo no. 24 t' = 31146 sec.; Ct = 2.0419 cm.[a]			Photo no. 30 t' = 49848 sec.; Ct = 1.6208 cm.[a]			Photo no. 33 t' = 63618 sec.; Ct = 1.4348 cm.[a]		
j	Y_j (cm.)	$Y_j/e^{-z_j^2}$ (cm.)	$\Omega \times 10^4$	Y_j (cm.)	$Y_j/e^{-z_j^2}$ (cm.)	$\Omega \times 10^4$	Y_j (cm.)	$Y_j/e^{-z_j^2}$ (cm.)	$\Omega \times 10^4$
0	1.9394	2.0421	−1	1.5394	1.6209	−1	1.3626	1.4347	0
1	1.8629	2.0426	−3	1.4787	1.6213	−3	1.3086	1.4348	0
2	1.8006	2.0424	−2	1.4287	1.6205	+1	1.2649	1.4348	0
3	1.7456	2.0423	−2	1.3856	1.6211	−2	1.2267	1.4352	−3
4	1.6963	2.0429	−4	1.3459	1.6209	−1	1.1917	1.4352	−3
5	1.6506	2.0433	−6	1.3094	1.6209	−1	1.1589	1.4346	+1
6	1.6069	2.0428	−4	1.2750	1.6209	0	1.1287	1.4349	−1
7	1.5659	2.0425	−2	1.2425	1.6207	+1	1.0997	1.4344	+2
8	1.5277	2.0435	−6	1.2117	1.6208	0	1.0725	1.4346	+1
9	1.4901	2.0431	−5	1.1820	1.6207	0	1.0461	1.4343	+2
10	1.4543	2.0436	−6	1.1535	1.6209	0	1.0208	1.4344	+1
12	1.3862	2.0435	−5	1.0990	1.6202	+2	0.9731	1.4346	+1
14	1.3215	2.0428	−3	1.0483	1.6205	+1	.9280	1.4345	+1
16	1.2609	2.0432	−4	1.0007	1.6216	−3	.8857	1.4352	−2
18	1.2030	2.0433	−5	0.9543	1.6209	0	.8449	1.4351	−1
20	1.1480	2.0440	−6	.9106	1.6214	−2	.8061	1.4353	−2
30	0.9004	2.0439	−5	.7138	1.6203	+1	.6319	1.4344	+1
40	.6889	2.0443	−4	.5463	1.6212	−1	.4834	1.4345	+1
50	.5037	2.0458	−5	.3993	1.6218	−2	.3534	1.4354	−1
60	.3400	2.0440	−2	.2697	1.6214	−1	.2383	1.4326	+2

[a] Obtained by extrapolation according to equation 16.

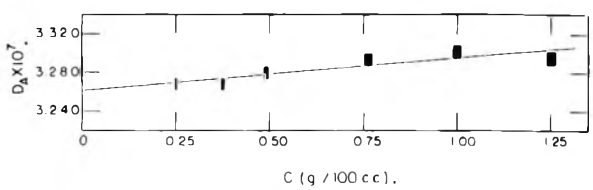

Fig. 11.—Dependence of the diffusion coefficient of bovine serum albumin on concentration. Rectangles represent error of ±1% in concentration and ±0.2% in D_A.

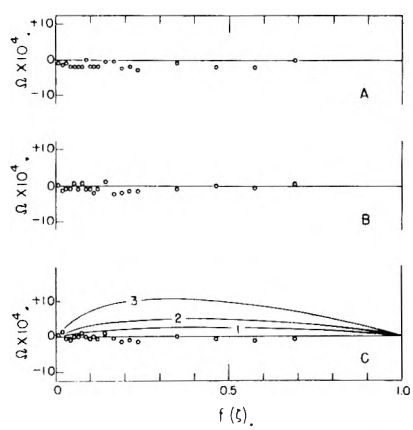

Fig. 12.—Relative fringe deviation Ω for bovine serum albumin. The points represent, in A and B the average of 4 photos from 2 different runs, and, in C, the average of 12 photos from 4 different runs. Ω does not appear to depend on concentration. The straight lines are drawn through the value of Ω = 0. Curves C (1, 2 and 3) have been calculated for D_1/D_2 = 1.5 and α_2 = 0.02, D_1/D_2 = 1.5 and α_2 = 0.03, and D_1/D_2 = 2.0 and α_2 = 0.02, respectively.

fringes as previously described and, as such, are known with a precision of about 0.03% without requiring a knowledge of a.

The values of D_A have been plotted in Fig. 11 against the mean concentration of solute. The rectangular points in this figure indicate an error of ±1% in $\bar{c}$ and ±0.2% in D_A. The least squares line drawn through the points and extrapolated to infinite dilution yields a value for the average diffusion coefficient, D_A° = 3.261 F at 1° in 0.5 M KCl at pH 5.14.

TABLE IV

DIFFUSION OF BOVINE SERUM ALBUMIN AT 1.00° IN 0.5 M KCl AT pH 5.14

$\bar{c}$[a] (g./100 cc.)	c_Λ[a] (g./100 cc.)	j_m[b]	Δt (sec.)	D_A, F	No. of photos	Av. dev.,[c] %
0.250	0.000	85.93	318	3.268	8	±0.06
.370	.120	86.17	202	3.268	8	± .09
.492	.242	87.96	298	3.280	15	± .04
.762	.512	87.44	303	3.294	12	± .08
1.000	.752	85.45	249	3.302	10	± .07
1.249	1.000	84.56	254	3.295	9	± .07

[a] Concentration known to ±1%. Δc = 0.5% g./100 cc. in all expt. [b] For explanation of variations in j_m, see text. [c] Average deviation of all D' values, after correction for Δt, from value of D_A at $1/t'$ = 0. This deviation represents only the precision in $1/Ct^2t$ (see Discussion).

Relative fringe deviations were calculated from three to four photos from each of four different runs and are plotted in Fig. 12 as a function[30] of $f(\zeta)$. Some of these values are listed in Table III. Due to the difficulties encountered near the undeviated slit, as previously described, no values of Ω are given beyond $f(\zeta)$ = 0.7. The straight lines in Fig. 12 have been drawn through Ω = 0 and are not meant to represent the experimental data. The precision here is about ±0.0003 and, within this experimental error, Ω is equal to zero for all fringes measured.

(30) The value of $f(\zeta)$ for a given fringe is actually different from one run to the next because of the variation in j_m, as is shown by equation 4. Since j_m for all albumin runs is roughly the same, values of $f(\zeta)$ for any j, do not differ by more than about 0.03 at most. The values of Ω for a given value of j have therefore been plotted on the $f(\zeta)$ scale taken arbitrarily from one run.

Discussion

According to the results obtained here, the precision obtainable for $1/C_t^2t$ with the Spinco Model H electrophoresis-diffusion apparatus appears to be about $\pm 0.1\%$ or less. The only significant discrepancy we have encountered is the nonlinearity of $Y_j/e^{-z_j^2}$ calculated for fringes close to the undeviated slit image and, since only the most deviated fringes are needed to calculate diffusion coefficients, this should introduce no serious error into the results. However, no interpretation of Ω can be given for $f(\zeta)$ greater than about 0.7.

The b distance of 152.8 cm. in this apparatus is the focal length of the Schlieren lens (the distance between the focal plane and the exit principal plane in air). It was obtained from measurements on an optical bench by the manufacturer before installation into the apparatus. After installation into the apparatus, it is necessary to adjust the position of the diaphragm until it is in the focal plane of the lens.[31] It is difficult to estimate exactly how precise this adjustment is. It has been found, however, that a movement of the diaphragm by about 0.05 cm. in either direction from its optimum position will produce a detectable tilt in the base line of the Schlieren pattern as viewed through the camera. It is reasonable to assume, therefore, that the b distance is known to about ± 0.05 cm. If values of $1/(C_t')^2t$, where $C_t = MC'_t$ and M is the cylindrical lens magnification factor, are plotted against $1/t'$ the probable error in the intercept[32] is about $\pm 0.05\%$. These errors in b and $(C_t')^2t$, combined with probable errors of $\pm 0.03\%$ and $\pm 0.05\%$ in j_m and M, respectively, lead to a probable error of about $\pm 0.16\%$ in the diffusion coefficient of sucrose.

Our value of 23.94 $\pm$ 0.04 F for the diffusion coefficient of sucrose at 1.00° and $\bar{c}$ = 0.375 g./100 cc. is seen to be somewhat lower than the values of 24.08 and 24.14 F reported by Gosting and Morris[33] and by Longsworth,[34] respectively, the latter having been obtained by the Rayleigh interference method. The deviation of our value from the 24.08 value is slightly larger than the discrepancy between the two literature values, and several times greater than would be indicated by the internal precision of our data. This *small* discrepancy persists at other concentrations. For example, at 1.00°, with $\bar{c}$ = 0.500 g./100 cc. and Δc = 0.500 g./100 cc., we obtained 23.89 F compared to the value 24.03 F of Gosting and Morris.[33]

In the albumin diffusion, the probable error in D_A at any given $\bar{c}$ is again $=0.16\%$ while the probable error in the intercept,[32] $D_A°$, is $\pm 0.13\%$. Our value of $D_A°$ = 3.261 $\pm$ 0.004 F for isoionic serum albumin (pH 5.14) at 1.00° and ionic strength 0.50 cannot properly be compared with other values reported in the literature due to a possible error involved in correcting from 1 to 20° or 25° using the Stokes–Einstein relation. If this correction is adopted, however, we obtain values of $(D_A)^0_{20,w}$ and $(D_A)^0_{25,w}$ of 5.805 $\pm$ 0.008 and 6.606 $\pm$ 0.009 F, respectively. At a value of $\bar{c}$ = 0.50 g./100 cc. we obtain values of $(D_A)_{20,w}$ = 5.835 F and $(D_A)_{25,w}$ = 6.641 F which are slightly lower than Akeley and Gosting's[16] values of 5.855 and 6.697 F, respectively; their measurements were made at 25° at the same (single) concentration. On the basis of increased hydration at 1°, one would expect to calculate a lower diffusion coefficient at 25° than would be determined experimentally at this higher temperature so the agreement between these two values is quite good. It should be remembered however that differences in pH, buffer and sample[35] may also affect this comparison.

The data for serum albumin plotted as D_A *vs.* $\bar{c}$ fall reasonably well on a straight line. The least-squares line drawn through all the points in Fig. 11 has a positive slope of 0.034×10^{-7} (for $\bar{c}$ in g./100 cc.) and has been extrapolated linearly to equal zero. Mandelkern and Flory[36] have shown that linear extrapolation may, in certain cases, introduce serious errors into the value of the diffusion coefficient at infinite dilution. For serum albumin at its isoionic point and at high ionic strength, where protein–salt interaction and Donnan effects are minimized, it appears justifiable to make the linear extrapolation.

It is worthwhile to consider the possible effect of heterogeneity on the foregoing analysis. The relative fringe deviation, Ω, for serum albumin remained, within the experimental error of ± 0.0003, equal to zero for $0 \leqslant f(\zeta) < 0.7$. An analysis of four different ultracentrifuge photographs, obtained from solutions prepared in a manner similar to those used in the diffusion runs and with the same preparation (Armour's lot N67009), showed the presence at 25° of 2 to 4% of a *faster sedimenting* second component. We have therefore calculated values of Ω from eq. 17 for a *slower diffusing* second component. In Fig. 12C, curve no. 1 has been calculated for $\alpha_2 = 2\%$ and $r_2 = D_1/D_2 = 1.5$; in curve 2, $\alpha_2 = 3\%$ and $r_2 = 1.5$; while in curve 3, $\alpha_2 = 2\%$ and $r_2 = 2.0$. It should be noted first that for a slower diffusing second component, the theoretical value of Ω reaches a maximum[16] in the region $f(\zeta) < 0.5$. It is for this reason that the anomalous behavior of Ω in the region $f(\zeta) > 0.7$ has not been considered as a serious deterrent to the present work. If the second component diffused *faster* than serum albumin, or if a buffer gradient existed, Ω would have reached its maximum around $f(\zeta) = 0.7$–0.8 and we would have been unable to analyze the relative fringe deviation graphs. Since it is unlikely that either of these latter conditions exist to any appreciable extent, we can consider further the region of $f(\zeta) < 0.7$. In Fig. 12C, curve 1 lies within the average deviation of Ω while curve 2 is just on the limit of the maximum deviation in Ω. Curve 3, on the other hand, is clearly outside of the range of Ω. Values of $\alpha_2 = 2$ to 3% where $r_2 = 1.5$ are thus compatible with both the sedimentation and the diffusion data while a value of $r_2 \geqslant 2$, even with α_2 at its minimum of 2%, is not. Values

(31) L. G. Longsworth, *Ind. Eng. Chem., Anal. Ed.*, **18**, 219 (1946).
(32) Calculated as 0.6745 × standard deviation of the intercept.
(33) Calculated from equation 16, ref. 10.
(34) L. G. Longsworth, *J. Am. Chem. Soc.*, **74**, 4155 (1952).
(35) Some preliminary diffusion data obtained from Armour lot 370295-B lead to values of D_A about 1% higher than those reported here.
(36) L. Mandelkern and P. J. Flory, *J. Chem. Phys.*, **17**, 984 (1951).

of α_2 larger than 3% would require values of r_2 less than 1.5 in order to obtain agreement with the data. In this connection, it should be mentioned again that as r_2 approaches 1.0, Ω approaches zero for any value of α_2, hence it would be possible to fit the data with any value of α_2 providing a value of r_2 close to unity were chosen.

Using the value $r_2 = 1.5$, and assuming α_2 to be independent of temperature, we obtain the following diffusion coefficients D_1 at 20° in water by means of equation 6.

$\bar{c}$ (g./100 cc.)	$\alpha_2 = 0.02$, F	$\alpha_2 = 0.03$, F
0	5.86	5.90
0.5	5.89	5.93

These values may be compared with Akeley and Gosting's[16] value of $(D_1)_{20,w}$ of 5.89 to 5.93 F at $\bar{c} = 0.5$ g./100 cc., the agreement being excellent.

The diffusion coefficient obtained here has been used, in conjunction with viscosity and sedimentation data, to obtain the hydrodynamic parameter[2] β, and, thereby, information about the size and shape of the equivalent hydrodynamic particle.[37] The relationship between the hydrodynamic properties of bovine serum albumin and the thermodynamics of various albumin reactions are also discussed elsewhere.[37,38]

(37) G. I. Loeb and H. A. Scheraga, to be submitted.

(38) H. A. Scheraga, G. I. Loeb and M. L. Wagner, *Federation Proc.*, **15**, 348 (1956).

A STUDY OF THE CONDUCTANCES OF SOME UNI-UNIVALENT ELECTROLYTES IN N,N-DIMETHYLACETAMIDE AT 25°[1]

BY GEORGE R. LESTER, THOMAS A. GOVER AND PAUL G. SEARS

Department of Chemistry, University of Kentucky, Lexington, Kentucky

Received March 19, 1956

The limiting equivalent conductances of thirteen potassium and sodium salts and of seven quaternary ammonium salts in N,N-dimethylacetamide have been determined at 25°. The concentration of the solute usually ranged from 1–50 $\times 10^{-4}$ N. Very unusual conductance behavior has been observed inasmuch as the limiting equivalent conductances of sodium salts in N,N-dimethylacetamide (DMA) are greater than those of corresponding potassium salts. In most cases the conductance data indicate that the salts are completely dissociated in dilute solutions. The results provide numerous examples which substantiate the law of independent ionic mobilities for solutions of electrolytes in DMA. Limiting ionic equivalent conductances which are based upon an assumed value for the conductance–viscosity product of the tetra-*n*-butylammonium ion have been evaluated.

Introduction

Several studies have been reported from this Laboratory concerning N,N-dimethylformamide (DMF) as an electrolytic solvent.[2-4] The results indicate that many salts are not only moderately soluble but also completely dissociated in DMF. Hence, the promising potentialities of DMF suggested the worthwhile nature of this initial investigation of the behavior of electrolytes in N,N-dimethylacetamide (DMA). Although the second member of a homologous series usually has a lower dielectric constant than that of the first, it is interesting to note that DMF and DMA have dielectric constants of 36.71 and 37.78, respectively, at 25°.[5] The viscosities of the former (0.00796 poise) and of the latter (0.00919 poise) differ only fifteen per cent. Consequently, on the basis of both chemical character and physical properties, DMA might be expected to very closely resemble DMF as an electrolytic solvent.

Experimental

1. **Preparation and Purification of Solvent.**—DMA was synthesized from glacial acetic acid and gaseous dimethylamine. After the acid was saturated with the amine, the solution was heated to simultaneously crack out and distil off water. The resulting binary maximum-boiling azeotrope of acetic acid and DMA was treated with solid potassium hydroxide until a separation of phases occurred. Precautions were taken to prevent the reaction flask from becoming hot during the neutralization and saturation procedure. The DMA layer was separated and then fractionally distilled two or more times through an efficient column at a reduced pressure. Each middle fraction of DMA which was retained had a density, refractive index and dielectric constant which checked very closely with corresponding data which have been reported in the literature.[5,6] The conductivity of the DMA thus obtained was in the range 0.8–2.0 $\times 10^{-7}$ ohm^{-1} cm.$^{-1}$.

2. **Purification of Salts.**—Potassium and sodium picrates were prepared by the neutralization of recrystallized picric acid with the proper reagent grade base. These picrates were recrystallized several times from ethanol–water mixtures.

Sodium benzenesulfonate and trimethylphenylammonium iodide (both Eastman grade) were recrystallized three times from methanol. Trimethylphenylammonium benzenesulfonate (practical grade) was treated with Norit prior to four recrystallizations from methanol.

The purifications of the other fifteen salts have been described in previous papers.[2,3] Prior to using, all salts were dried for several hours *in vacuo*. The length and temperature of the drying depended upon the nature of the salt. The melting points of the quaternary ammonium salts, which were determined using a Fisher–Johns melting point apparatus, showed good agreement with corresponding data which have been reported in the literature.

3. **Procedure and Apparatus.**—The dielectric constant of each retained fraction of DMA was measured at ten megacycles using the equipment and procedure which have been described by Leader.[7]

The viscosity of each of several fractions of DMA was determined using size-50 routine Cannon–Fenske viscometers which were calibrated by the Cannon Instrument

(1) This research was supported in part by a Frederick Gardner Cottrell grant from Research Corporation.

(2) P. G. Sears, E. D. Willhoit and L. R. Dawson, THIS JOURNAL, **59**, 373 (1955).

(3) D. P. Ames and P. G. Sears, *ibid.*, **59**, 16 (1955).

(4) P. G. Sears, E. D. Willhoit and L. R. Dawson, *J. Chem. Phys.*, **23**, 1274 (1955).

(5) G. R. Leader and J. F. Gormley, *J. Am. Chem. Soc.*, **73**, 5731 (1951).

(6) J. R. Ruhoff and E. E. Reid, *ibid.*, **59**, 401 (1937).

(7) G. R. Leader, *ibid.*, **73**, 856 (1951).

TABLE I

EQUIVALENT CONDUCTANCES OF SOME SALTS IN N,N-DIMETHYLACETAMIDE AT 25°

$C \times 10^4$	Λ	$C \times 10^4$	Λ	$C \times 10^4$	Λ	$C \times 10^4$	Λ	$C \times 10^4$	Λ
(a) Sodium thiocyanate		(b) Potassium thiocyanate		(c) Sodium nitrate		(m) Tetraethylammonium bromide		(n) Tetraethylammonium iodide	
1.512	72.93	0.8059	72.95	1.394	69.95	0.9882	74.52	0.7586	73.29
6.219	71.13	5.226	71.19	4.552	67.58	3.222	73.23	2.173	72.48
12.49	69.73	12.21	69.70	11.85	64.10	7.632	71.63	5.065	71.33
25.21	67.70	23.75	68.08	24.78	59.83	14.49	69.65	9.153	70.02
38.66	66.08	34.73	66.91	36.73	56.98	22.73	67.94	12.94	69.19
55.00	64.47	49.17	65.72	47.67	54.83	27.79	66.99	15.18	68.73
(d) Potassium nitrate		(e) Sodium bromide		(f) Potassium bromide		(o) Tetra-*n*-propylammonium bromide		(p) Tetra-*n*-propylammonium iodide	
1.179	69.93	0.9812	67.66	0.6005	67.39	0.6903	68.23	0.4528	67.03
4.128	68.26	4.639	65.88	1.793	66.63	2.106	67.24	1.910	66.10
10.38	66.04	11.60	63.92	4.979	65.43	5.750	65.67	5.345	64.83
21.51	63.29	27.17	61.02	9.483	64.30	11.12	64.10	10.04	63.66
30.28	61.62	43.88	58.90	14.88	63.25	19.67	62.16	18.37	62.05
37.47	60.39	55.34	57.61	19.58	62.45	26.52	60.94	24.27	61.13
(g) Sodium perchlorate		(h) Potassium perchlorate		(i) Sodium iodide		(q) Tetra-*n*-butylammonium iodide		(r) Sodium benzenesulfonate	
1.082	67.19	0.9743	66.86	1.739	65.92	0.8132	63.38	1.988	54.80
5.577	65.66	3.617	65.74	3.813	65.14	1.835	62.80	7.684	52.31
12.77	64.20	10.38	64.12	8.409	64.01	4.579	61.83	16.22	50.01
26.90	62.55	23.26	62.42	17.91	62.57	9.207	60.61	24.96	48.19
43.66	61.17	37.96	61.07	28.31	61.44	15.67	59.48	38.44	45.98
64.55	59.90	55.44	59.82	40.80	60.38	22.12	58.44	53.49	44.03
(j) Potassium iodide		(k) Sodium picrate		(l) Potassium picrate		(s) Trimethylphenylammonium iodide		(t) Trimethylphenylammonium benzenesulfonate	
0.6215	66.09	1.052	55.99	1.108	55.51	1.800	68.30	1.063	58.00
2.722	64.98	2.496	55.34	2.935	54.74	4.369	67.23	3.581	56.71
5.792	64.10	6.972	54.15	8.419	53.42	11.30	65.47	7.722	55.26
12.47	62.87	16.47	52.59	22.17	51.54	22.72	63.31	12.16	54.09
20.84	61.76	26.07	51.49	29.68	50.78	33.62	61.78	18.36	52.73
29.12	60.90	31.99	50.95	32.61	50.54	42.01	60.73	24.93	51.56

Company. Kinetic energy corrections were assumed to be negligible.

The bridge, cells, temperature bath and control, and the procedures involved in the preparation of solutions and the measurement of resistances have been described previously.[3,4]

The following data for DMA at 25° were used in the calculations: density, 0.9366 g./ml.; viscosity, 0.00919 poise; dielectric constant, 37.8. Values of the necessary fundamental constants were taken from a recent report of the Subcommittee on Fundamental Constants.[8]

Results and Discussion

Corresponding values of the equivalent conductance, Λ, and the concentration in gram-equivalents per liter, C, for each of the twenty salts are presented in Table I.

Plots of the equivalent conductance against the square root of the concentration are linear for all salts in DMA for concentrations less than 0.001 N. For greater concentrations, various types of behavior are observed. Some of the plots remain linear whereas others curve thereby becoming convex or concave with respect to the concentration axis. The plots of Λ *versus* $\sqrt{c}$ for the six pairs of corresponding potassium and sodium salts are of particular interest. The plots remain parallel in the cases of the iodides, perchlorates and picrates; in contrast, the plots intersect in the cases of the nitrates, thiocyanates and bromides.

(8) F. D. Rossini, F. T. Gucker, Jr., H. L. Johnston, L. Pauling and G. W. Vinal, *J. Am. Chem. Soc.*, **74**, 2699 (1952).

The Onsager equation[9] for a uni-univalent electrolyte may be written in a generalized form as

$$\Lambda = \Lambda_0 - \left[\frac{82.42}{(DT)^{1/2}\eta} + \frac{8.204 \times 10^5}{(DT)^{3/2}}\Lambda_0\right]\sqrt{C} \quad (1)$$

Substitution of the proper numerical values for the dielectric constant (D), the viscosity (η) and the absolute temperature into equation 1 gives the following equation for dilute solutions of electrolytes in DMA at 25°

$$\Lambda = \Lambda_0 - [84.5 + 0.686\Lambda_0]\sqrt{C} \quad (2)$$

Table II contains data pertinent to the applicability of this theoretical equation in describing the conductance behavior of electrolytes in DMA.

Compared to the theoretical slope of equation 2, $-[84.5 + 0.686\ \Lambda_0]$, both more negative slopes (positive deviations) and less negative slopes (negative deviations) are observed. For thirteen salts, the experimental and the theoretical behavior agree within 10%. For the other seven salts, observed deviations are in the range 19–96%.

In each case where there is close agreement between the experimental and the theoretical behavior, the Shedlovsky rearrangement of the Onsager equation[10] is particularly useful for calculating the

(9) L. Onsager, *Physik. Z.*, **28** 277 (1927).

(10) T. Shedlovsky, *J. Am. Chem. Soc.*, **54**, 1405 (1932).

TABLE II

DATA PERTINENT TO THE APPLICABILITY OF THE ONSAGER EQUATION TO THE CONDUCTANCES OF SOME SALTS IN N,N-DIMETHYLACETAMIDE AT 25°

Salt	Limiting exptl. slope (S_E)	Onsager theor. slope (S_T)	% Dev. $\frac{(S_E - S_T)100}{S_T}$
NaSCN	−137	−136	1
KSCN	−126	−135	−7
$NaNO_3$	−262	−134	96
KNO_3	−178	−134	33
NaBr	−156	−132	18
KBr	−134	−131	2
$NaClO_4$	−124	−132	−6
$KClO_4$	−122	−131	−7
NaI	−122	−131	−7
KI	−120	−130	−8
NaPi[a]	−115	−124	−7
KPi	−112	−123	−10
Et_4NBr	−172	−137	26
Et_4NI	−149	−136	10
Pr_4NBr	−166	−132	25
Pr_4NI	−138	−131	5
Bu_4NI	−128	−129	−1
$NaSO_3Ph$	−184	−124	48
Me_3PhNI	−146	−133	10
Me_3PhNSO_3Ph	−156	−125	25

[a] Pi represents the picrate ion.

limiting equivalent conductance directly from the individual values of Λ as shown in equation 3.

$$\Lambda_0' = \frac{\Lambda + 84.5\sqrt{C}}{1 - 0.686\sqrt{C}} = \Lambda_0 + BC \qquad (3)$$

The calculated values, Λ'_0, are plotted against the concentration, C, and the resulting plot is extrapolated to infinite dilution. The value of the ordinate at the point of intersection is taken as the actual limiting equivalent conductance, Λ_0. The slope, B, is evaluated by the conventional method. Table III contains values of the intercepts and the slopes which are based on plots of Λ'_0 *versus* C for several salts in DMA. The slope B has no theoretical significance; furthermore, values of B' (ratio of B to Λ_0) show no consistent trends which are comparable to those which have been observed for some of the same salts in water and hydrogen cyanide.[11]

TABLE III

DATA PERTINENT TO PLOTS OF EQUATION 3 FOR SOME SALTS IN N,N-DIMETHYLACETAMIDE AT 25°

Salt	Λ_0	$B \times 10$	Salt	Λ_0	$B \times 10$
NaSCN	74.55	−1	NaPi	57.25	23
KSCN	74.15	22	KPi	56.75	28
KBr	68.40	−6	Et_4NI	74.50	−35
$NaClO_4$	68.56	31	Me_3PhNI	70.10	−40
$KClO_4$	68.11	29	Pr_4NI	67.94	−15
NaI	67.57	30	Bu_4NI	64.55	0
KI	67.04	33			

The plots of Λ'_0 *versus* C for the seven salts in DMA exhibiting the most pronounced deviations from the behavior predicted by the Onsager equation are curved and cannot be extrapolated accurately. Recourse was made, therefore, to the Fuoss–Shedlovsky treatment[12] of data for these salts. The fundamental equation which is involved may be written as

$$S\Lambda = \Lambda_0 - \frac{cf^2S^2\Lambda^2}{K\Lambda_0} \qquad (4)$$

According to equation 4, if a plot of $S\Lambda$ *versus* $cf^2S^2\Lambda^2$ is linear, the value of the ordinate intercept may be taken as Λ_0, and the slope is equivalent to $-1/K\Lambda_0$, where K is the dissociation constant. This method produces a linear plot for each of the seven salts in DMA which show large deviations from the theoretical behavior predicted by the Onsager equation. Data based on plots of equation 4 are presented in Table IV. The dissociation constants which appear in Table IV are to be considered only qualitative in nature inasmuch as values of K of this magnitude which are based upon conductance measurements may be subject to appreciable error.[11]

TABLE IV

DATA PERTINENT TO PLOTS OF EQUATION 4 FOR SOME SALTS IN N,N-DIMETHYLACETAMIDE AT 25°

Salt	Λ_0	Slope	$K \times 10^3$
KNO_3	72.02	0.387	4
$NaNO_3$	71.53	.925	2
NaBr	69.02	.234	6
$NaSO_3Ph$	56.82	.710	3
Et_4NBr	76.01	.261	5
Pr_4NBr	69.40	.320	5
Me_3PhNSO_3Ph	59.43	.446	4

It may be noted from the results in Tables II and IV, in the cases of the bromides, nitrates and thiocyanates, that the sodium salts appear to be dissociated to a lesser extent at finite concentrations than are the potassium salts. This indicates that the relative charge density of the sodium ion in solution is probably greater than that of the potassium ion and, hence, would be more susceptible to participation in ion-pair formation.

There are numerous combinations of the values of Λ_0 in Tables III and IV which substantiate the Kohlrausch law of independent ionic mobilities for solutions of electrolytes in DMA. This substantiation is indicative of both the general consistency and reliability of the results.

Almost without exception, the limiting equivalent conductances of the alkali metal ions decrease as

$$Rb^+ > K^+ > Na^+ > Li^+$$

Owing to solvation effects, the relative effective sizes of these ions in solution apparently are reversed with respect to the sizes of the unsolvated ions. However, a very unusual phenomenon exists for DMA solutions inasmuch as the limiting equivalent conductance of a sodium salt is numerically greater than that of the corresponding potassium salt. Results for the six pairs of salts which were studied show that the sodium salt is 0.5 ± 0.1 ohm^{-1} $cm.^2$ $equiv.^{-1}$ more conducting than the similar potassium salt. Although this difference is small, it is approximately four times greater than

(11) C. A. Kraus, THIS JOURNAL, **58**, 673 (1954).

(12) R. M. Fuoss and T. Shedlovsky, *J. Am. Chem. Soc.*, **71**, 1496 (1949).

the estimated experimental error and appears to constitute a real effect. Only one other reversal in the conductances of alkali metal salts has been reported in the literature. According to Coates and Taylor,[13] lithium salts are more conducting than corresponding sodium salts in hydrogen cyanide. They postulated that the relative increase in size due to the solvation of the lithium ion is insufficient to compensate for the difference in the sizes of the unsolvated ions. The result is that the lithium ion in hydrogen cyanide is characterized by the smaller effective size and, hence, is more conducting than the sodium ion. A similar explanation for the reversal of the limiting equivalent conductances of the sodium and potassium ions in DMA appears satisfactory. Whereas no other case of a reversal in the limiting equivalent conductances of the sodium and the potassium ions is known to have been reported in the literature, another study which now is in progress in this Laboratory and which is to be reported in the near future, has shown that the same reversal occurs in N,N-dimethylpropionamide solutions.

Octadecyltrimethylammonium octadecylsulfate, which is sometimes used to evaluate limiting ionic equivalent conductances,[14] was found to be essentially insoluble in DMA. As an alternative method, approximate values of the limiting ionic equivalent conductances in DMA have been calculated assuming that the conductance–viscosity product of the tetra-*n*-butylammonium ion is 0.209 ohm^{-1} $cm.^2$ $equiv.^{-1}$ poise. Pickering and Kraus[15] and Healey and Martell[16] have discussed the favorable aspects of this indirect method of evaluating limiting ionic equivalent conductances. Table V contains the resulting data for several ions in DMA.

TABLE V

LIMITING IONIC EQUIVALENT CONDUCTANCES IN N,N-DIMETHYLACETAMIDE BASED ON THE CONDUCTANCE-VISCOSITY PRODUCT OF THE TETRA-*n*-BUTYLAMMONIUM ION

Cation	λ_0^+	Anion	λ_0^-
Et_4N^+	32.7	SCN^-	48.8
Me_3PhN^+	28.3	NO_3^-	46.3
Pr_4N^+	26.2	Br^-	43.2
Na^-	25.8	ClO_4^-	42.8
K^+	25.3	I^-	41.8
Bu_4N^+	22.8	$PhSO_3^-$	31.0
		Pi^-	31.5

It is interesting to note that the resulting conductance–viscosity product for the picrate ion is 0.289 in DMA. Whereas this value is about 8% greater than the 0.267 in several solvents as reported by Walden,[17] it is nevertheless comparable to the 0.297 in pyridine[18] and the 0.290 in nitrobenzene.[19]

The series of decreasing relative anionic equivalent conductances in DMA, $SCN^- > NO_3^- > Br^- > ClO_4^- > I^- > Pi^-$, has the same arrangement as those for the same ions in electron-donor solvents such as DMF,[1,2,20] acetone,[21] nitrobenzene[19] and nitromethane.[22] As for other well-known electron-donor solvents, the series in DMA differs only slightly from series for the same ions in pyridine[18] and dimethyl sulfoxide,[23] but it differs radically from those for the same ions in acetonitrile[24] and methyl ethyl ketone.[25]

The series of decreasing relative cationic equivalent conductances in DMA may be written as

$$Et_4N^+ > Me_3PhN^+ > Pr_4N^+ > Na^+ > K^+ > Bu_4N^+$$

This series is characterized by the normal relative positions of the quaternary ammonium ions; however, the very unusual reversal of the sodium and potassium conductances appears. It is interesting to note that these results indicate that the effective sizes of the sodium and potassium ions are intermediate between those of the Pr_4N^+ and Bu_4N^+ ions. For comparison purposes, their apparent effective sizes are intermediate between Et_4N^+ and Pr_4N^+ ions in DMF.[1] Thus, it would appear that larger solvodynamic species are present in DMA; this fact is further supported by conductance–viscosity products in DMA being of smaller magnitude than the corresponding products in DMF.

From the over-all results it may be concluded that DMA, like DMF, is a potentially promising electrolytic solvent. Generally, salts are moderately soluble in DMA and appear to be completely dissociated in dilute solutions. Although it has not been illustrated in this investigation, DMA has one important advantage over DMF in that it is solely an amide and is not susceptible to certain reactions which are characteristic of a formyl group. Theoretically, the evidence which has been obtained relative to the unusual conductances of the sodium and the potassium ions provides an excellent stimulus for further research involving solutions of alkali metal ions in DMA as well as in other disubstituted amides of higher molecular weight.

(13) G. E. Coates and E. G. Taylor, *J. Chem. Soc.*, 1245 (1936).
(14) W. E. Thompson and C. A. Kraus, *J. Am. Chem. Soc.*, **69**, 1016 (1947).
(15) H. L. Pickering and C. A. Kraus, *ibid.*, **71**, 3288 (1949).
(16) F. H. Healey and A. E. Martell, *ibid.*, **73**, 3296 (1951).
(17) P. Walden, "Elektrochemie nicht-wasseriger Losungen," Barth, Leipzig, 1924.
(18) D. S. Burgess and C. A. Kraus, *J. Am. Chem. Soc.*, **70**, 706 (1948).
(19) C. R. Witschonke and C. A. Kraus, *ibid.*, **69**, 2472 (1947).
(20) R. K. Wolford, Thesis, University of Kentucky, 1955.
(21) M. B. Reynolds and C. A. Kraus, *J. Am. Chem. Soc.*, **70**, 1709 (1948).
(22) C. P. Wright, D. M. Murray-Rust and H. Hartley, *J. Chem. Soc.*, 199 (1931).
(23) G. R. Lester, Thesis, University of Kentucky, 1956.
(24) P. Walden and E. J. Birr, *Z. physik. Chem.*, **144**, 269 (1929).
(25) P. Walden and E. J. Birr, *ibid.*, **153**, 1 (1931).

COMBUSTION CALORIMETRY OF ORGANIC FLUORINE COMPOUNDS BY A ROTATING-BOMB METHOD[1]

By W. D. Good, D. W. Scott and Guy Waddington

Contribution No. 56 from the Thermodynamics Laboratory, Petroleum Experiment Station, Bureau of Mines, Bartlesville, Oklahoma

Received March 21, 1956

A rotating-bomb method was developed for the combustion calorimetry of organic fluorine compounds. Conventional methods of handling volatile samples could not be used, and a special technique with sealed, fused-quartz ampoules was devised. Some auxiliary data necessary for reduction of the calorimetric results to standard states were lacking; this difficulty was circumvented by use of suitable comparison or "blank" experiments. The following values, in kcal. mole^{-1}, are reported for the standard heats of formation, $\Delta Hf°_{298.16}$, of some organic fluorine compounds from graphite and gaseous hydrogen, oxygen and fluorine: *o*-fluorobenzoic acid (c), −134.38; *m*-fluorobenzoic acid (c), −137.84; *p*-fluorobenzoic acid (c), −138.95; fluorobenzene (liq.), −34.75; benzotrifluoride (liq.), −147.85 and polytetrafluoroethylene (granular, no heat treatment), −193.5. The samples of fluorobenzoic acids were purified by zone melting. *p*-Fluorobenzoic acid is proposed as a reference substance for intercomparison of bomb-calorimetric data for fluorine compounds among different laboratories.

The combustion calorimetry of organic fluorine compounds has received little attention. Virtually the only thermochemical data available for liquid and solid organic fluorine compounds are those obtained by Swarts[2] in his pioneering researches before 1916. No studies of this class of compounds have been made previously by the methods of modern precision combustion-bomb calorimetry.

Accurate values of the heats of combustion and formation of organic fluorine compounds are important for both theoretical and practical applications. The main obstacle to obtaining such values by bomb calorimetry, apart from the corrosive nature of the hydrofluoric acid formed as a combustion product, has been the difficulty of obtaining a well-defined, equilibrium final state of the combustion process in a conventional stationary bomb. This obstacle was removed in principle by the development of rotating-bomb calorimetry, first at the University of Lund in Sweden[3] and later in this Laboratory,[4] to overcome the same difficulty in the combustion calorimetry of organic sulfur compounds.

The present investigation was undertaken to develop a rotating-bomb method for combustion calorimetry of organic fluorine compounds. A new and improved rotating-bomb calorimeter was constructed. With this apparatus, calorimetric studies were made with six organic fluorine compounds selected to include volatile liquids, nonvolatile solids, a group of isomeric compounds, and compounds with a wide range of fluorine content (14–76 wt. %). The results show that the rotating-bomb method can be used for accurate heat-of-combustion determinations for most, if not all, organic fluorine compounds normally liquid or solid at room temperature. The method is being used in this Laboratory in a continuing program of thermochemical studies of organic fluorine compounds.

(1) This research was supported by the United States Air Force, through the Office of Scientific Research of the Air Research and Development Command.

(2) F. Swarts, *J. chim. phys.*, **17**, 3 (1949).

(3) S. Sunner, Thesis, University of Lund, 1949.

(4) W. N. Hubbard, C. Katz and G. Waddington, This Journal, **58**, 142 (1954).

Experimental

Calorimeter and Bomb.—The calorimeter, laboratory designation BMR2, is similar in most essential features to the earlier model described by Hubbard, *et al.*[4] The most significant change is in the method of rotating the bomb. Instead of withdrawal of a wire wound around a pulley, a direct gear drive is used. Thereby rotation time is not limited by the maximum practical length of wire, and the bomb may be rotated as long as desired. Figure 1 is a schematic sectional view to illustrate the direct drive mechanism. The bomb A is shown in position in the calorimeter can B which in turn is in position in the well C′ of the constant-temperature jacket. The well is covered by the con-

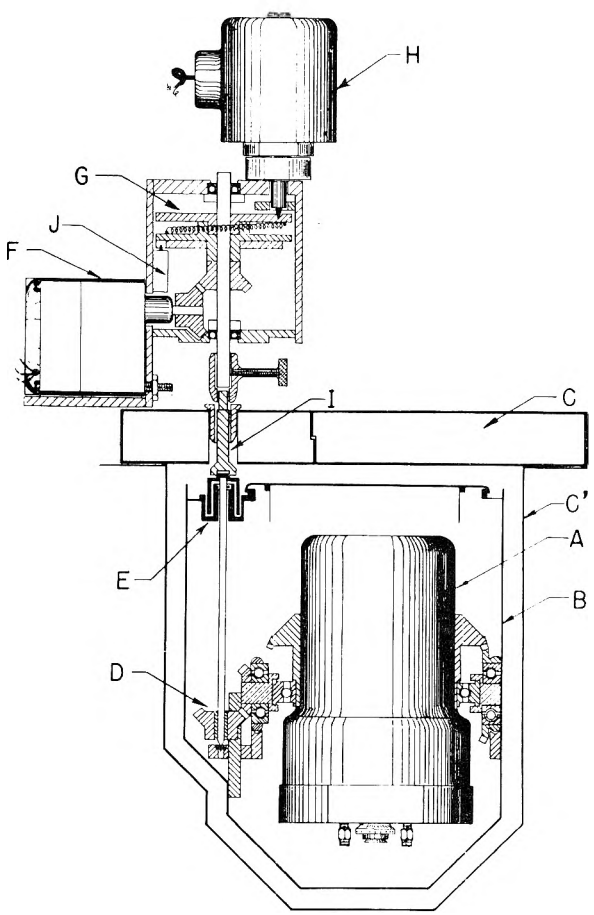

Fig. 1.—Schematic sectional view to illustrate the direct drive mechanism of the rotating bomb.

stant-temperature lid C. The drive shaft, actuated through a pair of miter gears by a 10-r.p.m. synchronous motor F, enters the calorimeter can through oil-seal E and actuates the rotating mechanism of the bomb through miter gear D. The portion of the drive shaft I immediately above the calorimeter can is of plastic to minimize heat conduction along the shaft. The mechanism in which the bomb rotates is identical in operation with that of Hubbard, *et al.*[4] The drive shaft and extra gears are accommodated in the calorimeter can with only a small increase in volume, equivalent to about 2% of the energy equivalent.

For greater versatility provision is made for automatic stopping of the rotation and positioning of the bomb, although such provision was not necessary for the experiments described in this paper. When the bomb is not rotating, the drive mechanism is prevented from turning by a pin in a hole in the wheel G. During rotation of the bomb the pin is held out of the hole by solenoid H, connected in parallel, with the motor circuit. A cam-actuated switch J sends an electrical impulse to a Microflex Counter once in each complete rotation of the bomb. The Microflex Counter counts the number of rotations and shuts off power to the motor and solenoid after any preset number. When the power is shut off, the bomb coasts by inertia until it returns to its original position, whereupon the pin drops into the hole in the wheel G and holds the bomb in position. A spring device takes up the shock from the abrupt stopping of the bomb. With this automatic arrangement the operator must merely push a button at the appropriate time to start rotation of the bomb and thereafter can devote his full attention to time–temperature observations.

For the experiments described in this paper, rotation of the bomb was continued throughout the after period to the end of the calorimetric experiment and not limited to part of the reaction period. The correction for heat generated in the calorimeter by rotation of the bomb was handled in the following manner. Rotation of the bomb was started when the calorimeter attained a predetermined temperature that had been found from previous experience to correspond closely to the midtime T_m of the calorimetric experiment. This midtime is defined by the relationship

$$\int_{T_i}^{T_m} (t - t_i)\mathrm{d}T = \int_{T_m}^{T_f} (t_f - t)\mathrm{d}T \qquad (1)$$

in which t denotes the temperature of the calorimeter and T the time. T_i and t_i are the time and temperature, respectively, at the beginning of the reaction period, and T_f and t_f are these quantities at the end of the reaction period. The rate of change of the calorimeter temperature at the beginning and end of the reaction period is given by the expressions

$$(\mathrm{d}t/\mathrm{d}T)_i = z + \alpha(t_{env.} - t_i) \qquad (2)$$

$$(\mathrm{d}t/\mathrm{d}T)_f = z + y + \alpha(t_{env.} - t_f) \qquad (3)$$

in which z is the constant rate from stirring the water in the calorimeter, y is the constant rate from rotating the bomb, and the last term in each equation is the rate from Newtonian heat exchange with the jacket, the temperature of which is $t_{env.}$. When rotation of the bomb starts at the midtime T_m, the total correction to the observed change in temperature in the reaction period is

$$\Delta t_{cor} = \int_{T_i}^{T_m} [z + \alpha(t_{env.} - t)]\mathrm{d}T + \int_{T_m}^{T_f} [z + y + \alpha(t_{env.} - t)]\mathrm{d}T \qquad (4)$$

By use of equations 1, 2 and 3, equation 4 may be reduced to

$$\Delta t_{cor} = (\mathrm{d}t/\mathrm{d}T)_i (T_m - T_i) + (\mathrm{d}T/\mathrm{d}T)_f (T_f - T_m) \qquad (5)$$

Equation 5 is the usual relationship that applies either to a conventional calorimeter with a stationary bomb or to a rotating-bomb calorimeter when the bomb rotates only during part of the reaction period.[5] When rotation of the bomb starts at the midtime T_m and continues throughout the remainder of the calorimetric experiment, the heat generated by rotation of the bomb is automatically included in the conventional correction for stirring and Newtonian heat exchange. The advantage of continuous rotation of the bomb throughout the after period is that the rate y must remain constant only throughout each individual experiment. When the bomb rotates only during part of the reaction period, the heat generated is included as part of the energy equivalent of the calorimetric system, and there is the much more stringent requirement that this heat be the same throughout a whole series of calibration and combustion experiments. A further advantage is the better opportunity for obtaining a homogeneous liquid phase and equilibrium between the bomb gases and the liquid when the contents of the bomb are agitated continuously rather than for a short time.

The constant-temperature lid of the jacket (C in Fig. 1) is divided into two parts. The calorimeter-stirrer shaft and thermometer (not shown in Fig. 1) go through the same part of the lid as the drive shaft for the rotating mechanism. The other part of the lid is free and allows access to the bomb and calorimeter for adjustment and servicing when all parts are assembled in operating condition. The calorimeter can is designed to accommodate a standard calorimetric-type platinum resistance thermometer.

The bomb, laboratory designation Pt-5, is made of stainless steel and lined with platinum 0.02 inch thick. It is equipped with two valves fabricated from monel. The sealing gasket, $^1/_{16}$ inch thick, is made of fine gold. The inlet tube, electrodes, gimbal, crucible and other internal fittings are all platinum. Teflon gaskets are used where the insulated electrode and valve ports enter through the platinum lining. The internal volume of the bomb is 0.353 l.

Technique for Volatile Samples.—The introduction of volatile samples of organic fluorine compounds into the bomb presented a unique problem. Glass ampoules, such as are used for most other classes of compounds, were unsuitable because the glass reacted with hydrofluoric acid in the combustion products with a thermal effect for which correction would be difficult. The technique of sealing samples in the crucible with a combustible material, such as adhesive cellulose tape, did not seem capable of refinement to the desired accuracy. (Swarts[2] used that technique, the combustible material being either a collodion film or a naphthalene plug.) The ideal solution of the problem would have been a container of some material entirely inert to hydrofluoric acid; however, efforts to devise such a container were unsuccessful. The practical compromise was to use a material that is relatively inert to hydrofluoric acid and for which the thermochemical correction for what reaction does occur is small and can be determined accurately enough. Ampoules of fused quartz were found satisfactory in these respects and were used to contain the samples of volatile fluorine compounds. Except for the use of fused quartz instead of soft glass, the ampoule technique was the same as that described in an earlier publication for this Laboratory.[6] Uniform ampoules of less than 70 mg. mass were consistently satisfactory; in a few experiments with heavier ampoules there was evidence that some of the sample had been ejected from the crucible by violent rupture of these mechanically stronger ampoules.

The fragments of fused quartz were recovered quantitatively at the end of a combustion experiment. The difference in mass of the original ampoule and the recovered fragments measured the amount that was dissolved by hydrofluoric acid. Most of the chemical attack on the fused quartz occurred during the actual combustion when the hot fragments were in contact with the fluorine-containing combustion gases. However, some additional attack occurred after rotation of the bomb started and the fragments were bathed in hydrofluoric acid at about 25°. This additional attack continued until the bomb was discharged and opened and the fragments were washed free of hydrofluoric acid. If this additional attack occurred at a constant rate, the thermal effect was accounted for in the calculation of Δt_{cor}, the correction to the observed change in temperature in the reaction period. (The foregoing statement follows if y in equation 3 of the previous subsection is redefined as the constant rate from rotating the bomb *and from the chemical attack on the fused quartz.*) However, a thermochemical correction was required for the attack that occurred during the actual combustion. The amount of additional attack that occurred after rotation of the bomb started was determined by an appropriate blank

(5) See, for instance, W. N. Hubbard, D. W. Scott and G. Waddington, THIS JOURNAL, **58**, 152 (1954), footnote 21, eq. X.

(6) G. B. Guthrie, Jr., D. W. Scott, W. N. Hubbard, C. Katz, J. P. McCullough, M. E. Gross, K. D. Williamson and G. Waddington, *J. Am. Chem. Soc.*, **74**, 4662 (1952).

experiment, and the amount of attack during the actual combustion was then obtained by difference.

The blank experiment was performed as part of the comparison experiment (*cf.* next subsection). An empty ampoule, which was a "twin" to the one used in the combustion experiment, *i.e.*, of similar mass and surface area, was suspended on a platinum hook outside the crucible (see Fig. 2). A tiny hole in the ampoule permitted pressure equalization when the bomb was charged with oxygen. This ampoule was not exposed to chemical attack during the actual combustion; but, when rotation of the bomb began, it was dropped from the hook and crushed, and the resulting fragments were bathed in a solution of the same concentration as that to which the fragments from the combustion experiment were exposed. The mass of fused quartz dissolved in this blank experiment could then be taken equal to the additional amount dissolved in the combustion experiment after rotation of the bomb started.

The heat of solution of fused quartz in hydrofluoric acid was calculated from values in Circular 500.[7]

$$SiO_2(\text{vitreous}) + 6HF(\text{aq.}) = H_2SiF_6(\text{aq.}) + 2H_2O(\text{liq.})$$
$$\Delta E = -37.7 \text{ kcal.}$$

The thermochemical corrections, per combustion experiment, were in the range 2–7 cal. for fluorobenzene samples and in the range 9–25 cal. for benzotrifluoride samples.

Comparison Experiments.—The reduction of the calorimetric results to standard states in the conventional manner would have required data not available in the literature and difficult to obtain experimentally. In particular, the solubility and heat of solution of carbon dioxide in aqueous solutions of HF (or HF and H_2SiF_6) have not been determined as a function of concentration. This difficulty was avoided by using comparison experiments so designed that the final state of the bomb process was nearly identical with that obtained in a combustion experiment with a fluorine compound. In a comparison experiment the sample consisted of benzoic acid and either succinic acid or a hydrocarbon oil, the heat of combustion of which had been determined previously. The amounts of the two materials were selected so that combustion of the sample produced an evolution of energy and a quantity of carbon dioxide both nearly the same as in the combustion of the fluorine compound. (For unit evolution of energy, combustion of the oil produces less and succinic acid more carbon dioxide than combustion of benzoic acid.) The bomb initially contained an aqueous solution of HF (or HF and H_2SiF_6), which, upon dilution with water produced by combustion of the sample, gave a solution of nearly the same amount and concentration as obtained from combustion of the fluorine compound.

Ideally, the calorimeter was used merely as an instrument to compare the masses of benzoic acid and succinic acid, or of benzoic acid and hydrocarbon oil, with the mass of fluorine compound required to produce the same evolution of energy in combustion to the same final state, the combustion of the former taking place in a bomb that contained a solution of HF (or HF and H_2SiF_6) and that of the latter in a bomb that contained water. No absolute calibration of the calorimeter was needed, and it was necessary to correct only the *initial* states of the bomb processes to standard states.

The design of the comparison experiments will be illustrated by three numerical examples.

In example I, for the combustion experiment, the sample consisted of 1.50690 g. of *o*-fluorobenzoic acid and 0.00305 g. of filter paper fuse (empirical formula, $CH_{1.686}O_{0.843}$), and the bomb initially contained 9.950 g. of water. For the comparison experiment, the sample consisted of 0.99828 g. of benzoic acid, 0.53636 g. of succinic acid and 0.00373 g. of filter paper fuse, and the bomb initially contained 9.87 g. of a 2.181 wt. % solution of HF.

In example II, for the combustion experiment, the sample consisted of 1.38414 g. of benzotrifluoride, 0.02313 g. of hydrocarbon oil (empirical formula, $CH_{1.891}$) and 0.00321 g. of filter paper fuse, and the bomb initially contained 9.950 g. of water. During the actual combustion, 0.01832 g. of the fused quartz ampoule used to contain the benzotrifluoride was dissolved. For the comparison experiment the sample consisted of 1.01240 g. of benzoic acid, 0.13825 g. of the same hydrocarbon oil and 0.00314 g. of filter paper fuse. The bomb initially contained 10.12 g. of solution that contained 5.123 wt. % HF and 0.591 wt. % H_2SiF_6.

In example III, for the combustion experiment, the sample consisted of 6.22982 g. of polytetrafluoroethylene (Teflon) and 0.00273 g. of filter paper fuse, and the bomb initially contained 9.212 g. of water. Analysis of the combustion products showed that 0.04580 mole of HF was formed. (The remainder of the fluorine in the sample appeared in the combustion products as CF_4). For the comparison experiment, the sample consisted of 1.10508 g. of benzoic acid, 0.31179 g. of succinic acid and 0.00326 g. of filter paper fuse, and the bomb initially contained 9.09 g. of a 10.08 wt. % solution of HF. In all cases, the bomb was charged to an initial pressure of 30.00 atm. with oxygen.

The following tabulation compares the energy of the isothermal bomb process, $\Delta E_{I.B.P.}$, and the contents of the bomb in the final state, for the three pairs of combustion and comparison experiments.

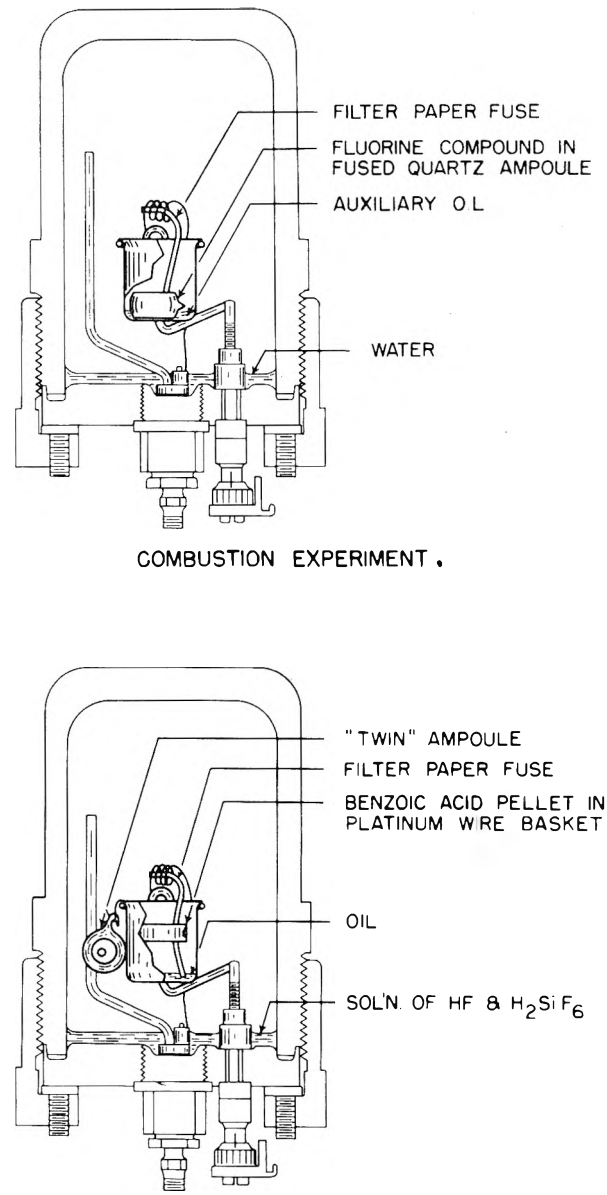

Fig. 2.—Schematic sectional views of the bomb to illustrate a combustion experiment with a volatile fluorine compound in a fused quartz ampoule and the corresponding comparison experiment.

(7) F. D. Rossini, D. D. Wagman, W. H. Evans, S. Levine and I. Jaffe, "Selected Values of Chemical Thermodynamic Properties," N. B. S. Circular 500, 1952.

	Example I o-Fluorobenzoic acid		Example II Benzotrifluoride		Example III Teflon	
	Combustion	Comparison	Combustion	Comparison	Combustion	Comparison
$\Delta E_{\text{I.B.P.}}$, cal.	−7950.2	−7948.4	−7922.4	−7933.8	−7948.7	−7942.6
O_2, moles	0.352	0.350	0.353	0.350	0.363	0.351
CO_2, moles	0.0754	0.0755	0.0681	0.0681	0.0738	0.0740
H_2O, moles	0.574	0.574	0.564	0.564	0.488	0.489
HF, moles	0.0108	0.0108	0.0266	0.0259	0.0458	0.0458
H_2SiF_6, moles	...	...	0.00030	0.00042	...	...
HNO_3, moles	0.00015	0.00007	0.00010	0.00012	0.00001	0.00008
CF_4, moles	...	...	...	...	0.0508	..

It is seen that the evolution of energy and the contents of the bomb in the final state (CF_4 excepted) could be made nearly the same in the comparison experiment as in the combustion experiment.

When the sample was benzoic acid and succinic acid, pellets of the two substances were placed in the crucible. When the sample was benzoic acid and oil, the oil was placed in the bottom of the crucible, and the benzoic acid pellet was suspended in a platinum wire basket so that it did not contact the oil (see Fig. 2).

Reduction to Standard States.—To correct for the minor differences in energy evolution and final state between the combustion and comparison experiments, the data were treated formally as though the comparison experiments were *bona fide* calibration experiments, and corrections to standard states were applied to both initial and final states of all experiments. For this purpose, the procedure of Hubbard, Scott and Waddington[8] was modified to apply to fluorine compounds instead of sulfur compounds.[9] Estimated values were used if experimental data needed for the corrections were lacking. In particular, the solubility and heat of solution of carbon dioxide and oxygen in aqueous solutions of HF (or HF and H_2SiF_6) were assumed to be the same as in pure water. Other less serious assumptions were made when necessary. The use of comparison experiments assures that errors from these assumptions relative to the final state of the bomb process will cancel in computing ΔE_c° for the organic fluorine compound. Errors relative to the initial state of the bomb process, which are not canceled by use of comparison experiments, are much smaller than those relative to the final state and, at worst, are scarcely significant.

In general, values of the *apparent* energy equivalent from comparison experiments [ε_{app}(calor.)] were slightly smaller than values of the energy equivalent from regular calibrations with benzoic acid [ε(calor.)], the more so the higher the concentration of HF used in the comparison experiments. The differences were in the direction to be expected if the product of the solubility and heat of solution of CO_2 in aqueous HF is greater than in pure water. These differences, although partly masked by precision uncertainties in the calibration and comparison experiments, permit crude estimates of the errors in $\Delta E_c^\circ/M$ for fluorine compounds that would result if comparison experiments were not used. For 10 ml. of water initially in the bomb and 0.07 mole of CO_2 produced in the combustion process, the estimates are

Final concn. of HF in bomb, wt. %	2	5	10
Error, %	0.01	0.04	0.10

Although these estimates have only order-of-magnitude significance, they show clearly that, until accurate enough values are available for the solubility and heat of solution of CO_2 in aqueous HF and the other physical constants that enter the corrections to standard states, it will be necessary to use comparison experiments in accurate work.

When tetrafluoromethane, CF_4, was a combustion product, it was necessary to estimate, for the three-component mixture, O_2–CO_2–CF_4, values of $(\partial E/\partial P)_T$ and the gas imperfection parameter, μ in the equation of state, $PV = nRT(1 - \mu P)$. The equations used were

$$(\partial E/\partial P)_T = -1.574\{1 + 1.69x(CO_2)[1 + x(CO_2)] + 1.36x(CF_4)[1 + x(CF_4)]\} \text{ cal. mole}^{-1} \text{ atm.}^{-1} \text{ at } 25^\circ$$

$$\mu = 0.00061\{1 + 3.21x(CO_2)[1 + 1.33x(CO_2)] + 2.20x(CF_4)[1 + 1.33x(CF_4)]\} \text{ atm.}^{-1} \text{ at } 25^\circ.$$

in which $x(CO_2)$ and $x(CF_4)$ are the mole fractions of CO_2 and CF_4, respectively. If $x(CF_4)$ is zero, these expressions reduce to those for O_2–CO_2 mixtures,[8] and if $x(CF_4)$ is unity, these reduce to values for pure CF_4 calculated from data of state.[10] The solubility of CF_4 in the aqueous phase is negligibly small.[11]

Experimental Procedures.—For most combustion experiments with fluorine compounds the bomb initially contained 10 ml. of water. The exception was the series of experiments with Teflon or Teflon–oil mixtures, in which the initial amount of water was varied to keep the composition of the final solution near $HF{\cdot}10H_2O$. The bomb was purged with about 2 l. of oxygen and then charged to a pressure of 30 atm. The bomb was placed in the calorimeter in the inverted position shown in Fig. 2, so that the valves and gaskets were protected from the combustion blast by the water or aqueous solution. In general, the calorimetric procedure was the same as that described in detail in ref. 4, except that rotation of the bomb was continued to the end of the calorimetric experiment.

The electrical energy introduced to ignite the sample was shown by experiment to be the same, whether the bomb initially contained water, as in the combustion experiments, or aqueous HF (or HF and H_2SiF_6), as in the comparison experiments.

The procedure for analyzing the final contents of the bomb varied depending on whether it was critically important to separate fused-quartz fragments rapidly from the bomb solution or to determine accurately the amount of HF in the combustion products. In the former instance, the bomb was discharged rapidly (with a small loss of HF as vapor or spray) and opened. The bomb solution was filtered into a platinum dish, and the interior parts of the bomb were thoroughly rinsed with distilled water. All fused-quartz fragments were transferred to the filter paper. The total time the fragments had been in contact with the bomb solution was recorded. The filter paper containing the fragments was ignited in a weighed platinum crucible, and the mass of the fragments was determined. The combined bomb solution and washings were titrated with standard NaOH solution in the following manner. Slightly more than half of the expected total amount of NaOH solution was first added to ensure that all of the HF was converted to HF_2^- ion. The solution was then heated to incipient boiling to expel dissolved CO_2; and, while the solution was still hot, the titration was continued to the phenolphthalein end-point. The neutralized solution was transferred to a volumetric flask, allowed to come to room temperature, and made up to a volume of 500 ml. with distilled water. A 100-ml. aliquot of the resultant solution was used for determining nitrate ion by Devarda's method (sometimes done in duplicate). In some experiments hydrous silica, from hydrolysis of $SiF_6^=$ ion by titration with the NaOH solution, was recovered by filtration, ignited and weighed as SiO_2 as an approximate check of the amount of fused quartz dissolved. The comparison experiments, in which known amounts of HF (or HF and H_2SiF_6) were initially added to the bomb, served as blank experiments to estimate the small amount of HF lost in rapid discharge of the bomb.

When it was important to determine accurately the amount of HF in the combustion products, the bomb was discharged slowly, the gas was passed through a scrubber that contained 50 ml. of 0.1*M* NaF solution, and this solution was then heated to incipient boiling to expel CO_2 and

(8) W. N. Hubbard, D. W. Scott and G. Waddington, THIS JOURNAL, **58**, 152 (1954).

(9) Copies of the complete computation form for organic fluorine compounds may be obtained from the authors upon request.

(10) K. E. MacCormack and W. G. Schneider, *J. Chem. Phys.*, **19**, 845 (1951).

(11) H. M. Parmelee, *Refrig. Eng.*, **61**, 1341 (1953).

titrated with standard NaOH solution to the phenolphthalein end-point. This step determined the small amount of HF carried out of the bomb with the discharge gases. The bomb was opened, and the bomb solution was washed quantitatively into a platinum dish. The combined bomb solution and washings were then titrated with standard NaOH solution and analyzed for nitrate ion, as already described.

In titration of the total acidity of the bomb solution, the number of equivalents of base required equals the number of gram-atoms of fluorine from combustion of the sample (or added as HF and H_2SiF_6 in a comparison experiment) plus the number of equivalents of nitric acid produced in the bomb process. It is immaterial whether the fluorine is present as HF or H_2SiF_6, because each requires one equivalent of base per gram atom of fluorine when titrated in a hot solution.

$$HF + OH^- = H_2O + F^-$$

$$H_2SiF_6 + 6\ OH^- = SiO_2 + 4\ H_2O + 6\ F^-$$

In some instances the determination of fluorine in the combustion products by acid–base titration was checked by direct determination of fluoride ion in aliquots of the neutralized bomb solution. The determinations were made either volumetrically, by titration with thorium nitrate solution according to the procedure of Kimball and Tufts,[12] or gravimetrically, by precipitation as PbClF.[13] Samples of the discharge gases, freed from HF, were retained after some experiments for mass-spectrometer scanning. Occasional tests of the discharge gases for carbon monoxide always gave negative results. Qualitative tests of bomb solutions for nitrite ion and for the metals used for the lining, fittings and valves of the bomb (platinum, gold, palladium, nickel and copper) were likewise negative.

Materials

Benzoic Acid.—The benzoic acid was National Bureau of Standards standard sample 39g, with a certified heat of combustion of 26.4338 ± 0.0026 abs. kj. (6317.83 ± 0.62 cal.)/g. mass under certificate conditions. Conversion from certificate conditions to standard conditions by the method of ref. 8 gives −6312.91 ± 0.62 cal./g. mass for $\Delta E_c^\circ/M$, the energy of the idealized combustion reaction.

Auxiliary Oil.—The auxiliary oil was a sample of redistilled mineral oil, laboratory designation USBM-P3a, empirical formula $CH_{1.891}$. The value of $\Delta E_c^\circ/M$, as determined by a series of combustion experiments in this Laboratory, was −10,983.8 ± 2.2 cal. g.$^{-1}$

Succinic Acid.—The sample used in this work was prepared by recrystallizing Mallinckrodt analytical reagent-grade material four times from distilled water, oven drying at 105–110°, and storing in a vacuum desiccator. Duplicate determinations of the neutralization equivalent gave 99.98 and 99.97% of the theoretical value. The material gave a negative spot test for acid anhydride.[14] The heat of combustion was determined concurrently with each of the two series for which succinic acid was used for comparison experiments. The values obtained for $\Delta E_c^\circ/M$ were −3018.6 ± 1.8 and −3019.1 ± 0.6 cal. g.$^{-1}$ These values are slightly lower than those obtained by Huffman,[15] −3020.2 ± 0.8 cal. g.$^{-1}$ [16], and by Pilcher and Sutton,[17] −3020.57 ± 0.43 cal. g.$^{-1}$. The reason for the difference is not evident. If the sample used in this work had not been pure, that circumstance would be of little consequence. It was only necessary that $\Delta E_c^\circ/M$ be known accurately for the actual material used in the comparison experiments; this material did not need to be highly pure succinic acid.

***o*-, *m*- and *p*-Fluorobenzoic Acids.**—Two samples each of *o*-, *m*- and *p*-fluorobenzoic acid were used. One set of samples, hereafter designated "A," was supplied by the Illinois State Geological Survey Division through the courtesy of Dr. G. C. Finger. These had been purified by recrystallization from 50% aqueous ethanol and then vacuum sublimed at 130–140°. These samples were used as received. The other samples, hereafter designated "B," were prepared with materials from a commercial source. These were purified, first by recrystallization from 50% aqueous ethanol, and then by zone melting.

The zone-melting procedure was an adaptation of that of Herrington and co-workers[18] to permit all heating of the material to be done in a closed glass system under an inert atmosphere. The main parts of the apparatus are illustrated in Fig. 3. The fluorobenzoic acid, with 0.01 mole % or less of indanthrene dye added as impurity indicator, was first melted into the long, heavy-walled tube under dry helium. The head was then sealed to the tube, and the assembly was evacuated, filled with dry helium and sealed off. The small, cylindrical heater was made to move over the outside of the tube away from the head at such a rate that the melted zone traversed the length of the tube in 15 to 20 hours. The tube could be either vertical, as in Fig. 3, or inclined slightly from horizontal. The hot air bath was used to prevent sublimation of material into the head. Passages of the melted zone were repeated until the dye was concentrated in a short section at the end of the tube. The *o*- and *p*-fluorobenzoic acids crystallized from the melt as large, nearly perfect crystals, and 4 to 6 passages of the melted zone were adequate. The *m*-fluorobenzoic acid, on the other hand, crystallized as a network of fine, needle-shaped crystals, which trapped impurity-laden melt. With this substance a single passage of the melted zone was much less effective, and about 20 passages were necessary. The purified material, that is, that from which all visible traces of dye had been removed, was recovered by inverting the tube, warming only the section of purified material, and allowing it to flow into the receiver in the head as it melted.

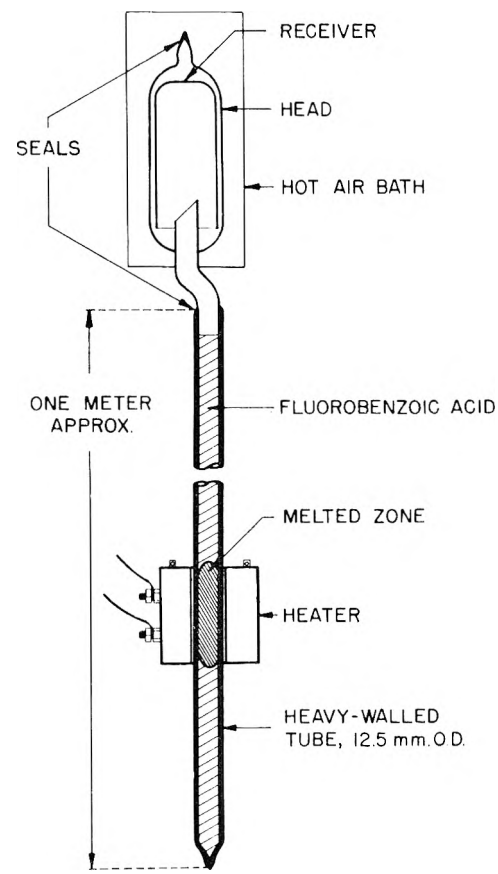

Fig. 3.—Apparatus for purifying fluorobenzoic acids by zone melting.

(12) R. H. Kimball and L. E. Tufts, *Anal. Chem.*, **19**, 150 (1947).

(13) W. W. Scott, "Standard Methods of Chemical Analysis," Vol. I, 5th ed., D. Van Nostrand Co., Inc., New York, N. Y., 1939, p. 405.

(14) F. Feigl, "Qualitative Analysis by Spot Tests," 3rd Eng. ed., Elsevier Publishing Co., Inc., New York, N. Y., 1947, p. 359.

(15) H. M. Huffman, *J. Am. Chem. Soc.*, **60**, 1171 (1938).

(16) This value has been corrected to the revised value for the heat of combustion of benzoic acid. See R. S. Jessup, *J. Research Natl. Bur. Standards*, **29**, 247 (1942).

(17) G. Pilcher and L. E. Sutton, *Trans. Roy. Soc.* (*London*), **A248**, 23 (1955).

(18) See, *Research*, **7**, 465 (1954).

Neutralization equivalents were determined for both sets of samples with the following results, expressed as per cent. of the theoretical values.

Compound	"A" Sample	"B" Sample
o-Fluorobenzoic acid	99.86	99.89
m-Fluorobenzoic acid	99.78	99.91
p-Fluorobenzoic acid	99.93	99.93

All six samples gave negative spot tests for acid anhydride.[14] No quantitative determinations of purity were made for these crystalline materials. However, as the pairs of samples purified by fundamentally different means gave concordant values of $\Delta E_c^\circ/M$, it is unlikely that they contained enough impurity to alter the heat of combustion significantly.

Fluorobenzene.—Fluorobenzene, supplied by the Illinois State Geological Survey Division through the courtesy of Dr. G. C. Finger, was distilled in an efficient fractionating column by the Chemistry and Refining Branch of this station. The composite of selected fractions taken as sample had a purity of 99.95 ± 0.03 mole %, as determined by a calorimetric study of melting point as a function of the fraction melted. Immediately before filling ampoules for combustion calorimetry, the material was dried by passing the vapor through anhydrous $Mg(ClO_4)_2$.

Benzotrifluoride.—Benzotrifluoride (α,α,α-trifluorotoluene), from the Hooker Electrochemical Co., was distilled in an efficient fractionating column by the Chemistry and Refining Branch of this station. The composite of selected fractions taken as sample had a purity of 99.999 ± 0.001 mole %, as determined by a calorimetric study of melting point as a function of the fraction melted. The sample was dried by treatment with calcium hydride.

Polytetrafluoroethylene.—Polytetrafluoroethylene (Teflon) was furnished through the courtesy of Dr. E. E. Lewis, Polychemicals Department, E. I. du Pont de Nemours & Co. This material, a granular powder that had received no heat treatment, was used as received.

Heats of Combustion

Units of Measurement and Auxiliary Quantities.—The results of the combustion calorimetry are expressed in terms of the defined calorie equal to 4.1840 abs. joules and refer to the isothermal process at 25° and to the true mass. The molecular weights were computed from the 1951 table of international atomic weights.[19] For use in reducing weights in air to *in vacuo*, in correcting the energy of the actual bomb process to the isothermal process and in correcting to standard states, the following values (for 25°) of density, ρ, specific heat, c_p, and $(\partial E/\partial P)_T$ for the various substances were used.

	ρ, g. ml.$^{-1}$	c_p, cal. deg.$^{-1}$ g.$^{-1}$	$(\partial E/\partial P)_T$ cal. atm.$^{-1}$ g.$^{-1}$
Benzoic acid	1.320	0.289	−0.0028
Auxiliary oil	0.87	(0.53)	−0.0060
Succinic acid	1.56	0.287	(−0.0028)
o-Fluorobenzoic acid	1.460	(0.269)	(−0.0028)
m-Fluorobenzoic acid	1.474	(0.269)	(−0.0028)
p-Fluorobenzoic acid	1.479	(0.269)	(−0.0028)
Fluorobenzene	1.0191	0.364	−0.0083
Benzotrifluoride	1.1814	(0.36)	−0.0072
Polytetrafluoroethylene	2.24	0.28	−0.010

These values were obtained from the literature and from unpublished measurements in Bureau of Mines laboratories, or, in parentheses, estimated by analogy with structurally similar substances. For $\Delta E_c^\circ/M$ of the filter paper fuse, the value −3923 cal. g.$^{-1}$ was used.

Typical Calorimetric Experiments.—Calorimetric experiments selected as typical of each of the several series are summarized in Table I. In this table m (material) denotes the mass of the designated material (benzoic acid, oil, succinic acid or compound) in the sample that underwent combustion. The symbol n^i(material) denotes the number of moles of the designated material (H_2O, HF, or H_2SiF_6) initially present in the bomb. The quantity $\Delta t_c = t_f - t_i - \Delta t_{cor.}$ is the observed temperature rise of the calorimeter corrected for Newtonian heat exchange, and the energy from stirring, from rotation of the bomb and, where applicable, from solution of fused quartz in the bomb solution after rotation of the bomb had started. The symbol $\Delta E_c^\circ/M$(material) denotes the energy of the idealized combustion reaction for 1 g. of the designated material. The terms ΔE^f_{dec}-(HNO_3) and $\Delta E^f_{hydr}(H_2SiF_6)$ denote the thermochemical corrections for formation of HNO_3 and for attack on the fused quartz during the actual combustion. The term ΔE cor. to st. states denotes the sum of all corrections to standard states. The term ΔE_{ign} denotes the electrical energy used to ignite the fuse. The symbols ε(cont.), ε(calor.) and ε_{app}(calor.) denote the energy equivalent of the contents of the bomb, the energy equivalent of the calorimetric system, and the apparent energy equivalent of the calorimetric system as determined by a comparison experiment, respectively.

***o*-, *m*- and *p*-Fluorobenzoic Acids.**—Nine series of experiments, *i.e.*, combustion experiments with each of the two samples of *o*-, *m*-, and *p*-fluorobenzoic acids, comparison experiments, combustion experiments with succinic acid and standard calibrations with benzoic acid were done concurrently. By operating in this manner, any errors from time-dependent effects were minimized. For three combustion experiments in which care was taken to avoid loss of HF in discharge of the bomb, the average amount of HF in the products, as determined by acid–base titration and correction for the nitric acid present, was 99.81 ± 0.01% of that expected for complete conversion of fluorine to HF. For twenty experiments in which the bomb was discharged rapidly, the corresponding average recovery of HF was 99.17 ± 0.06%; the average loss of HF in rapid discharge of the bomb, as determined from six comparison experiments, was 0.81 ± 0.18%; the corrected recovery was therefore 99.98 ± 0.19%. Mass-spectrometer scanning of HF free discharge gas from a non-calorimetric combustion of *p*-fluorobenzoic acid showed O_2, CO_2, A, N_2 and H_2O but no detectable amount of any fluorine-containing gas. These analytical results indicate that fluorine in fluorobenzoic acids is converted quantitatively to HF in the combustion process.

The values of $\Delta E_c^\circ/M$ (in cal. g.$^{-1}$) obtained in all of the combustion experiments are listed below. These refer to the reaction

$$C_7H_5O_2F(c) + 7O_2(g) + 48H_2O(liq.) = 7CO_2(g) + HF\cdot 50H_2O\ (liq.).$$

(19) E. Wichers, *J. Am. Chem. Soc.*, **74**, 2447 (1952).

	o-Fluorobenzoic acid	*m*-Fluorobenzoic acid	*p*-Fluorobenzoic acid
"A" Sample	−5258.5	−5233.6	−5219.9
	−5252.2	−5229.5	−5223.9
	−5253.3	−5230.4	−5218.7
	−5252.4	−5229.7	−5219.6
"B" Sample	−5259.6	−5229.2	−5223.8
	−5252.4	−5230.3	−5223.9
	−5258.9	−5230.0	−5225.2
	−5252.6	−5229.6	−5224.1
Mean:	−5255.0	−5230.3	−5222.4
Standard dev. of mean (comb. expts. only)	±1.2 (0.023%)	±0.5 (0.010%)	±0.9 (0.017%)
Standard dev. of mean (comb. and comp. expts.)	±1.3 (0.024%)	±0.7 (0.013%)	±1.0 (0.019%)

x	0.0285	0.0564	0.1178	0.2577	0.2678	0.3645	0.5388	0.5702	0.7973	0.8104	0.8162
$\Delta E_c°/M$, cal./g.	−1582.6	−1580.5	−1568.0	−1501.5	−1498.8	−1458.1	−1384.2	−1374.5	−1276.9	−1271.3	−1270.8
$\Delta E_c°$, kcal. mono-mole^{-1}	−158.3	−158.1	−156.8	−150.2	−149.9	−145.8	−138.5	−137.5	−127.7	−127.2	−127.1
$\Delta H_c°$, kcal. mono-mole^{-1}	−157.7 ±1.8	−157.5 ±1.3	−156.2 ±0.9	−149.6 ±0.6	−149.3 ±0.5	−145.2 ±0.5	−137.9 ±0.2	−136.9 ±0.2	−127.1 ±0.1	−126.6 ±0.1	−126.5 ±0.1

TABLE I

SUMMARY OF TYPICAL CALORIMETRIC EXPERIMENTS

	o-Fluorobenzoic acid[a]	Fluorobenzene	Benzotri-fluoride	Teflon	Teflon and oil	Succinic acid
Comparison experiments						
m(benzoic acid), g.	0.99843	0.65867	0.98098	1.08051	0.36919	1.25095
m(oil), g.		0.34193	0.15663		0.50924	
m(succinic acid), g.	0.53715			0.36427		
$n^i(H_2O)$, moles	0.5359	0.5382	0.5210	0.4520	0.4028	0.0559
n^i(HF), moles	0.01076	0.00884	0.02403	0.04722	0.02322	
$n^i(H_2SiF_6)$, moles		0.00008	0.00057			
Δt_c, deg.	1.98099	1.97832	1.97773	1.98227	1.98183	1.97670
$m\Delta E_c°/M$(benzoic acid,) cal.	−6303.0	−4158.1	−6192.8	−6821.2	−2330.7	−7897.1
$m\Delta E_c°/M$(oil), cal.		−3755.7	−1720.4		−5593.4	
$m\Delta E_c°/M$(succinic acid,) cal.	−1621.7[b]			−1099.6[d]		
$m\Delta E_c°/M$(fuse), cal.	−12.2	−12.2	−10.6	−11.5	−12.2	−11.7
$-\Delta E^f_{dec}(HNO_3)$, cal.	−1.0	−0.4	−1.6	−1.6	−0.8	−0.8
$-\Delta E$, cor. to st. states, cal.	−12.1	−8.6	−10.1	−11.3	−6.5	−6.2
$-\Delta E_{ign}$, cal.	−1.4	−1.3	−1.3	−1.3	−1.3	−1.4
ε(cont.)(Δt_c), cal.	+26.2	+26.1	+26.0	+23.6	+20.8	+8.9
ε_{app}(calor.) $(-\Delta t_c)$, cal.	−7925.2	−7910.2	−7910.8	−7922.9	−7924.1	−7908.3
ε_{app}(calor.), cal. deg.$^{-1}$	4000.6	3998.4	3999.9	3996.9	3998.4	4000.7[g]
Combustion Experiments						
m(compound), g.	1.50607	0.89520	1.33710	6.22701	0.61528	2.62048
m(oil), g.		0.09085	0.04717		0.63439	
$n^i(H_2O)$, moles	0.5523	0.5523	0.5523	0.5113	0.4150	0.0559
Δt_c, deg.	1.97793	1.97616	1.97794	1.98228	1.98596	1.98208
ε_{app}(calor.) $(-\Delta t_c)$, cal.	−7912.7[c]	−7901.5	−7911.6	−7923.0	−7940.6	−7930.1[h]
ε(cont.) $(-\Delta t_c)$, cal.	−26.5	−26.4	−26.8	−27.8	−21.3	−9.6
ΔE_{ign}, cal.	+1.4	+1.3	+1.3	+1.3	+1.3	+1.4
ΔE, cor. to st. states, cal.	12.3	8.7	10.5	20.9	7.6	10.2
$\Delta E^f_{dec}(HNO_3)$, cal.	0.9	0.6	1.7	0.5	0.4	0.7
$\Delta E^f_{hydr}(H_2SiF_6)$, cal.		2.5	24.2			
$-m\Delta E_c°/M$(fuse), cal.	12.8	12.0	13.0	11.9	12.1	15.7
$-m\Delta E_c°/M$(oil,) cal.		997.9	518.1		6968.0	
$m\Delta E_c°/M$(compound), cal.	−7911.8	−6904.9	−7369.6	−7916.2	−972.5	−7911.7
$\Delta E_c°/M$(compound), cal. g.$^{-1}$	−5253.3	−7713.2	−5511.6	−1271.3[e]	−1580.5[f]	−3019.2

[a] Typical of experiments with all three isomers. [b] Using value of $\Delta E_c°/M$(succinic acid,) 3019.1 cal. g.$^{-1}$, determined concurrent with this series. [c] Calculated from average value of ε_{app} (calor.), 4000.5 cal. deg.$^{-1}$, from eight comparison experiments. [d] Using value of $\Delta E_c°/M$(succinic acid), 3018.6 cal. g.$^{-1}$, determined concurrently with this series. [e] In this experiment, 81.04% of the fluorine in the sample appeared in the products as CF_4. [f] In this experiment, 5.64% of the fluorine in the sample appeared in the products as CF_4. [g] Value of ε(calor.) from standard calibration with benzoic acid. [h] Calculated from average value of ε(calor.), 4000.9 cal. deg.$^{-1}$, from five calibration experiments.

All combustion experiments for the three isomers were so similar that the same comparison experiments could be used. The values of $\Delta E_c^\circ/M$ for the individual combustion experiments were computed by use of the average value of ε_{app}(calor.), 4000.5 ± 0.3 cal. deg.$^{-1}$, from eight comparison experiments. The standard deviation of the mean computed to include precision uncertainty in the comparison experiments is comparable with the standard deviation of the mean for the experiments with fluorobenzene and benzotrifluoride, in which it was necessary to pair each combustion experiment with its individual comparison experiment.

Fluorobenzene.—Seven acceptable combustion experiments with fluorobenzene were obtained out of sixteen attempts. The average recovery of HF was 99.77 ± 0.04%; the loss in discharge of the bomb, as determined from the comparison experiments, was 0.20 ± 0.07%; the corrected recovery was therefore 99.97 ± 0.08%. These determinations of HF recovery by acid–base titration were checked by volumetric determinations of fluoride ion in the neutralized bomb solutions. Mass-spectrometer scanning of HF-free discharge gases showed no detectable amount of fluorine-containing gas. These analytical results indicate that fluorine in fluorobenzene is converted quantitatively to HF in the combustion process.

The results of the seven combustion experiments follow. The values of $\Delta E_c^\circ/M$ refer to the reaction

$$C_6H_5F(liq.) + 7O_2(g) + 58H_2O(liq.) = 6CO_2(g) + HF\cdot 60H_2O(liq.).$$

$\Delta E_c^\circ/M$: −7719.8, −7709.0, −7717.5, −7711.4, −7713.2, −7710.8, −7713.1 cal. g.$^{-1}$

Mean −7713.5 cal. g.$^{-1}$

Standard dev. of the mean ±1.4 cal. g.$^{-1}$ (0.019%)

Benzotrifluoride.—Six acceptable combustion experiments with benzotrifluoride were obtained out of eleven attempts. The average recovery of HF was 99.28 ± 0.12%; the loss in discharge of the bomb, as determined from the comparison experiments, was 0.56 ± 0.13%; the corrected recovery was therefore 99.84 ± 0.18%. Mass-spectrometer scanning of HF-free discharge gases showed no detectable amount of fluorine-containing gas. These analytical results indicate that fluorine in benzotrifluoride is converted quantitatively to HF in the combustion process.

The results of the six combustion experiments follow. The values of $\Delta E_c^\circ/M$ refer to the reaction

$$C_7H_5F_3(liq.) + 15/2O_2(g) + 59H_2O(liq.) = 7CO_2(g) + 3HF\cdot 20H_2O(liq.).$$

$\Delta E_c^\circ/M$: −5515.5, −5509.4, −5511.6, −5516.2, −5508.4, −5514.0 cal. g.$^{-1}$

Mean −5512.5 cal. g.$^{-1}$

Standard dev. of the mean: ±1.3 cal. g.$^{-1}$ (0.024%)

Polytetrafluoroethylene (Teflon).—A brief account of the studies with Teflon has already been published.[20] Teflon differed from the other organic fluorine compounds studied in this investigation in that CF_4 as well as HF was a product of the combustion process. When the sample was pure Teflon, about 80% of the fluorine appeared in the products as CF_4. When the sample was a mixture of Teflon and auxiliary oil, the percentage of fluorine appearing as CF_4 could be reduced to any desired value by suitably varying the relative amounts of Teflon and oil. This circumstance permitted a simple determination of the heats of hydrolysis and formation of CF_4.

Preliminary experiments showed that clean combustions were obtained in ordinary platinum crucibles when the sample was Teflon alone but that mixtures of Teflon and oil left gray deposits. This difficulty was avoided by use of a crucible perforated with small holes above the oil level to permit better access of oxygen to the reaction zone. This perforated crucible was used for all calorimetric experiments with mixtures of Teflon and oil, and clean combustions were always obtained.

The fraction of the fluorine in the sample that appeared in the combustion products as HF was determined from the total acidity of the bomb solution and discharge gases after correction for the nitric acid present. The determinations of HF by acid–base titration were checked by gravimetric determinations of fluoride ion in the neutralized bomb solutions. The fraction of fluorine that appeared as CF_4 was obtained by difference. Mass-spectrometer scanning of the HF-free discharge gases showed that no detectable amounts of fluorine-containing gases other than CF_4 were present. No quantitative determinations of CF_4 were made, but the heights of the mass peaks for CF_4 correlated well with the calculated mole fractions of CF_4 in the samples of discharge gases.

Since the initial temperature of the calorimetric experiments, 23°, lies in the temperature range in which Teflon has one and probably two transitions and shows hysteresis in its thermal and volumetric properties,[21] it was necessary for all of the samples to have similar thermal histories before ignition, so that, if they were not in a state of complete equilibrium, at least all would be in states in which differences in enthalpy would be negligible. The samples, stored at ambient temperature, were at the temperature of the air-conditioned laboratory (25–30°) for at least the period of about two hours required to prepare the experiment. They were cooled to slightly below 23° when the bomb was placed into the calorimeter and then immediately warmed to 23° when the calorimeter was brought to the starting temperature. A period of 19 ± 4 minutes then elapsed before calorimetric observations began. It is thought that the thermal histories of the samples were similar enough that the desired end was achieved.

In some of the experiments the samples of Teflon were pressed into pellets; in others, the samples were put into the crucible as the original powder. No difference could be detected between the results with samples in the pellet or powder form (see Fig. 4).

Eleven satisfactory pairs of combustion and comparison experiments were obtained—three with samples of Teflon alone and eight with mixtures of Teflon and oil selected to give a large variation

(20) D. W. Scott, W. D. Good and G. Waddington, *J. Am. Chem. Soc.*, **77**, 245 (1955).

(21) G. T. Furukawa, R. E. McCoskey and G. J. King, *J. Research Natl. Bur. Standards*, **49**, 273 (1952) and references cited therein.

of the fraction of fluorine that appeared in the products as CF_4. The results are as follows. The values of $\Delta E_c^\circ/M$, ΔE_c° and ΔH_c° refer to the reaction

$$C_2F_4(\text{solid polymer}) + O_2(g) + (42 - 42x)H_2O(\text{liq.}) = (2 - x)CO_2(g) + xCF_4(g) + (4 - 4x)\ HF\cdot 10H_2O(\text{liq.})$$

in which x is the fraction of fluorine that appears in the products as CF_4.

The uncertainty assigned to the values of ΔH_c° was calculated from an estimated over-all uncertainty of 0.1% in the combustion and comparison experiments. The uncertainty is greater at smaller values of x because more of the heat measured calorimetrically came from combustion of the admixed oil and less from the Teflon. The values of ΔH_c° are plotted as a function of x in Fig. 4. The equation of the straight line in Fig. 4, which represents the experimental values within their estimated uncertainty, is

$$\Delta H_c^\circ = -160.34 + 41.55\ x \text{ kcal. monomole}^{-1}$$

For the limits of x equal to 0 and 1

$$C_2F_4(\text{solid polymer}) + O_2(g) + 42H_2O(\text{liq.}) = 2CO_2(g) + 4HF\cdot 10H_2O(\text{liq.})$$
$$\Delta H^\circ_{298.16} = -160.3 \pm 0.9 \text{ kcal. monomole}^{-1}$$
$$C_2F_4(\text{solid polymer}) + O_2(g) = CO_2(g) + CF_4(g)$$
$$\Delta H^\circ_{298.16} = -118.8 \pm 0.5 \text{ kcal. monomole}^{-1}$$

The difference of the foregoing two equations gives the heat of hydrolysis of CF_4.

$$CF_4(g) + 42H_2O\ (\text{liq.}) = CO_2(g) + 4HF\cdot 10H_2O\ (\text{liq.})$$
$$\Delta H^\circ_{298.16} = -41.5 \pm 1.0 \text{ kcal. mole}^{-1}$$

The value of the heat of hydrolysis of CF_4 is independent of the particular thermodynamic state, *i.e.*, degree of crystallinity, of the Teflon sample. Use of values for the standard heats of formation of $CO_2(g)$, $H_2O(\text{liq.})$ and HF (in $10H_2O$) at 298.16°K.[7] leads to the derived value for the heat of formation of CF_4.

$$C(\text{graphite}) + 2F_2(g) = CF_4(g)$$
$$\Delta H^\circ_{298.16} = -218.3 \text{ kcal. mole}^{-1}$$

Derived Data.—In Table II are listed the derived data for all six substances. The uncertainties given for ΔE_c° and ΔH_c° are the uncertainty intervals equal to twice the final "over-all" standard deviation.[22] The latter includes uncertainties not only in the combustion and comparison experiments but also in the heats of combustion of the benzoic acid, auxiliary oil and succinic acid used in the comparison experiments. To compute the values of standard heat of formation, $\Delta Hf°$, the following values were used for the standard heats of formation of carbon dioxide, water and hydrofluoric acid, $\Delta Hf°$, in kcal. mole^{-1} at 298.16°K.[7]

$CO_2(g)$	−94.0518
$H_2O(\text{liq.})$	−68.3174
HF(in $10H_2O$)	−75.605
HF(in $20H_2O$)	−75.634
HF(in $50H_2O$)	−75.660
HF(in $60H_2O$)	−75.666

Discussion

Comparison with Previous Work.—Aside from the results reported here, virtually all of the thermochemical data available for solid and liquid organic fluorine compounds are from the early work of Swarts.[2] It is now possible to appraise the reliability of Swarts' data, since five of the compounds studied in this research were also studied by Swarts. A comparison of the results of this research with those of Swarts follows.

(22) F. D. Rossini and W. E. Deming, *J. Wash. Acad. Sci.*, **29**, 116 (1939).

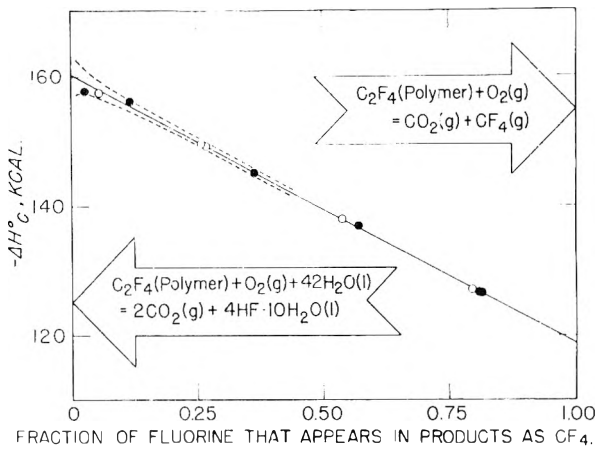

Fig. 4.—$\Delta Hc°$ for the combustion of polytetrafluoroethylene (Teflon) as a function of x, the fraction of fluorine that appears in the products as CF_4. Open circles, samples not pelleted. Filled circles, samples pelleted. The dashed lines correspond to an uncertainty of ±0.1% in the calorimetry.

	$-\Delta E_c^\circ/M$, cal. g.$^{-1}$ This investigation	Heat of combustion, cal. g.$^{-1}$, Swarts	Difference, cal. g.$^{-1}$
o-Fluorobenzoic acid	5255.0	5285.2	30.2
m-Fluorobenzoic acid	5230.3	5266.85	36.5
p-Fluorobenzoic acid	5222.4	5281.7	59.3
Fluorobenzene	7713 5	7773.6	60.1
Benzotrifluoride	5512.5	5547.1	34.6

It is seen that the values of heat of combustion reported by Swarts are from ½% to more than 1% higher than the values of $-\Delta Ec°/M$ of this research. The two sets of values are not strictly comparable for several reasons. Swarts' values apply to a lower temperature, not specified but near 19°, and to lower, but also not specified, concentrations of HF in the final state. The calibration of Swarts' calorimetric system was based on values for the heats of combustion of his calibrating substances, naphthalene, sucrose and benzoic acid, significantly different from present accepted values. Finally, Swarts' values were not corrected to standard states. The correction to standard states would be large for Swarts' experimental conditions because of solution of CO_2 in the large volume of solution in his bomb (50 ml. of water added initially). Swarts did not give enough experimental details, such as volume of the bomb, sample size, initial pressure of oxygen, initial and final temperatures, and details of calibration experiments, to permit recalculation of his data to a basis comparable with the results of this research. Even if possible, such a recalculation would not be meaningful, because Swarts probably did not obtain a homogeneous solution of HF nor equilibrium solution of CO_2 in the final solution in his stationary bomb.

***p*-Fluorobenzoic Acid as a Reference Substance.**—In the combustion calorimetry of any class of organic compounds, it is desirable to have one or

TABLE II

DERIVED DATA AT 298.16°K., KCAL. MOLE^{-1}

Compound and state	Concn. of HF to which $\Delta E_c°$ and $\Delta H_c°$ apply	$\Delta E_c°$, kcal. mole^{-1}	$\Delta H_c°$, kcal. mole^{-1}	$\Delta Hf°$, kcal. mole^{-1}
o-Fluorobenzoic acid(c)	$HF \cdot 50H_2O$	-736.28 ± 0.36	-736.28 ± 0.36	-134.38
m-Fluorobenzoic acid(c)	$HF \cdot 50H_2O$	-732.81 ± 0.20	-732.81 ± 0.20	-137.84
p-Fluorobenzoic acid(c)	$HF \cdot 50H_2O$	-731.71 ± 0.29	-731.71 ± 0.29	-138.95
Fluorobenzene(liq.)	$HF \cdot 60H_2O$	-741.27 ± 0.29	-741.86 ± 0.29	-34.75
Benzotrifluoride(liq.)	$HF \cdot 20H_2O$	-805.43 ± 0.39	-805.73 ± 0.39	-147.85
Polytetrafluoroethylene (Teflon) (solid polymer)[a]	$HF \cdot 10H_2O$	-160.9 ± 0.9[b,c]	-160.3 ± 0.9[b,c]	-193.5[b]

[a] Values apply only for the particular sample of Teflon used in this work. [b] Unit: kcal. monomole^{-1}. [c] Estimated uncertainty.

more reference substances for intercomparison of results among different laboratories. Succinic acid for compounds of carbon, hydrogen and oxygen, hippuric acid for nitrogen compounds, and thianthrene for sulfur compounds have attained varying degrees of acceptance as reference substances. For fluorine compounds, it will be desirable to have several reference substances representative of compounds with different fluorine content. In 1936 the Permanent Commission on Thermochemistry of the International Union of Chemistry recommended *m*-trifluorotoluic acid, *m*-$CF_3C_6H_4COOH$; this substance (29.98 wt. % F) is representative of compounds with intermediate fluorine content. It is now proposed that *p*-fluorobenzoic acid (13.56 wt. % F) is a suitable reference substance representative of compounds of low fluorine content. The *p*-isomer is selected because its lower solubility relative to the *o*- and *m*-isomers makes it easier to free from isomeric impurity by fractional crystallization. *p*-Fluorobenzoic acid fulfills the minimum requirements for a reference substance.[23] It is easy to dry and free from residual solvent, *e.g.*, by vacuum sublimation, and remains dry without special precautions. It is stable at elevated temperatures, as shown by the zone-melting purification in which the material was repeatedly heated above its melting point, 183.5°, without detectable decomposition. It is essentially non-volatile at room temperature, it is readily flammable, and it undergoes complete combustion. It is easily made into pellets. The pellets are somewhat more fragile than those made with benzoic acid, but this property is no disadvantage if the pellets are weighed directly in the crucible.

(23) M. Beckers, *Bull. soc. chim. Belges*, **40**, 518 (1931).

Appraisal of the Method.—The results with compounds of different physical state, volatility and fluorine content show that the rotating-bomb method is satisfactory for accurate combustion calorimetry of most solid and liquid organic fluorine compounds. The precision obtained, uncertainty intervals in the range ± 0.20 to ± 0.40 kcal. mole^{-1}, is nearly, but not quite, as good as that currently obtainable in combustion calorimetry with compounds of carbon, hydrogen, oxygen, nitrogen and sulfur. The chemistry of the combustion process appears to be well defined. For compounds of low fluorine content, the fluorine is converted quantitatively to HF. For Teflon, and probably for other compounds of high fluorine content, the fluorine appears in the combustion products both as HF and as CF_4, but there is no evidence for any other fluorine-containing combustion product. The use of comparison experiments and the special technique for volatile samples are cumbersome and time-consuming procedures, which, however, are necessary if accuracy is to be achieved.

TETRAETHYLLEAD: HEAT OF FORMATION BY ROTATING-BOMB CALORIMETRY

By D. W. Scott, W. D. Good and Guy Waddington

Contribution No. 57 from the Thermodynamics Laboratory, Petroleum Experiment Station, Bureau of Mines, U.S. Department of the Interior, Bartlesville, Okla.

Received March 21, 1956

The heat of formation of tetraethyllead was determined by combustion calorimetry. A rotating-bomb method was employed, and a solution of nitric acid and arsenious acid was used in the bomb to convert all lead-containing products of combustion to Pb^{++} ion. Fused quartz was used both for the ampoule to contain the tetraethyllead sample and for the crucible in which the combustion occurred. Thermochemical corrections were applied for chemical attack on the fused quartz in the bomb process. The combustion reaction was referred to solid $Pb(NO_3)_2$ as a product by suitable comparison experiments, which also tended to eliminate errors in reduction of the data to standard states. The calorimetric experiments gave for the reaction $C_8H_{20}Pb(liq.) + 2HNO_3(in\ 30H_2O) + 13.5O_2(g) = Pb(NO_3)_2(c) + 11H_2O(liq.) + 8CO_2(g)$ the value $\Delta H^\circ_{298.16} = -1525.6 \pm 0.6$ kcal. The derived value for the heat of formation of liquid tetraethyllead from graphite, hydrogen gas and lead metal, $\Delta Hf^\circ_{298.16}$, is +12.8 kcal. mole^{-1}. Combustion calorimetry of lead oxalate was done to develop and test the method for tetraethyllead. The experiments gave for the reaction $PbC_2O_4(c) + 2HNO_3(in\ 32.1\ H_2O) + 1/2O_2(g) = Pb(NO_3)_2(c) + H_2O(liq.) + 2CO_2(g)$, the value $\Delta H^\circ_{298.16} = -62.1 \pm 1.2$ kcal. The derived value for the heat of formation of lead oxalate, $\Delta Hf^\circ_{298.16}$, is −203.2 kcal. mole^{-1}.

This investigation on tetraethyllead was part of a continuing program of chemical thermodynamic studies of compounds important in petroleum technology. Despite its commercial importance as an antiknock agent in motor fuels, no reliable value has been available for the heat of formation of tetraethyllead. The most versatile method for determining heats of formation of organic compounds is combustion-bomb calorimetry. However, the standard methods of combustion-bomb calorimetry are not applicable to tetraethyllead for two reasons. First, the combustion of tetraethyllead produces a complex mixture of solid inorganic lead compounds, and it is not possible to analyze this complex mixture accurately and thereby define the final thermodynamic state of the combustion process. Second, the standard procedures of containing liquid samples in glass ampoules and of using platinum for the crucible in which combustions take place cannot be used with tetraethyllead, because molten lead oxides and lead metal produced upon combustion would react with glass and alloy with platinum.

The rotating-bomb method of combustion calorimetry that was developed in this Laboratory[1,2] made it possible to surmount the first difficulty. With the rotating-bomb method a suitable solution could be used in the bomb to dissolve the complex mixture of solid products and produce a final state that could be defined readily by chemical analysis. This method was applied to the combustion calorimetry of tetraethyllead and used to determine the heats of combustion and formation. The second difficulty mentioned above was surmounted by finding satisfactory substitutes for glass ampoules and platinum crucibles.

Experimental

Calorimeter and Bomb.—The calorimeter, laboratory designation BMR2, is described in the preceding paper.[2] The provision for continuous rotation of the bomb was particularly necessary in this investigation because of the relatively long time required to dissolve the solid combustion products.

The bomb, laboratory designation B57I, was constructed especially for this investigation. It was necessary that all interior parts of the bomb be inert to the 10 wt. % nitric acid in the bomb solution used. However, a platinum-lined bomb was not used because of the possibility of damage to the thin lining in case of accidental spattering of molten lead or oxides. Instead, most parts exposed to the bomb solution were constructed of nickel–chromium alloys inert to nitric acid. Illium was used for the bomb cylinder and head, for the valve bodies and stems, and for the locking nuts. Carpenter No. 20 alloy was used for the inlet tube. The sealing gasket, 1/16 inch thick, was made of fine gold. The support and ring, which together constituted the gimbal in which the crucible was suspended, were made of pure platinum. This gimbal was interchangeable with a double gimbal, also of pure platinum, which was used to suspend the two crucibles that were used in comparison experiments (see Fig. 1). These parts, of 1/16-inch-diameter platinum rod, were not liable to serious damage from accidental spattering of molten lead or oxides. The support, which also served as the insulated electrode for the ignition circuit, was mounted on a post integral with the head of the bomb (see Fig. 1). This arrangement was necessary to prevent short circuit of the ignition current through the solution ot strong electrolyte in the bomb. The bomb was equipped with two valves to permit purging with oxygen before charging. The internal volume of the bomb was 0.328 l. with the single gimbal support and 0.327 l. with the double gimbal support.

Initial Bomb Solution.—It was necessary to introduce into the bomb a solution that would completely dissolve all of the solid inorganic lead compounds in the combustion products within a reasonable time to yield a well-defined final state of the bomb process. It was also necessary that the final bomb solution be suitable for the required analytical determinations. The initial bomb solution that was selected on the basis of numerous exploratory experiments was one that contained about 10 wt. % nitric acid and 0.1 wt. % arsenious acid. The nitric acid dissolves all the solid lead compounds in the +2 oxidation state (PbO, $PbCO_3$ and basic carbonates). The nitric acid, saturated with oxygen at 40 atm. pressure, is also effective in dissolving finely divided metallic lead. The arsenious acid, in the presence of nitric acid, reduces lead compounds of higher valence states (Pb_3O_4 and PbO_2) to Pb^{++} ion in solution. Enough solution was required in the bomb to assure that the crucible, which after the combustion contained a fused mass of solid lead compounds, was repeatedly bathed in the solution by rotation of the bomb; 50 ml. of solution was found adequate and was used in all calorimetric experiments with tetraethyllead.

The phase-rule studies of Denham and Kidson[3] show that concentrations of nitric acid in a range of roughly 6 to 16 wt. % are most favorable for solution of +2 lead. At lower concentrations, $Pb(NO_3)_2 \cdot PbO \cdot 2.5H_2O$ and, at higher concentrations, anhydrous $Pb(NO_3)_2$ become less soluble. The concentration used for the initial bomb solution lies in the

(1) W. N. Hubbard, C. Katz and G. Waddington, This Journal, **58**, 142 (1954).

(2) W. D. Good, D. W. Scott and G. Waddington, *ibid.*, **60**, 1080 (1956).

(3) H. G. Denham and J. G. Kidson, *J. Chem. Soc.*, 1757 (1931).

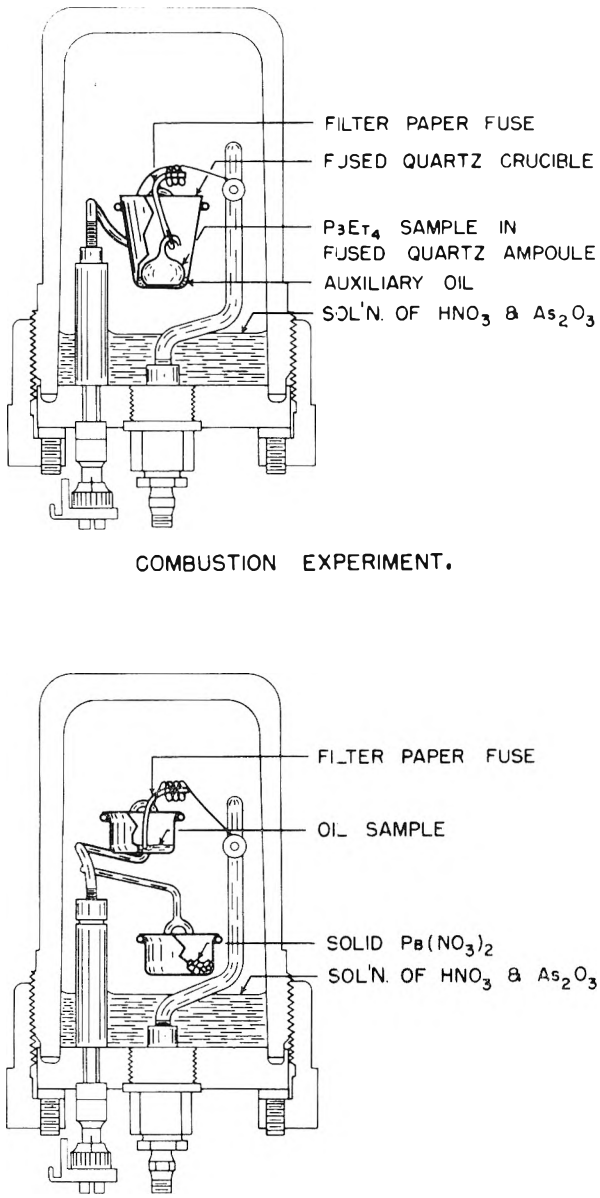

Fig. 1.—Schematic sectional views of the bomb to illustrate a combustion experiment with tetraethyllead and the corresponding comparison experiment.

favorable range. Fortuitously, this concentration is also in the range in which $\Delta Hf^\circ_{298.16}$ for aqueous HNO_3 passes through a broad minimum, and heat of dilution effects are very small.

The amount of arsenious acid in the initial bomb solution was selected to be a safe excess over that needed to reduce all Pb_3O_4 and PbO_2 in the combustion products. Thermochemical corrections, in the range 4–21 cal. per combustion experiment, were applied for oxidation of the arsenious acid.

$$As_2O_3(aq.) = As_2O_3(aq.) + O_2(g)^4 \quad \Delta E^\circ_{298.16} = 74.4 \text{ kcal.}$$

The foregoing value of $\Delta E^\circ_{298.16}$ was calculated from data in Circular 500.[5]

Fused-quartz Ampoules and Crucibles.—As mentioned in the Introduction, it was necessary to find satisfactory substitutes for the glass ampoules and platinum crucibles customarily used in the combustion calorimetry of organic liquids. Of various materials considered or tried in exploratory experiments, fused quartz proved to be most satisfactory for *both* ampoules and crucibles. Ideally, it was desirable to have ampoules and crucibles of materials entirely inert to the hot lead or oxides produced upon combustion of tetraethyllead. However, no such materials could be found that had the necessary physical and mechanical properties and were also inert to oxygen at high temperatures and to the nitric acid in the bomb solution. Fused quartz is not entirely inert to hot lead oxides. However, since it is a pure chemical substance, the chemistry of the reaction that does occur with hot lead oxides is relatively simple, and the application of appropriate thermochemical corrections is straightforward.

At the time of the combustion, hot lead oxides react with the fused quartz, with the formation of lead silicate. Later, when the bomb is rotated and the fragments of ampoule and crucible are bathed in the bomb solution, the lead silicate on the surface is dissolved by the nitric acid, with the formation of silicic acid in solution. However, the lead silicate that is occluded (or in solution) in the fused quartz is unaffected by the bomb solution. Thermochemical corrections must therefore be applied both for the fused quartz that is converted to silicic acid and for the lead silicate that remains in the final state of the bomb process.

$$SiO_2(aq.) = SiO_2(gls.) \quad \Delta E^\circ_{298.16} = -1.5 \text{ kcal.}$$

$$PbSiO_3(amorp.) + 2\,HNO_3(aq.) = Pb(NO_3)_2(aq.) + SiO_2(gls.) + H_2O(liq.) \quad \Delta E^\circ_{298.16} = -14.7 \text{ kcal.}$$

The values of $\Delta E^\circ_{298.16}$ were calculated from data in Circular 500.[5] The sum of the two corrections was in the range 2–5 cal. per combustion experiment.

The fused-quartz ampoules were about 14 mm. in diameter, weighed 45 to 80 mg., and were flattened on the bottom. The stems were drawn down to fine capillaries and bent over (see Fig. 1). Except for the use of fused quartz, the ampoule technique was that described by Hubbard, Knowlton and Huffman.[6]

The fused-quartz crucibles, obtained from The Thermal Syndicate, Ltd., were about 30 mm. high and 25 mm. in diameter at the top and weighed less than 5 g. In most experiments the crucible was broken, either by thermal shock from falling, while still hot, into the bomb solution when rotation of the bomb started, or by mechanical shock as the crucible, along with the heavy gimbal ring, bounced around inside the rotating bomb. Therefore, it was usually necessary to use a new crucible for each combustion experiment.

Comparison Experiments.—There are several possible sources of error in determining the heat of formation of tetraethyllead by the rotating-bomb method of combustion calorimetry as described thus far. (a) The lead nitrate that is a product of the over-all bomb process exists in the final state in an aqueous solution that also contains nitric, arsenious and arsenic acids. The heat of formation of lead nitrate in that particular state is not known and may differ significantly from the standard heat of formation of aqueous lead nitrate. Thus, even if the standard change of energy, ΔE°, is known accurately for the combustion reaction, that datum cannot be used to compute a reliable value for the heat of formation of tetraethyllead. (b) The correction of the calorimetric results to standard states requires values of certain physical constants that are not known accurately enough for that purpose. In particular, the solubility and heat of solution of carbon dioxide in aqueous solutions of nitric acid, lead nitrate, arsenious acid and arsenic acid, as functions of concentration, have not been determined and cannot be estimated accurately. The correction for dissolved carbon dioxide is especially large in the present case, because of the large volume of the final bomb solution (about 51 ml.). (c) The calorimetry in a combustion experiment with tetraethyllead differs from that in a calibration experiment with benzoic acid under certificate conditions in the initial volume of bomb solution (50 ml. instead of 1 ml.) and the duration of the reaction period

(4) Arsenious and arsenic acids exist in solution predominately as $HAsO_2$ and H_3AsO_4. However, it is easier to discuss the stoichiometry and makes no real difference otherwise if they are regarded as solutions of the anhydrides. This convention is well established with respect to the use of arsenious acid as a reductant in the combustion calorimetry of chlorine and bromine compounds.

(5) F. D. Rossini, D. D. Wagman, W. H. Evans, S. Levine and I. Jaffe, "Selected Values of Chemical Thermodynamic Properties," N. B. S. Circular 500, 1952.

(6) W. N. Hubbard, J. W. Knowlton and H. M. Huffman, THIS JOURNAL, **58**, 396 (1954).

(about 40 min. instead of about 15 min., because of the time required for the solid combustion products to dissolve). The calorimetry is therefore not strictly a substitution method, and systematic errors could arise from differences in the combustion and calibration experiments.

These difficulties were either avoided, or the possible errors therefrom greatly reduced, by the use of suitable comparison experiments. In the comparison experiments, the sample was a hydrocarbon oil, the heat of combustion of which was known. A second crucible contained solid lead nitrate, which dissolved in the bomb solution when rotation of the bomb was started. The amounts of oil and lead nitrate, and the amount and concentration of the initial bomb solution, were made such that the evolution of energy and the amount and composition of the final bomb solution were essentially the same as for the combustion experiment with tetraethyllead. The final amounts of carbon dioxide could not also be made the same in the two experiments because combustion of tetraethyllead produces less carbon dioxide per unit evolution of energy than any substance or mixture of substances that would have been suitable as samples in the comparison experiments.[7]

The design of a comparison experiment will be illustrated by a numerical example. In the combustion experiment the sample consisted of 1.46396 g. tetraethyllead, 0.10789 g. auxiliary oil (empirical formula, $CH_{1.891}$) and 0.00273 g. filter paper fuse (empirical formula, $CH_{1.686}O_{0.843}$). The initial bomb solution contained 2.626 moles water, 0.08168 mole HNO_3 and 0.000351 mole As_2O_3. Chemical analysis of the final contents of the bomb showed that 0.000095 mole of As_2O_3 had been oxidized to As_2O_5, 0.000155 mole of $PbSiO_3$ was occluded in fused quartz, and 0.000921 mole of SiO_2 had been dissolved. In the comparison experiment the sample consisted of 0.73553 g. of auxiliary oil and 0.00308 g. filter paper fuse. The second crucible contained 1.45123 g. of solid $Pb(NO_3)_2$. The initial bomb solution contained 2.633 moles of water, 0.07292 mole of HNO_3 and 0.000351 mole of As_2O_3. Chemical analysis of the final contents of the bomb showed that there had been no detectable oxidation of As_2O_3. In each experiment the bomb was initially charged to a pressure of 40 atm. with oxygen. The following list compares the energy of the isothermal bomb process, $\Delta E_{I.B.P.}$, and the contents of the bomb in the final state, for the combustion and comparison experiments, respectively: $\Delta E_{I.B.P.}$, −8084.8, −8094.2 cal.; O_2, 0.390, 0.385 mole; CO_2, 0.04406, 0.05296 mole; $PbSiO_3$, 0.000155 mole, none; H_2O, 2.683, 2.683 moles; HNO_3, 0.07294, 0.07292 mole; $Pb(NO_3)_2$, 0.004371, 0.004381 mole; As_2O_3, 0.000256, 0.000351 mole; As_2O_5, 0.000095 mole, none; SiO_2(aq.), 0.000921 mole, none.

It is seen that the evolution of energy was nearly the same in the two experiments and that, except for the very small concentration of silicic acid and the substitution of arsenic acid for part of the arsenious acid, the final bomb solution was nearly the same in the combustion as in the comparison experiment.

The comparison experiments eliminate, or greatly reduce errors from, the difficulties that have been mentioned. (a) The comparison experiments allow the combustion reaction to be referred to solid lead nitrate as a product. The heat of formation of lead nitrate is known for the solid state, and the value of $\Delta Ec°$ referred to solid lead nitrate can be used to compute the heat of formation of tetraethyllead. (b) The corrections to standard states are nearly the same for the combustion and comparison experiments, and errors in these corrections will nearly cancel in the final value of $\Delta Ec°$. The important correction for dissolved carbon dioxide is not exactly the same in the two experiments because of the different amounts of carbon dioxide formed. However, any error in this correction is reduced to about one fifth of what it would have been if comparison experiments had not been used. (c) The calorimetry is similar in the combustion and comparison experiments. In both the bomb contains about 50 ml. of solution. The duration of the reaction period is arbitrarily made as long in the comparison experiment as in the combustion experiment, even though essentially the same value is calculated for the corrected temperature rise with a reaction period of normal duration. Any systematic errors from the non-standard calorimetry will be present in both combustion and comparison experiments and therefore largely cancel.

The arrangement of the interior part of the bomb for combustion and comparison experiments is illustrated in Fig. 1.

Special Oxygen.—Usually in combustion calorimetry the bomb is charged with ordinary commercial oxygen, the amount of nitric acid formed in the combustion process from nitrogen impurity in the oxygen is determined, and the appropriate thermochemical correction is applied. However, in this investigation it was impossible to determine a small amount of nitric acid formed in the combustion process in the presence of the large amount of nitric acid already present in the bomb. It was therefore essential to reduce the formation of nitric acid in the combustion process by charging the bomb with oxygen that contained very little nitrogen. Special electrolytic oxygen was used. The main impurity in this oxygen was hydrogen, which was removed quantitatively by the usual purification train for removing combustible impurities (heated CuO, $Mg(ClO_4)_2$, Ascarite, P_2O_5). The bomb was purged with about 3 l. of the gas before charging. The formation of nitric acid in the combustion process was reduced but not eliminated by this procedure. In calibration experiments with benzoic acid, the nitric acid formed was equivalent to 0.3–0.6 cal. per combustion experiment. If the same amounts of nitric acid, on the average, were formed in the combustion and comparison experiments, the errors in the individual experiments would cancel in the final value of $\Delta Ec°$ for tetraethyllead. However, the combustion of tetraethyllead is more rapid than that of oil, as shown by the time–temperature behavior of the calorimeter. As the more intense heat of rapid combustion is known to favor formation of nitric acid, it is likely that somewhat more nitric acid was formed in the combustion experiments than in the comparison experiments. However, it is unlikely that error from this source exceeded 0.1 kcal. mole^{-1} in the final values of $\Delta Ec°$ and $\Delta Hf°_{298.16}$ for tetraethyllead.

Reduction to Standard States.—The calorimetric results were corrected to standard states by a procedure similar to that of Hubbard, Scott and Waddington,[8] but modified to apply to organic lead compounds instead of sulfur compounds.[9] Certain physical constants needed for the corrections have not been determined accurately enough, and others must be estimated because experimental data are lacking. The use of comparison experiments assures that errors from inaccurate values of physical constants used in the corrections to standard states will largely cancel when the final value of $\Delta Ec°$ is computed.

Experimental Procedures.—The bomb was placed in the calorimeter in the inverted position shown in Fig. 1, so that the valves and gaskets were protected from the combustion blast by the aqueous solution. The calorimetric observations were made as described in detail in ref. 1, except that rotation of the bomb continued to the end of the calorimetric experiment and a longer reaction period was needed to allow solid combustion products to dissolve. In Fig. 2 a typical time–temperature curve for a combustion experiment with tetraethyllead is compared with typical curves for a comparison experiment and a calibration experiment with benzoic acid.

When the calorimetric observations were complete, the bomb was taken out of the calorimeter, discharged and opened. The bomb solution was transferred to a beaker, and the interior parts of the bomb were rinsed thoroughly with distilled water. All fused quartz fragments were transferred to the beaker. The combined bomb solution and washings were titrated with 0.1 *N* potassium permanganate solution to determine arsenious acid. The fragments of fused quartz were then separated by filtration, the filter paper containing the fragments was ignited in a weighed platinum crucible, and the mass of the fragments was determined. The filtrate was used for gravimetric determination of lead as the sulfate. In the comparison experiments the

(7) In principle, the amounts of carbon dioxide could have been made the same by use in the *combustion* experiment of an auxiliary substance, such as oxalic or succinic acid, the combustion of which produces a large amount of carbon dioxide per unit evolution of energy. However, it was felt that the extra complexity of such a procedure would cancel the advantage of having equal amounts of carbon dioxide produced.

(8) W. N. Hubbard, D. W. Scott and G. Waddington, This Journal, **58**, 152 (1954).

(9) Copies of the complete computation form for organic lead compounds may be obtained from the authors upon request.

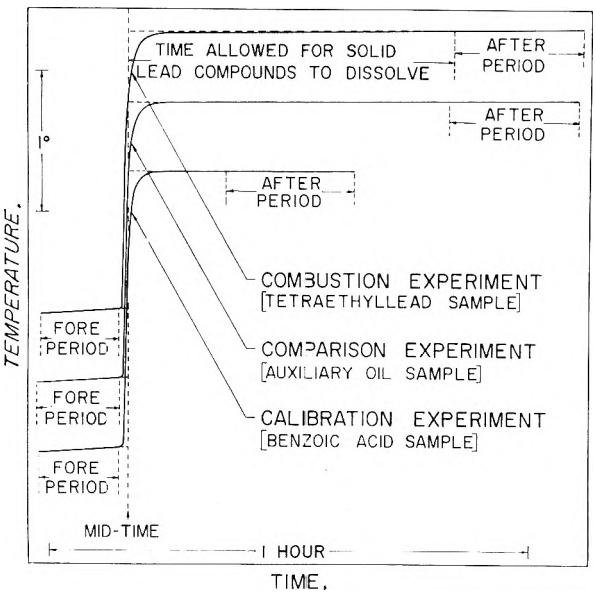

Fig. 2.—Typical time-temperature curves for a combustion experiment with tetraethyllead, a comparison experiment and a calibration experiment with benzoic acid. The vertical scales are offset for clarity.

final bomb solutions contained known amounts of lead nitrate. Determinations of lead in these solutions served as control experiments for the gravimetric method.

The difference between the number of gram-atoms of lead in the tetraethyllead sample and in the final bomb solution was a measure of the number of moles of PbO that had reacted with fused quartz to produce lead silicate. The original mass of crucible and ampoule, plus the mass of PbO that reacted to form lead silicate, minus the mass of recovered fused-quartz fragments, was a measure of the mass of fused quartz that had dissolved to form silicic acid.

In one experiment the recovered fragments were dissolved in HF, and lead was determined in the residue. The amount of lead found checked that calculated by difference. Fragments recovered from another experiment, but not ignited, were examined by X-ray and electron diffraction by Dr. Frances W. Lamb, Research Laboratories, Ethyl Corporation. No evidence of crystalline material was found.

Materials

Tetraethyllead.—The tetraethyllead was contributed by the Research Laboratories of the Ethyl Corporation. The reported purity was 99.9 mole % or higher. A weighed sample was digested with bromine in carbon tetrachloride, and lead in the resulting solution was determined gravimetrically as the sulfate. $PbSO_4/C_8H_{20}Pb$; theory, 0.9376; found, 0.9384.

To fill ampoules, the tetraethyllead was distilled from a calibrated bulb heated by a water-bath directly into the ice-cooled receiver that contained the empty ampoules. The system was evacuated with a diffusion pump throughout the distillation. By this procedure, any water in the sample was pumped off. If there had been any decomposition in storage to metallic lead and light hydrocarbons, the latter were also pumped off by this procedure. When enough distillate was collected in the receiver, dry helium was admitted slowly to force the liquid into the evacuated ampoules. On some occasions the material was dried with calcium hydride before distilling into the receiver. This preliminary drying made no observable difference in the heat of combustion. Handling of the tetraethyllead was done in subdued light as much as possible, as a precaution against photochemical decomposition.

Benzoic Acid.—The benzoic acid was National Bureau of Standards standard sample 39 g. with a certified heat of combustion of 26.4338 ± 0.0026 abs. kj. (6317.83 ± 0.62 cal.)/g. mass under certificate conditions. Conversion from certificate conditions to standard conditions by the method of ref. 7 gives −6312.91 ± 0.62 cal./g. mass for $\Delta Ec^\circ/M$, the energy of the idealized combustion reaction.

Auxiliary Oil.—The auxiliary oil was a sample of redistilled mineral oil, laboratory designation USBM-P3a, empirical formula $CH_{1.891}$. The value of $\Delta Ec^\circ/M$, as determined in a recent series of combustion experiments in this Laboratory, is −10,984.8 ± 1.6 cal. g.$^{-1}$, in satisfactory agreement with the earlier value, −10,983.8 ± 2.2 cal. g.$^{-1}$.

Lead Nitrate.—Eimer and Amend tested purity reagent lead nitrate was stored in a desiccator over P_2O_5 before use.

Oxygen.—Special electrolytic oxygen was purchased from Stuart Oxygen Co.

Results

Units of Measurements and Auxiliary Quantities.—The results of the combustion calorimetry are expressed in terms of the defined calorie equal to 4.1840 abs. joules and refer to the isothermal process at 25° and to true mass. The molecular weights were computed from the 1951 table of international atomic weights.[10] For use in reducing weights in air to *in vacuo*, in correcting the energy of the actual bomb process to the isothermal bomb process and in correcting to standard states, the following values (for 25°) of density, ρ, specific heat, c_p, and $(\partial E/\partial P)_T$ for the various substances were used.

	ρ, g. ml.$^{-1}$	c_p, cal. deg.$^{-1}$ g.$^{-1}$	$(\partial E/\partial P)_T$, cal. atm.$^{-1}$ g.$^{-1}$
Tetraethyllead	1.649	0.229	−0.0038
Benzoic acid	1.320	0.289	−0.0028
Auxiliary oil	0.87	0.53	−0.0060
Lead nitrate	4.53	0.11	negligible
Fused quartz	2.2	0.18	negligible

For $\Delta Ec^\circ/M$ of the filter paper fuse, the value −3923 cal. g.$^{-1}$ was used. The energy equivalent of the calorimetric system, as determined by five calibration experiments with benzoic acid, was 4053.7 ± 0.3 cal. deg.$^{-1}$.

Preliminary Experiments with Lead Oxalate.—In preliminary experiments, it was convenient to use a solid non-volatile organic lead compound that could be weighed directly in the crucible. Lead oxalate was selected because it has the desired physical properties and also because the heat of formation has been determined by solution calorimetry.[11] To obtain complete combustion of lead oxalate, it was necessary to use a nearly equal mass of auxiliary oil. Six satisfactory pairs of combustion and comparison experiments led to the following average values.

$$\Delta Ec^\circ/M = -213.4 \pm 4.1 \text{ cal. g.}^{-1};\quad \Delta Ec^\circ = -63.0 \pm 1.2 \text{ kcal. mole}^{-1}$$
$$\Delta Hc^\circ = -62.1 \pm 1.2 \text{ kcal. mole}^{-1}$$

These values refer to the reaction

$$PbC_2O_4(c) + 2HNO_3(\text{in } 32.1\ H_2O) + 1/2O_2(g) = Pb(NO_3)_2(c) + H_2O(\text{liq.}) + 2\ CO_2(g)$$

and the uncertainties given are the uncertainty intervals equal to twice the final "over-all" standard deviation.[12] The combustion calorimetry of lead oxalate was only incidental to developing and testing a method for tetraethyllead. The sample was ordinary C.P. lead oxalate, used without further purification, and the bomb was charged with commercial oxygen to conserve the limited supply

(10) E. Wichers, *J. Am. Chem. Soc.*, **74**, 2447 (1952).

(11) M. P. E. Berthelot, *Ann. chim. phys.*, **4**, 160 (1875).

(12) F. D. Rossini and W. E. Deming, *J. Wash. Acad. Sci.*, **29**, 416 (1939).

of special electrolytic oxygen. The results may therefore be subject to minor systematic error from impurity in the sample and failure to correct for formation of nitric acid in the bomb process.

The derived value of the heat of formation of lead oxalate, $\Delta Hf°_{298.16}$, is -203.2 kcal. mole^{-1}. For comparison, the value given in Circular 500[5] is -205.1 kcal. mole^{-1}. The experimental uncertainty of the latter value may be several kcal. mole^{-1}. The foregoing comparison is intended merely to show that the method of combustion calorimetry employed here is free from any gross undetected systematic error.

Results with Tetraethyllead.—Nine satisfactory combustion experiments with tetraethyllead were obtained out of 26 attempts. Of the other 17 experiments, 4 failed from diverse calorimetric difficulties, 4 failed because violent rupture of the ampoule ejected unreacted sample from the crucible, 4 failed because the solid lead compounds did not completely dissolve within the allotted time, and 5 failed because of incomplete combustion, as shown by traces of soot on the fused quartz fragments or other interior parts of the bomb. The 5 cases of incomplete combustion included 3 experiments in which the bomb was charged to an initial pressure of only 30 atm. and 1 experiment in which it was charged to only 20 atm.

A typical combustion experiment with tetraethyllead and the corresponding comparison experiment are summarized in Table I. In this table, m(material) denotes the mass of the designated material that was used, and n^i(material), denotes the number of moles of the designated material initially present in the bomb. The quantity, $\Delta t_c = t_f - t_i - \Delta t_{cor}$, is the observed increase of the calorimeter temperature, corrected for Newtonian heat exchange and for the energy from stirring the calorimeter and from rotation of the bomb. The symbols, $\mathcal{E}$(calor.) and $\mathcal{E}$(cont.), denote the energy equivalent of the calorimetric system and of the contents of the bomb, respectively. The term ΔE_{ign} denotes the electrical energy used to ignite the fuse. The term ΔE, cor. to st. states, denotes the sum of all corrections to standard states. The terms $\Delta E^f_{soln}(SiO_2)$, $\Delta E^f_{soln}(PbSiO_3)$ and $\Delta E^f_{dec}(As_2O_5)$ are the thermochemical corrections for formation of silicic acid, for formation of lead silicate and for oxidation of arsenious acid, respectively. The symbol $\Delta Ec°/M$(material) denotes the energy of the idealized combustion reaction for 1 g. of the designated material.

Table I

Typical Pair of Combustion and Comparison Experiments with Tetraethyllead

	Combustion experiment	Comparison experiment
m(tetraethyllead), g.	1.51570	....
m(oil), g.	0.08661	0.73565
m[$Pb(NO_3)_2$], g.	....	1.55217
$n^i(H_2O)$, moles	2.626	2.633
$n^i(HNO_3)$, moles	0.08168	0.07230
$n^i(As_2O_3)$, moles	0.000257	0.000257
Δt_c, deg.	1.97325	1.97167
$\mathcal{E}$(calor.)$(-\Delta t_c)$, cal.	−7999.0	−7992.6
$\mathcal{E}$(cont.)$(-\Delta t_c)$, cal.	−100.3	−102.2
ΔE_{ign}, cal.	+1.4	+1.4
ΔE, cor. to st. states, cal.	+17.1	+22.0
$\Delta E^f_{soln}(SiO_2)$, cal.	−1.6	....
$\Delta E^f_{soln}(PbSiO_3)$, cal.	−2.9	....
$\Delta E^f_{dec}(As_2O_5)$, cal.	+12.6	−0.1
$-m\Delta Ec°/M$(fuse), cal.	+11.1	+12.5
$-m\Delta Ec°/M$(oil), cal.	+951.4	+8081.0
$m\Delta Ec°/M$(tetraethyllead), cal.	−7110.2	
$\Delta Ec°/M$(tetraethyllead), cal. g.$^{-1}$	−4691.0	
$\Delta Ec°$(tetraethyllead), kcal. mole^{-1}	−1517.3	
$m\Delta E°/M$[$Pb(NO_3)_2$], cal.		+21.9
$\Delta E°/M$[$Pb(NO_3)_2$], cal. g.$^{-1}$		+14.1
$\Delta E°$[$Pb(NO_3)_2$], kcal. mole^{-1}		+4.7

If the small concentrations of As_2O_3 and As_2O_5 in the bomb solutions are neglected, the values of $\Delta Ec°$(tetraethyllead) and of $-\Delta E°[Pb(NO_3)_2]$ in Table I refer to equations I and II below. Formally, two dilution corrections are necessary, but, because of the favorable range of nitric acid concentrations, these are negligibly small. The first, equation III below, corrects for the difference in concentration of the initial bomb solutions, and the second, equation IV below, refers each experiment to the same initial concentration of nitric acid, HNO_3(in 30 H_2O).

$$C_8H_{20}Pb + 17.84HNO_3{\cdot}573.6H_2O + 13.5O_2 + 1.5H_2O = Pb(NO_3)_2{\cdot}15.84HNO_3{\cdot}586.1H_2O + 8\,CO_2 \quad (I)$$
$$\Delta E°_{298.16} = -1517.3 \text{ kcal.}$$

$$Pb(NO_3)_2{\cdot}15.84HNO_3{\cdot}586.1H_2O = Pb(NO_3)_2 + 15.84HNO_3{\cdot}575.1H_2O + 11.0H_2O \quad (II)$$
$$\Delta E°_{298.16} = -4.7 \text{ kcal}$$

$$15.84\ HNO_3{\cdot}575.1H_2O = 15.84\ HNO_3{\cdot}509.3H_2O + 65.8H_2O \quad (III)$$
$$\Delta E°_{298.16} = 0.0 \text{ kcal.}$$

$$2HNO_3{\cdot}60H_2O + 4.3H_2O = 2HNO_3{\cdot}64.3H_2O \quad (IV)$$
$$\Delta E°_{298.16} = 0.0 \text{ kcal.}$$

The sum of equations I through IV is

$$C_8H_{20}Pb + 2HNO_3(\text{in } 30H_2O) + 13.5O_2 = Pb(NO_3)_2 + 11H_2O + 8CO_2 \quad (V)$$
$$\Delta E°_{298.16} = -1522.0 \text{ kcal.}$$

The results of all nine pairs of combustion and comparison experiments are given in Table II. The value of $\Delta H°_{298.16}$ (eq. V) in Table II is the direct result of the calorimetric studies; aside from small thermochemical corrections, this value depends only on calorimetric experiments done in this Laboratory and the certificate value for the heat of combustion of the benzoic acid used for calibration.

Derived Results.—The values given in Circular 500[5] for the standard heats of formation, in kcal. mole^{-1}, of HNO_3 (in $30H_2O$), -49.234; $Pb(NO_3)_2$ (c), -107.35; H_2O(liq.), -68.3174, and CO_2(g), -94.0514, were used to obtain a derived value for the heat of formation of tetraethyllead. An unpublished value obtained in this Laboratory for the entropy of liquid tetraethyllead, $S°_{298.16} = 111.92 \pm 0.20$ cal. deg.$^{-1}$ mole^{-1}, together with entropy values for C(graphite), $S°_{298.16} = 1.3609$ cal. deg.$^{-1}$ mole^{-1}[5]; H_2(g), $S°_{298.16} = 31.211$ cal. deg.$^{-1}$ mole^{-1}[5]; and Pb(c), $S°_{298.16} = 15.51$ cal. deg.$^{-1}$ mole^{-1},[5] were used to compute the standard entropy, free energy

and logarithm of the equilibrium constant of formation.

$$8C \text{ (graphite)} + 10H_2(g) + Pb(c) = C_8H_{20}Pb(liq.)$$

$\Delta Hf°_{298.16} = +12.8$ kcal. mole^{-1}

$\Delta Sf°_{298.16} = -226.6$ cal. deg^{-1} mole^{-1}

$\Delta Ff°_{298.16} = +80.4$ kcal. mole^{-1} $\log_{10} Kf_{298.16} = -58.9$

Discussion

This investigation has demonstrated the applicability of the rotating-bomb method to combustion calorimetry of compounds that normally yield ill-defined solid combustion products. With this method, the solid products can be dissolved to give a well-defined final state of the combustion process. Comparison experiments can be devised to refer the combustion reaction to products in states for which the heats of formation are known. The rotating-bomb method should have wide application in thermochemical studies, not only of organometallic compounds, but of many inorganic compounds as well.

Acknowledgment.—The Research Laboratories of the Ethyl Corporation have contributed financial support and a sample of purified tetraethyllead to this investigation. This assistance and helpful discussion with G. W. Thomson and H. Shapiro of Ethyl Corporation are gratefully acknowledged.

TABLE II

SUMMARY OF CALORIMETRIC EXPERIMENTS WITH TETRAETHYLLEAD

$\Delta E_c°$(tetraethyllead) (from combustion expt.), kcal. mole^{-1}	$-\Delta E°$[Pb(NO$_3$)$_2$] (from comparison expt.), kcal. mole^{-1}	Sum of dilution cor., kcal. mole^{-1}	$\Delta E°_{298.16}$ (eq. V), kcal. mole^{-1}
−1517.3	−4.7	0.0	−1522.0
−1517.6	−4.5	0.0	−1522.1
−1517.4	−5.4	0.0	−1522.8
−1517.6	−4.7	0.0	−1522.3
−1517.7	−4.7	0.0	−1522.4
−1518.7	−5.1	0.0	−1523.8
−1517.8	−5.1	−0.1	−1523.0
−1516.2	−4.7	0.0	−1520.9
−1517.5	−4.5	0.0	−1522.0
$\Delta E°_{298.16}$(eq. V), mean			−1522.4 kcal. mole^{-1}
$\Delta H°_{298.16}$(eq. V)			−1525.6 kcal. mole^{-1}
Standard dev. of the mean			±0.3 kcal. mole^{-1}
Uncertainty interval[12]			±0.6 kcal. mole^{-1}

THE EFFECT OF PHYSICAL ADSORPTION ON THE ABSOLUTE DECOMPOSITION RATES OF CRYSTALLINE AMMONIUM CHLORIDE AND CUPRIC SULFATE TRIHYDRATE[1]

BY ROBERT D. SCHULTZ AND ALBERT O. DEKKER

Aerojet-General Corporation, Azusa, California

Received March 23, 1956

The linear decomposition rates for the decomposition reactions $NH_4Cl \rightarrow NH_3 + HCl$ and $CuSO_4 \cdot 3H_2O \rightarrow CuSO_4 \cdot H_2O$ are interpreted on the basis of a modified Langmuir–Hinshelwood bimolecular surface reaction mechanism. An absolute rate treatment (similar in method to that developed by Laidler, Glasstone and Eyring for heterogeneous processes) accounts for the unusually low reaction probabilities per collision of gaseous product molecules with the reaction interface in terms of interference by a physically adsorbed product layer.

Introduction

The purpose of this paper is to account for certain anomalies observed in the rates of decomposition of ammonium chloride and cupric sulfate trihydrate. The experimental pre-exponential rate factors for the linear vaporization of ammonium chloride

$$NH_4Cl(solid) \longrightarrow NH_3(gas) + HCl(gas) \quad (1)$$

and the linear dehydration of cupric sulfate trihydrate

$$CuSO_4 \cdot 3H_2O(solid) \longrightarrow CuSO_4 \cdot H_2O(solid) + 2H_2O(gas) \quad (2)$$

are unusually low in comparison with decomposition rate factors for other crystals (see Table I). Another remarkable feature of these two reactions is the fact that the values of the reaction coefficient, ϕ, per collision of gaseous product molecules with the reaction interface, are extremely low. The NH_4Cl decomposition is also remarkable in that the corresponding activation energy is much lower than the endothermicity of reaction per mole of vapor (*i.e.*, $E_{act} = 13.5$ kcal. g. mole^{-1}, $(\Delta H°_{298.1°K.}/2) = 21.1$ kcal. g. mole^{-1}).[2]

The discussion which follows will demonstrate that these unusual observations are consistent with a modified bimolecular Langmuir–Hinshelwood surface reaction mechanism occurring in a physically adsorbed product layer at the reaction interface. An absolute rate treatment corresponding to this mechanism will be presented. Since little is known of the configuration of the potential energy surface for reaction, it will not be possible to evaluate activation energies and partition function ratios entirely from first principles. Instead, the absolute rate treatment will be used in conjunction with experimental decomposition rate data to obtain information about the properties of the potential energy surface. This type of approach, although partly intuitive and less fundamental than desired, has been employed with considerable success by

(1) Part of the research described in this paper was supported under Contract AF 18(600)-1026 by the United States Air Force, through the Office of Scientific Research of the Air Research & Development Command, and was first reported in Technical Note OSR-TN-55-141 (July 1955).

(2) See C. C. Stephenson, *J. Chem. Phys.*, **12**, 318 (1944), for a discussion of the value of $\Delta H°_{298.1°K.}$ for the decomposition of NH_4Cl.

Laidler, Glasstone and Eyring[3] and by Laidler[4] to interpret rate data for various heterogeneous processes occurring on surfaces of solids. As a preliminary to the absolute rate treatment, an equation for the reaction coefficient ϕ will be derived by means of classical gas kinetic theory.

The Reaction Coefficient ϕ of the Decomposition Interface.—By analogy with the Knudsen condensation coefficient α, the reaction coefficient ϕ for the reversible reaction

$$\text{A(gas)} + \text{D(gas or solid)} \underset{\text{b}}{\overset{\text{a}}{\rightleftharpoons}} \text{AD(solid)} \qquad (3)$$

is defined as the fraction of the gaseous molecules of a given species colliding with the decomposition interface which react to form product. If every molecule of A which collided with the decomposition interface were to react (*i.e.*, $\phi = 1$), the hypothetical rate of the partial reaction (3a), expressed as a linear growth rate, would be

$$B_{\text{hyp}} = \frac{M_{\text{AD}}}{\rho_{\text{AD}} M_{\text{A}}} \left[5.833 \times 10^{-2} P_{\text{A}} \sqrt{\frac{M_{\text{A}}}{T}} \right] \text{cm. sec.}^{-1} \qquad (4)$$

where

M_{AD} = formula weight of AD(solid), g. g.-mole^{-1}
ρ_{AD} = density of AD(solid), g. cm.$^{-3}$
P_{A} = vapor pressure of A(gas) in equilibrium with AD(solid), mm.
M_{A} = molecular weight of A(gas), g. g.-mole^{-1}
T = absolute temperature, °K.

The term in brackets in equation 4 will be recognized as the classical gas-kinetic theory formula for the mass of gas A incident on unit area per unit time.[5] The reaction probability ϕ_{A} per collision of gaseous A with the reaction interface is simply

$$\phi_{\text{A}} = \frac{B_{3b}}{B_{\text{hyp}}} \qquad (5)$$

where

B_{3b} = expt. linear decomposition rate of AD(solid) *in vacuo* (at temp., T), cm. sec.$^{-1}$

Implicit in equation 5 is the assumption that the rate of the partial reaction (3b) is identical under vacuum and equilibrium conditions.

The reaction probability ϕ_{NH_3} for ammonia vapor at the surface of crystalline ammonium chloride is calculated from (5) as

$$\phi_{\text{NH}_3} = \frac{B_{3b}}{B_{\text{hyp}}} = \frac{1.2 \times 10^{2} \exp(-13.5/RT)}{5.9 \times 10^{7} \exp(-19.3/RT)} \qquad (6)$$

or

$$\phi_{\text{NH}_3} = 2.1 \times 10^{-6} \exp(5.8/RT) \qquad (7)$$

where

R = gas constant, kcal. g.-mole^{-1}

Equation 7 is based upon vapor pressure data by Spingler[6] and the vacuum decomposition rate data of Table I. In the same way, the reaction probability ϕ_{HCl} for hydrogen chloride at the NH_4Cl surface is calculated as

$$\phi_{\text{HCl}} = 1.4 \times 10^{-8} \exp(5.8/RT) \qquad (8)$$

Similarly, the reaction probability for water vapor at the $CuSO_4 \cdot 3H_2O$ decomposition interface is calculated as

$$\phi_{\text{H2O}} = 1.6 \times 10^{-7} \exp(-2.3/RT) \qquad (9)$$

using vapor pressure data compiled by Randall, Nielsen and West[7] and decomposition data from Table I. These reaction probabilities are exceptionally low. By way of comparison it is noted that the Knudsen condensation coefficient α for KCl vapor at the (100) face of KCl crystal is 0.72 ± 0.015, independent of temperature.[8]

The low reaction probabilities found for the gaseous products from NH_4Cl and $CuSO_4 \cdot 3H_2O$ are suggestive of the presence of an adsorbed product layer at the decomposition interface which hinders the direct reaction between the interface and colliding gaseous product molecules. This concept is developed further in the following section.

A Modified Langmuir-Hinshelwood Reaction Mechanism at the Decomposition Interface.—The conventional Langmuir–Hinshelwood mechanism for the reaction between gas molecules X and Y at a surface may be formulated as[9]

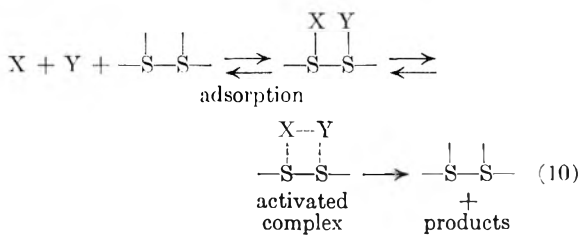

For the present case the Langmuir–Hinshelwood mechanism is modified slightly as

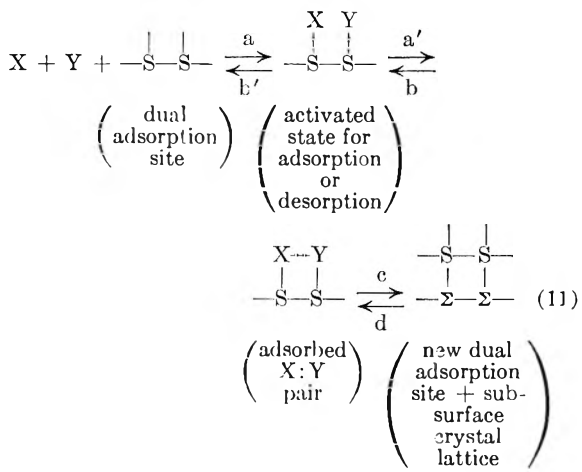

Reaction 11c represents the conversion of the adsorbed X:Y pair into the ionic or molecular groups of the surface lattice, which thereby creates a new dual adsorption site. Simultaneously the ionic or

(3) (a) K. J. Laidler, S. Glasstone and H. Eyring, *J. Chem. Phys.*, **8**, 659, 667 (1940); (b) S. Glasstone, K. J. Laidler and H. Eyring, "Theory of Rate Processes," McGraw-Hill Book Co., New York, N. Y., 1941, Chapter VII.

(4) K. J. Laidler, "Absolute Rates of Surface Reactions," in "Catalysis," Vol. I, P. H. Emmett, ed., Reinhold Publ. Corp., New York, N. Y., 1954, Chapter V.

(5) S. Dushman, "Scientific Foundations of Vacuum Technique," John Wiley and Sons, Inc., New York, N. Y., 1949, p. 17, eq. 6b.

(6) K. Spingler, *Z. physik. Chem.*, **B52**, 90 (1942).

(7) M. Randall, F. F. Nielsen and G. H. West, *Ind. Eng. Chem.*, **23**, 388 (1931).

(8) R. S. Bradley and P. Volans, *Proc. Roy. Soc.* (*London*), **A217**, 508 (1953).

(9) K. J. Laidler, "Chemical Kinetics," McGraw-Hill Book Co., New York, N. Y., 1950, p. 153.

molecular group which provided the initial dual adsorption site is incorporated into the subsurface crystal lattice designated by the symbol $-\Sigma-\Sigma-$. The reaction scheme (11) in the case of NH_4Cl is assumed to occur at random anywhere on an exposed crystal face. However, for $CuSO_4 \cdot 3H_2O$ the reaction scheme must be assumed to occur preferentially at the interface between the trihydrate and monohydrate phases. To assume otherwise would mean that during decomposition monohydrate could form anywhere on the surface, so that finally a mixture of the monohydrate and dihydrate in patches of molecular dimensions would result (*i.e.*, a solid solution), contrary to experimental observation.[10]

The observed behavior of ammonium chloride and cupric sulfate trihydrate may be explained on the assumption that reaction 11b is the rate-controlling step in decomposition, while 11c is the rate-controlling step in crystal formation. No rate data are available for reactions 11c and 11d. However, it is possible to interpret reactions 11a and 11b by the absolute rate treatment of surface reactions developed by Laidler, Glasstone and Eyring[3] and extended by Laidler.[4] The absolute rate of reaction is given by

$$v = \frac{(1/2)sc_g c_g' \Lambda}{(1 + Kc_g + K'c_g')^2} \frac{kT}{h} \frac{f^\ddagger}{F_g F_g' f_{s2}} \exp(-\epsilon_0/kT) \quad (12)$$

The nomenclature and form of eq. 12 are virtually the same as that of eq. 63, page 215 of reference 4, except that the symbol Λ has been substituted for the symbol L; Λ is now the number of single adsorption sites per square centimeter of reaction interface. (In applying transition theory to solid decomposition reactions, the authors prefer to reserve the symbol L for the thickness of the monomolecular surface layer.) Also, the symbols c_g, K and F_g now refer to component X (instead of A) and the corresponding primed symbols refer to component Y (instead of B).

If the desorption reaction 11b is rate controlling in decomposition and the reaction 11c is rate controlling in crystal formation, the reaction interface could be almost completely covered with an adsorbed monomolecular layer. In this case $(Kc_g + K'c_g')$ is large compared with unity. If c_g/c_s and c_g'/c_s are comparable in magnitude, the following approximation is valid

$$(Kc_g + K'c_g')^2 \sim 4Kc_gK'c_g' \quad (13)$$

It is possible to express both K and K' in terms of partition function ratios

$$K = \frac{c_a}{c_g c_s} = \frac{f_a}{F_g f_s} \exp(\epsilon_x/kT) \quad (14)$$

$$K' = \frac{c_a'}{c_g' c_s} = \frac{f_a'}{F_g' f_s} \exp(\epsilon_y/kT) \quad (15)$$

where c_a and c_a' are the concentrations of adsorbed X and adsorbed Y, respectively, and ϵ_x and ϵ_y represent the energy liberated at 0°K. per respective molecule adsorbed at the reaction interface.

(10) The reader is referred to the classic discussion of the auto catalytic role of the solid decomposition interface by I. Langmuir, *J. Am. Chem. Soc.*, **38**, 2263 (1916). See also the discussion by N. K. Adam, "The Physics and Chemistry of Surfaces," 3rd Ed., Oxford University Press, 1941, pp. 241–244.

With the reasonable assumption that the coördination number (s) of the reaction interface is 4 and that adsorption site partition functions f_s and f_{s2} are approximately unity, substitution of (13), (14) and (15) into (12) yields

$$v = \frac{1}{2} \Lambda \frac{kT}{h} \frac{f^\ddagger}{f_a f_a'} \exp[-(\epsilon_x + \epsilon_y + \epsilon_0)/kT] \quad (16)$$

as the rate equation for the adsorption reaction 11a. The apparent activation energy for this reaction thus includes the energies of adsorption of gaseous X and Y. The reason for this result is that a molecule of X and a molecule of Y must both be desorbed from a dual site before a new adsorbed X:Y pair can be formed from another set of gaseous molecules. In other words, reaction 11a is essentially a bimolecular exchange reaction between the adsorbed material on the surface and the gas phase. It is not implied that reaction 11a would be solely responsible for any experimentally observed exchange since there is the possibility of monomolecular exchange reactions between the gas phase and the surface, *i.e.*

$$X^* + \begin{matrix} X\text{---}Y \\ | \quad | \\ -S-S- \end{matrix} \rightleftharpoons X + \begin{matrix} X^*\text{---}Y \\ | \quad | \\ -S-S- \end{matrix}$$

This last type of exchange could proceed independently of the bimolecular exchange reaction without affecting the mechanism of the latter or of the reactions involved in the dynamic equilibrium scheme (11).

Rate equation 16 which has been derived for the adsorption reaction 11a, should be identical with the rate equation for the reverse desorption reaction 11b under equilibrium conditions. It is assumed that the transmission coefficients for 11a and 11b are identical.

The Activation Energy for Adsorption–Desorption at the Reaction Interface.—The experimental activation energies for the decomposition of ammonium chloride and cupric sulfate trihydrate are consistent with a physical (*i.e.*, van der Waals) adsorbed state of the X:Y pair at the reaction interface. From the data obtained by Crawford and Tompkins[11] for the adsorption of SO_2, NH_3, N_2O and CO_2 on BaF_2 crystals, the average enthalpy of physical adsorption of a given component at the surface of an ionic crystal is nearly equal to the enthalpy of sublimation of the pure component. Accordingly, the apparent activation energy for the adsorption reaction 11a or the desorption reaction 11b is approximated as

$$E_{app} \simeq E_0 + (\Delta H_{sx} - RT_{sx}) + (\Delta H_{sy} - RT_{sy}) \quad (17)$$

where

E_{app} = $N(\epsilon_x + \epsilon_y + \epsilon_0)$, the activation energy for the interaction of gaseous X and Y with an occupied dual adsorption site to form a new adsorbed X:Y pair, kcal. g.-mole^{-1}

N = Avogadro's number, molecules g.-mole^{-1}

E_0 = $N\epsilon_0$, the activation energy for the interaction of gaseous X and Y with an unoccupied surface site, kcal. g.-mole^{-1}

ΔH_{sx}, ΔH_{sy} = enthalpy of sublimation of pure components, X, Y measured at T_{sx}, T_{sy}, respectively, kcal. g.-mole^{-1}

R = gas constant, kcal. g.-mole^{-1}, °K.$^{-1}$

(11) V. A. Crawford and F. C. Tompkins, *Trans. Faraday Soc.*, **44**, 698 (1948).

Since the intermolecular bonding between X and Y in the physically adsorbed state is assumed to be very weak, E_0 should be correspondingly small. E_0, however, may represent the potential energy barrier to collision between X and Y on the surface. In that case it would be reasonable to identify E_0 with the height V_{tx} of the potential energy barrier to surface translation for component X plus the corresponding quantity V_{ty} for Y at the reaction interface. Hill[12] has estimated the height of such a barrier to be about 0.3–1.0 kcal. g.-mole^{-1}. With this assumption, the estimated value of E_{app} for the NH_3–HCl desorption–adsorption reaction would be about 10.4 + (0.6 to 2.0) kcal. g. mole^{-1}. Another approximation, still consistent with the aforementioned estimate by Hill, consists in equating V_{tx}, V_{ty} to about half of the respective heats of fusion ΔH_{mx}, ΔH_{my} of the pure components, so that

$$E_{app} \simeq 1/2\,(\Delta H_{mx} + \Delta H_{my}) + \Delta H_{sx} + \Delta H_{sy} - R(T_{sy} + T_{sx}) \quad (18)$$

This last approximation gives $E_{app} \simeq 11.3$ kcal. g.-mole^{-1} for the desorption–adsorption activation energy of NH_3 + HCl from NH_4Cl, in fair agreement with the 13.5 kcal. g.-mole^{-1} experimental activation energy for decomposition. (It is noted that if decomposition proceeds in the crystals under consideration *via* a multistage process, the experimentally observed activation energy of the rate-controlling step may be either smaller or greater than the endothermicity of the over-all reaction.)

Equation 18 when applied to the desorption–adsorption of $2H_2O$ at the $CuSO_4{\cdot}3H_2O$–$CuSO_4{\cdot}H_2O$ interface gives a high value, *i.e.*, $E_{app} \simeq$ 24.1 kcal. g.-mole^{-1}, in poor agreement with the 15.6 kcal. g.-mole^{-1} experimental activation energy for dehydration as given by equation 4. This discrepancy could be the result of the large effect of hydrogen bonding energy on the heat of fusion of water. If only a limited amount of hydrogen bonding exists in the physically adsorbed water layer at the decomposition interface, it is reasonable for the experimental activation energy for dehydration to be less than 24.1 kcal. g.-mole^{-1}. Thermodynamic data for the adsorption of water on Graphon indicates that the hydrogen bonding energy of water in the first monomolecular physically adsorbed layer is about 5 kcal. g.-mole^{-1} less than the hydrogen bonding energy of the liquid state.[13] This correction, when applied to equation 18 for each of the two water molecules involved in the $CuSO_4{\cdot}3H_2O$–$CuSO_4{\cdot}H_2O$ equilibrium, results in a value of $E_{app} \simeq$ 14 kcal. g.-mole^{-1}, in reasonable agreement with the experimental dehydration rate data summarized in Table I. Accordingly, equation 18 will be rewritten as

$$E_{app} \simeq 1/2(\Delta H_{mx} + \Delta H_{my}) + \Delta H_{sx} + \Delta H_{sy} - R(T_{sx} + T_{sy}) - C_h \quad (18a)$$

where C_h is a correction for the effect of hydrogen bonding. (Except where otherwise mentioned, all thermodynamic data used in this discussion were obtained from a compilation by the U. S. Bureau of Standards.[14])

(12) T. L. Hill, *J. Chem. Phys.*, **16**, 181 (1948).

(13) G. J. Young, J. J. Chessick, F. H. Healey and A. C. Zettlemoyer, THIS JOURNAL, **58**, 313 (1954).

(14) U. S. Bureau of Standards, Circular 500, "Selected Values of Chemical Thermodynamic Properties," 1952.

TABLE I

LINEAR DECOMPOSITION RATES OF VARIOUS CRYSTALS *in vacuo*

Crystal	B, cm. sec.$^{-1}$	Ref.
BaN_6	$4.8 \times 10^6 \exp(-23.5/RT)$	*a*
Ag_2CO_3	$1.3 \times 10^5 \exp(-23.4/RT)$	*b*
$CuSO_4{\cdot}5H_2O$	$3.3 \times 10^7 \exp(-18.3/RT)$	*c*
$NiSO_4{\cdot}7H_2O$	$8.0 \times 10^8 \exp(-19.0/RT)$	*d*
$KCr(SO_4)_2{\cdot}12H_2O$		
at 15 to 35°	$2.8 \times 10^{11} \exp(-22.6/RT)$	*e*
at −12.01 to 1.71°	$5 \times 10^{16} \exp(-29.9/RT)$	*e*
at 15 to 35°	$8.9 \times 10^{17} \exp(-31.2/RT)$	*f*
$NH_4Al(SO_4)_2{\cdot}12H_2O$	$9.3 \times 10^5 \exp(-16.4/RT)$	*g*
$KAl(SO_4)_2{\cdot}12H_2O$	$1.2 \times 10^6 \exp(-16.6/RT)$	*g*
NH_4Cl	$1.2 \times 10^2 \exp(-13.5/RT)$	*h*, *i*, *j*
$CuSO_4{\cdot}3H_2O$	$2.8 \times 10^2 \exp(-15.6/RT)$	*k*

[a] A. Wischin, *Proc. Roy. Soc.* (*London*), **A172**, 314 (1939). [b] W. D. Spencer and B. Topley, *J. Chem. Soc.*, **124**, 2633 (1929). [c] M. L. Smith and B. Topley, *Proc. Roy. Soc.* (*London*), **A134**, 224 (1931). [d] W. E. Garner and W. E. Southon, *J. Chem. Soc.*, 1705 (1935). [e] M. M. T. Anous, R. S. Bradley and J. Colvin, *ibid.*, 3348 (1951). [f] W. E. Garner and J. A. Cooper, *Proc. Roy. Soc.* (*London*), **A174**, 487 (1940). [g] G. P. Acock, W. E. Garner, J. Milstead and H. J. Willavoys, *ibid.*, **A189**, 508 (1946). [h] K. Spingler, *Z. physik. Chem.*, **B52**, 90 (1942). [i] R. D. Schultz and A. O. Dekker, "Fifth Symposium (International) on Combustion," Reinhold Publ. Corp., New York, N. Y., 1955, pp. 260–7. [j] K. W. Bills, G. M. Therneau, E. Mishuck and R. D. Schultz, Aerojet-General Corporation Technical Note OSR-TN-55-117 prepared for the Office of Scientific Research of the Air Research and Development Command, U. S. Air Force (1955). [k] M. M. Cooper, J. Colvin and J. Hume, *Trans. Faraday Soc.*, **24**, 576 (1933).

A Simplified Model of the Desorption Process at the Reaction Interface.—The following assumptions provide a simplified model of the desorption process at the reaction interface and lead to theoretical values of the partition function ratio $f_\ddagger/f_a f_a'$ consistent with the experimental rate equations for NH_4Cl and $CuSO_4{\cdot}3H_2O$. The assumptions are the following.

a. The activated state arises from a collision between X and Y in a physically adsorbed layer at the reaction interface.

b. The position of the point of collision between X and Y in the activated state is localized with respect to one coördinate in the adsorbed layer at the reaction interface. More precisely, it is assumed that a projection of the center of gravity of the X–Y pair of the activated state falls within a narrow segment ($\delta \simeq 2 \times 10^{-9}$ cm.) of a line drawn in the plane of the physically adsorbed layer. This particular line connects the center of motion of X and the center of motion of Y in the initial physically adsorbed state.

c. The activated-state motion of the projected center of gravity within this segment ($\delta \simeq 2 \times 10^{-9}$ cm.) may be approximated as the motion of a quantum mechanical particle in a one-dimensional box. The effective mass, $m_\ddagger$, of this particle is taken as equal to the mass of the X–Y pair.

d. The activated-state motion of the centers of gravity of X and Y relative to each other in the plane of the physically adsorbed layer corresponds to the motion of the system along the reaction coordinate of the potential energy surface. The

partition function for this motion is considered to be included in the kT/h factor of eq. 16.

e. The initial state motions of X and Y along the line drawn between their respective centers of motion may be adequately described as two independent quantum-mechanical harmonic oscillations of frequency ν_a and ν_a', respectively, in the plane of the physically adsorbed layer at the reaction interface.

f. The remaining modes of motion of the X–Y pair at the reaction interface are nearly identical in the initial and activated states.

The last assumption permits cancellation of equivalent terms in the numerator and denominator of the partition function ratio, so that

$$\frac{f_{\pm}}{f_a f_a'} \simeq \frac{(2\pi m_{\pm} kT)^{1/2}\,\delta/h}{[1 - \exp(-h\nu_a/kT)]^{-1}[1 - \exp(-h\nu_a'/kT)]^{-1}} \tag{19}$$

The frequencies ν_a and ν_a' may be estimated in the manner of Hill[12] and Drenan and Hill[15] by use of the equation

$$\nu \simeq (v_t/4m_a d^2)^{1/2} = 1.025 \times 10^{13}(V_t/M_a D^2)^{1/2}\ \text{sec.}^{-1} \tag{20}$$

where

v_t = max. potential energy barrier to translation in the plane of the physically adsorbed layer, ergs
V_t = same as v_t except for units, kcal. g.-mole^{-1}
m_a = mass of adsorbed molecule, g.
M_a = mol. wt. of adsorbed molecule, g. g.-mole^{-1}
d = distance between successive potential min. along a principal axis in the surface lattice (assumed simple cubic), cm.
D = same as d except for units, Å.

The distance d between successive potential minima in the surface lattice is estimated to be about equal to the cube root of the volume occupied by a molecule of the undecomposed crystal; *i.e.*

$$d \simeq \left(\frac{M_c}{N\rho_c}\right)^{1/3} \tag{21}$$

where

M_c = formula weight of crystal, g. g.-mole^{-1}
N = Avogadro's number, molecules g.-mole^{-1}
ρ_c = density of crystal, g. cm.$^{-3}$

The potential energy barrier V_t was estimated in the previous section as about equal to half the heat of fusion, ΔH_m, of the pure component, so that

$$\nu_a \simeq 1.025 \times 10^5 \frac{(0.5\Delta H_{mx}/M_x)^{1/2}}{(M_c/N\rho_c)^{1/3}} \tag{22}$$

$$\nu_a' \simeq 1.025 \times 10^5 \frac{(0.5(\Delta H_{my}/M_y)^{1/2}}{(M_c/N\rho_c)^{1/3}} \tag{23}$$

The frequencies ν_a and ν_a' at the NH_4Cl decomposition interface are estimated by (22) and (23) as

$$\nu_a = \nu_{NH_3} \simeq 5.3 \times 10^{11}\ \text{sec.}^{-1} \tag{24}$$

$$\nu_a' = \nu_{HCl} \simeq 2.1 \times 10^{11}\ \text{sec.}^{-1} \tag{25}$$

Similarly, the frequencies ν_a and ν_a' at the $CuSO_4 \cdot 3H_2O$ decomposition interface are estimated to be

$$\nu_a = \nu_a' = \nu_{H_2O} \simeq 4.0 \times 10^{11}\ \text{sec.}^{-1} \tag{26}$$

Comparison of Theory with Data.—Before comparing theoretical desorption–adsorption rate expressions obtained from (16) with the experimental decomposition rate equations it is necessary to adopt a consistent set of units. The units of eq. 16 are molecules cm.$^{-2}$ sec.$^{-1}$. The rate equations of Table I may be converted to these units by multiplication by the factor $(\rho_c N/M_c)$. Alternatively eq. 16 may be converted to units of cm. sec.$^{-1}$ by multiplication by the reciprocal factor $(M_c/\rho_c N)$. It is noted that the number of single adsorption sites per square centimeter of reaction interface is approximately

$$\Lambda \simeq (\rho_c N/M_c)^{2/3} \tag{27}$$

Equation 16 may now be written in cm. sec.$^{-1}$ units as

$$B_{\text{theory}} \simeq \frac{1}{2}\left(\frac{M_c}{\rho_c N}\right)^{1/3} \frac{kT}{h} \frac{f_{\pm}}{f_a f_a'} \exp(-E_{\text{app}}/RT) \tag{28}$$

where $(f_{\pm}/f_a f_a')$ is given by eq. 19 and where E_{app} is given by eq. 18a.

The rate of the physical desorption reaction 11b, which is equal to the rate of the physical adsorption reaction 11a at equilibrium, may now be evaluated for $NH_3 + HCl$ at the NH_4Cl decomposition interface as

$$B_{NH_4Cl} \simeq 3.5 \times 10^2 \exp(-11.3/RT)\ \text{cm. sec.}^{-1} \quad \text{(theory)} \tag{29}$$

in reasonable agreement with the experimental vacuum decomposition rate expression (Table I)

$$B_{NH_4Cl} \sim 1.2 \times 10^2 \exp(-13.5/RT)\ \text{cm. sec.}^{-1} \quad \text{(expt.)} \tag{30}$$

where $T_{av.} = 596°$K. and $R = 1.99 \times 10^{-3}$ kcal. g.-mole^{-1} °K.$^{-1}$. Similarly, the rate of the physical desorption reaction 11b for $2H_2O$ at the $CuSO_4 \cdot 3H_2O$–$CuSO_4 \cdot H_2O$ interface is evaluated as

$$B_{CuSO_4 \cdot 3H_2O} \simeq 7.1 \times 10^2 \exp(-14.1/RT)\ \text{cm. sec.}^{-1} \quad \text{(theory)} \tag{31}$$

where $T_{av.} = 317°$K. and $R = 1.99 \times 10^{-3}$ kcal. g.-mole^{-1} °K.$^{-1}$; also in reasonable agreement with the experimental vacuum decomposition rate expression (Table I)

$$B_{CuSO_4 \cdot 3H_2O} \sim 2.8 \times 10^2 \exp(-15.6/RT)\ \text{cm. sec.}^{-1} \tag{32}$$

Note Regarding NH_4Cl Vaporization Rate Data in Table I.—The rate equation for the ammonium chloride vaporization was calculated by Schultz and Dekker[3] from the original vacuum sublimation rate data by Spingler.[4] This rate equation has been verified up to 807°K. by an improved linear pyrolysis technique in which a solid sample is pressed against a hot plate maintained at a series of constant temperatures. Experimental details are presently available as an Aerojet–General technical note(OSR-TN-55-117) prepared for the Office of Scientific Research.[5] The reproducibility of the hot-plate data and the agreement with vacuum sublimation data indicate that small amounts of moisture acquired by the solid NH_4Cl samples from the atmosphere prior to each run have little effect on the observed rates.

Summary and Conclusions

A modification of the Langmuir–Hinshelwood bimolecular surface reaction mechanism has been proposed to explain the thermal decomposition of ammonium chloride and cupric sulfate trihydrate. An absolute rate treatment based on this mechanism accounts for the unusually low reaction coefficients

(15) J. W. Drenan and T. L. Hill, *J. Chem. Phys.*, **17**, 775 (1949).

per collision of gaseous product molecules with the reaction interface in terms of interference by a physically adsorbed product layer. The correspondingly low experimental pre-exponential rate factors and the apparent experimental activation energies appear to be consistent with the proposed mechanism.

Because of the simplifying assumptions required to make the problem tractable, this treatment must be regarded as primarily heuristic in nature.

The writers are pleased to acknowledge an interesting discussion with Dr. Eli Mishuck of Aerojet-General Corporation, which discussion served as the stimulus for this paper. The helpful criticism of Dr. Bertram Keilin who corrected the final manuscript is also gratefully acknowledged.

COMPARATIVE PRODUCTION OF ACTIVE NITROGEN FROM NITROGEN, NITRIC OXIDE AND AMMONIA, AND FROM NITROGEN AT DIFFERENT DISCHARGE POTENTIALS[1]

BY D. A. ARMSTRONG[2] AND C. A. WINKLER

Contribution from the Physical Chemistry Laboratory, McGill University, Montreal, Canada

Received March 23, 1956

Active nitrogen was obtained from nitrogen and ammonia in roughly equal amounts when these gases were subjected to a condensed electrical discharge under comparable conditions. Nitric oxide gave a smaller yield of active nitrogen, probably owing to consumption of active nitrogen by reaction with the parent gas. The behavior suggests that all three gases were almost completely dissociated in the discharge tube to yield nitrogen atoms as the main reactive component of active nitrogen. However, variation of the voltage across a nitrogen discharge indicated that a second species was probably also present in considerable amounts.

Introduction

The chemical reactivity of active nitrogen, produced by an electrical discharge through nitrogen, has been ascribed to various entities such as atomic nitrogen, excited molecular nitrogen and N_3. It seemed that some information about the nature of active nitrogen might be obtained by studying its production from such gases as nitric oxide and ammonia, which contain only one atom of nitrogen in the molecule. It was also of interest to determine whether any change in the nature of active nitrogen with change in voltage across the discharge tube might be detected by taking advantage of an earlier observation[3] that the maximum extent of ammonia decomposition by active nitrogen represented only about one-sixth the activity inferred from hydrogen cyanide production from ethylene.

Experimental

The apparatus and analytical techniques were similar to those described in earlier papers.[3,4] The energy input to the condensed discharge was controlled by a variac transformer in the primary of the power transformer and a rotating spark gap was in series with the discharge tube to maintain a constant flash rate irrespective of the nature of the gas in the discharge tube.

Argon at a flow rate of 7.3×10^{-5} mole/sec. was used as a diluent for the nitrogen-containing gas (NO, NH_3 or N_2), the flow rate of which was generally 1.0×10^{-5} mole/sec.

In experiments with nitric oxide, where some ozone might have been present in the gas from the discharge tube, an alcohol–isopentane slurry cooled to $-135°$ was used to cool the traps. In other experiments, the traps were immersed in liquid nitrogen.

Results and Discussion

A. Comparison of Nitrogen, Nitric Oxide and Ammonia, as Sources of Active Nitrogen.—With 95 v. across the primary of the power transformer, and a flash rate of 22/sec., at least 94% of the nitric oxide or ammonia that entered the discharge tube was decomposed. Only traces of acidic oxides of nitrogen were formed from nitric oxide, while the discharge through ammonia yielded neither hydrazine nor the blue deposit indicative of NH radicals; this latter observation agrees with the results of Rice and Freamo.[5]

The products from the discharge through ammonia had the yellow color characteristic of active nitrogen, whereas those from the discharge through nitric oxide showed a faint blue afterglow at higher, and green afterglow at lower energy input to the discharge tube.

The production of hydrogen cyanide in the presence of excess ethylene was used to estimate the amount of active nitrogen.[6] The molar flow rate of HCN expressed as a percentage of the nitrogen admitted to the discharge is referred to as the "per cent. activity" and used as a measure of the relative extents to which each of the nitrogen-containing gases yielded active nitrogen in the reaction vessel. The per cent. activities obtained from the three gases under several different conditions are given in Table I. The effect of varying the energy input to the discharge on the per cent. activity obtained from NH_3 and N_2 at a constant flash rate of 6.4/sec. is illustrated graphically in Fig. 1. The energy values were calculated from the known con-

(1) With financial assistance from the National Research Council and the Consolidated Mining and Smelting Company, Trail, British Columbia.

(2) Holder of a Cominco Fellowship, 1954–1955.

(3) G. R. Freeman and C. A. Winkler, THIS JOURNAL, **59**, 371 (1955).

(4) D. A. Armstrong and C. A. Winkler, *Can. J. Chem.*, **33**, 1649 (1955).

(5) (a) F. O. Rice and M. Freamo, *J. Am. Chem. Soc.*, **73**, 5529 (1951); (b) **75**, 548 (1953).

(6) (a) J. Greenblatt and C. A. Winkler, *Can. J. Research*, **B27**, 732 (1949); (b) J. Versteeg and C. A. Winkler, *Can. J. Chem.*, **31**, 1 (1953).

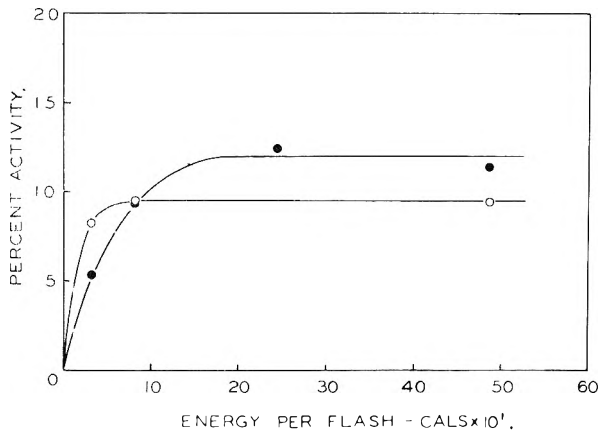

Fig. 1.

denser capacity and measured discharge potentials for different variac settings, using the relation

$$\text{energy} = {}^1/_2\,(\text{condenser capacity})\,(\text{condenser potential})^2$$

TABLE I

PER CENT. ACTIVITY OF ACTIVE NITROGEN OBTAINED BY ELECTRICAL DISCHARGE THROUGH NITROGEN, NITRIC OXIDE AND AMMONIA

Flow rate of diluent (Argon), 7.3×10^{-5} mole/sec. (except column b)
Flow rates of N_2, NO or NH_3, 1.0×10^{-5} mole/sec.
Flash rate, 22 per sec. (except column c)
Primary voltage, 95 v.

Gas	(a) Conditions as above	(b) No diluent	(c) Flash rate reduced to 6.4/sec.	(d) Length of discharge tube halved	(e) Discharge tube heated to 300°	(f) A.C. discharge
N_2	27[a]	17[a]	10	20[a]	23[a]	1.6[a]
NO	25[a]	4.4[a]	—	14[a]	14[a]	—
NH_3	31[a]	24[a]	12	21	27[a]	2.7

[a] Alcohol slurry (−135°) used to cool traps.

The values are undoubtedly rough approximations, but probably adequate for present purposes.

It will be noted that under the most favorable conditions of the study, the per cent. activity from all three gases was in the range 25–31%, and that roughly comparable activities were obtained from ammonia and nitrogen under all conditions. Furthermore, as the energy expended in the discharge was increased, the activity reached an upper limit. A reasonable interpretation of these results would seem to be that, at the plateau, all three gases were completely dissociated in the discharge tube, and that virtually all the nitrogen present was converted to atomic nitrogen. The amount of active nitrogen reaching the reaction vessel would then be determined by its rate of decay in transit from the discharge tube to the reaction vessel. Since for comparable flow rates, the initial concentration of nitrogen atoms derived from molecular nitrogen should be greater than that from ammonia, the loss of nitrogen atoms should be greater in the former than in the latter system, and the slightly greater percentage activity at the reaction vessel when ammonia is the parent gas can be explained. On the other hand, the fraction of the nitrogen that might appear as excited molecules, formed either by direct excitation or by recombination of nitrogen atoms, should be much higher for nitrogen than for ammonia. Thus, the results indicate clearly that such molecules do not react to a significant extent with ethylene, though they might contribute to reactivity in other systems. The consistently lower activity obtained from nitric oxide can be attributed to consumption of some nitrogen atoms by reaction with nitric oxide.[7]

It is interesting that a reduction in the number of flashes to which the gas was subjected as it flowed through the discharge tube (Table I, columns (c) and (d)) did not favor the production of active nitrogen from molecular nitrogen over its production from ammonia. It would seem, therefore, that formation of active nitrogen from ammonia does not require that dissociation of the molecule be followed by recombination of the nitrogen atoms to form nitrogen molecules which are then excited to a still higher state by a subsequent flash. Hence the observed chemical reactivity of the active nitrogen apparently is not due to molecules brought into a highly excited state *by the discharge*.

Rather, it would appear to be due mainly to atomic nitrogen, with perhaps some contribution from a product of the recombination of nitrogen atoms. Recent results of mass spectrometric examination of active nitrogen support such a conclusion.[8,9]

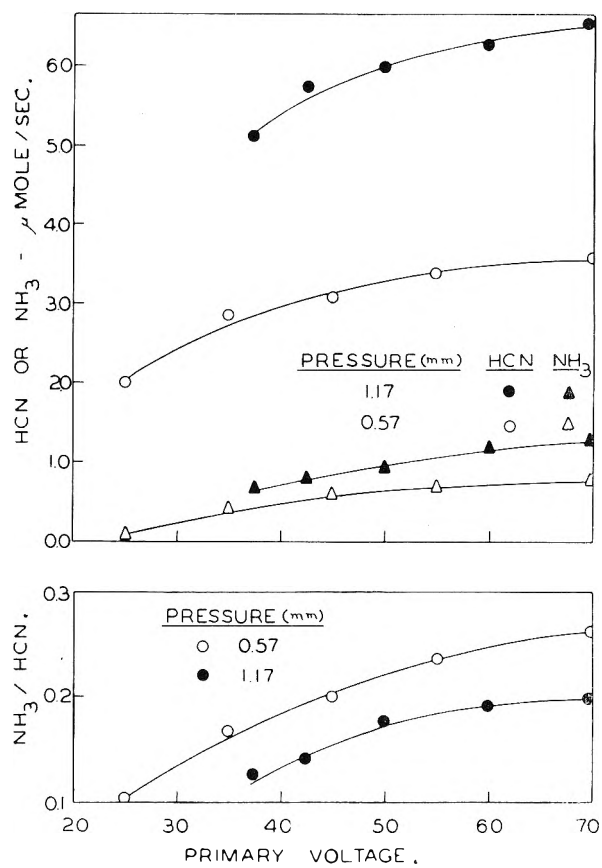

Fig. 2.

(7) M. L. Spealman and W. H. Rodebush, *J. Am. Chem. Soc.*, **57** 1474 (1935).
(8) D. S. Jackson and H. I. Schiff, *J. Chem. Phys.*, **21**, 2233 (1953).
(9) D. S. Jackson and H. I. Schiff, *ibid.*, **23**, 2333 (1955).

B. Effect of Voltage on the Nature of Active Nitrogen.—Increase in the voltage across the primary of the power transformer with constant flash rate (*ca.* 8/sec.) through the discharge caused a marked increase in the ratio of the maximum amount of ammonia decomposed to the maximum yield of hydrogen cyanide from ethylene, as shown in Fig. 2. Although it was not possible to extend the experiments to higher voltages with the equipment available, there is little doubt that the ratio would reach a plateau value slightly beyond the upper limit of the range studied.

To explain the behavior shown by Fig. 2, it seems necessary to revert to an earlier suggestion[3] that there are two reactive species in active nitrogen, only one of which is capable of destroying ammonia while the other, or both, may react with ethylene. Within the range of voltages studied, the species that reacts with ethylene appears to increase in amount proportionately less with increase of total activity than does the species that reacts with ammonia. This might be explained by assuming that atomic nitrogen is largely responsible for the reaction with ethylene and that the destruction of ammonia is caused by a second species derived from recombination of nitrogen atoms in increasing proportion as the atom concentration is increased by increase of voltage across the discharge tube.

The identity of such a second species is a matter for speculation; the available information has been reviewed for a further paper, with a view to suggesting a probable species.

THE OSMOTIC AND ACTIVITY COEFFICIENTS OF SOME SULFONIC ACIDS AND THEIR RELATIONSHIP TO ION EXCHANGE EQUILIBRIA[1]

BY O. D. BONNER, V. F. HOLLAND AND LINDA LOU SMITH

Department of Chemistry of the University of South Carolina, Columbia, South Carolina

Received March 28, 1956

Osmotic and activity coefficients have been determined for several monosulfonic and disulfonic acids. Activity coefficient ratios, $\gamma_{acid}/\gamma_{Na\ salt}$, have been calculated for the system 80% *p*-toluenesulfonate–20% 2,5-dimethylbenzenesulfonate. These data have been used in the modified McKay–Perring equation for the calculation of ion-exchange selectivities. It has been deduced that ion-exchange resins must be treated as polymeric *n*,1 electrolytes rather than 1,1 or 1,0 electrolytes. The conclusion of Myers and Boyd that more than one type of functional group is probably present in ion-exchange resins has been further verified.

The exchange of two univalent cations on a synthetic strong acid type ion exchanger such as Dowex 50 may be represented by the equation

$$(A^+)_o + (B^+)_i = (A^+)_i + (B^+)_o \qquad (1)$$

where A^+ and B^+ represent the ions being exchanged and i and o represent the resin phase and outside solution phase, respectively. The selectivity coefficient, k, which defines the relative affinity of the two ions for the resin is

$$k = \frac{N_{(A^+)_i}\, m_{(B^+)_o}}{N_{(B^+)_i}\, m_{(A^+)_o}} = \frac{m_{(A^+)_i}\, m_{(B^+)_o}}{m_{(B^+)_i}\, m_{(A^+)_o}} \qquad (2)$$

where N is the mole fraction of the ion in the resin phase and m is the molality of the ion in the solution or resin phase. This selectivity coefficient is not a constant at constant temperature but varies with the mole fraction of ion A^+ in the resin phase. It is related to the thermodynamic equilibrium constant, K, by the equation

$$K = k\, \frac{\gamma_{(A^+)_i}\, \gamma_{(B^+)_o}}{\gamma_{(B^+)_i}\, \gamma_{(A^+)_o}} \qquad (3)$$

It has been demonstrated[2-4] that a selectivity scale for the various univalent ions may be established if the standard state for the resin phase is chosen to be the resin anion associated with only one cationic species and the usual standard state, *i.e.*, the hypothetical one molal solution in which the electrolyte behaves as it does at infinite dilution, is chosen for the aqueous phase. If, however, one chooses the same standard reference state for the resin phase as for the aqueous phase and recognizes that the partition of the ions between the two phases must be governed by a Donnan membrane equilibrium, then K, the thermodynamic equilibrium constant, must be unity and the resin selectivity is given by the equation[5]

$$\log k = P(\bar{v}_{B^+} - \bar{v}_{A^+})_i/2.3RT + \log (\gamma_{B^+}/\gamma_{A^+})_i - \log (\gamma_{B^+}/\gamma_{A^+})_o \qquad (4)$$

the swelling pressure, P, is greater for the higher cross-linked resins and is the pressure necessary to increase the "escaping tendency" of the solvent in the concentrated resin phase to that in the dilute outer solution. It is the purpose of this report to describe some efforts to evaluate k by means of equation 4 for a series of exchange reactions involving sodium ion and hydrogen ion, and to compare these values with the experimentally determined values for the same system. The sodium-hydrogen system was chosen because it is probably the most difficult to explain on account of the change of the values for log k from positive to negative at high sodium loadings for resins of greater than 8% DVB content. This exchange should furnish a most severe test for equation 4.

The term log $(\gamma_{B^+}/\gamma_{A^+})_i$ makes the major contribution to the value of log k. The final term, log

(1) A portion of the results were developed under a Project sponsored by the United States Atomic Energy Commission.

(2) W. J. Argersinger, Jr., A. W. Davidson and O. D. Bonner, *Trans. Kansas Acad. Sci.*, **53**, 404 (1950).

(3) E. Högfeldt, E. Ekedahl and L. G. Sillen, *Acta Chem. Scand.*, **4**, 828 (1950).

(4) O. D. Bonner, THIS JOURNAL, **59**, 719 (1955).

(5) G. E. Myers and G. E. Boyd, *ibid.*, **60**, 521 (1956).

$(\gamma_{B^+}/\gamma_{A^+})_o$, may be neglected if the outer solution is sufficiently dilute. An evaluation of the contribution of the pressure–volume term is more difficult. It may be estimated to contribute perhaps 2–15% of the total value of log k, the lower value probably being more nearly correct. The difference $(\bar{v}_{H^+} - \bar{v}_{Na^+})$ for solutions of chlorides and nitrates is in the approximate range + 1.5 cc. for dilute solutions to − 2.5 cc. for concentrated solutions. The swelling pressure, P, is probably 200–600 atm.[5] for highly cross-linked resins. The maximum value of the term $\pi\Delta\bar{v}/2.303\ RT$ would therefore be perhaps (600)(2.5)/(2.303)(82.06)(298) = 0.027. An adaptation[6] of the McKay–Perring equation[7] may be used for the evaluation of the term log $(\gamma_{B^+}/\gamma_{A^+})_i$. This equation is

$$2.303 \log \frac{\gamma_{HRes}}{\gamma_{NaRes}} = \int_0^{m\varphi} \left(\frac{\partial(1/m)}{\partial X_{HRes}}\right)_{m\varphi} d(m\varphi) \quad (5)$$

where m is the total number of equivalents of resin per 1000 g. of water, X_{HRes} is the mole fraction of the resin in the acid form and φ is the practical osmotic coefficient. It is of interest to note that the equilibrium constant for a given exchange system, such as was used in the establishment of the selectivity scale,[4] may be calculated from the equation

$$\ln K = \int_0^1 \ln k\, dX_{NaRes} = \int_0^{m\varphi}\int_0^1 \left(\frac{\partial(1/m)}{\partial X_{HRes}}\right)_{m\varphi} dX_{NaRes}\, d(m\varphi) = \int_0^{m\varphi} \left(\frac{1}{m_{HRes}} - \frac{1}{m_{NaRes}}\right)_{m\varphi} d(m\varphi) \quad (6)$$

if one considers only the contribution of the second term on the right side of equation 4. The difficulty in the evaluation of ln $\gamma_{HRes}/\gamma_{NaRes}$ at any resin loading or ln K in this manner arises from the necessity of extrapolating $(\partial(1/m)/\partial X_{HRes})_{m\varphi}$ or $\left(\frac{1}{m_{HRes}} - \frac{1}{m_{NaRes}}\right)_{m\varphi}$ to infinitely dilute solutions. The experimental realization of infinitely dilute solutions for highly cross-linked exchangers is impossible because of their limited swelling.

At least one attempt has been made, prior to this report, to circumvent this difficulty. In this previously reported work and in the present work, model compounds which are similar in structure to the highly cross-linked resins and are presumably similar in properties, but which permit the measurement of the osmotic properties of the solution at greater dilutions, have been used as "substitutes" for the resin. Myers and Boyd[5] use a very weakly cross-linked resin as the model compound. This approximately 0.5% DVB resin will swell sufficiently to form relatively dilute solutions and will therefore allow reasonably accurate extrapolations to infinite dilution. Concentrations equivalent to those in the higher cross-linked resins may be obtained by equilibration of this resin with solutions of the proper water activity. These workers were able to obtain fair agreement between calculated and observed selectivities for exchanges between sodium and lithium, potassium and sodium, and cesium and sodium ions. Poorer agreement with no indication of the reversal which occurs experimentally, was obtained in the calculation of selectivities for the sodium–hydrogen system. The authors cited attribute this lack of agreement at least partially to the presence of more than one type of exchange site on the cross-linked resin. This conclusion is logical, since the sulfonate exchange sites on the weakly cross-linked resins are probably of the type

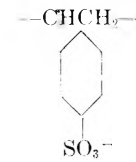

while the highly cross-linked resins have at least one additional type of exchange site, namely

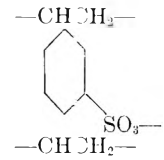

Monosulfonic Acid Data.—A second type of model system which should approach the behavior of an ion-exchange resin and which would permit extrapolations to infinitely dilute solutions would appear to be a solution of two sulfonic acids, similar in structure to the two monomeric units of the resin and present in approximately the same ratio in the solution as the units appear in the resin structure. Solutions of the acid and sodium salt of *p*-toluenesulfonic acid and 2,5-dimethylbenzenesulfonic acid were therefore chosen, since these compounds are commercially available in very pure form. Osmotic and activity coefficients (Table I) were first determined for solutions of pure 2,5-dimethylbenzenesulfonic acid. The experimental procedure of isopiestic equilibration and the equations for the calculation of these coefficients have been given previously.[8]

TABLE I

TABLE OF OSMOTIC AND ACTIVITY COEFFICIENTS FOR 2,5-DIMETHYLBENZENESULFONIC ACID

m	φ	γ	m	φ	γ
0.1	0.913	0.749	1.4	0.728	0.406
0.2	.885	.679	1.6	.721	.389
0.3	.864	.634	1.8	.718	.374
0.4	.844	.596	2.0	.713	.362
0.5	.826	.565	2.5	.709	.338
0.6	.811	.537	3.0	.711	.321
0.7	.795	.513	3.5	.718	.310
0.8	.782	.493	4.0	.734	.303
0.9	.771	.474	4.5	.752	.300
1.0	.758	.456	5.0	.774	.299
1.2	.740	.429			

Mixtures containing 20% 2,5-dimethylbenzenesulfonate and 80% *p*-toluenesulfonate, and sodium to hydrogen ion ratios of 0, 1/9, 2/8, 4/6, 6/4, 8/2, 9/1 and ∞, were then equilibrated isopiestically with standard lithium chloride solutions rang-

(6) O. D. Bonner and V. F. Holland, *J. Am. Chem. Soc.*, **77**, 5828 (1955).

(7) H. A. C. McKay and J. K. Perring, *Trans. Faraday Soc.*, **49**, 163 (1953).

(8) O. D. Bonner, G. D. Easterling, D. L. West and V. F. Holland, *J. Am. Chem. Soc.*, **77**, 242 (1955).

ing from 0.1 to 2.5 molal. Evaluation of the term $\gamma_{acid}/\gamma_{salt}$ at various concentrations and ratios of acid to salt was accomplished by means of the modified McKay–Perring equation (Table II). Since there were present two anionic species as well as two cationic species, this value of $\gamma_{acid}/\gamma_{salt}$ represents the mean values of the ratios of the activity coefficients of the acids and sodium salts present. The more concentrated solutions of constant water activity ($m\varphi = 2.5$) are equivalent to concentrations of 3.13 m for the $X_{acid} = 1$ solutions and 3.52 m for the $X_{Na\ salt} = 1$ solutions, and represent the limit of solubility of the sodium salts. Ion-exchange resins of about 20% DVB content have equivalental moisture uptakes of about 100 g. of water in the sodium form and 120 g. of water in the acid form. These correspond to "molalities" of 10 and 8.2, respectively. Although an extrapolation of the sulfonate data to these concentrations is impractical, it is obvious that the calculated selectivity coefficient of about 1.1 would be too small for resins of low sodium ion loading.[5] The experimentally observed value is about 4. It is believed, however, that the change in the sign of log $\gamma_{acid}/\gamma_{salt}$ at constant water activity in a manner similar to that which is observed in the ion exchange system is of significance. Since this behavior was not observed by Myers and Boyd, it probably is due to the presence of two types of sulfonate groups.

TABLE II

ACTIVITY COEFFICIENT RATIO OF ACID TO SODIUM SALT IN AQUEOUS MIXTURES OF 80% *p*-TOLUENESULFONIC ACID, 20% 2,5-DIMETHYLBENZENESULFONIC ACID AT CONSTANT WATER ACTIVITY

	Mole fraction acid					
$m\varphi$	0.0	0.2	0.4	0.6	0.8	1.0
0.2	0.988	0.996	0.997	0.998	0 999	0 999
0.4	.964	.990	.992	.995	.997	.997
0.6	.941	.985	.987	.991	.993	.993
0.8	.920	.979	.983	.986	.989	.989
1.0	.901	.974	.979	.984	.986	.986
1.2	.882	.971	.977	.982	.984	.985
1.4	.866	.971	.978	.983	.985	.986
1.6	.856	.972	.981	.986	988	989
1.8	.853	.975	.986	.990	.992	.993
2.0	.854	.979	.990	.995	.997	.998
2.2	.858	.983	.995	1 000	1.002	1.003
2.5	.866	.992	1.004	1.009	1.011	1.012

Disulfonic Acid Data.—While the above model is superior to that of Myers and Boyd for the representation of the ion exchanger in that there is more than one type of sulfonate group present, it is inferior to their model in that it does not permit an estimation of the effect which neighboring sulfonic acid groups have upon one another. These sulfonate groups on the monomeric compounds are separated by relatively great distances in very dilute solutions, while those on the polymeric compounds are fixed by the polymer matrix. Consequently it was believed that a solution of two dimeric sulfonates such as disulfonated 4,4′-dimethylbibenzyl and 4,4′-bibenzyldisulfonic acid which have structures similar to the above monomers would constitute an improved model. These compounds were prepared and purified by recrystallization of the barium salts. The barium ion was replaced quantitatively by hydrogen ion by passing a solution of the barium salt through an ion-exchange column in the acid form.

Upon completion of these syntheses, it was found that the solubility of the sodium salts of the disulfonic acids was too small ($m \approx 0.2$) for significant isopiestic comparisons. The acids were quite soluble, however, and solutions of 4,4′-bibenzyldisulfonic acid were isopiestically compared with standard solutions of sodium chloride. The concentration of the sulfonic acid was taken to be

$$m' = \frac{\text{equivalents of acid}}{\text{wt. of } H_2O} \times 1000$$

and the number of ions $\gamma' = 2$. This procedure of assuming the molal unit to be one half of the bibenzyldisulfonic acid molecule is identical with that of previous investigators in the field of polyelectrolytes.[9–12] Values of the function $(\gamma'\varphi')$ calculated from the relationship

$$\gamma' m' \varphi' = \gamma_r m_r \varphi_r$$

are given in Table III. These data lead to a value of $\gamma'\varphi' = \gamma' = 1.5$ at infinite dilution. Glueckauf[9] first observed that the extrapolated value of $\gamma\varphi$ was unity at infinite dilution for weakly cross-linked sulfonic acid type ion exchangers when treated in this manner. He accounted for this value of $\gamma = 1$ by assuming that the sulfonate groups on the polymeric matrix are osmotically inactive. It may be demonstrated, however, that the results obtained for both the polymer and the dimer may be accounted for without this assumption. If the sulfonate groups in a dimer or a polymer are attached to adjacent rings, the interaction between them is such that one must not treat them as uni-univalent or 1,0 electrolytes but rather as n,1 electrolytes where n is the number of fixed anionic groups. The correct concentration is then

$$m = \frac{n \times \text{no. of equiv. of polyelectrolyte} \times 1000}{\text{no. of grams of water}}$$

TABLE III

APPARENT OSMOTIC COEFFICIENTS OF 4,4′-BIBENZYLDISULFONIC ACID

m'	$\gamma'\varphi'$
0.0	1.500 (extrap.)
0.2	1.286
0.4	1.220
0.6	1.200
0.8	1.188
1.0	1.179

and the number of ions is $\nu = n + 1$. The relationship between ν' and ν and m' and m is thus $\nu = \nu' + n - 1 = n + 1$ and $m = m'/n$. For solutions of equal water activity the relationship

$$\nu_r m_r \varphi_r = \nu m \varphi = (n+1)(m'/n)\varphi = \frac{n+1}{n} m'\varphi$$

(9) E. Glueckauf, *Proc. Roy. Soc.* (*London*), **214**, 207 (1952).
(10) J. F. Duncan, *ibid.*, **214**, 344 (1952).
(11) D. Reichenberg, *Research*, **6**, 98 (1953).
(12) G. E. Boyd and B. A. Soldano, *Z. Elektrochem.*, **57**, 162 (1953).

may now be applied. If m' is thus incorrectly taken to be m, the apparent value of ν at infinite dilution is $(n + 1)/n$. This corresponds to the first observed value of $\nu = 1.5$ when ν' was incorrectly taken to be 2 for the disulfonic acid and to the value obtained by Glueckauf of $\nu \approx 1$ for a polysulfonic acid having a very large value for n. It should be realized that equations 5 and 6 are still applicable to ion exchangers or polyelectrolytes even when the value of ν is unknown because m may be taken to be the number of equivalents of a common ion, the resin or polymeric anion, per 1000 g. of water.

Osmotic and activity coefficient data for two disulfonic acids, 4,4′-bibenzyldisulfonic acid and *m*-benzenedisulfonic acid are given in Table IV. The former compound is the better model for an ion exchanger and therefore these data should furnish an indication of the order of magnitude of the activity coefficients in the resin. The data on the latter compound indicate the effect which would be expected if disulfonation of a single ring occurred in the preparation of the ion exchange resin since the activity coefficients of this compound in concentrated solutions are relatively large when compared with those of 2,5-dimethylbenzenesulfonic acid, *p*-toluenesulfonic acid[8] or 4,4′-bibenzyldisulfonic acid.

In summary, these sulfonic acid activity coefficient data suggest that there are at least two types of resin exchange sites. The sulfonated styrene and the sulfonated DVB sites are probably significantly different in character since the similar monomeric compounds, *p*-toluenesulfonic acid and 2,5-dimethylbenzenesulfonic acid, have quite different activity coefficients in concentrated solutions. If there is any disulfonation of a single ring in the resin, a third type of exchange site is also present.

TABLE IV

TABLE OF OSMOTIC AND ACTIVITY COEFFICIENTS

	4,4′-Bibenzyldisulfonic acid		*m*-Benzenedisulfonic acid	
m	φ	γ	φ	γ
0.1	0.857	0.640	0.891	0.686
0.2	.813	.545	.905	.646
0.3	.800	.500	.937	.647
0.4	.792	.465	.968	.657
0.5	.786	.442	.997	.674
0.6	.782	.426	1.027	.694
0.7	.784	.412	1.057	.715
0.8	.796	.403	1.088	.738
0.9	.807	.398	1.120	.763
1.0	.822	.397	1.151	.790
1.2	.857	.399	1.222	.856
1.4	.899	.410	1.293	.931
1.6	.944	.424	1.362	1.015
1.8	.992	.443	1.437	1.108
2.0	1.042	.467		
2.2	1.098	.496		
2.4	1.161	.533		

SORPTION OF AMMONIA BY HOMOIONIC BENTONITES[1,2]

BY W. H. SLABAUGH AND RICHARD H. SIEGEL

Department of Chemistry, Oregon State College, Corvallis, Oregon

Received April 6, 1956

Isotherms were determined for the adsorption of ammonia by oven-dried and freeze-dried Ca, Na and H bentonites at −45°. Samples were humidified at 51% relative humidity before weighing. Surface areas from B.E.T. plots were corrected for amounts of water adsorbed to give the surface area per gram of dry clay. Surface areas of sodium and hydrogen clays were found to be on the order of 300 m.²/g. Surface areas were 363.5 m.²/g. for oven-dried and 420 m.²/g. for freeze-dried calcium clays. Assumption of only a single layer between platelets at the point V_m gives values for the total surface area comparable to the theoretical value of 800 m.²/g. The hydrogen clays apparently adsorb ammonia more strongly than do the sodium clays although no more adsorption takes place upon them. It is suggested that the increased adsorption of calcium clays is due to greater coördination about the base exchange cation. The data do not fit the Harkins-Jura equation.

Introduction

Cornet,[3] Barrer and MacLeod[4] and others[5-7] have made studies of the adsorption of ammonia by montmorillonite or bentonite. However, little work has been done at sufficiently low temperatures in order to allow complete isotherms, including high relative pressures, to be run. Furthermore, no adequate study of carefully characterized, homoionic bentonites has been made.

Studies which have been made with ammonia indicate, in some cases, surface areas of about 300 to 350 m.²/g. for the total area of the clay.[5,7] Ammonia, being a polar molecule, is capable of forcing the platelets of clay particles apart and entering between the platelets thus becoming available to the entire surface for adsorption. Besides possessing the ability to penetrate between the clay platelets, ammonia would be expected to exhibit special affinity for hydrogen bentonite which is a fairly strong ($K_a = 2 \times 10^{-1}$) acid in aqueous suspension.

It was felt that there was need for a set of complete isotherms at a low temperature on a group of well characterized homoionic bentonites using ammonia as the adsorbate. Accordingly, this study was made on Ca, H and Na bentonites at −45°. The clays used were both oven-dried and freeze-dried.[8] Investigations of the reproducibility of the isotherms were also carried out as no previous mention has been made of this factor in the literature.

(1) Taken from the M. S. thesis of Richard H. Siegel, Oregon State College, 1956.

(2) Supported by a research grant from the Baroid Division, National Lead Company.

(3) I. Cornet, *J. Chem. Phys.*, **11**, 217 (1943).

(4) R. M. Barrer and D. M. MacLeod, *Trans. Faraday Soc.*, **50**, 980 (1954).

(5) C. Sato, *J. Chem. Soc. Japan, Pure Chem. Sect.*, **74**, 167 (1953).

(6) von P. Weiden and H. Balduin, *Kolloid Z.*, **127**, 30 (1952).

(7) S. Teichner, *Compt. rend.*, **231**, 1063 (1950).

(8) F. Call, *Nature*, **172**, 126 (1953).

Experimental

Apparatus.—The gravimetric apparatus utilized a copper-beryllium spring maintained at 26 ± 0.1° in a vacuum system. The bentonite samples were suspended from this spring in a small glass bucket and the amount of ammonia adsorbed was measured by observing the distension of the spring with a travelling microscope capable of reproducing readings to within 0.002 mm. A mercury manometer was provided for measurement of the pressure of ammonia in the system. A low temperature thermostating system was devised to maintain the sample at −45°. Variations in bath temperature were estimated to be no more than ±0.025°. Differences in temperatures between individual runs were no more than 0.2°.

Preparation of the Bentonite.—The homoionic clays were prepared by passing a 1.5% suspension of clarified Wyoming bentonite through an ion-exchange resin (Amberlite IR-120) charged with the appropriate cation. This resulted in an essentially homoionic bentonite. The suspension was then either dried by placing it in an oven at 105°, or by freeze-drying at −5°. The oven-dried clay was ground with a mortar and pestle to 200 mesh. Freeze-drying consisted of freezing an 8 to 10% clay gel to the walls of a 1-liter round-bottom flask and evacuating the flask by use of a vacuum pump and a cold trap. The gel was kept frozen until all the water had been sublimed from it.

Purification of the Ammonia.—Anhydrous tank ammonia from the Penn Salt Company was purified by passage through a soda-lime column and trapped in a liquid nitrogen cold trap. The ammonia was then exhaustively pumped to remove non-condensable vapors and distilled into a second liquid nitrogen trap where it was again pumped before using it as an adsorbate.

Conditioning of the Samples.—The bentonite samples were stored in a constant humidity container maintained at 51% relative humidity by means of a saturated solution of $Ca(NO_3)_2$. Samples of each type of clay were also placed in a desiccator containing magnesium perchlorate and the difference in water content of the dry clay and the clay at 51% relative humidity was determined.

Determination of Isotherms.—Weighed samples of about 0.3 g. of bentonite were suspended from the spring and evacuated slowly. The samples were then outgassed for 2 hours at 100°. Determination of the effect of buoyancy was made by use of dry air. The sample was then cooled −45° and appropriate increments of ammonia admitted. After equilibrium was obtained (6 to 10 hr.) readings of the spring distension and the pressure of the ammonia were made. At the end of each run enough ammonia was admitted to the system to allow P_0, the vapor pressure of the ammonia at the sample temperature, to be determined.

Reproducibility of Isotherms

Isotherms were determined on Na, Ca and H bentonites both oven-dried and freeze-dried. Some isotherms were made with clays which had not been humidified in the constant humidity container. What appeared to be a lack of reproducibility was in effect the difference in sample weight caused by variations in water content of the samples. Therefore, it was necessary to equilibrate all samples at a constant relative humidity prior to weighing. Thus, all isotherms are plotted on the basis of clays weighed at 51% relative humidity.

Reproducibility of the isotherms is apparently good. The data, both corrected and standard, coincide well and are distributed in a manner which indicates reproducibility. Further and more convincing proof of reproducibility is provided by the data on freeze-dried Na bentonite. Two separate runs were made with humidified clay. No correction factor was applied to the data. As may be seen from the isotherm the two sets of data fall closely along the curve.

Deviations in the data do not exceed a few per cent., most points being within 2 or 3% of the values indicated by plotting of smooth curves for the isotherms.

Conclusions

All isotherms obtained in this study were good examples of type II, S-shaped isotherms (see figures). There was no tendency toward stepwise isotherms. Cornet[3] has reported stepwise isotherms with ammonia on hydrogen montmorillonite at very low relative pressures at room temperature. Our work does not disclose any steps, probably on account of the widely different temperatures used and the resultant effect on the adsorption and the relative pressures.

B.E.T. plots of the adsorption data yield very good straight lines up to relative pressure values of about 0.3. Above this point however the data begin to deviate from a linear plot. Surface areas for the clays were calculated on the basis of humidified clay (see Table I). On this basis Na and H clays, whether freeze- or oven-dried, exhibit practically the same surface area. The surface areas of these clays are within 2.1% of each other and this is undoubtedly within the experimental error for the data.

Comparison of the isotherms on sodium and hydrogen bentonite reveal slightly more ammonia sorbed at the lower pressures by the hydrogen clay.

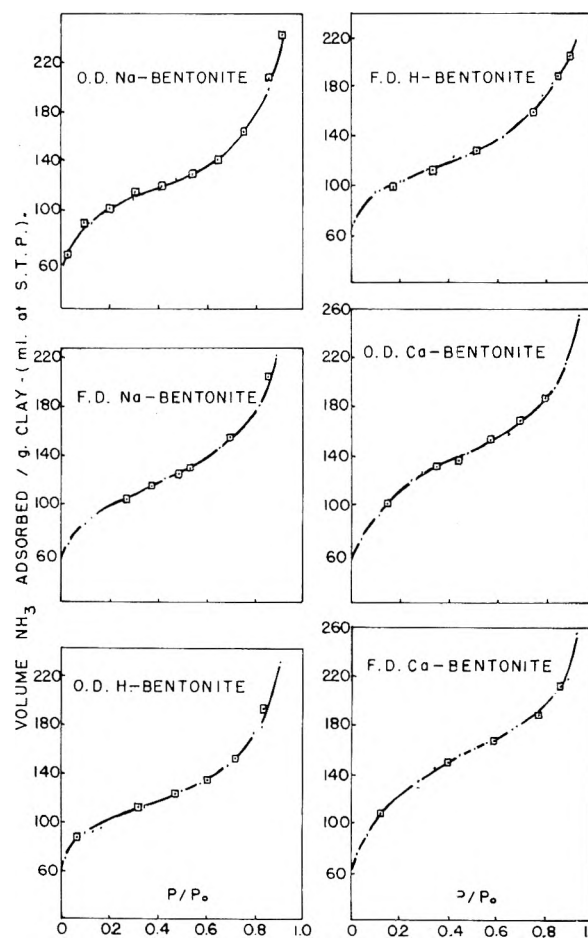

Fig. 1.—Adsorption isotherms at −45° of ammonia on various homoionic bentonites. The two sets of data in each instance represent two independent determinations of the isotherm.

The difference is very small, however, and becomes smaller as the pressure increases. It is felt that this does not show that the hydrogen clay exhibits a greater capacity for the sorption of ammonia but rather that the hydrogen clay sorbs the ammonia more strongly than does the sodium. This is borne out by comparison of surface areas of the two clays. Stronger attraction for ammonia by hydrogen bentonite would be expected since it is acidic and should attract the basic ammonia. This attraction would logically be expected to take the form of stronger active sites rather than a greater number of active sites since both clays have the same base exchange capacity and therefore the same number of exchange cations. Each base exchange cation can be taken as an active site on the clay. However, other types of active sites may also be present on both clays.

One would expect the forces between the sodium ions in the clay and ammonia to be strictly those for the formation of coördination compounds of some sort, whereas those between hydrogen and ammonia should also include a stronger component due to the acid–base characteristics of the reactants. There is ample evidence that ammonia reacts anhydrously with hydrogen clay to form an ammonium clay according to the reaction[3]

$$\text{H-bentonite} + NH_3 \longrightarrow NH_4\text{-bentonite}$$

The surface area values are great enough to indicate that the ammonia penetrates between platelets of the clay and thus becomes available to the entire surfaces of the bentonite. This has been substantiated by other investigators.[3,4,9]

It is not fruitful to further investigate the relationship between the surface areas of the various clays without making allowance for the water vapor adsorbed on the clay surface when it is weighed and its effect on the apparent weight and hence the surface area of the clay. The amounts of water vapor adsorbed are presented as percentages in Table II. These values were used to arrive at the corrected surface areas listed in Table I. It is seen that appreciable amounts of water are adsorbed by the clay and that the amount of this adsorption depends markedly upon the exchangeable ion present on the clay and the method used to prepare the clay.

It should be noted that in general the freeze-dried clays exhibit a larger surface area than do oven-dried clays with the same cation. This would be expected since freeze-drying seems to result in a more dispersed clay. Call[8] has reported values for nitrogen areas on freeze-dried clays which are slightly larger than external areas reported by other workers on oven-dried clays.[10] Freeze-drying apparently breaks up the clay particles to a larger extent than does oven-drying resulting in a particle with more of the platelet surface exposed in such a manner that nitrogen can adsorb on it.

Recent X-ray studies[10] have shown that only one layer of water is present between two adjacent platelets in bentonite at the point given by V_m. This suggests that the B.E.T. theory does not, in this case, give a value for the volume necessary to form a monolayer on each and every surface but rather that two adjacent bentonite platelets share the same monolayer. Therefore, calculations of the surface area using this value of V_m do not give a measure of the total surface. These calculations instead give a value for the surface which actually is about one-half that of the true surface area.

(9) R. M. Barrer and N. Mackenzie, THIS JOURNAL, **58**, 560 (1954).

(10) R. W. Mooney, A. G. Keenan and L. A. Wood, *J. Am. Chem. Soc.*, **74**, 1367 (1952).

TABLE I

SURFACE AREAS OF HOMOIONIC BENTONITES IN m.²/g.

Type of clay	Uncor. V_m	Uncor. surf. area	Cor. V_m	Cor. surf. area	N_2 area	Total surf. area
O. D. Na	83.7	290	90.7	314	33	595
O. D. H.	82.1	284	92.3	319	40	598
O. D. Ca	92.2	319	105	363.5	50	677
F. D. Na	83.0	287	91.3	316	49	583
F. D. H.	83.9	290	97.5	338	58	616
F. D. Ca	105	362.5	121.3	420	70	770

TABLE II

PERCENTAGE BY WEIGHT OF H_2O ADSORBED (AT 51% RELATIVE HUMIDITY)

Type of clay	% of H_2O adsorbed	Type of clay	% of H_2O adsorbed
O. D. Na	7.7%	F. D. Na	9.1
O. D. H	11.0	F. D. H	14.0
O. D. Ca	12.2	F. D. Ca	13.7

It would seem reasonable that ammonia should exhibit the same phenomena as water in this respect. Experimental evidence through X-ray work would be necessary to prove this, however. Comparison of surface areas obtained in this study with those by water vapor on montmorillonite by Mooney, *et al.*, seem to indicate that a similar process is occurring. Calculations based on this assumption are listed in Table I under total surface area. Even though comparisons are made to the results of other workers who may probably have used clays from different sources and pretreated differently, the correlations appear of sufficient interest to warrant a direct comparison.

The nitrogen area presumably gives only the external area whereas the large surface area values for ammonia include the external area plus one-half the internal area. Therefore the total surface area, external and internal, should be obtained by subtracting the nitrogen area from twice the ammonia area. The nitrogen areas listed in Table I for freeze-dried clays are after Call. The areas for oven-dried sodium and hydrogen are after Mooney, *et al.* The value for oven-dried calcium is an estimate.

Calculations based on the dimensions of the clay lattice give values of about 800 m.²/g. for the total surface of a completely dispersed bentonite. The values obtained for total surface, as calculated by the method outlined above, are somewhat below this value but this may be due to the possibility that the ammonia cannot penetrate to all parts of the clay lattice. Both types of sodium and hydrogen clays have total surfaces in the vicinity of 600 m.²/g. but the calcium clays exhibit considerably larger total surfaces. Furthermore the freeze-dried calcium has a very appreciably larger surface than does the oven-dried.

Two interdependent factors may account for this. It has been shown that the calcium ion in an exchange site exerts forces tending to hold two ad-

jacent platelets together.[11] It is possible that these forces are not completely overcome by ammonia molecules tending to enter between the platelets. However, in freeze-drying some of these bonds may be broken resulting in more of the surface becoming accessible to the ammonia. Furthermore it is probable that some ammonia molecules coördinate about the calcium ions. Possibly the disrupting of the forces between the platelets which occurs in freeze-drying allows the calcium ions on the freeze-dried clay to coördinate with more ammonia molecules than the calcium on oven-dried clay is capable of doing.

Insufficient data are present to allow one to explain thoroughly why the calcium bentonites exhibit such a markedly larger surface area than do the sodium and hydrogen clays. It is possible that this is due more to increased coördination of ammonia with the calcium than it is to an increase in the actual surface area of the clay. Mooney has pointed out that calcium does show greater coördination with water than do sodium and hydrogen. No significant calculations can be made in this case however.

The data do not give linear Harkins–Jura plots. The Harkins–Jura equation is applicable only if a condensed film is formed on the adsorbent while the B.E.T. theory is applicable to the upper intermediate film and the lower condensed film.[12] Apparently the ammonia does not occur on the clay surface in a condensed phase but rather in a more expanded adsorbed state.

(11) W. H. Slabaugh and J. L. Culbertson, THIS JOURNAL, **55**, 1131 (1951).

(12) W. D. Harkins and G. Jura, *J. Am. Chem. Soc.*, **66**, 1366 (1944).

THE PHYSICAL-CHEMICAL BEHAVIOR OF OIL-DISPERSIBLE SOAP SOLUTIONS. II. ALKALI AND ALKALINE EARTH PHENYLSTEARATES IN BENZENE[1,2]

BY JOHN G. HONIG AND C. R. SINGLETERRY

Surface Chemistry Branch, Naval Research Laboratory, Washington 25, D. C.

Received April 9, 1956

Alkali metal phenylstearates in dilute, anhydrous solutions (*c*-1–2.5%) formed viscous, slightly non-Newtonian systems analogous to polymeric solutions. The effectiveness of the soaps in forming such systems varied inversely with the size of the cation involved. A reverse order of effectiveness in forming similar systems was observed for the alkaline earth phenylstearates. Addition of polar substances caused a breakdown of these structures, the effectiveness in producing this breakdown decreasing in the order: phenylstearic acid, water, phenol or ethanol. In the alkali metal soap solutions, bifunctional groups such as water or glycol caused a secondary aggregation to a highly elastic, viscous system, this effect being most pronounced with lithium soaps and least with cesium soaps. Alkaline earth phenylstearates did not show this phenomenon. Addition of about 2 moles of water per equivalent of soap to magnesium or calcium soap solutions, or 4 to 5 moles water per mole soap to alkali metal soap solutions (except lithium), caused precipitation Under controlled conditions highly birefringent soap-rich phases separated at the onset of precipitation. A method was developed for the derivation of the size and shape of colloidal particles from viscosity and fluorescence depolarization data and was applied to the small micelle (low viscosity) systems.

Introduction

Previous publications have reported the high viscosity of dilute, anhydrous benzene solutions of calcium xenylstearate[3] and sodium phenylstearate[4] and the extraordinary sensitivity of these systems to traces of water, phenylstearic acid, phenol and ethanol. Bifunctional polar additives, such as water and glycol, produced secondary aggregation phenomena in dilute sodium phenylstearate solutions, while an excess of water caused the soap to precipitate. A study of these phenomena has now been extended to benzene solutions of other alkali and alkaline earth phenylstearates to provide further data from which inferences may be made about the structures of the soap aggregates, the forces responsible for these structures and the interaction mechanisms involved. Viscosity and fluorescence depolarization data have been combined to estimate micelle size and shape in the low viscosity systems.

Experimental Procedure

Materials Used.—**Phenylstearic acid** supplied by a commercial laboratory was molecularly distilled. The acid fraction used had a neutral equivalent of 362.4 (theoretical 360.6) and a refractive index of 1.4912 at 20°. Examination by a urea adduct technique[5] indicated the presence of approximately 0.4% of straight chain impurities in the purified acid. Repeated passes through a molecular still at 120° and a pressure of 4 to 5 μ yielded a large fraction of acid with a refractive index of 1.4910 at 20° which is somewhat higher than the values reported elsewhere.[6,7]

Sodium, lithium, potassium and cesium phenylstearate were prepared by neutralizing the acid in the absence of carbon dioxide. The soaps were then freeze-dried and stored in ampoules as described previously.[4,8]

Magnesium and calcium phenylstearate were prepared by precipitation from alcoholic sodium phenylstearate solutions with solutions of their respective halides (made alkaline to phenolphthalein). The soaps were dissolved, freeze-dried and stored as described previously.[4]

(1) Taken from a thesis submitted by John G. Honig to the Graduate School of Georgetown University in partial fulfillment of the Ph.D. degree.

(2) Presented at the 129th Meeting of the American Chemical Society, Dallas, Texas, April, 1956.

(3) L. S. Arkin and C. R. Singleterry, *J. Colloid Sci.*, **4**, 537 (1949).

(4) J. G. Honig and C. R. Singleterry, THIS JOURNAL, **58**, 201 (1954).

(5) D. Swern, *Ind. Eng. Chem.*, **47**, 216 (1955).

(6) A. J. Stirton, *et al.*, *J. Am. Oil Chemists' Soc.*, **25**, 365 (1948).

(7) B. H. Nicolet and C. M. de Milt, *J. Am. Chem. Soc.*, **49**, 1103 (1927).

(8) C. R. Singleterry and L. A. Weinberger, *ibid.*, **73**, 4574 (1951).

Barium phenylstearate was prepared by allowing $Ba(OH)_2 \cdot 8H_2O$ to react with phenylstearic acid dissolved in a benzene–isopropyl alcohol mixture; the mixture was shaken continuously for four days. The solution was titrated to the phenolphthalein end-point with phenylstearic acid, freeze-dried and stored as the others.

Sodium dinonylnaphthalene sulfonate was part of a stock described in a previous publication.[9]

Methods Used.—The size of small micelles was determined by means of the fluorescence depolarization method[8] using purified Rhodamine B. Absorption measurements required in connection with this method were carried out in an assembled instrument using a Perkin–Elmer monochromator and an Aminco microphotometer. The same glass-stoppered 3-cm. cell was used for both absorption and fluorescence measurements in order to minimize contamination of the solution with atmospheric moisture and carbon dioxide.

Viscosity data used in conjunction with the fluorescence depolarization data were obtained with an Ostwald–Fenske viscometer in a constant temperature bath at 25 ± 0.003°. The three-level capillary viscometer for the study of non-Newtonian solutions in sealed systems[10] was used to study the effect of polar additives on the rheological behavior of different soap solutions as described previously.[4] The average shearing stresses for the three levels varied in the ratio 1:2:4 and were of the order of 4, 8 and 16 dynes/cm.^{2}, respectively.

Densities were measured in a Sprengel–Ostwald pycnometer fitted with ground-glass caps to prevent evaporation. The pycnometers were conditioned in a constant temperature bath at 25 ± 0.003°.

All soap solution manipulations were carried out in a specially constructed box in which a positive pressure of dry helium was maintained and the amount of atmospheric contamination was kept to 3% or below.

The Determination of the Size and Shape of Micelles.—In the absence of information as to the shape of micelles, fluorescence depolarization data furnish information only as to the volume of a sphere hydrodynamically equivalent to the actual particle in solution. Considerably more information is available if the departure of the micellar solutions from the rheological behavior predicted by the Einstein equation is also considered. If a solvated spherical particle is assumed, fluorescence depolarization data will establish the volume of this particle. The degree of solvation can be estimated from the departure of the viscosity behavior from that predicted by the Einstein equation. If an unsolvated ellipsoid of revolution is assumed, its asymmetry can be determined from viscosity data; with the asymmetry known fluorescence depolarization data will furnish the actual volume of this ellipsoid.

Simha[11] has expressed this viscosity deviation for solutions of ellipsoids of rotation as a function of their axial ratio. In this equation

$$\frac{\eta - \eta_0}{\eta_0} = \phi\Lambda(J) \qquad (1)$$

η and η_0 are the viscosities of the solution and the solvent, respectively, ϕ is the volume concentration of the solute, and $\Lambda(J)$ is a function of the axial ratio J. This equation, or a slight modification in which ϕ was expanded to include all the solute species present in the micelle, was used to estimate the particle shape from the measured viscosities of the soap solutions.

The information as to asymmetry was used in conjunction with fluorescence depolarization data for the same solution to arrive at an estimate of the particle size. Perrin's equation[12] describes the ratios of the relaxation times for the rotation about the major axis, ρ_1, or the minor axis, ρ_2, of a rotational ellipsoid and the relaxation time for the rotation of a sphere of equal volume, ρ_0, as a function of the half axes of the ellipsoid. This equation may be restated in terms of the axial ratio, J, of the ellipsoid of revolution as

$$n_1 = \frac{\rho_1}{\rho_0} = \frac{2}{3}\,\frac{J^4 - 1}{(2J^2 - 1)\dfrac{J}{\sqrt{J^2 - 1}}\log\left(J + \sqrt{J^2 - 1}\right) - J^2} \qquad (2)$$

$$n_2 = \frac{\rho_2}{\rho_0} = \frac{4}{3}\,\frac{J^4 - 1}{(J^2 - 2)\dfrac{J}{\sqrt{J^2 - 1}}\log\left(J + \sqrt{J^2 - 1}\right) + J^4}$$

where ($J > 1$ for prolate ellipsoid). The values for n_1 and n_2 were plotted against J. Since J was determined from viscosity data using Simha's equation, n_1 and n_2 could be found either from the graph or calculated using equations 2.

Perrin[8,13] derived an equation for the relationship between the volume and the depolarization of the fluorescence emitted from spherical particles in dilute solution. Weber[14] has expanded this equation for use with non-spherical particles undergoing Brownian movement.

$$\left(\frac{1}{p} \pm \frac{1}{3}\right) = \left(\frac{1}{p_0} \pm \frac{1}{3}\right)\frac{\left(1 + \frac{3}{n_1}\frac{\tau}{\rho_0}\right)\left[1 + \frac{\tau}{\rho_0}\left(\frac{4}{n_2} - \frac{1}{n_1}\right)\right]}{1 + \frac{1}{2}\frac{\tau}{\rho_0}\left(\frac{5}{n_2} + \frac{1}{n_1}\right) - \frac{9}{8}\frac{\tau^2}{\rho_0^2}\left[\frac{\left(\frac{1}{n_1} - \frac{1}{n_2}\right)^2}{1 + \frac{\tau}{\rho_0}\left(\frac{2}{n_1} + \frac{1}{n_2}\right)}\right]} \qquad (3)$$

The polarization, p, of the dye molecules associated with the micelles in solution was determined experimentally. The polarization, p_0, of a completely immobilized dye molecule was estimated from published data[8] and the average excited life, τ, of the dye molecule was estimated from observed fluorescence efficiencies. Substituting the values for n_1 and n_2 in this equation the rotational relaxation time of a sphere of volume V_e equal to that of the ellipsoid was calculated. Since

$$\rho_0 = \frac{3\eta_0 V_e}{RT} \qquad (4)$$

where R is the gas constant and T the absolute temperature, the volume of the ellipsoid with an axial ratio of J could be calculated.

There are several theoretical limitations which must be considered when rheological and fluorescence depolarization data are used to establish the shape and size of particles as small as those considered here from data taken at finite concentrations. Equation 1 was derived by Simha[11] for systems at infinite dilution where no particle-particle interaction occurs. In the present study it was not possible to use solutions more dilute than those reported here because of the uncertainty as to the amount of additive present in the micelles in more dilute solutions. Hence extrapolation to infinite dilution was not considered. Various methods can be used to estimate the error of using the viscosity number[15] at finite concentrations instead of the limiting viscosity number for the determination of particle shape in moderately dilute solutions.[16–18] Huggins[16] proposed the equation

$$\eta = \eta_0(1 + a_1 c + a_2 c^2 + \ldots) \qquad (5)$$

where a_1 is the limiting viscosity number, and a_2 a parameter such that $a_2 = k_1 a_1^2$. If polystyrene solutions in benzene are assumed to be somewhat analogous to micellar phenylstearate solutions and if Streeter and Boyer's value[19] of $k_1 = 0.225$ is used, it is found that for a limiting viscosity number of 4.0, the viscosity number at a volume concentration of 0.02 ml. solute/ml. solution exceeds the limiting value by only 1.8%. Rothman, Simha and Weissberg[20]

(9) S. Kaufman and C. R. Singleterry, *J. Colloid Sci.*, **10**, 139 (1954).

(10) J. G. Honig and C. R. Singleterry, *Anal. Chem.*, **26**, 677 (1954).

(11) R. Simha, THIS JOURNAL, **44**, 25 (1940); *Proc. Intern. Congr. Rheology*, Holland 1948, Part II, **70** (1948).

(12) F. Perrin, *J. Phys. radium*, [VII] **5**, 497 (1934).

(13) F. Perrin, *ibid.*, [VI] **7**, 390 (1926).

(14) G. Weber, *Biochem. J. (London)*, **51**, 145 (1952).

(15) The rheological nomenclature used in this paper is that recommended by the International Union of Chemistry: *J. Polymer Sci.*, **8**, 257 (1952).

(16) M. L. Huggins, *J. Am. Chem. Soc.*, **64**, 2716 (1942).

(17) R. Simha, *J. Research Natl. Bur. Standards*, **42**, 409 (1949).

(18) A. Peterlin, *Proc. Intern. Congr. Rheology*, 2nd Congr., Oxford, 1953, 343 (1954).

(19) D. J. Streeter and R. F. Boyer, *Ind. Eng. Chem.*, **43**, 1790 (1951).

(20) S. Rothman, R. Simha and S. G. Weissberg, *J. Polymer Sci.*, **5**, 141 (1950).

have shown that for very dilute solutions of polystyrene in toluene, Baker's equation holds for n equals 2.9. Assuming the systems studied here to be analogous to the above solutions it was found that the difference between the viscosity number at finite and at infinite dilution is less than 3% if the viscosity ratio of the solution is less than 1.10. The effect of concentration on the viscosity number can also be estimated using Eilers' equation[21] and assuming a voluminosity of 1.5 in this case, the viscosity effect due to concentration is calculated to be about 3% when the concentration is 1% by volume.

In addition to the error due to concentration, the particle–particle interactions will be affected by the maximum extension of the particles, the error increasing with increasing asymmetry of the particles.

The Einstein equation and its variations, as well as the fluorescence depolarization equations, are derived for particles which are relatively large compared to the solvent molecules so that the solvent can be considered a continuous fluid for which the laws of hydrodynamics hold. It has been shown that Perrin's equations for rotational diffusion[12] are not valid when the solvent and the solute molecule are of similar size[22,23]; however, the minimum permissible ratio of solute–solvent particle size is ill-defined. Sadron[24] suggested that the limiting ratio may be about 10. The deviations resulting when the equations are applied to solute particles between five and ten times the linear dimensions of the solvent molecule have not been determined explicitly.

The use of the solvent viscosity in fluorescence depolarization equations is also limited by concentration effects. However, since the rotation of a particle in the solvent should be less affected by the neighboring particles than the translation of the same particles, the concentration effect should be less with fluorescence depolarization measurements than with viscosity measurements.[18]

Experimental Results

The Effect of Polar Additives on the Rheological Behavior of the Soap Solutions.—It is convenient to compare the rheological behavior of the different soaps studied with that of the sodium phenylstearate solutions reported in detail previously.[4,25] Successive additions of water to sodium phenylstearate solution caused the viscosity of the very viscous, slightly non-Newtonian, anhydrous soap solution to fall sharply, pass through a minimum, and to rise again to form a non-Newtonian, highly elastic, viscous system. When 4.5 to 5 s.r.u.[26] of water had been added the soap precipitated. The potassium and cesium soap solutions showed similar but less pronounced patterns of viscosity variation (Fig. 1). The effectiveness of equal amounts of soap in producing both the anhydrous and the elastic structure decreased with increasing alkali cation size (Fig. 2). The soap containing the smallest ion, lithium phenylstearate, was even more effective than sodium in building high viscosity structures. Experiments with more dilute lithium soap solutions indicated that the first water added, instead of causing a viscosity decrease such as was shown by the sodium soap solutions, caused a viscosity increase (Figs. 3a and 3b). Even in the most dilute lithium soap solution (Fig. 3a) the first water addition produced a powerful gelling action resulting in relatively large, transparent gel fragments. Gelling action and rheological inhomogeneity of the solution caused viscosity measurements in region C to be unreliable.

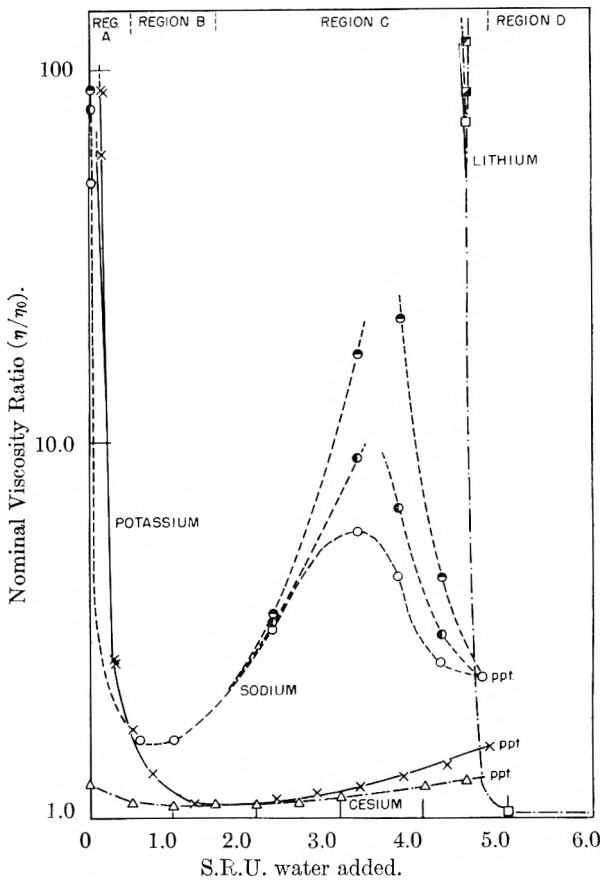

Fig. 1.—The effect of adding water to benzene solutions of the alkali metal phenylstearates: O–◐–●, sodium phenylstearate (c = 0.0158 g./ml.; at high, intermediate and low shearing stress): □–◪–◩, lithium phenylstearate (c = 0.00927 g./ml.; at high, intermediate and low shearing stress); X—XX, potassium phenylstearate (c = 0.0214 g./ml.; at high and intermediate shearing stress); and △–△–△, cesium phenylstearate (c = 0.0265 g./ml.). The nominal viscosity is the viscosity of a Newtonian liquid which has the same flow-time under the same shearing stress as the solution measured.

The prolonged plateau in region C of the most dilute lithium soap solution (Fig. 3a) could result from the competition between the micelles and benzene for the minute amounts of water added, since 1 s.r.u. of water for this solution amounts only to 0.00898 g. water/100 cc. solution while the solubility of water in benzene is 0.045 g. water/100 cc. benzene at 25°.[27] This indicates that sufficient water must be present to nearly saturate the benzene before enough water is incorporated in the micelle to cause this viscosity drop. On the other hand, the initial rise in viscosity resulting from the first addition of water indicates that the lithium

(21) H. Eilers, *Kolloid-Z.*, **96**, 313 (1941).

(22) C. P. Smyth, THIS JOURNAL, **58**, 580 (1954); *J. Am. Chem. Soc.*, **78**, 20 (1956).

(23) R. J. W. Le Fevre and J. Tardif, *Chem. and Ind.*, 1674 (1955).

(24) Ch. Sadron, "Flow Properties of Disperse Systems," J. J. Hermans, ed., Interscience Publishers, Inc., New York, N. Y., 1953, p. 132.

(25) Since that publication the phenylstearic acid used in the preparation of the soaps has been purified further and the effect of atmospheric carbon dioxide on the hydrolysis of the soap has been recognized [H. R. Baker and C. R. Singleterry, *Ind. Eng. Chem.*, **48**, 1190 (1956); R. E. Kagarise, THIS JOURNAL, **59**, 271 (1955)]. Some of the measurements for the sodium soap were therefore repeated with the purified material, using special precautions to exclude carbon dioxide. It was found that the new results followed the same qualitative pattern as the earlier data, although the numerical values were slightly different.

(26) s.r.u. = solute ratio units = moles of solute added per equivalent dissolved soap.

(27) G. G. Joris and H. S. Taylor, *J. Chem. Phys.* **16**, 45 (1948).

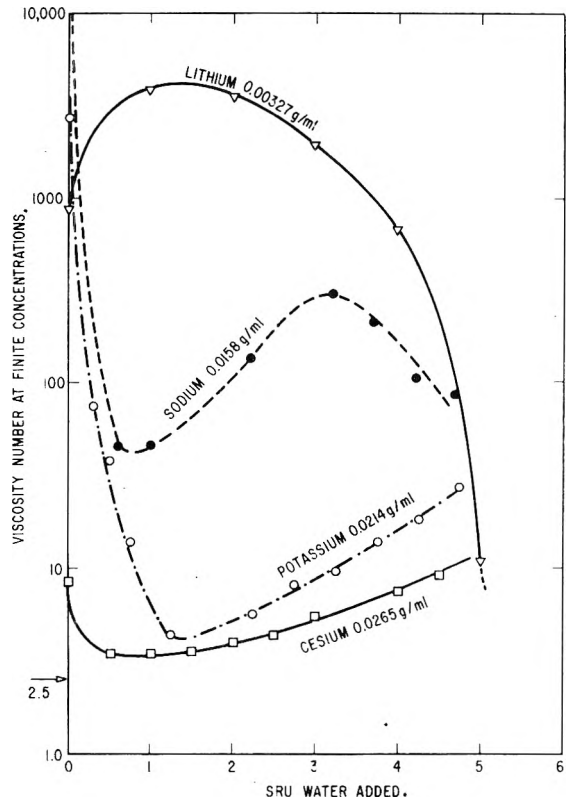

Fig. 2.—The effect of added water on the viscosity of alkali metal phenylstearate solutions at similar shearing stresses.

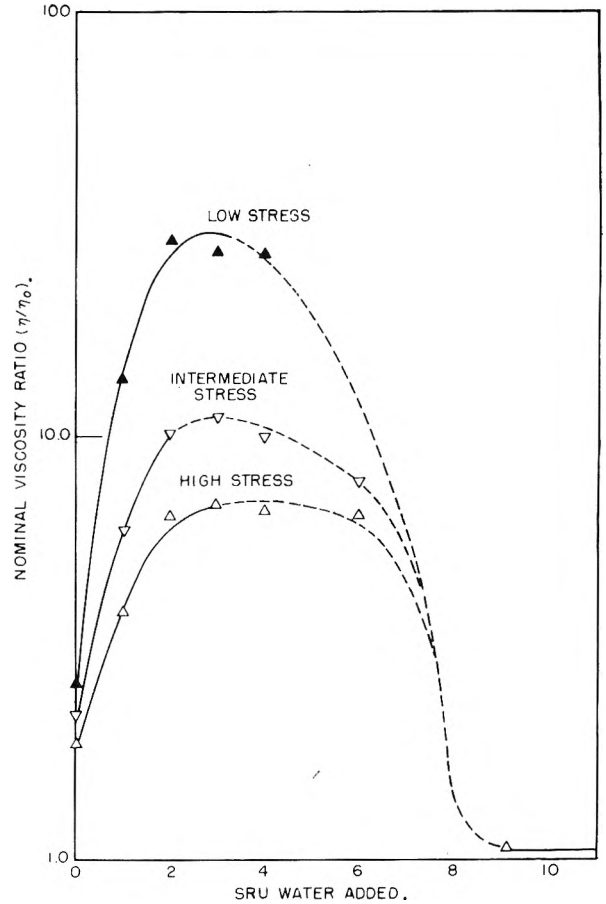

Fig. 3a.—The effect of added water to the most dilute benzene solution of lithium phenylstearate (c = 0.0018 g./ml.) at different shearing stresses.

soap can remove some water from a benzene solution containing only a small fraction of the water necessary for saturation.

The decreased sensitivity of the solutions to secondary aggregation in region C with increased cation diameter led also to lower minimum viscosities of the various soap solutions in region B. From Fig. 1 and Table I it can be seen that the minimum viscosity reached by the solutions of the different soaps varies inversely with the size of the respective cation. Since lithium soap solutions showed no viscosity drop in region B, the viscosity reached by a lithium soap solution in region D is recorded in Table I for comparison.

TABLE I

THE MINIMUM VISCOSITY NUMBERS OF THE ALKALI METAL SOAP SOLUTIONS

	Soap concn. (g./ml. soln. × 100)	Water added (s.r.u.)	$\left(\frac{\eta - \eta_0}{\eta_0 c}\right)$
Lithium phenylstearate	0.964	5.0	4.4
Sodium phenylstearate	1.58	0.6	45
Potassium phenylstearate	1.600	1.4	4.65
Cesium phenylstearate	2.65	1.5	3.5

All alkali soaps, except lithium, precipitated after a total of approximately 4.5 to 5 s.r.u. of water had been added. This precipitation phenomenon was temperature reversible provided only a small excess of water was present in the system. After a total of 4.5 s.r.u. of water had been added to the more concentrated lithium soap solutions the viscosity dropped sharply to a minimum value which was maintained for all further water additions (region D). Even after 16.5 s.r.u. of water had been added the lithium soap system showed no signs of precipitation. The unusual ability of lithium soap to solubilize large amounts of water is being given further study.

Solutions of the alkaline earth soaps exhibited characteristically different behavior on addition of water. Their effectiveness in forming high viscosity anhydrous systems increased with increasing cation size, which is the reverse of the order observed with the alkali soaps. Furthermore, no secondary aggregation phenomena were found with any of the alkaline earth soap systems (Fig. 4). Both the barium soap solution and the calcium soap solution formed high viscosity systems in the absence of water, but none was found with magnesium soap solutions. The high viscosity barium soap solutions were more stable toward small additions of water than the corresponding calcium soap solutions. When 1.6 s.r.u. of water had been added to an anhydrous barium phenylstearate solution the viscosity ratio, η/η_0, of the solution had been reduced only to 3.40 (corresponding to a viscosity number of 152). At this point a small drop of undissolved water with a cloudy surface persisted indefinitely. On cooling the whole liquid turned turbid, a phenomenon which was temperature reversible. The magnesium and calcium soap solutions precipitated

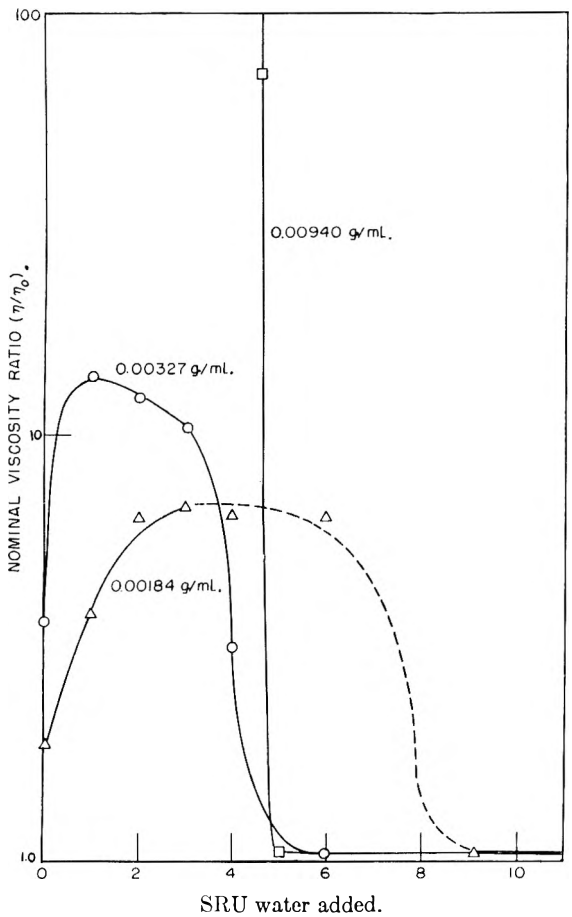

Fig. 3b.—The effect of adding water to lithium phenylstearate solutions of different concentrations at similar shearing stresses.

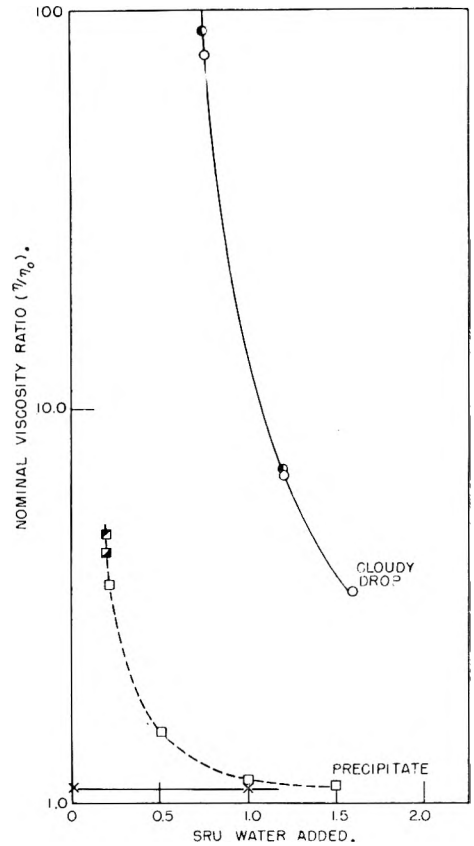

Fig. 4.—The effect of adding water to benzene solutions of alkaline earth metal phenylstearates: □--◪--◩, calcium phenylstearate (c = 0.0174 g./ml.; at high, intermediate and low shearing stress); ○—●, barium phenylstearate (c = 0.0167 g./ml.; at high and intermediate shearing stress; and ×—×, magnesium phenylstearate (c = 0.0218 g./ml.).

after 1.5 to 2.0 s.r.u. of water had been added to the solution.

In view of the similar applications of the carboxylate soaps and the organic sulfonates, measurements were made of the effect of water on a sodium dinonylnaphthalene sulfonate solution (c = 0.02101 g./ml. solution). It was found that the anhydrous solution gave a viscosity number of only 2.5 and that this value did not change upon addition of more water. After approximately 7.4 s.r.u. of water had been added a drop persisted, but no precipitate was formed. This drop disappeared on cooling and reappeared on warming the solution.

The stability of the high viscosity lithium soap structure is further evidenced by the fact that it took slightly more than 1 s.r.u. of phenylstearic acid to produce a low viscosity system in a lithium phenylstearate solution (c = 0.00927 g./ml.), while less than 0.2 s.r.u. of acid reduced a sodium soap solution (c = 0.0159 g./ml.) to a very low viscosity. The reduction in viscosity of the lithium soap solution upon the addition of acid was gradual and very regular (Fig. 5). Even after 2 s.r.u. of acid had been added to the lithium soap solution the viscosity number was still 11.5 compared to a viscosity number of 4.62 for a sodium phenylstearate solution containing 0.2 s.r.u. of acid. The great resistance of the lithium soap solutions to breakdown by acid parallels a similar resistance of the solid films of the same soap to reaction with carbon dioxide as found from infrared spectroscopy studies.[28]

The structure of a high viscosity system of calcium phenylstearate solution (c = 0.0161 g./ml. solution) was broken down very effectively by only 0.05 s.r.u. of phenylstearic acid. Further additions of acid produced a stable, low viscosity system which never precipitated. Acid was less effective in breaking down the high viscosity structure of a barium phenylstearate solution. When 0.25 s.r.u. of phenylstearic acid had been added to a barium phenylstearate solution (c = 0.00611C g./ml. solution) the resulting viscosity number was still 10.1 compared to 5.34 for the calcium soap solution containing only 0.107 s.r.u. of acid.

Fluorescence Depolarization of the Small Micelles.—The method combining the fluorescence depolarization and viscosity data to determine the size and shape of colloidal particles was applied to the small micelles occurring in the regions B and D. This method was not used with the more viscous solutions because particle–particle interactions occurring in such solutions were considered to invalidate the interpretation of such data.

Table II shows the sizes estimated for the small micelles. The nature of the sodium soap was such that the breakdown to the small micelles in region

(28) R. E. Kagarise, THIS JOURNAL, **59**, 271 (1955).

TABLE II

THE SIZE OF THE SMALL MICELLES FROM FLUORESCENCE DEPOLARIZATION AND VISCOSITY DATA

	Concn. (g./ml. soln. × 100)	Water added (s.r.u.)	$\frac{\eta - \eta_0}{\eta_0 c}$	Polarization	V_{sphere} (cc./g.-micelle)	$V_{ellipsoid}$ (cc./g.-micelle)
Lithium	0.9636	5.0	4.4	0.230	10,700	6,700
Sodium	1.5153	0.6	43.4	.457	279,000	99,000
Potassium	1.690	1.4	4.65	.251	17,600	8,400
Cesium	2.211	0.5	3.58	.202	8,500[a]	4,400[a]
Magnesium	1.785	anhydrous	5.10	.261	17,800	9,340
Calcium	0.7580	0.7	4.09	.325	25,400	15,000

[a] Assuming average fluorescence efficiency.

B was not complete before the secondary aggregation to a C-region system commenced.

The lithium soap did not form small micelles in region B but the small micelles of the D-region were investigated. The fluorescence depolarization of lithium soap solutions of various dilutions containing several moles of water per mole of soap indicated that the micelle size was not significantly altered by dilution (Table III). Similar results have been reported for calcium xenylstearate.[29]

TABLE III

THE EFFECT OF CONCENTRATION ON THE SIZE OF SMALL LITHIUM SOAP MICELLES AS ESTIMATED FROM FLUORESCENCE DEPOLARIZATION DATA

Concn. (g./ml. soln.)	Water content (s.r.u.)	Polarization	V_{sphere} (cc./g. micelle)
0.009363	5.0	0.230	10,700
.009189	6.5	.236	11,000
.004482	*ca.* 10	.262	13,300
.00867	>10	.240	11,400[a]

[a] Assuming average fluorescence efficiency.

The micelle size shown in Table II for the cesium soap is provisional only, because the light absorption of the colored form of the dye was too low for reliable efficiency measurements. The size reported was calculated on the assumption of an average value for this efficiency. The barium phenylstearate solution never reached a low viscosity or a small micelle region by water addition. Even 0.25 s.r.u. of acid added to this soap did not produce the small micelles found for the other soaps.

The Region of Precipitation.—When approximately 5 s.r.u. of water had been added to any alkali soap solution (except lithium soap solutions) the system became turbid and an amorphous, flocculent, white precipitate usually separated. However, in the presence of only a small excess of water a soap-rich, strongly birefringent phase, which might be either clear or turbid, was observed.

When 5.2 s.r.u. of water had been added to 44.4 ml. of a carbon dioxide-free sodium soap solution containing 0.7004 g. of soap (c = 0.0158 g./ml. solution) a turbid phase (3.6 ml.) was formed which exhibited pronounced birefringence. The soap concentration in this highly oriented phase was 0.1163 g./ml., or roughly 7.4 times the original soap concentration. Another 0.5 s.r.u. of water was added to the system, which was warmed to about 40° until homogeneous and then cooled to 25°. Over a period of days three distinct layers formed: a clear top layer, which contained only

(29) S. Kaufman and C. R. Singleterry, *J. Colloid Sci.*, **7**, 453 (1952).

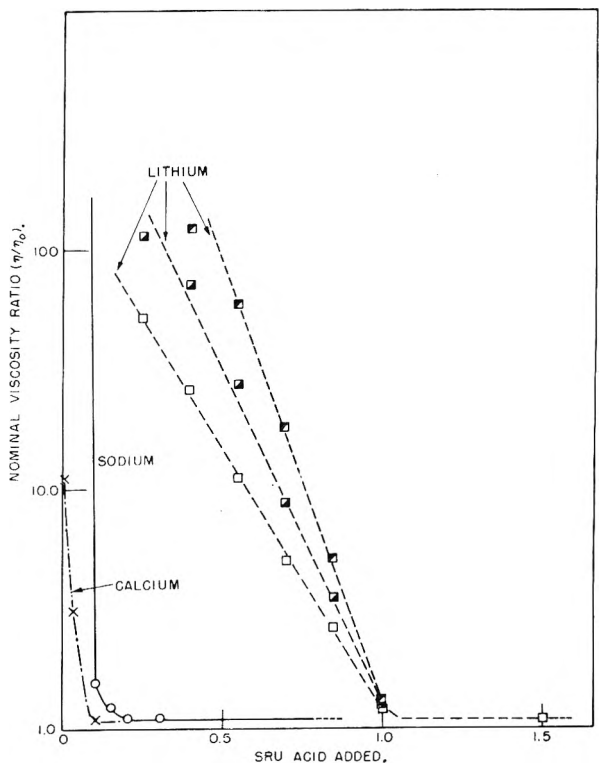

Fig. 5.—The effect of adding phenylstearic acid to phenylstearate solutions in benzene: O—O—O, sodium phenylstearate (c = 0.0159 g./ml.); ×-·-×, calcium phenylstearate (c = 0.0161 g./ml.); and □--◪--◩, lithium phenylstearate (c = 0.00927 g./ml., at high, intermediate and low shearing stress).

1.673×10^{-5} g. soap/ml., a slightly turbid, strongly birefringent, intermediate layer, and an opaque bottom layer. The intermediate layer cleared up over a period of time but retained its birefringence.

Similar effects were observed when 1.5 to 2.0 s.r.u. of water had been added to a magnesium or calcium soap solution. With careful adjustment of temperature most of these precipitation phenomena could be reversed provided the excess of water present was small. Even the barium phenylstearate solution, which did not give a precipitate when saturated with water, exhibited turbidity when cooled below room temperature.

Apparent Molar Volumes.—The apparent molar volumes occupied by the soap molecules in micelles, and by phenylstearic acid molecules in solution as computed from density measurements and formula weights are shown in Table IV.

A direct comparison of the closeness of packing of the molecules in different soap micelles may be

TABLE IV

THE APPARENT MOLAR VOLUMES OF PHENYLSTEARATE SOAPS AND PHENYLSTEARIC ACID IN BENZENE SOLUTION AT 25°

	Apparent density (g./cc.)	Formula wt.	Apparent molar vol. (cc./mole)	Vol. assigned to the metal ion (cc./mole)	Vol. of phenylstearate radical (cc./mole)
Lithium	0.991	366.54	369.9	1.6	368.3
Sodium	1.020	382.6	375.1	4.2	370.9
Potassium	1.054	398.7	378.3	11.5	366.8
Cesium	1.216	492.5	405.0	21.4	383.6
Magnesium	0.985	743.52	754.8	1.7	376.6
Calcium	1.044	759.52	727.2	5.0	361.1
Barium	1.160	856.6	738.4	13.7	362.4
Phenylstearic acid (1.9% soln.)	0.952	360.5	378.7	...	(375.7)
Phenylstearic acid (bulk)	0.9369	360.5	384.9	...	...

approximated by subtracting the volumes associated with each of the metal ions in the crystalline state from the measured volumes of the respective soap molecules. This metal ion volume was estimated by apportioning the volume of a cell unit of the appropriate alkali metal fluoride crystal[30] or of the alkaline earth metal sulfide crystal[30] between the two ions of the cell unit in proportion to the cubes of their respective ionic radii.[31]

The volume of the acid molecules in bulk is larger than the apparent volume occupied by the acid molecules in dilute solution. The estimated apparent volume of the phenylstearate radical in dilute solutions of the alkali metal soaps was significantly larger than that in solutions of alkaline earth metal soaps. The apparent volumes associated with the acid radical in the magnesium and cesium soap solutions were much larger, which suggests a difference in structure in these two cases.

Acknowledgment.—The authors wish to express their appreciation to Mr. Philip D. Faurote and Mr. Charles M. Henderson for molecularly distilling the phenylstearic acid and measuring the refractive index of the fractions.

(30) R. W. G. Wyckoff, "Crystal Structures," Interscience Publishers Inc., New York, N. Y., 1951, Table III, p. 2.

(31) N. V. Sidgwick, "The Chemical Elements and Their Compounds," Oxford University Press, London, 1950, Vol. I, Groups IA and IIA.

THE PHYSICAL-CHEMICAL BEHAVIOR OF OIL-DISPERSIBLE SOAP SOLUTIONS. III. COLLOID STRUCTURE IN DILUTE ARYLSTEARATE–BENZENE SYSTEMS[1,2]

BY JOHN G. HONIG AND C. R. SINGLETERRY

Naval Research Laboratory, Washington 25, D. C.

Received April 9, 1956

A consideration of the viscosity effects of alkali and alkaline earth phenylstearates in dilute benzene solutions indicates that the high viscosities encountered result from the formation of linear soap polymers through coördinate linkages between metal ions and carboxylate oxygen. For the alkaline earth soaps the structure proposed provides also for chelation effects which augment the stability. The viscosity decreases produced by additions of phenylstearic acid, water, ethanol or phenol result from competition between the additive and the carboxylate ion for positions in the coördination sphere of the metal ion. The secondary aggregation of alkali metal soaps produced by water is attributed to hydrogen bonding between micelles by coördinately held water molecules. A combination of viscometric and fluorescence depolarization data indicates that the small micelles formed in the presence of suitable amounts of water are either strongly solvated or distinctly asymmetric in shape. The latter alternative appears more probable, and suggests that these small micelles are ellipsoids having axial ratios of 4 to 1, or less, and containing from twenty to forty phenylstearate radicals. The hydrocarbon sheath of the micelle appears to be more liquid-like than crystalline in structure.

Introduction

Some general aspects of micelle formation in nonaqueous systems have been reviewed elsewhere.[3] Two previous publications of this series[4,5] have dealt with the effect of additions of water, phenylstearic acid, phenol, ethanol and glycol on the rheological behavior and the micellar structure of benzene solutions of sodium phenylstearate, and with the effect of water or acid additions on physical-chemical properties of benzene solutions of the phenylstearates of other alkali and alkaline earth metals. The viscometric behavior of the phenylstearate solutions suggests the appearance of distinctly different structures as the amount of water in the systems is increased. For example, anhydrous dilute sodium phenylstearate solutions are extremely viscous; progressive additions of water cause a rapid decrease in viscosity to a minimum, then a thickening to a viscous, elastic semi-gel, and finally a viscosity decrease and precipitation. For convenience of reference these stages are identified[5] as regions A, B, C and D, respectively. The present communication undertakes to interpret these data in terms of micellar structure.

The Anhydrous Systems.—The phenylstearate soaps differ from the oil-soluble sulfonates[6] in that their dilute anhydrous solutions in benzene are shear-birefringent, highly viscous and slightly non-

(1) Taken from a thesis submitted to the Graduate School of Georgetown University by John G. Honig in partial fulfillment of the requirements for the Ph.D. degree.

(2) Presented at the 129th Meeting of the American Chemical Society, Dallas, Texas, April, 1956.

(3) C. R. Singleterry, *J. Am. Oil Chemists' Soc.*, **32**, 446 (1955).

(4) J. G. Honig and C. R. Singleterry, THIS JOURNAL, **58**, 201 (1954).

(5) J. G. Honig and C. R. Singleterry, *ibid.*, **60**, 1108 (1956).

(6) S. Kaufman and C. R. Singleterry, *J. Colloid Sci.*, **10**, 139 (1955).

Newtonian in flow. For such systems it is postulated that the soap molecules are organized into extensive linear structures. Lawrence[7] has suggested similar polymeric structures for the highly viscous plastic stage in more concentrated soap–oil systems. Since dinonylnaphthalene sulfonates, which do not form highly viscous dilute solutions, are certainly as strongly ionic as the alkali carboxylates, it seems necessary to look beyond a simple dipole interaction between ion pairs for the forces linking the latter into polymer-like chains. The relative tendencies of the various alkali and alkaline earth phenylstearates to form such structures, as reported here, parallels closely the tendencies of the corresponding cations to form stable chelate compounds. This parallelism suggests that coördination phenomena are responsible for chain formation. When such polymeric soap chains do not interact to form either a precipitate or a three-dimensional gel it must be assumed the polar portions of different chains are either chemically saturated or sterically hindered from such interaction by the chain structure.

A structure meeting these requirements has been proposed earlier for sodium phenylstearate.[4] This model, which is shown in Fig. 1, is also consistent with the data obtained for three other alkali soaps, the stability of the polymeric structure found decreasing with increasing atomic diameters.

The basic structure is considered to be the coordinately bonded single chain of alternating cations and anions. Some additional decrease in the free energy of the system can occur if portions of such chains are juxtaposed by coiling or folding, or by parallel alignment as indicated schematically in the figure. This chain structure allows full resonance of the carboxylate group even when the coördination effect leads to something less than full ionic character of the soap. The full equivalence of the two carboxylate oxygens has been deduced from infrared studies.[8] Infrared spectra also show that the strength of the C–O linkage, as revealed by the ω_2 carboxylate ion band in the 1500–1600 cm.$^{-1}$ region, is linearly related to the Pauling electronegativity of the alkali ion present.[9] This points to some specific interaction between the metal and the carboxylate ions, such as might arise if coördination occurred but which would not be expected if the soaps were fully ionic. Other coördination complexes between the alkali metal ions and carbonyl oxygens, phenolic oxygens or water are known in which the metal ion exhibits a coördination number of 4 to 6.[10]

Since the properties of the carboxyl group are constant for the different alkali metal soaps, the strength of the coördination bonds should increase with increasing charge of the metal ion and decrease with increasing size of the metal ion. Assuming the ions to be spherical, Born[11] has shown that the energy of solution (or solvation) of gaseous ions should vary as e^2/r, where e is the ionic charge and r the ionic radius. Since the stability of the complexes is related to the energy involved in coördination, it should also vary as e^2/r. This was actually shown to be the case for a number of chelate complexes.[12] Table I gives the e^2/r values for the metal ions involved. The direct correlation between the e^2/r values and the tendency of the various alkali soaps to form large chain-like micelles is apparent. Lithium phenylstearate in 0.9% concentration forms a solution too viscous for convenient measurement, while the cesium soap, even at 2.65% concentration gives a solution only slightly more viscous than pure benzene.

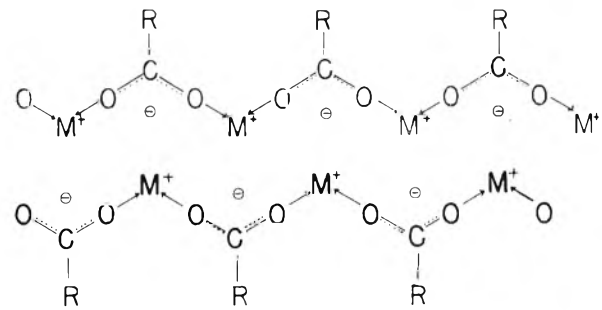

Fig. 1.—Proposed configuration for alkali metal soap micelles.

TABLE I

IONIC RADIUS AND CHARGE^2/RADIUS FOR CATIONS STUDIED

	Ionic radius (Å.)	e^2/r		Ionic radius (Å.)	e^2/r
Lithium	0.78	1.3	Magnesium	0.78	5.13
Sodium	0.98	1.0	Calcium	1.05	3.81
Potassium	1.33	0.75	Barium	1.43	2.80
Cesium	1.65	0.60			

A different, but related, coördinated structure is proposed for the alkaline earth metal soaps in anhydrous solution. Such a structure (Fig. 2) was first suggested by D. C. Smith as an explanation of unpublished infrared spectra of calcium arylstearate soaps prepared at this Laboratory in 1946.[13] This structure assigns a coördination number of 4 to each alkaline earth ion, and makes each a member of two eight-membered rings which might be expected to enhance the stability of the system as chelation would. It has also been suggested that coördinate bonding is responsible for the structure of aluminum soaps in hydrocarbon solvents[14] and that peptizers of zinc soaps act by a coördination mechanism.[15]

It has been proposed[10] that magnesium acetate in aqueous solution forms "autocomplexes," is similar to the structure shown in Fig. 2, in which polymerization occurs by the formation of chains of chelate rings. The fact that the tendencies of the alkaline earth soaps to long chain aggregation do not parallel the tendencies of the corresponding ions to form simple coördinate compounds is sur-

(7) A. S. C. Lawrence, THIS JOURNAL, **52**, 1504 (1948).

(8) C. L. Duval, J. Lecomte and E. Douvillé, *Ann. Phys.*, **17**, 5 (1942).

(9) R. E. Kagarise, THIS JOURNAL, **59**, 271 (1955).

(10) N. V. Sidgwick, "The Chemical Elements and their Compounds," Oxford University Press, London, 1950, Vol. I, Groups IA and IIA.

(11) M. Born, *Z. Physik*, **1**, 45 (1920).

(12) A. E. Martell and M. Calvin, "Chemistry of the Metal Chelate Compounds," Prentice-Hall, Inc., New York, N. Y., 1952, Ch. 5.

(13) D. C. Smith, unpublished data.

(14) W. O. Ludke, S. E. Wiberley, J. Goldenson and W. H. Bauer, THIS JOURNAL, **59**, 222 (1955).

(15) V. D. Tughan and R. C. Pink, *J. Chem. Soc.*, 1804 (1951).

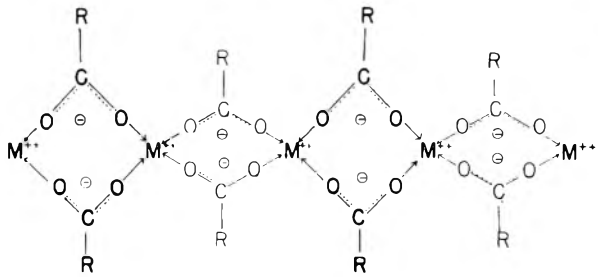

Fig. 2.—Proposed configuration for alkaline earth soap micelles.

prising, but a similar anomaly has been noted in the stability of some of their chelate complexes.[12] This reversal may reflect steric difficulties in adjusting the bulky hydrocarbon tails about a chain whose repeating unit is shortened as the diameter of the ion is decreased. It has been shown that the carboxylates of certain strongly coördinated small ions tend to form compact or closed configurations rather than linear ones. Basic beryllium soaps form such configurations having four beryllium atoms tetrahedrally disposed about a central oxygen; the beryllium ions are linked to each other by chelation with carboxyl groups along the six edges of the tetrahedron. These compounds dissolve in benzene to give solutions of low viscosity.[10] Zinc soaps, which have not been found to form high viscosity systems in dilute solutions, form complexes in the same way as beryllium soaps.

In order to make an estimate of the steric problem involved, a configuration is assumed for the polar links in which the metal ion is surrounded by the four coördinating oxygens in a tetrahedral arrangement. This places the like oxygens farther from each other than they would be in a planar configuration having the same oxygen–metal distance. On this basis, and assuming no specific bond angle for the oxygen–metal interaction, the length of a polar repeating unit can be calculated. This leads to values of 4.7, 5.0 and 5.5 Å. for the fully extended units in magnesium, calcium and barium soaps, respectively.

The diameter of the straight fatty acid chain in condensed films at zero compression as estimated from the area of 20.5 Å.^{2} per molecule is 5.1 Å.[16] It seems reasonable to assume a similar effective diameter of the aliphatic portion of the molecule in the micelle. Two such chains extend out from each repeating unit of the polymer. If the configuration of the tails about the micelle core is such that the neighboring units are not free to overlap, or if their thermal motion creates a two-dimensional pressure in the hydrocarbon sheath, the strain on the linkages forming the chain will increase as the length of the repeating polar unit is decreased. Consequently the magnesium soap would experience the greatest resistance to long chain formation and barium the least. Resistance to overlapping would result if the hydrocarbon portions of the molecules tended to lie as compactly against the core as possible rather than to extend as far as possible into the solvent. By the use of atom models it can be shown that in the former arrangement the hydrocarbon tails will effectively fill the space within 10 Å. of the central core; the latter arrangement provides a 28 Å. maximum extension of these tails but leaves some unoccupied space near the core. The actual configuration probably lies somewhere between these extremes, but the fact that one end of each hydrocarbon residue is firmly attached to the polar core makes it more likely statistically that parts of this residue, rather than solvent molecules, will occupy space near the core.

Assuming that the repeating units in the polar core are fully extended in the axis direction, the minimum possible diameter of an indefinitely long polymer of calcium phenylstearate will lie in the neighborhood of 18 Å. If there is a mixing of solvent molecules and hydrocarbon sheath, the effective hydrodynamic radius will be correspondingly larger.

In the case of the sodium soap the fully extended polymer chain, if calculated as a solid cylinder of unsolvated soap, would have a diameter of only 11 Å.; this appears improbably small and suggests that some folding or coiling of the central core is probable. A straightforward combination of the viscosity and fluorescence depolarization data leads to an estimated diameter of 24 Å. for a sodium phenylstearate micelle which must be assigned a highly elongated shape to account for the properties of the solution. In this case there is only one hydrocarbon chain per repeating unit, so the polymer chain would have to have contracted to less than one-half its maximum extension to give a densely packed structure of the diameter indicated.

The Breakdown and Secondary Aggregation of Soap Structures.—The breakdown of the anhydrous soap structure on addition of polar compounds was previously ascribed primarily to a hydrolytic mechanism.[4] It was shown that acid was several times as effective as water and that excess alkali prevented the breakdown of the sodium phenylstearate structure otherwise resulting from the addition of water. In view of the evidence that water can be bound coördinately to the alkali metal ions in similar complexes,[10] it is probable that water may also participate directly in structure breakdown. The breakdown may be considered to result from competition between the oxygen of the added polar substance and the soap carboxyl oxygens for coördination with the metal ion. Experimentally, acid is most effective in breaking down the chain, water is less effective, and ethanol is least effective; this is the order of the stability for the coördination of the respective oxygens with the metal ion[10]; when water is present in the system in large excess the mass effect on the coördination equilibria may be sufficient to replace appreciable numbers of the metal-to-carboxyl linkages by metal–water coördination, thus reducing the polymer to smaller aggregates. It will be noted that the viscosity of lithium phenylstearate solutions decreased sharply after more than four moles of water per lithium ion had been added; the maximum coördination number of this ion is four.

The fact that the dry lithium soap system increased in viscosity with small additions of water, instead of first decreasing to a minimum value in the B-region as the other alkali soaps did, is a result of

(16) N. K. Adam, "The Physics and Chemistry of Surfaces," Oxford University Press, London, 1941, p. 50.

the unusual resistance of the strongly coördinated lithium carboxylate chain to breakdown by any additive studied. Any slight breaking of the polymer chains that may occur is masked by the powerful interaction between the hydrated chains to form cross-linked, secondary aggregates. The less strongly coördinated sodium phenylstearate structure is more readily broken, and a substantial decrease in viscosity results before secondary reaggregation neutralizes the effect of the primary chain-breaking reaction.

The increase in viscosity in the C-region is attributed to the formation of larger structural units by the secondary aggregation of small micelles in the presence of bifunctional hydrogen bonding compounds, such as water or glycol. The micelle interaction is conceived as occurring by bridging between the polar cores through hydrogen bonding by one or more water or glycol molecules to form a cross-linked, or three-dimensional, elastic, but shear-sensitive, structure. The close parallel between reaggregation phenomena in region C and the tendency of the respective metal ions to form coördination complexes suggests that coördination of water or glycol with the metal ions is the factor controlling the stability of such secondary aggregates. Doscher and Vold[17] have found similar inflection points in curves relating the water content and stability of sodium stearate–cetane–water systems.

The failure of the alkaline earth soaps to exhibit the secondary aggregation (C-region) phenomena shown by the alkali soaps may be explained on the basis of the structures shown in Figs. 1 and 2. The alkaline earth soaps carry two acid residues per repeating unit, instead of one as in the alkali soaps; hence for the former the polar core of the polymer chain in its maximum extension will be more effectively shielded from interaction with the polar portion of other chains.

In addition the models suggested provide a fourfold coördination of the alkaline earth ions as against twofold coördination of the alkali ions. Since coördination numbers of four (or more) are characteristic of all of these ions, the alkali soaps should coördinate the water involved in the secondary aggregation process more readily than alkaline earth soaps do.

The Nature of the Small Micelles.—The effect of carboxylic acids and water in breaking down the soap structure initially present in anhydrous systems is attributed to chain breaking resulting from the competition of these additives with the soap carboxylate ions for coördination sites on the metal ions. It should then follow that the small micelles first appearing in the B-region are essentially fragments of the original polymer. They should have a similar linear core structure, but experience slightly less lateral crowding of the hydrocarbon residues on the exterior. With cesium phenylstearate, which shows little evidence of linear polymer formation even in the anhydrous state, and with the lithium soap containing five or more moles of water per mole of soap, the assumption of a linear structure is on uncertain ground. Here the forces holding the core together may be dipole interactions or H-bonding between hydrated ion pairs.

The combination of viscosity and fluorescence depolarization data offers an attractive approach to the problem of the shape of such small micelles provided the inherent limitations of the method are kept in mind. In addition to the question of the validity of the Einstein–Simha and Perrin equations for very small micelles,[5] two special limitations call for comment.

(1) There is an ambiguity as to whether enhanced viscosity effects are a result of solvation or of non-spherical shapes. In these hydrocarbon solutions the energy decrease available by solvation of the hydrocarbon portion exposed in an inverted micelle is negligible, so that the only solvation to be anticipated would be the entanglement of benzene molecules among randomly disposed hydrocarbon tails of the micelle. As has been pointed out, such entanglement is less likely than might at first appear, because of the anchorage of all the tails to a compact polar core.

(2) A second possible uncertainty in the combination of viscosity and fluorescence data to estimate micelle shapes arises if the soap micelles in a given equilibrated soap solution are not essentially monodisperse. If a wide range of micelle sizes or shapes coexist at equilibrium one may question whether the results of viscosity and fluorescence depolarization measurements are equally sensitive to each micelle size present The concordance found between osmotic pressure and fluorescence depolarization estimates of the micelle size of calcium xenylstearate[18] as well as the essentially constant micelle size found for the same soap over a thousandfold range in concentration[19] argue strongly for an approximately uniform size in systems containing small micelles at equilibrium. It must be borne in mind, however, that the approach to equilibrium is extraordinarily slow in some of these systems at 25°.

In recognition of the possibility of either solvation or asymmetry of the small soap micelles, calculations were made (Table II) on the separate assumptions (a) that these micelles are solvated spheres, or (b) that they are unsolvated ellipsoids conforming to the Simha equation. Data are not available for the barium phenylstearate solutions because the soap was precipitated by water before the structure had broken down to small micelles. The results for the cesium soap, because of the absence of information as to the fluorescence efficiency, cannot be given equal weight with the remaining values.

The data for all the "small" micelles, except those of sodium phenylstearate, are formally compatible with the assumption of either asymmetry or solvation. Those for the sodium soap give an unreasonable diameter of 90 Å. (approximately four times the length of the stearic acid chain), for a solvated, spherical model, but acceptable dimensions for an unsolvated ellipsoidal particle. When unsolvated asymmetric micelles are assumed the minor axes found for micelles of all the soaps in

(17) T. M. Doscher and R. D. Vold, *J. Am. Oil Chemists' Soc.*, **26**, 515 (1949).

(18) C. R. Singleterry and L. A. Weinberger, *J. Am. Chem. Soc.*, **73**, 4574 (1951).

(19) S. Kaufman and C. R. Singleterry, *J. Colloid Sci.*, **7**, 453 (1952).

TABLE II

THE SIZE AND SHAPE OF SOME SMALL MICELLES FROM FLUORESCENCE DEPOLARIZATION AND VISCOSITY DATA

	Hydrodynamically equiv. sphere		Solvation assumed		Asymmetry assumed			
	Vol. (cc. per g.-micelle)	Dia. (Å.)	Micellar vol. occupied by benzene (%)	Phenylstearate radicals in micelle	Vol. (cc. per g.-micelle)	Minor axis (Å.)	Major axis (Å.)	Phenylstearate radicals in micelle
Lithium	10,700	32.4	26	22	6,690	19.6	55.0	18
Sodium	279,000	96.0	92.1	58	98,700	24.0	542	260
Potassium	17,600	38.2	45.9	24	8,400	18.5	78.0	21
Cesium	8,500[a]	30[a]	38.6[a]	11[a]	4,400[a]	15.6[a]	57.8[a]	9[a]
Magnesium	17,800	38.4	47.2	23	8,340	18.3	79.4	22
Calcium	25,400	43.2	36.3	43	15,000	23.8	83.3	39

[a] Fluorescence efficiency not measured; average fluorescence efficiency assumed.

Table II agree reasonably and their average value corresponds roughly with the minimum diameter calculated for infinitely long and fully extended polymer chains of the alkaline earth soaps. It is therefore suggested that these small micelles are unsolvated, or only slightly solvated, ellipsoids having an approximately linear configuration of the polar units in the core and a compact folding of the hydrocarbon portion to occupy the space near this core.

If a few benzene molecules are actually caught in the micelle structure, their presence would modify the interpretation in a way to lead to a thicker and somewhat shorter model of the micelle, but the number of soap molecules implied per micelle would not be significantly changed. The result would be similar if the hydrocarbon tails of the molecules comprising the micelles were extended more or less radially to form a rough or spiculate surface with a higher frictional constant than that of a smooth spheroid containing an equal number of molecules.

A review of the possible errors affecting the viscosity measurements reveals a preponderance of sources which might lead to high viscosity numbers. Such errors, if present, would lead to excessive estimates of the degree of asymmetry or solvation, and give too small an aggregation number for the soap. The theoretical and experimental uncertainties associated with the fluorescence depolarization method are largely such as to produce too small an estimate of the micellar volume. The preceding discussion may therefore be considered to set an upper limit for the asymmetry and a lower limit for the volumes of these small carboxylate micelles.

It has been suggested elsewhere[3] that the size-limiting factor for small micelles in soap hydrocarbon systems is the balance between the cohesive forces in the polar core and the lateral expansion pressure of the thermally agitated tails in the hydrocarbon sheath. It was pointed out that when the number or mode of interaction of the units in the polar core led to a departure from spherical symmetry, the prolate spheroid was more probable because it allowed a looser arrangement of the hydrocarbon tails for a given micelle size than did the oblate spheroid. The present data support this generalization. The attempt to apply the data found to an oblate micelle leads to an improbably small value for the minor axes, or thickness.

Nature of the Phase Precipitated by Water.—With the exception of lithium phenylstearate, all of the soaps studied separated from solution when sufficient water had been added. The precipitate was usually an amorphous flock, but the viscous, birefringent, liquid-crystalline phases which were obtained under special conditions throw an interesting light on the composition of the soap-rich phase and the probable reasons for separation. They are especially interesting since they are the most extensively ordered systems so far observed for these soaps. (The phenylstearic acid used as a starting material is a mixture of position isomers and crystallizes only rarely and very slowly at subzero temperatures. The solid soaps are amorphous, horny materials; their anhydrous benzene solutions are birefringent only under shear.) The composition of the liquid crystal phase is not constant; a typical system for sodium phenylstearate was found to contain 5 moles of water and 32 moles of benzene per mole of soap. It appears that at this approximate composition the cross-section of the hydrated ionic head becomes comparable with the maximum cross-sectional requirement of the phenyl-substituted tail, so that, given sufficient solvent to fill in between the straight chain portions of the phenylstearate radical, it is possible for the soap molecules to order themselves in linear or planar configurations of macrodimensions. The varied location of the phenyl substituent on the aliphatic chain is then no deterrent to orderly arrangement. Stated another way, the presence of this much water cancels the geometrical restraints which led to micelles as the arrangement of lowest free energy; the micelles open out and coalesce into a new phase in which benzene has a limited solubility dictated by the organization of the system. Winsor[20] has suggested a transition from micellar to extended lamellar structure as one characteristic stage in his general theory of structure in colloidal soap systems. The structure suggested is analogous to the repeating lamellar structure discussed by Hess,[21] Harkins,[22] McBain[23,24] and others[25] to explain X-ray scattering by concentrated aqueous soap solutions. If the optimum proportion of water is exceeded, or if the precipitated

(20) P. A. Winsor, *Trans. Faraday Soc.*, **44**, 376 (1948).

(21) K. Hess, *Fette und Seifen*, **46**, 572 (1939).

(22) W. D. Harkins, R. W. Mattoon and M. L. Corrin, *J. Colloid Sci.*, **1**, 105 (1946).

(23) J. W. McBain, "Advances in Colloid Science," Vol. I, ed. by E. O. Kraemer, Interscience Publishers, Inc., New York, N. Y., 1942, p. 124.

(24) J. W. McBain, *Nature*, **145**, 702 (1940).

(25) H. Kiessig and W. Philippoff, *Naturwissenschaften*, **27**, 593 (1939).

phase is too viscous to allow reorganization of the coagulum into large, ordered domains, the precipitate remains amorphous. Its composition, however, must still be rather close to that of the mesomorphic phase occasionally isolated. The ability of the lithium phenylstearate to take up, without precipitation, several times as many water molecules per mole of soap as any of the other soaps examined is difficult to explain. This, as well as the observation that a solution of sodium dinonylnaphthalene sulfonate formed no precipitate even after it had taken up 7 moles of water per mole of soap, and was in contact with excess bulk water, indicates that the phenomena of precipitation are more specific than the generalized discussion just given would imply. The re-dissolving of these precipitates at higher temperatures reflects both the decreased stability of the hydrogen bonds holding the water and carboxylate groups together, and the increased solubility of water in the hydrocarbon phase at elevated temperatures.

Density of Packing in Micelles.—Although the apparent densities of the soaps were determined primarily for use in computing micellar weights from micellar volumes, the molar volumes computed from them throw further light on the organization of the micelle. The apparent molar volume of phenylstearic acid in dilute benzene solution provides a reference datum for the phenylstearate molecule in a fully liquid environment. If 3 cc. is subtracted from this as the probable contribution of the hydrogen atom, the liquid volume assignable to the phenylstearate radical is 376 cc. Comparison of this value with those estimated for the phenylstearate radical in the soaps[5] shows that the constraints on movement imposed by the micelle structure have reduced the space from which each molecule excludes solvent or other molecules. The reduction is greater for the alkaline earth than for the alkali soaps, as would be expected with the multiple linked core structure suggested for the former. However, the reduction of 2.0% for most of the alkali soaps and 3.7% for the calcium and barium soaps is much less than the decrease of approximately 10% noted when long chain fatty acids, such as lauric, stearic or oleic acid, pass from the liquid to the crystalline state. This suggests that the degree of ordering in the micelle is closer to that of the liquid state than to that of a crystalline solid. Small decreases in density upon micelle formation have been found elsewhere.[26] The higher apparent volumes found for the magnesium and cesium soaps may be a result of the same peculiar properties which prevent their forming extensive polymer structures.

(26) M. E. L. McBain and E. Hutchinson, "Solubilization and Related Phenomena," Academic Press, Inc., New York, N. Y., 1955.

THE SOLID SOLUTION KRYPTON–XENON FROM 90 TO 120°K., THE VAPOR PRESSURES OF ARGON, KRYPTON AND XENON[1]

BY MARK P. FREEMAN[2] AND G. D. HALSEY, JR.

Department of Chemistry, University of Washington, Seattle 5, Wash.

Received April 16, 1956

The solid solutions of krypton and xenon have been studied by means of vapor pressure measurements over the temperature range 90 to 120°K. The data have been analyzed in terms of the strictly regular solution theory of Fowler and Guggenheim. The "heat of solution parameter" has been shown to be a function of temperature with values fitted to the form $w_{AB} = 680 - 3.4T$ in calories per mole. The critical solution temperature for phase separation has been estimated to be 91°K. The vapor pressures, triple points and boiling points for argon, krypton and xenon are reported.

Introduction

The rare gases argon and krypton form a solid solution at 77°K. that shows a positive deviation from Raoult's law.[3] It seemed desirable to make a more thorough study of this system over a range of temperature, but the desired low temperatures in the anticipated range of phase separation were not readily available to us. We turned therefore to the next heavier pair of rare gases, krypton and xenon. Similar solutions were encountered.

Theoretical.—The analysis reported here was largely carried out by means of the theory of strictly regular solutions discussed by Fowler and Guggenheim.[4,5] We shall use their notation, and discuss only deviations from their presentation. The restriction that the energy of mixing parameter, w_{AB}, is temperature independent, used in Fowler and Guggenheim's section 817, can be removed by carrying out the differentiation that leads to 817.10 with respect to w_{AB}/kT instead of $1/T$. The modified result is

$$\bar{X} = \partial(F'/kT)/\partial(w_{AB}/kT) \qquad (1)$$

Their quasi-chemical expression for $\bar{X}$ (eq. 819.1) is derived isothermally and so is correct as it stands; eq. 1 can be integrated directly to give 819.5. Now the argument for the boundary condition is that when w_{AB}/kT is zero, the excess free energy of mixing F' is also zero (ideal solution). Then Fowler and Guggenheim proceed to derive their eq. 819.12 for the excess partial potential

$$\mu_A'/kT = (z/2) \log \frac{(\beta - 1 + 2x)}{x(\beta + 1)} \qquad (2)$$

where

$$\beta = \{1 + 4x(1 - x)[\exp\{2w_{AB}/zkT\} - 1]\}^{1/2} \qquad (3)$$

(1) Presented in partial fulfillment of the requirements for the degree of Doctor of Philosophy by M. P. Freeman.

(2) National Science Foundation Pre-doctoral Fellow 1954–1956.

(3) J. H. Singleton and G. D. Halsey, THIS JOURNAL, **58**, 1011 (1954).

(4) R. H. Fowler and E. A. Guggenheim, "Statistical Thermodynamics," Cambridge University Press, Cambridge, 1939, Chapt. 8.

(5) E. A. Guggenheim, "Mixtures," Oxford University Press, Amen House, London E.C.4, 1952, Chapt. 4.

and x is the mole fraction of A and z is the coordination number. If the gas phase behaves ideally, the relationship

$$\mu_A'/kT = \log (P_A/xP_A^\circ) \quad (4)$$

holds, and thus w_{AB} can be expressed directly in terms of gas pressure and mole fraction of A in the solid.

$$w_{AB} = kT' \log \left\{ 1 - \frac{1 - (P_A/xP_A^\circ)^{2/z}}{[1 - x(P_A/xP_A^\circ)^{2/z}]^2} \right\}^{z/2} \quad (5)$$

To study the temperature dependence of w_{AB} it is convenient to consider eq. 2 at the equimolar concentration $x = 1/2$. There

$$\mu_A'/kT = (1/4)(w_{AB}/kT') - (z/2)\log\cosh(w_{AB}/2zkT') \quad (6)$$

We then define two functions

$$h = \partial(w_{AB}/kT)/\partial(1/kT') \quad (7)$$

and

$$s = -\partial w_{AB}/\partial T'$$

so that

$$w_{AB} = h - Ts \quad (8)$$

Then, at $x = 1/2$, the partial molar energy becomes

$$\bar{E}_A' = \bar{H}_A' = \partial(\mu_A'/kT')/\partial(1/kT') = (h/4) \times (1 - \tanh(w_{AB}/2zkT')) \quad (9)$$

which serves to determine h, and (with eq. 8) s, in terms of the experimental values of excess partial potential μ_A', and its temperature variation.

If eq. 2 is expanded in (w_{AB}/zkT') and all but the first-order term discarded, the simple random-mixing formulas emerge. They are

$$\mu_A'/kT' = (1 - x)^2 (w_{AB}/kT') \quad (10)$$

$$\bar{E}_A' = \bar{H}_A' = (1 - x)^2 h \quad (11)$$

$$\bar{S}_A' = -\partial\mu_A'/\partial T = (1 - x)^2 s \quad (12)$$

The error introduced by the use of these simple formulas is not large. For example, if $z = 12$ and $w_{AB}/kT = 2$, eq. 9 and 11 differ by 8%. The random-mixing expressions for the integral excess quantities are also simple

$$F' = G' = x(1 - x)w_{AB} \quad (13)$$

$$E' = H' = x(1 - x)h$$

and

$$S' = x(1 - x)s$$

Experimental

The reagent gases used were obtained from the Air Reduction Sales Co., Jersey City, N.J. The argon was reported by them as mass spectrometrically pure. The krypton had 0.04% A as a maximum impurity while the xenon was reported to have 0.18% Kr. After repeated expansions into and recondensations out of a large volume, the vapor pressures of Xe and Kr were observed to be independent of the quantity of the gas employed and so they may be considered pure.

The oxygen and carbon dioxide were generated in apparatus identical to that of Loomis and Walters[6] using reagent grade potassium permanganate and sodium bicarbonate, respectively. The only purity checks made on these gases were to measure the vapor pressure for widely different quantities of gas. The reproducibility was well within the precision of the manometers.

(6) A. G. Loomis and J. E. Walters, *J. Am. Chem. Soc.*, **48**, 3101 (1926).

The apparatus consisted of a conventional gas transfer apparatus, using a gas buret and free leg manometer to measure quantities of gas, connected to a constant volume system consisting of a cryostat and a constant volume manometer. This constant volume manometer was used for determining the total equilibrium vapor pressure over the solutions and so had a valve in the mercury line to prevent the meniscus from moving while equilibrium was being attained.

The cryostat is schematically shown in Fig. 1. It consisted of a massive copper block (about 2 kg.), A, whose temperature was measured by a capsule-type platinum resistance thermometer, B. The copper probe, C, passing through a stainless steel thimble and finally anchoring in the pool of grease, K, served a twofold purpose. First, it permitted the introduction of xenon into the block without endangering the stem, G, (which may burst if xenon is sublimed into it) and second, by inverting the order of deposition of the solids on the walls of the cryostat it permitted equilibrium pressure to be approached from either side. The temperature differential between the probe and block was indicated by the copper–constantan thermocouple, D. As it did not really register the temperature of the probe it had to be calibrated for a "neutral reading" at every temperature investigated. When the vapor pressures of the pure gases were being run, this probe was merely left substantially warm, but for solutions it had to be nearly neutral or it disturbed solution equilibrium. The neutral e.m.f. of this thermocouple was taken to be that below which it had an effect on the vapor pressure of either krypton or xenon (depending on the temperature). A thermal leak, J, as well as the probe, block and stem each had its separately-controlled bifilar-wound constantan heater, E. The stem block differential temperature was measured by the copper–constantan couple, F, which had a double cold junction in a hole in the block not shown in the diagram. This differential temperature had to be carefully regulated throughout a run to make reproducible the "apparent volume" described below. The thermocouple junction on the stainless steel stem which runs into the block through a stainless steel bushing was kept from 20 to 80 degrees hotter than the block to minimize the danger of subliming xenon into the stem. The block was surrounded by a 10^{-3} mm. vacuum which was contained in a 4 in., Pyrex pipe with a test-tube end. The whole assembly was immersed in liquid nitrogen to roughly the indicated level which was automatically maintained by a storage Dewar flask and a Kr vapor pressure thermometer which actuated an automatic filler.

The manometers were of 17 mm. Pyrex tubing selected for straightness and clarity of glass. All legs were back lighted with horizontally focused and polarized light. The index for the constant volume leg was a fine glass point which was observed with a short range telescope while fine adjustments were made to the mercury level. Fine adjustments to the mercury level were made by closing off the line to the reservoir and altering the mercury level through pinching a rubber hose. The zero of the manometer was easily reproduced to ±0.01 mm. The vacuum leg of this manometer and both legs of the free leg manometer were compared with a Gaertner meter bar type M-1010, which had been compared to a calibrated standard meter and found not to differ significantly from a meter in length in the range of room temperatures encountered. These elements were mounted on the circle of focus of an especially designed Gaertner cathetometer which was used for interpolation between millimeter marks on the bar and could be read to 0.001 mm. The absolute accuracy of either manometer is better than ±0.05 mm. Pressure changes of as little as 0.01 mm. could be detected with facility which helped to determine when equilibrium was reached. The manometer readings were corrected to the density of mercury at 0° and to standard gravity.[7] The temperature of the mercury column was taken to be that of a mercury-in-glass thermometer located close to the middle of the manometers and read to 0.1°.

Using the nomograph of V. Goler[8] it was determined that satisfactory composition equilibrium of the gases in the line connecting the cryostat and manometer should be ob-

(7) J. A. Beattie, *et al.*, *Proc. Amer. Acad. Arts Sci.*, **74**, 327 (1941).

(8) W. Jost, "Diffusion in Solids, Liquids, Gases," Academic Press Inc., New York, N. Y., p. 21.

tained in less than 10 hours. Most solid solution equilibrium times encountered were of the order of 24 hours although equilibrium was obtained faster at the lower temperatures.

Temperature was measured with a platinum resistance thermometer constructed in this Laboratory and calibrated in a carefully constructed comparator with a Leeds and Northrup bayonet platinum resistance thermometer calibrated at the National Bureau of Standards for the international Celsius temperature scale. The triple point of water was determined for both thermometers locally and the nominal temperatures for comparison were −45, −78 and −183°. The measured resistances for these four points were used to determine the constants for the modified Callendar equation which was then used as the interpolation formula. The local and calibrated thermometers were both of the potential lead type and their resistances were measured on a Leeds and Northrup Mueller bridge, type 8067, which was checked and found self consistent to within ±0.0002 ohm.

During the measurement of the vapor pressures of the pure gases, the temperature was held constant for from 5 to 15 minutes by carefully balancing the heat input against loss. This was not difficult because of the large mass of the block. For the pure gases, the vapor pressures were measured at temperatures held to ±0.001°.

When holding the temperature for the week or so needed for an isotherm other methods were employed. The block was automatically heated and cooled past a central value of the N leg resistance reading. The average cycle took about 1 minute and the variation in the resistance of this leg corresponded to a temperature change of ±0.01°. As the N-R difference was free to drift, no better than ±0.03° can be claimed for the temperature stability in the course of a week's run. The control was accomplished by putting a properly biased photocell in the grid circuit of a sensitive relay cascade manufactured by the Metal Marine Pilot of Tacoma, Washington. The photocell was activated by the galvanometer lamp of the Mueller bridge and the relay switched the block heater on and off.

Using the method of gas analysis described below, it was found necessary to determine a quantity δ such that when multiplied by the pressure of krypton it would give a measure of the amount of krypton in the gas phase. Before solution at a given temperature was investigated, pure krypton was introduced into the system at less than condensation pressure for that temperature in measured amounts. The quantity δ was then determined as a function of pressure. With caution, this quantity could be reproduced in the fourth significant figure.

The data were taken with a combination of isosteres and isotherms. When gas is added to a solution, the equilibrium is approached from above, but when an isostere is taken to a higher temperature, the equilibrium pressure is approached from below. In addition, proper use of the probe can also cause an equilibrium to be approached from below. From $1/3$ to $1/2$ of all points at any temperature were approached from below and the remainder from above.

The quantity of xenon introduced was varied between runs at the same temperature and in general less was used at the lower temperatures. The amounts varied from 10^{-5} to 10^{-4} mole. Unless quantities somewhat smaller than this were employed, the results were found to be independent of quantity.

Although the total pressure over the solutions as well as the vapor pressure of xenon was determined with the constant volume manometer, the vapor pressure of krypton and argon were determined on the free leg manometer as the precision of this manometer was slightly better. The much larger volume of the free leg manometer made it inconvenient for xenon which comes in 100-ml. packages.

Vapor Pressure of Pure Gases.—In Table I may be found tabulated points of interest for the gases studied in this work. Oxygen and carbon dioxide were investigated as a check on the absolute accuracy of the apparatus. Included in the table are results obtained by other investigators for these gases. No reliable modern results could be found for either the solid or liquid phases of xenon, but certainly argon and to a somewhat lesser extent krypton seem to have become quite reproducible.

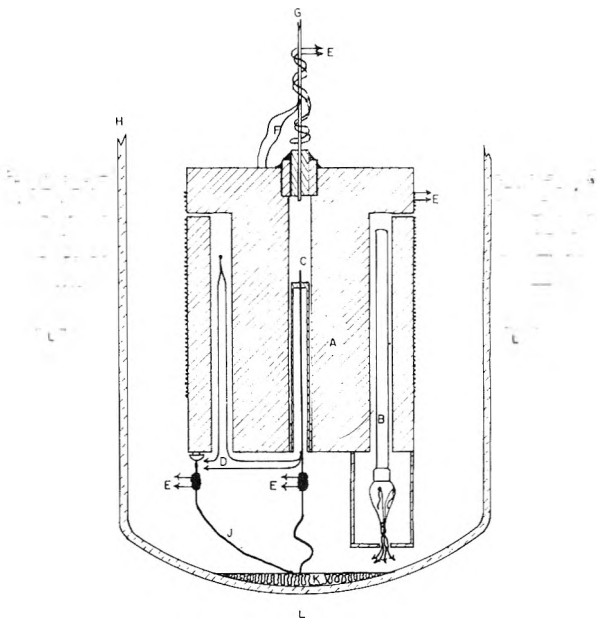

Fig. 1.—Schematic diagram of the cryostat assembly.

TABLE I

Gas	Triple pt. T (°K.)	P (mm.)	B.p. T (°K.)
Argon	83.77 (83.78)[a]	514.1 (515.7)[a]	87.29 (87.29)[a]
	(83.78)[b]	(516.8)[b]	(87.29)[b]
			(87.25)[c]
Krypton	115.6 (115.94)[d]	538.1 (549)[d]	119.82 (120.9)[e]
	(116.1)[e]	(522.2)[e]	(120.3)[f]
	(116.6)[f]	(557)[f]	(122.2)[g]
	(116.2)[g]	(522.2)[g]	
Xenon	160.56 (16_1.)[f]	575.6(6_{00})[f]	165.00 (166.1)[f]
	(161.2)[g]	(615.5)[g]	(164.6)[g]
Oxygen			90.18 (90.18)[h]
Carbon dioxide			194.60 (194.65)[h]

[a] A. M. Clark, F. Din and J. Robb, *Physica*, 17, 876 (1951), London. [b] K. Clusius and A. Frank, *Z. Elektrochem.*, 49, 308 (1943). [c] Clark, Din and Robb, 1951, Amsterdam. [d] W. H. Keesom, J. Mazur and J. J. Meihuizen, *Physica*, 2, 669 (1935). [e] Eduard Justi, *Physik. Z.*, 36, 571 (1935). [f] F. J. Allen and R. B. Moore, *J. Am. Chem. Soc.*, 53, 2522 (1931). [g] K. Peters and K. Weil, *Z. physik. Chem.*, A148, 27 (1930). [h] International Kelvin temperature scale of 1948.

A Clapeyron plot was made of the vapor pressure data and the best straight lines drawn through each phase by the method of least squares. Only in the case of solid xenon was there detected any deviation from these straight lines and this was a small deviation encountered at vapor pressures less than 1 mm. These data were omitted in determining the best straight line. To a high degree of accuracy, then, say ±0.02%, the vapor pressures of the six helium group phases studied are given by

$$\log_{10} P_{(\mathrm{mm.})} = A - B/T \qquad (14)$$

where the constants A and B are given for each phase in the appropriate temperature range in Table II.

It should be noted that the International temperature scale is properly measured by our thermometer only above 90.18°K. (int. 1948). All temperatures quoted here below this point simply use the extrapolation of the modified Callendar

TABLE II

Phase	A	B	From °K.	To °K.
Liquid argon	6.9224	352.8	83.77	88.2
Solid argon	7.7353	420.9	82.0	83.77
Liquid krypton	6.9861	491.9	115.6	121.0
Solid krypton	7.7447	579.6	87.2	115.6
Liquid xenon	7.2488	720.7	160.56	166.2
Solid xenon	7.7371	799.1	110.00	160.56

equation valid from 0.00 to −182.97° (int. 1948).

Method of Gas Analysis.—The composition of the gas and solid are determined mathematically. This procedure may be readily justified.

As the krypton has about 100 times the vapor pressure of xenon in the range studied, it would have been justifiable in many cases to attribute the entire equilibrium pressure over the solution to krypton. Knowing the total amount of each gas introduced into the constant volume cryostat system and having measured the "apparent volume" of the system as described above, it would then be simple to calculate the relative amounts and hence the mole fraction of the two constituents in solution. P_{Kr}/P°_{Kr} then follows directly and from the well known symmetry of the regular solution problem, P_{Xe}/P°_{Xe} also follows. To this approximation the solution would be completely analyzed.

A refinement on this approximation would be to assume that the vapor pressure of xenon is either constant at the pressure of pure xenon at that temperature, or equally good, that the xenon pressure obeys Raoult's law for ideal solutions. If the second alternative is chosen, successive approximations may be used to determine the composition of gas and solid. In either case it should be considered that the xenon might not have the same "apparent volume" as the krypton, but due to the low pressure of the xenon, the error in the amount of xenon calculated to be in solution would be small.

The analysis may be refined still further by assuming the random mixing or so-called zeroth approximation to the quasi-chemical solution theory.[9] If the parameter w_{AB}/kT is left adjustable, the resulting isotherm equation is found to fit the data well and hence should represent a good approach to gas analysis. The constancy of this parameter as a function of mole fraction at any given temperature should be a measure of the validity of the method. This is the procedure used.

In deriving the equations for gas analysis, these assumptions were made: (A) equal "apparent volumes" for the two gases; (B) no mixed virial interaction; (C) Random mixing model of s-regular solutions.[9] From assumption (B)

$$P_{total} = P = P_{Xe} + P_{Kr} \tag{15}$$

The "apparent volume," δ, was measured so that the total moles in the gas phase, n^G may be taken to be $P\delta$. It follows from assumptions (A) and (B) above

$$n^G_{Xe} = P_{Xe}\delta \qquad n^G_{Kr} = P_{Kr}\delta \tag{16}$$

(9) Ref. 5, pp. 29–30, 42.

If we denote quantities measured in the gas buret with a posterior superscript B and those in solid solution with S, then

$$n^B_{Kr} = n^G_{Kr} + n^S_{Kr} \tag{17}$$

with an identical expression for xenon. The mole fraction of krypton in solution is denoted by x and defined in the usual way (see equation 20 below), then the random mixing model may be expressed[10]

$$\begin{aligned} P_{Kr}/P^{\circ}_{Kr} &= x \exp\{(1-x)^2 w_{AB}/kT\} \\ P_{Xe}/P^{\circ}_{X} &= (1-x)\exp\{x^2 w_{AB}/kT\} \end{aligned} \tag{18}$$

Eliminating w_{AB}/kT between equations 18 yields

$$\frac{1}{(1-x)^2}\ln\{P_{Kr}/P^{\circ}_{Kr}(x)\} = \frac{1}{x^2}\ln\{P_{Xe}/P^{\circ}_{Xe}(1-x)\} \tag{19}$$

Combining equations 15 and 16 with the definition of mole fraction

$$x = n^S_{Kr}/(n^S_{Kr} + n^S_{Xe}) = \frac{n^B_{Kr} - P_{Kr}\delta}{n^B_{K} + n^B_{Xe} - P\delta} \tag{20}$$

Equations 15, 19 and 20 are three equations in the unknowns x, P_{Kr} and P_{Xe}. For every experimental point, these three equations were simultaneously solved to determine the first two quantities. Substituting back into either of equations 18 gives in addition the value of the parameter w_{AB}/kT. In Table III may be found this parameter calculated for mixtures of several compositions at one temperature. Allowing for the greater uncertainty encountered in dilute solutions, it is seen that this parameter is effectively independent of mole fraction. This justifies the use of this expression in analyzing the mixture. Included in the same table are values of this parameter calculated from the quasi chemical theory (equation 5). The constancy of the parameter is not appreciably better, which supports the use of the more tractable random mixing model.

TABLE III

w_{AB}/kT FOR SOLUTIONS OF KR IN XE AT −114.2°K.

Mole fraction Kr x	Random mix w_{AB}/kT	Quasi-chemical w_{AB}/kT
0.048	1.40	1.42
.115	1.34	1.37
.157	1.51	1.56
.214	1.27	1.31
.217	1.19	1.23
.383	1.20	1.25
.428	1.22	1.27
.446	1.13	1.18
.507	1.23	1.26
	av. 1.280	av. 1.317

A more sophisticated approach to the gas analysis would have considered the imperfections in the gas. It can be shown that equations 18 are valid (*i.e.*, they obey the Duhem–Margules relation) if absolute activity is substituted for the partial pressures of the components.

$$\lambda_{Kr}/\lambda^{\circ}_{Kr} = x\exp\{(1-x)^2 w_{AB}/kT\} \tag{21a}$$

$$\lambda_{Xe}/\lambda^{\circ}_{Xe} = (1-x)\exp\{x^2 w_{AB}/kT\} \tag{21b}$$

(10) Ref. 5, p. 32, eq. 4.05.5 and 4.05.6. (Note different definition of x.)

Now x may be defined in terms of the moles of each substance in the gas phase

$$x = \frac{n^{B}_{Kr} - n^{G}_{Kr}}{(n^{B}_{Kr} + n^{B}_{Xe}) - (n^{G}_{Kr} + n^{G}_{Xe})} \quad (22)$$

The mole fraction of Kr in the gas phase must now be defined

$$N = \frac{n^{G}_{Kr}}{(n^{G}_{Kr} + n^{G}_{Xe})} \quad (23)$$

Using this notation, the expression for the activity ratios of equations 21 in terms of the second virial coefficients is[11]

$$\lambda_{Kr}/\lambda^{\circ}_{Kr} = N \exp \left\{ \frac{P}{RT} (1 - N)^2 \times (2B_{Kr-Xe} - B_{Kr-Kr} - B_{Xe-Xe}) \right\} \quad (24a)$$

$$\lambda_{Xe}/\lambda^{\circ}_{Xe} = (1 - N) \exp \left\{ \frac{P}{RT} N^2 \times (2B_{Kr-Xe} - B_{Kr-Kr} - B_{Xe-Xe}) \right\} \quad (24b)$$

Finally, to determine the amount of gas in the gas phase, the mixed virial equation of state must be used[12]

$$P = kT \frac{n^{G}_{Kr} + n^{G}_{Xe}}{V} + \frac{kT}{V^2} \times \{B_{Kr-Kr} n^{G2}_{Kr} + 2B_{Kr-Xe} n^{G}_{Kr} n^{G}_{Xe} + B_{Xe-Xe} n^{G2}_{Xe}\} \quad (25)$$

Equations 21a, 21b, 22, 23, 24a, 24b and 25 make seven equations in seven unknowns. In particular, they may be solved for x, w_{AB}/kT, and the absolute activity ratios. This would represent a complete solution to the analysis without the restrictive assumptions (A) and (B) above. At the low pressures involved in this series of experiments, however, it was decided that uncertainties arising from other sources made the error caused by gas imperfections negligible.

Results

Solid solutions of krypton in xenon were studied at six temperatures. Table IV gives the average value of w_{AB}/kT for each temperature, calculated for the random mixing model (equation 18) and the quasi-chemical model (equation 5). The close agreement constitutes a good argument for using the simpler random mixing model for the analysis of the data.

TABLE IV

Temp., °K.	w_{AB}/kT Random mix	w_{AB}/kT Quasi-chemical
90.2	2.07	2.18
96.2	1.74	1.81
102.2	1.62	1.66
108.2	1.35	1.38
114.2	1.28	1.29
120.2	1.20	1.24

Figure 2 is a plot of the natural logarithm of the partial pressure of krypton, determined as described above, *vs.* mole fraction Kr. The interpolated values of pressure at 50% solution (crossed points) were found by inserting the average value for the parameter w_{AB}/kT at that temperature into equation 18 with $x = 1/2$ and with the measured value of the vapor pressure of pure krypton at that temperature.

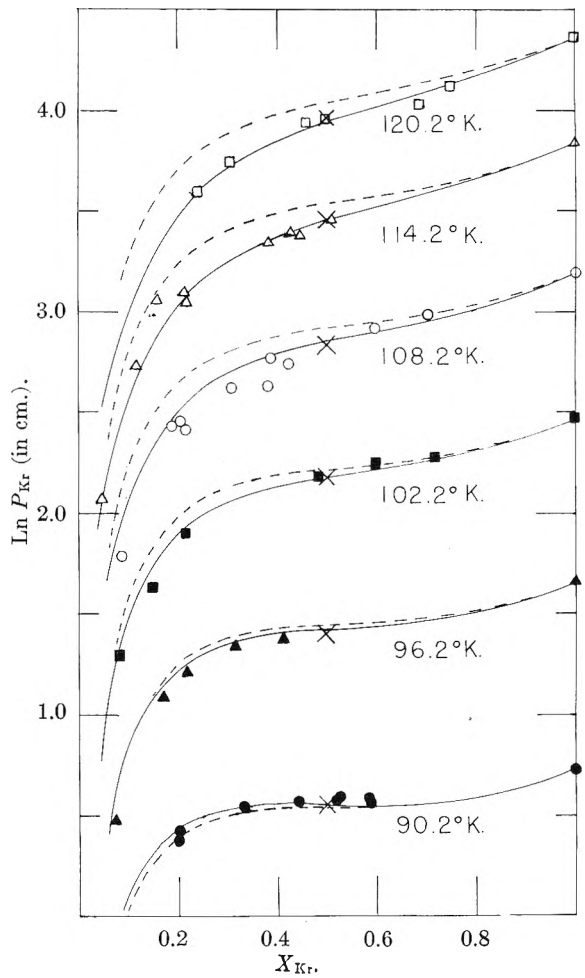

Fig. 2.—Ln P_{Kr} (in cm.) *vs.* mole fraction Kr for six temperatures: – – –, curves generated by random mixing approximation of quasi-chem. model with constant w_{AB}; ——, curves generated by same model with temperature dependent w_{AB}.

The dashed lines of Fig. 2 represent a first attempt to fit the data with a constant value of w_{AB}. Insofar as the pressure seemed to hold constant near 50% solution for the run at 90.2°K., the value of w_{AB} was rather arbitrarily taken to be 358 (corresponding to w_{AB}/kT equal to 2, the value required for phase separation). The dashed lines were generated, then, by using $w_{AB} = 358$ in equation 5. It is clear that a w_{AB} independent of temperature is not adequate since an adjustment in its value would improve the fit in one region, only to make it worse in another.

The simplest form for a temperature dependent w_{AB} is given by equation 6 with h and s independent of temperature. The constants h and s may be evaluated readily by equation 7 if the average w_{AB}/kT values are used on the left. For our data, $h = 680 \pm 30$ cal., $s = 3.4 \pm 0.5$ e.u. The data taken at 120.2°K. were not used in determining the temperature dependent parameter because melting and general experimental difficulties undermined our confidence in the data taken at this temperature. Figure 3 shows the calculated

(11) Ref. 5, p. 153 eq. 8.08.3.
(12) Ref. 4, p. 297 eq. 720.2

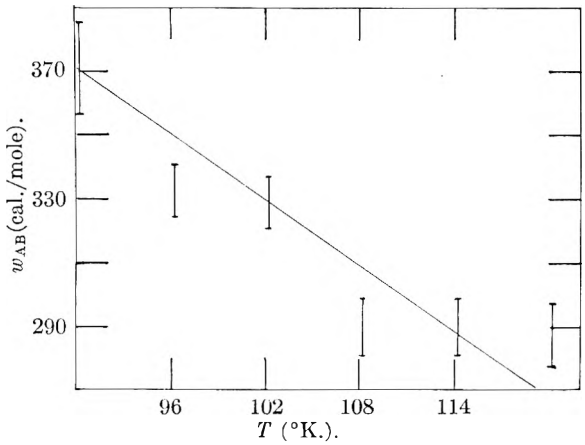

Fig. 3.—Measured values of the parameter w_{AB} at six temperatures shown with line representing the thermodynamically obtained temperature dependent w_{AB}.

temperature dependent w_{AB} together with the average values of w_{AB} determined at each temperature. The width of the points represents the probable error of the average. Although we have not generated the best straight line through the points, the fit is sufficiently good to be an independent justification of the method.

The solid lines in Fig. 2 have been generated by using this temperature dependent w_{AB} in equations 18. It is apparent that the fit is considerably improved. It is also clear that no further improvement can be made in the functional relationship between w_{AB} and T within the accuracy of the data.

That the difference between the random mixing model and the more refined quasi-chemical approximation is negligible is graphically illustrated in Fig. 4. The curves are from calculations of Guggenheim.[13] The solid line represents the predicted P_{Kr} line at the critical solution temperature for the random mixing model and the dashed line represents the most highly refined quasi-chemical calculation involving the effects of pairs, triplets and quadruplets, also at critical solution temperature. The data taken at 90.2°K. are also shown. It is seen that both lines are near fits but that neither is perfect. It would be difficult to choose the better fit on the basis of our data.

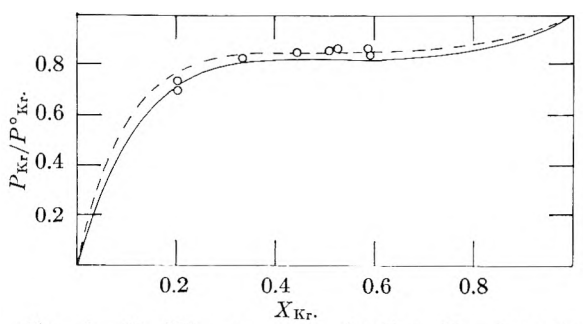

Fig. 4.—$P_{Kr}/P°_{Kr}$ *vs.* mole fraction Kr theoretical curves (——, random mixing; — — —, refined quasi-chemical) at the critical solution temperature shown with data taken at 90.2°K.

Critical Solution Temperature and Sub-critical Data.—The most objective way of estimating the critical temperature appeared to be from the w_{AB} line calculated from equations 4, 10, 11 and 12, (Fig. 3). Since this line was calculated from the random-mixing equations, the critical temperature is found where $w_{AB}/kT = 2$. This occurs at 92°K. Alternatively, we may use the smoothed values of w_{AB}/kT estimated from the shape of the mole fraction *vs.* ln p curves (Table IV). The random-mixing fits suggest $T_c = 93$°K. The quasi-chemical fits are in substantial agreement with 90°K. (It should be noted that, although the w_{AB}/kT_c values according to the two theories are substantially different, (about 10%), both theories give substantially the same thermodynamic account of the system in a limited region such as around the critical point. The w_{AB} values differ, because, thermodynamically, these relate to an ideal process taking place at 0°K. and $x = 0$; conditions remote from the critical ones). We may thus estimate the critical temperature for phase separation of the solid solution to be 91 ± 2°K.

An attempt was made to secure sub-critical temperature data. Because of the nearness of the liquid nitrogen bath temperature, reliable automatic control of the block temperature was practicable only to about 87.2°K. Several points were taken at this temperature, however. The results are shown in Fig. 5. The theoretical line is calculated from the random-mixing theory, with a value of w_{AB}/kT obtained from the extrapolation of the line in Fig. 3. The agreement is clearly not satisfactory; also there is no flat region in the pressure to clearly indicate phase separation. This difficultly will be explored further in an apparatus designed to operate at lower temperatures.

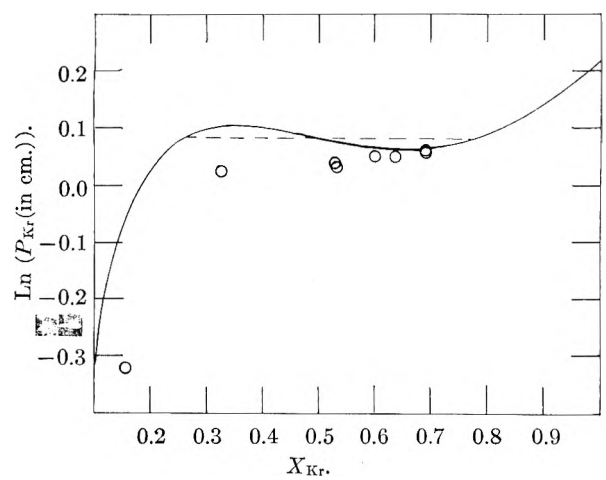

Fig. 5.—Ln P_{Kr} (in cm.) *vs.* mole fraction Kr theoretical curve generated by random mixing approximation with temperature dependent w_{AB} at 87.2°K. shown with data taken at 87.2°K: — — —, theoretical line assuming phase split.

Conclusion. The Variation of w_{AB} with Temperature.—The temperature variation of the "heat of solution parameter" for liquid solutions has been the subject of widespread interest. Scatchard[14] presented an early theoretical treatment,

(13) Ref. 5, p. 61.

(14) G. Scatchard, *Trans. Faraday Soc.*, **33**, 160 (1937).

and Fowler and Guggenheim[15,16] comment on the question. We have selected the recent calculations of Prigogine and Bellemans[17] which are based on the Lennard-Jones cell model for liquids, for comparison with our results. The cell model is based on molecular forces of the central-field, rare-gas type, and is more applicable to solid than liquid solutions, at least on the face of it. From the intermolecular force constants determined by Hirschfelder, *et al.*, by the analysis of gas viscosity[18] we have calculated the integral excess enthalpy, entropy and free energy of a 50% solution. It should be noted that the results are strongly dependent on the choice of these constants, and furthermore the mole fraction dependence of these quantities is substantially that predicted by the quasi-chemical theory. The calculated results at 50% are $H' = 95.9$ cal./mole (measured 169 cal./mole); $S' = 0.306$ e.u. (measured 0.85 e.u.) and $F' = 61.3$ cal./mole (measured 73 cal./mole). (Almost the entire enthalpy and entropy are due to size effect in these formulas.) There is at least qualitative agreement with the theory. However, we feel that when full data are available on the argon–krypton system, and other pairs of simple molecules, an analysis of the trends in the heat and entropy parts of w_{AB} will provide a more stringent test of the theories.

(15) Ref. 4, p. 370.

(16) Ref. 5, p. 78.

(17) I. Prigogine and A. Bellemans, *Disc. Faraday Soc.*, **15**, 80 (1953).

(18) Joseph O. Hirschfelder, R. Byron Bird and Ellen L. Spotz, *Chem. Revs.*, **44**, 205 (1949).

ELECTRICAL CONDUCTANCE AND DENSITY OF PURE MOLTEN ALKALI HALIDES[1]

BY I. S. YAFFE AND E. R. VAN ARTSDALEN

Chemistry Division, Oak Ridge National Laboratory,[2] Oak Ridge, Tennessee

Received April 20, 1956

Measurements of specific conductance and of density as functions of temperature have been made on all pure molten alkali chlorides, bromides and iodides. From these data, the equivalent conductance and the molar volume of each salt have been calculated at temperatures up to 200° above the melting point. In general, the equivalent conductance differs among these salts in a regular manner and may be correlated with fundamental properties of the constituent ions. It is necessary, however, to make comparisons at corresponding temperatures. Conductance has been treated as a rate process and the heat and the entropy of activation were calculated from the experimental results. The heat of activation varies with temperature with the sign of the temperature coefficient depending upon the cation. The calculated entropies of activation were found to be negative, of reasonable magnitude and nearly independent of temperature. The melting points of various alkali halides were redetermined by a method which takes advantage of the rapid change of resistance at the solidification point.

A previous paper by the authors[3] concerned the conductance and density of molten binary alkali halide systems. From a study of the data presented in that paper it was evident that before a detailed explanation of the variations of conductance and of density with temperature and with composition could be made, a better knowledge of the magnitudes of these properties of the pure alkali halides was required. Numerous authors[4-17] have previously reported on these properties but, in general, there has been considerable scatter in the data presented and wide discrepancies among the work of the various investigators. Thus it was felt expedient to measure the specific conductance and the density of all of the alkali halides in order to obtain a self-consistent, and perhaps a more accurate and precise, set of data.

As fluorides attack fused silica, it is not possible to measure with any high degree of accuracy the specific conductance of the alkali fluorides by the method used in this investigation. Such measurements await the development of a suitable cell material which is (1) non-reactive with molten fluorides, (2) non-porous and (3) an electrical insulator at high temperature, or else the development of measuring apparatus which can determine accurately the required resistance without the use of an insulating cell.

This paper presents new data of the specific conductance and of the density of eleven molten alkali halides. Combined with the data on the four pure

(1) Presented at the Symposium on Nonaqueous Electrochemistry at the 128th Meeting of the American Chemical Society, Minneapolis, Minn., September 15, 1955.

(2) Operated by Union Carbide Nuclear Company for the U. S. Atomic Energy Commission.

(3) E. R. Van Artsdalen and I. S. Yaffe, THIS JOURNAL, **59**, 118 (1955).

(4) H. Bloom, J. W. Knaggs, J. J. Molloy and D. Welch, *Trans. Faraday Soc.*, **49**, 1458 (1953).

(5) B. S. Harrap and E. Heymann, *ibid.*, **51**, 259, 268 (1955).

(6) J. D. Edwards, C. S. Taylor, A. S. Russell and L. F. Maranville, *J. Electrochem. Soc.*, **99**, 527 (1952).

(7) J. S. Peake and M. R. Bothwell, *J. Am. Chem. Soc.*, **76**, 2653 (1954).

(8) S. V. Karpachev, A. G. Stromberg and V. N. Padchainova, *Zhur. Obshchei Khim.*, **5**, 1517 (1953).

(9) S. V. Karpachev and A. G. Stromberg, *Zhur. Fiz. Khim.*, **11**, 852 (1938).

(10) P. W. Huber, E. V. Potter and H. W. St. Clair, U. S. Bureau of Mines, Report of Investigation 4858 (1952).

(11) E. K. Lee and E. P. Pearson, *Trans. Electrochem. Soc.*, **88**, 171 (1945).

(12) W. Biltz and W. Klemm, *Z. anorg. Chem.*, **152**, 267 (1926).

(13) M. E. Mantzell, *Z. Elektrochem.*, **49**, 283 (1943).

(14) F. M. Jaeger and B. Kampa, *Z. anorg. Chem.*, **113**, 27 (1920).

(15) F. M. Jaeger, *ibid.*, **101**, 1 (1917).

(16) B. P. Barzakowsky, *Izvest. Akad. Nauk. S.S.S.R., Otdel. Khim. Nauk*, **No. 5**, 825 (1940).

(17) B. P. Barzakowsky, *Zhur. Priklad. Khim.*, **13**, 1117 (1940).

halides previously reported by the authors,[3] they represent a self-consistent and interpretable set of measurements of all alkali halides which are at present capable of accurate determination.

Experimental

The methods and apparatus previously described[3] were used with the slight modification that, in the furnace assembly, a heavy-walled inconel tube equipped with a quartz liner was substituted for the combination of inconel and nickel tubes. The specific conductance was computed in the manner described previously[3] from the resistance at infinite frequency obtained by extrapolation of measurements made below 20,000 c.p.s.

All salts were carefully purified before use. LiBr and LiI were synthesized from purified Li_2CO_3 and the corresponding halogen acid, recrystallized from demineralized distilled water, and dehydrated under vacuum while slowly and uniformly raising the temperature to 350° over a period of 96 hours.[18] RbI and CsI were prepared by the addition of purified HI to the corresponding hydroxide, and recrystallized from water. RbBr and CsBr were made, successively, from the iodide, by adding purified bromine to an aqueous solution of the iodide, subliming off the liberated iodine and recrystallizing from water. RbCl was similarly prepared from RbBr by adding Cl_2 and boiling off the Br_2. All other salts were C.P. reagent chemicals which were further purified by recrystallization, and dehydrated according to the above procedure when necessary. Finally, all salts were premelted under vacuum or an inert atmosphere, and after slow solidification the center core of the solidified melt was discarded.

At the conclusion of each run, the salt was checked for decomposition and hydrolysis by dissolving a portion in water and adding phenolphthalein. With the exception of LiI, no data from runs showing evidence of hydrolysis are reported. In the two runs made with LiI, the salt partially decomposed (as evidenced by the evolution of I_2) at the higher experimental temperatures, and thus, the data for LiI are not considered to be as reliable as for the other salts.

As a further check of the purity of the salts used, the melting points were determined by a conductance method which is applicable only to pure substances. With the conductance cell immersed in the molten salt, the temperature of the melt is slowly lowered. At the melting point, the measured resistance increases quite rapidly as the salt solidifies while the temperature of the melt remains constant. The melting points so obtained were in no case lower within experimental error than those accepted for each salt, and in many cases were higher than the accepted values possibly indicating a higher degree of purity than that of the salts previously recorded in the literature. The observed melting points are listed in Table I.

TABLE I

MELTING POINTS OF VARIOUS ALKALI HALIDES

Salt	M.p., °C. This Study[a]	N.B.S.[19]	Other Values
LiBr	549	550	549[20]
LiI	465	449	469[21]
NaBr	745	750	743[20], 747[22]
NaI	659	662	660[20], 661[22]
KBr	735	735	733[20]
RbCl	722	717	711[20]
RbBr	692	680	
RbI	647	640	
CsCl	645	645	641[20], 640[22]
CsBr	636	636	
CsI	630	621	626[22]

[a] Estimated accuracy is ±2°.

Results and Discussion

The specific conductance, κ, and the density, ρ, of eleven pure alkali halides were measured over a 200° temperature range above their melting points. The data are listed in Tables II and III, and may be represented by either of two types of equations. As previously reported,[3] the specific conductance data can be expressed as quadratic functions of temperature and the density data by linear functions of temperature. Parameters of these equations for the salts investigated in this study together with those of the four alkali halides previously determined[3] are given in Table IV. Although the equations are useful for the calculation of the quantities involved, it should be emphasized that they are valid only in the temperature ranges investigated. Also, the experimentally determined κ's for most salts near the melting point are lower than those calculated from the equations. This has been previously interpreted[3] as evidence of a small amount of "long range" order still present in the melt at temperatures near the melting point.

Alternately, the data may be represented by exponential functions: the specific conductance data by $\kappa = \exp(A + B/T + CT)$ and the density data by $\rho = \exp(a + bT)$. The constants of these equations for two representative salts are given in Table V. These exponential equations might be preferred from a theoretical standpoint and they can be used to obtain a simple equation for Λ, but there is no clear explanation of the factors involved in the magnitudes of the parameters.

Jaeger[15] has previously determined the densities of most of the alkali halides; considering that he based his density–temperature equations upon very few experimental data (in most cases only three points), there is surprisingly good agreement between his data and those reported herein. The largest discrepancy between the new data and those in the literature is in the density of LiI, previously reported by Karpachev and Stromberg[9] who gave $\rho = 2.892 - 0.0057t$ g./cc. (t, °C.). In view of the fact that they obtained experimental data on the molten salt 21° below their own listed melting point (450°), and took no special precautions to prevent hydrolysis, their work cannot be regarded as reliable.

Comparison of the absolute magnitudes of the molar volume and the equivalent conductance of fused salts should be made at "corresponding temperatures." However, the definition of a corresponding temperature scale is not obvious. Isothermal comparison is not very fruitful as the equivalent conductance-temperature curve (and also $\log \Lambda$ *vs.* $1/T$ curve) of one salt frequently intersects that of another salt and interpretation would be dependent on temperature. Comparisons at equal fractions of the critical temperature might be meaningful; however, the critical temperatures of these salts are not sufficiently well known for this purpose. Comparisons made at temperatures corresponding to equal vapor pressures are also not

(18) R. Sampley, "Preparation of High-Purity Anhydrous Lithium Iodide," U. S. Atomic Energy Commission, Unclassified Report No. ORNL-1673 (1954).

(19) National Bureau of Standards, "Selected Values of Chemical Thermodynamic Properties," Circular No. 500, U. S. Government Printing Office (1952). References to other data listed therein.

(20) O. Schmitz-Dumont and E. Schmitz, *Z. anorg. Chem.*, **252**, 329 (1944).

(21) J. W. Johnson and M. A. Bredig, unpublished data.

(22) M. A. Bredig, H. R. Bronstein, J. W. Johnson and Wm. T. Smith, Jr., *J. Am. Chem. Soc.*, **77**, 307, 1454 (1955).

TABLE II

SPECIFIC CONDUCTANCE DATA OF SOME ALKALI HALIDES

Temp., °C.	κ, Ω^{-1} cm.$^{-1}$	Temp., °C.	κ, Ω^{-1} cm.$^{-1}$	Temp., °C.	κ, Ω^{-1} cm.$^{-1}$	Temp., °C.	κ, Ω^{-1} cm.$^{-1}$
LiBr		NaBr		RbCl		CsCl	
555.4	4.7265	880.3	3.3015	729.8	1.5250	653.3	1.1245
558.0	4.7422	906.1	3.3793	735.8	1.5444	689.0	1.2385
569.5	4.8039	929.2	3.4359	755.4	1.6050	712.4	1.3058
575.5	4.8341	955.8	3.5034	766.4	1.6309	720.8	1.3355
592.0	4.9258	NaI		776.1	1.6590	750.0	1.4232
628.3	5.1191			801.1	1.7296	766.4	1.4736
646.8	5.2162	663.0	2.2452	823.9	1.7864	804.4	1.5842
672.3	5.3466	672.4	2.2764	844.1	1.8339	820.6	1.6269
701.8	5.4891	675.0	2.2894	881.6	1.9256	833.1	1.6652
727.5	5.6224	691.9	2.3451	904.5	1.9779	868.5	1.7557
731.3	5.6413	700.5	2.3718	924.1	2.0202	896.8	1.8259
749.0	5.7232	711.3	2.4041				
		723.1	2.4392	RbBr		CsBr	
LiI		748.0	2.5188				
		761.2	2.5561	695.7	1.1217	644.6	0.8160
468.5	3.585	798.4	2.6616	710.5	1.1596	644.8	.8165
472.9	3.611	827.3	2.7408	733.0	1.2215	645.4	.8245
477.8	3.646	848.8	2.8045	751.8	1.2692	655.8	.8500
478.2	3.648	875.6	2.8645	777.4	1.3185	661.2	.8655
483.5	3.666	892.1	2.9040	802.9	1.3702	662.4	.8657
503.6	3.757	914.1	2.9576	826.3	1.4131	699.1	.9606
505.8	3.763	KBr		850.1	1.4475	733.0	1.0468
511.1	3.786			864.9	1.4705	758.2	1.1019
536.6	3.872	737.8	1.6108	894.0	1.5024	795.8	1.1968
547.7	3.898	739.6	1.6203	905.4	1.5183	824.0	1.2594
562.6	3.934	750.4	1.6547			836.9	1.2886
577.8	3.970	756.2	1.6656	RbI		857.7	1.3331
593.1	3.994	778.7	1.7311				
608.8	4.029	783.9	1.7430	656.3	0.8765	CsI	
627.1	4.051	784.8	1.7505	656.7	.8777		
637.1	4.071	800.9	1.7946	666.3	.8942	633.5	0.6391
668.5	4.099	815.5	1.8167	668.9	.9041	658.8	.7097
		825.9	1.8361	678.0	.9201	670.7	.7360
NaBr		829.4	1.8505	681.7	.9264	688.3	.7772
		847.9	1.8895	705.7	.9708	691.9	.7804
744.0	2.8720	853.3	1.8938	742.0	1.0323	722.1	.8456
751.7	2.9051	858.5	1.9058	746.8	1.0395	726.8	.8617
758.2	2.9265	869.6	1.9187	748.0	1.0439	756.7	.9162
763.9	2.9479	876.6	1.9386	751.8	1.0450	783.4	.9732
784.6	3.0103	892.0	1.9688	784.0	1.0983	791.3	.9776
784.7	3.0112	906.8	1.9858	810.4	1.1365	816.8	1.0286
811.8	3.0944	913.3	1.9971	815.9	1.1455	830.4	1.0504
820.9	3.1258	923.5	2.0012	818.2	1.1463	843.8	1.0811
839.7	3.1827	927.9	2.0136	852.8	1.1900	847.3	1.0851
858.8	3.2364	935.9	2.0208	885.0	1.2317	864.0	1.1147
870.7	3.2720	956.3	2.0372				

presently practical due to our lack of knowledge of the precise values of these pressures. However, the melting points of these salts are known and the transition point between solid and liquid may be considered a corresponding temperature. We have, accordingly, made our comparisons at equal fractions above the melting point.[23] We define a corresponding temperature, θ, as $\theta = T°K/T_m°K$ where $T_m°$ is the melting point

The coefficient of expansion for the several salts at corresponding θ varies in a rather regular manner from salt to salt. The coefficient of expansion is plotted in Fig. 1 as a function of formula weight. All potassium, rubidium and cesium chlorides, bromides and iodides have very nearly the same coefficient of expansion, although the iodides tend to be a little lower. The lithium salts are very roughly 30% lower while the sodium salts are intermediate. The fluoride data of Jaeger[15] show qualitatively similar behavior, though the coefficients are considerably lower for fluorides than for other halides. The exact dependence of molar volume upon fundamental properties of the constituent ions is unknown, but smooth curves can be obtained for plots of molar volume against molecular weight, interionic crystal distance, etc. The molar volumes of the liquid salts in conjunction with their coefficient of expansion show smooth dependence from

(23) H. Bloom and E. Heymann, *Proc. Roy. Soc.* (*London*), **188A**, 392 (1947), also employed a similar convention.

TABLE III

DENSITY DATA OF VARIOUS ALKALI HALIDES

Temp., °C.	Density, g./cc.	Temp., °C.	Density, g./ec.	Temp., °C.	Density, g./cc.	Temp., °C.	Density, g./cc.
LiBr		NaI		RbCl		CsCl	
552.2	2.5283	671.3	2.7316	791.2	2.1810	671.5	2.7638
553.6	2.5272	680.1	2.7227	813.2	2.1613	690.3	2.7424
579.6	2.5098	713.3	2.6905	844.5	2.1338	713.8	2.7181
612.0	2.4883	734.3	2.6719	884.0	2.0994	750.7	2.6777
641.8	2.4689	755.8	2.6512	922.7	2.0650	792.0	2.6355
672.3	2.4492	780.7	2.6268			828.8	2.5952
673.4	2.4485	802.7	2.6065	RbBr		870.6	2.5516
696.0	2.4343	803.6	2.6059	703.7	2.6927	905.4	2.5136
738.6	2.4070	831.1	2.5792	728.2	2.6661		
		851.6	2.5597	751.7	2.6405	CsBr	
LiI		877.6	2.5357	770.3	2.6201		
		911.9	2.5029	799.6	2.5894	637.0	3.1320
474.9	3.1040			823.7	2.5627	670.5	3.0902
500.0	3.0808	KBr		846.2	2.5391	694.8	3.0610
527.7	3.0556			870.9	2.5136	735.3	3.0110
551.9	3.0337	740.4	2.1233	906.8	2.4747	758.4	2.9826
578.4	3.0093	752.2	2.1132			797.0	2.9358
601.8	2.9873	785.4	2.0853	RbI		797.4	2.9355
633.9	2.9585	793.8	2.0783	654.9	2.8898	825.2	2.9019
667.1	2.9274	809.2	2.0656	662.3	2.8804	859.6	2.8590
		817.4	2.0581	662.4	2.8802		
NaBr		839.2	2.0405	662.9	2.8794	CsI	
		868.7	2 0161	669.9	2.8727		
753.3	2.3366	872.2	2 0129	682.8	2.8564	645.8	3.1541
767.5	2.3254	884.7	2.0028	701.8	2.8357	663.9	3.1318
791.9	2.3046	906.5	1.9851	715.8	2.8184	692.6	3.0984
819.2	2.2825	914.1	1.9787	719.3	2.8158	732.3	3.0510
842.4	2.2633	930.1	1.9660	745.1	2.7850	763.7	3.0143
867.9	2 2428			754.1	2.7751	797.3	2.9743
888.9	2 2256	RbCl		785.0	2.7399	830.4	2.9352
917.4	2.2023			785.1	2.7397	852.3	2.9094
944.9	2.1804	722.4	2.2417	815.5	2.7051		
		748.2	2.2191	821.4	2.6980		
		753.4	2 2146	852.8	2.6631		
		762.6	2.2067	857.9	2.6575		
		771.3	2.1989	901.8	2.6072		

TABLE IV

SPECIFIC CONDUCTANCE AND DENSITY EQUATIONS FOR MOLTEN ALKALI HALIDES

Salt	Specific conductance (Ω^{-1} cm.$^{-1}$) $\kappa = a + bt - ct^2$ a	$b \times 10^2$	$c \times 10^6$	Std. dev. σ (Ω^{-1} cm.$^{-1}$)	Applicable temp. range, °C.	Density $\rho = a - bt$ a	$b \times 10^3$	Std. dev. σ, g./cc.	Exptl. temp. range, °C.
LiCl[3]	+0.5282	1.125	4.554	0.008	630–790	1.7660	0.4328	0.0001	630–780
LiBr	+1.0095	0.7834	2.057	.002	555–750	2.8878	.6520	.0004	552–740
LiI	−0.578	1.348	9.695	.006	475–670	3.5397	.9176	.0003	475–670
NaCl[3]	−0.1697	0.6259	1.953	.006	810–1030	1.9911	.5430	.0007	803–1030
NaBr	−0.4392	0.5632	1.572	.002	750–960	2.9518	.8169	.0003	753–945
NaI	−0.8202	0.5940	1.976	.002	675–915	3.3683	.9491	.0004	670–915
KCl[3]	−1.7491	0.738	3.000	.003	790–930	1.9767	.5831	.0003	780–940
KBr	−3.2261	1.0124	4.828	.004	737–960	2.7333	.82525	.0005	740–930
KI[3]	−1.7100	0.6408	2.965	.003	720–920	3.0985	.9557	.0003	682–905
RbCl	−1.8097	0.6176	2.1985	.002	730–935	2.8799	.8832	.0002	722–925
RbBr	−3.0505	0.9104	4.510	.002	700–905	3.4464	1.0718	.0005	700–910
RbI	−1.0798	0.4055	1.6305	.002	655–885	3.6377	1.1435	.0005	655–905
CsCl	−1.8023	0.5628	1.765	.003	650–900	3.4782	1.0650	.0006	670–905
CsBr	−1.4137	0.4255	1.228	.002	644–860	3.9109	1.2234	.0003	637–860
CsI	−1.3313	0.3958	1.305	.003	640–865	3.9179	1.1834	.0002	645–855

one salt to the next in such a way as to confirm the conclusion of Johnson, Agron and Bredig[24] that on melting cesium bromide and iodide undergo a change in coördination number to approximate those of other alkali halides.

Figure 2 shows the equivalent conductance of the alkali halides as a function of θ. For the salts of each cation, excepting Li^+, the equivalent con-

(24) J. W. Johnson, P. A. Agron and M. A. Bredig, *J. Am. Chem. Soc.*, **77**, 2734 (1955).

TABLE V

REPRESENTATIVE EXPONENTIAL EQUATIONS FOR CONDUCTANCE AND DENSITY

LiBr: $\rho = \exp(1.1453 - 2.6395 \times 10^{-4}T)$ ($\sigma = 0.0002$)
(T, °K.)
$\kappa = \exp(2.2519 - 694.83/T + 0.16866 \times 10^{-2}T)$ ($\sigma = 0.0022$)
$\Lambda = \exp(5.5709 - 694.83/T + 0.43261 \times 10^{-3}T)$

CsBr: $\rho = \exp(1.5138 - 4.0834 \times 10^{-4}T)$ ($\sigma = 0.0010$)
$\kappa = \exp(5.5706 - 398.3/T - 1.5611 \times 10^{-3}T)$ ($\sigma = 0.0024$)
$\Lambda = \exp(9.4173 - 3980.3/T - 1.1528 \times 10^{-3}T)$

ductance varies in the order of $Cl^- > Br^- > I^-$, and the lithium salts also obey this order near the melting point. Likewise for the salts of each anion the order is $Li^+ > Na^+ > K^+ > Rb^+ > Cs^+$. In comparing the equivalent conductance of several salts at corresponding temperatures we may anticipate that the smaller and lighter the conducting ions the greater will be the conductance. The data of Fig. 2 illustrate a self-consistent set of trends which agree with this concept. In addition to dependence upon size and mass, we may expect the equivalent conductance of the ions to be some function of their moments of inertia, polarizability, charge, effective free volume or "void" space in the melt, etc. In the absence of any detailed theory of conduction in molten salts, one can only speculate upon the form of this function. When the equivalent conductance is plotted as a function of the radii of the constituent ions (see Fig. 3a), the curves for each anion contain points of inflection. Similarly, plots of Λ *versus* $1/m$ or $1/m^{1/2}$ are not smooth curves. However, smooth curves are obtained when Λ is plotted as a function of the product of the mass and volume of the ions, as seen in Fig. 3b. (Pauling's crystal radii[25] were used for these computations). Thus it can be deduced that while neither mass nor volume alone determines the magnitude of equivalent conductance, some function of the product of these two properties may be significant. Equivalent conductance at corresponding temperatures decreases with increasing polarizability of the ions, but whether this is a fundamental property or a reflection of the size and mass effect is not clear from the present data. Plots of equivalent conductance against free volume in melts illustrate qualitatively that conductance decreases with increasing free volume, but again no conclusion can be drawn as to the correct form of the function. These curves do illustrate, however, the self-consistency of the presented data, and do indicate that the corresponding temperature scale used is a reasonable one.

Frenkel[26] has proposed for pure molten salts the expression $\Lambda^m\eta$ = constant (η = viscosity in poises), which is essentially a modification of Walden's rule,[27] $\Lambda\eta$ = constant. The validity of these expressions connecting the conductance and viscosity of molten salts has been the concern of the above authors and such other workers as Erdey-Gruz[28] and Wetmore.[29] The present results do not differ sufficiently from previously reported data (at least for those salts for which there are viscosity data) to alter the conclusion that Frenkel's expression is obeyed by many ionic melts. However, we consider that the validity of the relationship does emphasize the important fact that the transport processes of conduction and viscous flow (and, very likely self-diffusion) are dependent upon the same fundamental properties of the constituent ions, although to different degrees, rather than upon each other. Hence nothing is gained by attributing the variation of conductance with temperature or composition to the variation of viscosity.

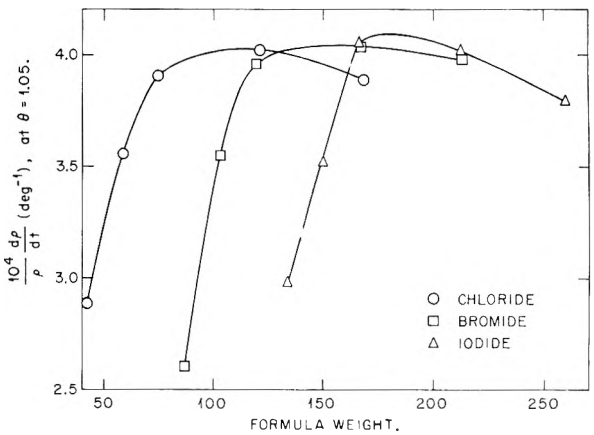

Fig. 1.—Coefficient of expansion of molten alkali halides.

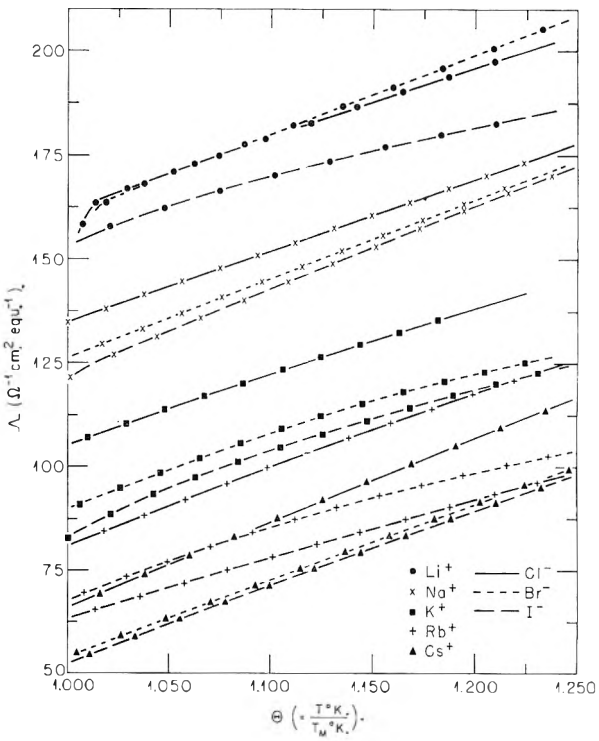

Fig. 2.—Equivalent conductance of molten alkali halides (points are calculated at 20° intervals from equations of Table IV).

(25) L. Pauling, "Nature of the Chemical Bond," 2nd Edition, p. 358, Cornell University Press, Ithaca, N. Y., 1940.

(26) J. Frenkel, "Kinetic Theory of Liquids," Oxford University Press, London, 1946, p. 441.

(27) P. Walden, *Z. physik. Chem.*, **A157**, 389 (1931).

(28) T. Erdey-Gruz, *ibid.*, **A178**, 138 (1937).

(29) F. A. Pugsley and F. E. W. Wetmore, *Can. J. Chem.*, **32**, 839 (1954).

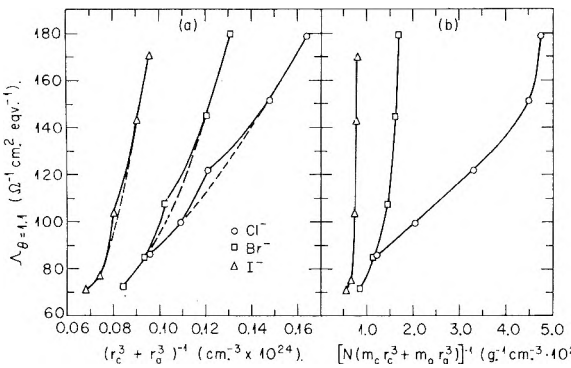

Fig. 3.—Equivalent conductance of molten alkali halides as functions of the mass and volume of the constituent ions.

Conduction being a rate process, the equation $\Lambda = Ae^{-\Delta H^{\ddagger}/RT}$ can be used to calculate the heat of activation, $\Delta H^{\ddagger}$, for the conductance process. The values are illustrated in Fig. 4, in which the abscissa is the number of degrees above the melting point. As previously observed,[3] the heats of activation are temperature dependent and for the halides of the

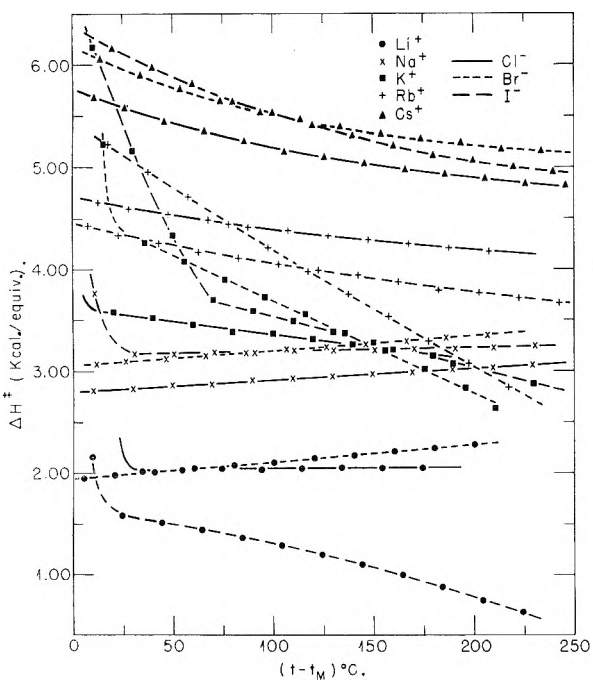

Fig. 4.—Heats of activation for conduction for molten alkali halides (points are calculated at 20° intervals from slopes of log Λ *vs.* $1/T$ plots.)

lighter alkali metals vary linearly with temperature. For each halide, the heat of activation decreases with decreasing size of the cation and, in general, the bromides have steeper slopes than the chlorides or iodides.

We consider that the heat of activation depends upon at least two opposing factors which may be thought of as follows. As the melt expands with rising temperature, the total coulombic forces among the constituent ions tend to lessen and thus the heat of activation for migration should decrease with rising temperature.[3] Opposing this effect as the liquid expands with rising temperature, the average number of nearest neighbors to any particular ion may decrease (due mainly to an increase in the number of holes). Thus the attractive force, per nearest neighbor, would increase and so increase the heat of activation. This latter effect should be more dominant the greater the disparity in ionic size and the former the smaller this disparity. In general, this is the case, with ΔH of the lithium and sodium salts increasing with temperature and those of the heavier alkali halides decreasing. LiI appears to be an exception to these generalities; here the opposite extremes in ion size could introduce a special spatial effect.

The explanation of the rapid rise in $\Delta H^{\ddagger}$ for several of the salts (*e.g.*, KI) as the melting point is approached is not obvious. The effect certainly is real. In the case of potassium iodide three separate melts from two different samples of salt were measured with highly reproducible and concordant results. The effect could be the result of some change of order in the liquid. Thus if there were partial molecule or polymer formation (which would detract from conduction) increasing with decreasing temperature the apparent heat of activation for conductance would increase abnormally as the temperature drops.

The Arrhenius equation can be expanded into the following form[3]

$$\Lambda = 5.18 \cdot 10^{18}(D + 2)d_i^2 e^{\Delta S^{\ddagger}/R} e^{-\Delta H^{\ddagger}/RT}$$

in which D is the "dielectric constant" of the conducting melt and d_i is the half-migration distance for the conducting ion. By use of this equation, the entropy of activation for the conduction process can be estimated from a measured value of Λ and the derived value of $\Delta H^{\ddagger}$ at the same temperature. The method of estimating d_i has been described previously.[3] D was assumed equal to 3 for all cases; but fortunately $\Delta S^{\ddagger}$ is not very sensitive to this choice and a change to $D = 15$ merely makes all $\Delta S^{\ddagger}$ values approximately 2 e.u. more negative. These values of $\Delta S^{\ddagger}$ at 850° are listed in Table VI; they are temperature-insensitive, of intuitively proper sign and of reasonable magnitude. Although there appears to be a general trend of the values of $I^- > Br^- > Cl^-$, and a maximum at the potassium salts of each halide, no conclusion can be drawn as to the meaning of these differences among the values due to the crude approximations made in their calculation.

Recently, Sakai[30] has proposed the following equation to represent the variation of specific conductance with temperature for pure molten salts

$$\kappa = K \times T^{a-1/2} e^{-U/RT}$$

Here K is a constant of the system, involving among other quantities the mass of the ions, and a is a positive number related to the mean free path, l, by the expression, $l = kT^a$, where k is a constant for any particular system. His equation for specific conductance is analogous in form to the equation previously employed by the present authors[3] for equivalent conductance of molten systems in which the heat of activation varies linearly with temperature. However, when the specific conductance data of the alkali halides are analyzed in line with Sakai's theory, a is found to be temperature-dependent and

(30) K. Sakai, *J. Chem. Soc., Japan*, **75**, 182 (1954).

to vary too widely to be able to ascribe any physical significance to its magnitude.

TABLE VI

ENTROPY OF ACTIVATION FOR THE CONDUCTANCE PROCESS FOR MOLTEN ALKALI HALIDES AT 850°

Salt	$-\Delta S^{\ddagger}$ (e.u./equiv.)	Salt	$-\Delta S^{\ddagger}$ (e.u./equiv.)
LiCl	6.1	KI	7.4
LiBr	6.2	RbCl	6.2
LiI	8.2	RbBr	7.3
NaCl	6.4	RbI	7.1
NaBr	6.3	CsCl	6.2
NaI	6.4	CsBr	6.3
KCl	6.7	CsI	6.7
KBr	6.9		

Before a detailed theory of conduction in molten salts is developed, the structure of molten salts and the factors influencing the structure should be determined. Some work has been and is being done[31,32] on diffraction measurements in molten salts. Data for self-diffusion in melts will also shed light on the mechanism of transport and work is already in progress along this line.[33,34]

Acknowledgment.—We wish to acknowledge the assistance of Mr. D. E. LaValle who prepared our pure samples of CsBr, CsI, RbCl, RbBr and RbI, and of Mr. R. Sampley who prepared our pure LiBr.

(31) K. Lark-Horovitz and E. P. Miller, *Phys. Rev.*, **49**, 418 (1936); **51**, 61 (1937).

(32) Kunitomi, *J. Chem. Soc. Japan*, **65**, 74 (1944), (cited by Sakai, ref. 30.)

(33) A. Klemm, *Z. Naturforschung*, **8a**, 397, 400 (1953).

(34) E. R. Van Artsdalen, D. Brown, A. S. Dworkin and F. J. Miller, *J. Am. Chem. Soc.*, **78**, 1772 (1956). Also E. R. Van Artsdalen, I. S. Yaffe and F. J. Miller, "Electrical Conductance and Ionic Migration in Molten Salts," presented before the 107th meeting of the Electrochemical Society, Cincinnati, Ohio, 1955.

THE SALTING IN OF SUBSTITUTED BENZENES BY LARGE ION SALTS[1,2]

BY R. L. BERGEN, JR., AND F. A. LONG

Contribution from the Department of Chemistry, Cornell University, Ithaca, N. Y.

Received April 20, 1956

The effects of salts on the activity coefficients of a series of acidic and basic derivatives of benzene in aqueous solutions have been measured at 25° by either solubility or distribution procedures. Salts of such large ions as tetraethylammonium and toluenesulfonate lead to salting in for all cases. There is a pronounced dependence of the extent of salting in by the large ion salts on the acidic and basic character of the non-electrolytes. The direction of the dependence is opposite to that observed for very small cations. Possible explanations are discussed.

Several recent studies[3-7] have emphasized that the influences of salts on the activity coefficients of non-electrolytes in aqueous solution are decidedly specific and also that salts with either large anions or large cations generally cause salting in. A recent review[8] summarizes available data on these points and discusses explanations.

Since theories for treating the salting in of non-electrolytes are at best incomplete, an important need is for data to point up the major variables. This paper reports a systematic study of the influence of both variations in the salt size and type and variations in the acidic or basic character of the non-electrolyte. The salts studied include examples with both large anions and large cations. The non-electrolytes studied are all simple derivatives or analogs of benzene and as a result have quite similar molar volumes and dipole moments.

Experimental

Activity coefficients of the non-electrolytes were measured by either a solubility or a distribution procedure. A convenient parameter for discussion of the salt effects is the salting out parameter, k_s, which for either of the experimental procedures is given by the general equation[8]

$$\log \frac{f_i}{f_i^{\circ}} = k_s C_s + k_i (C_i - C_i^{\circ}) \qquad (1)$$

where C_s is normality of the salt solution and f_i and f_i° are activity coefficients of the non-electrolyte in the salt solution and in the reference state, respectively. (Normal practice is to choose a dilute solution of the non-electrolyte as the reference state so that $\log f_i^{\circ}$ is zero by definition.) The second term on the right is called the self interaction term; k_i is the self interaction parameter and is generally negative; C_i and C_i° are concentrations of non-electrolyte in the actual and reference solutions, respectively. As suggested by the empirical Setschenow equation, $\log f_i = KC_s$, one normally obtains k_s from the slope of plots of $\log f_i$ *vs.* C_s. However, to do this one must be sure the self interaction term is negligible or is corrected for. When $\log f_i$ is determined from distribution experiments the non-electrolyte concentrations can be adjusted so that both C_i and C_i° and hence this term are very small. For solubility experiments one can generally neglect the self interaction term if S_i°, the solubility of the non-electrolyte, is below about 0.04 molar. However, even with a low value of S_i°, the term $k_i(S_i - S_i^{\circ}) \equiv k_i(C_i - C_i^{\circ})$ can be significant if there is extensive salting in since S_i can then become sizable. In the present study this occurred in a few cases and corrections were made using known or estimated values of k_i. For benzoic acid the measured value of $k_i = -0.9$ was used.[9] For phthalic acid, salicylic acid and benzene estimated values of -0.5, -0.5 and -0.2, respectively, were used.

The non-electrolytes are listed in Table I along with some pertinent properties. The phenol, salicylic and benzoic acids were reagent grade and were used without further purification. Phthalic acid was recrystallized from water. Benzylamine, piperidine, aniline and benzene were reagent grade and were redistilled.

(1) Presented in part at the 127th meeting of the American Chemical Society, Cincinnati, Ohio, March, 1955.

(2) Work supported in part by a grant from the Atomic Energy Commission.

(3) F. A. Long and R. L. Bergen Jr., THIS JOURNAL, **58**, 166 (1954).

(4) W. F. McDevit and F. A. Long, *J. Am. Chem. Soc.*, **74**, 1773 (1952).

(5) J. H. Saylor, A. I. Whitten, I. Claiborne and P. M. Gross, *ibid.*, **74**, 1778 (1952).

(6) M. A. Paul, *ibid.*, **74**, 5274 (1952).

(7) J. O'M. Bockris, J. Bowler-Reed and J. A. Kitchener, *Trans. Faraday Soc.*, **47**, 184 (1951).

(8) F. A. Long and W. F. McDevit, *Chem. Revs.*, **51**, 119 (1952).

(9) M. A. Paul, *J. Am. Chem. Soc.*, **75**, 2513 (1953).

TABLE I

NON-ELECTROLYTES STUDIED

Non-electrolyte	μ (Debye)	Molar vol., ml.	pK_A	pK_B	Wave length (mμ)
Phthalic acid	..	104.3 (solid)	2.90		281.0
Salicylic acid	2.6	95.7 (solid)	2.98		296.5
Benzoic acid	1.6	109.3	4.20		270.0
Phenol	1.7	87.9	9.89		271.0
Benzene	0	89.5			254.0
Aniline	1.5	91.6		9.42	287.5
Benzylamine	..	109.2		4.70	268.5
Piperidine	1.2	99.4		2.94	...

The large ion salts which were studied are listed in Table II in approximate order of ion size as judged from ionic conductances. When the data were not otherwise available, salting out studies were also made with the salts lithium, sodium and potassium chloride. All of the large ion salts were purified by recrystallization, usually from absolute ethanol, and were dried to constant weight.

TABLE II

LARGE ION SALTS

Salt	Equiv. ionic conductance of large ion
Ammonium thiocyanate	67.3
Tetramethylammonium bromide	44.93
Sodium benzenesulfonate	36.0
Sodium benzoate	34.9
Tetraethylammonium bromide	32.67
Trimethylphenylammonium chloride	....
Sodium *p*-toluenesulfonate	30.2
Tetra-*n*-propylammonium bromide	23.4

Activity coefficients of the following non-electrolytes were determined from solubility experiments: salicylic, phthalic and benzoic acids and benzene. Roughly 10-cc. samples of salt solutions containing excess non-electrolyte were placed in stoppered bottles which were attached to a rotating drum and permitted to equilibrate for at least 24 hours. All studies were made at 25.00 ± 0.01°.

A similar equilibration procedure was used for the distribution experiments except that here 10.00 ± 0.05 ml. of both the salt solution and the organic reference solvent were used plus a measured quantity of non-electrolyte. Procedures for experiments with piperidine (reference solvent benzene) were slightly different and have been described elsewhere.[3] For the other non-electrolytes, phenol, aniline and benzene, the reference solvent was spectro grade isooctane. This was found to be quite satisfactory since the solubility in isooctane of water and of the various salts is very low. The necessary information on the distribution of non-electrolyte between the isooctane and the salt-free aqueous phase was obtained by preliminary experiments employing a range of concentrations of each non-electrolyte.

The piperidine solutions were analyzed by titration. All the other non-electrolyte solutions with the exception of some runs with benzene were analyzed using an ultraviolet spectrophotometer. The wave lengths which were used for analysis of the various non-electrolytes are listed in the last column of Table I. Beer's law was found to apply for all non-electrolytes at all the concentrations measured. In the majority of cases the salts neither absorbed at the wave lengths used nor in any case shifted the wave length of maximum absorption. Corrections were made for salt absorption where this occurred. In a few cases the salts absorbed so strongly that it was not possible to analyze the aqueous solution to determine the non-electrolyte concentration. In the distribution experiments the water layer concentrations were determined by difference since the total amount of non-electrolyte added and the amount in the isooctane phase were known. Fortunately, these techniques enabled us to perform most of the desired experiments. Only the sodium benzoate effects on the solubility of salicylic and phthalic acids were omitted because of experimental difficulties.

Measurement of the solubility of benzene in solutions of salts which absorb in the ultraviolet region was done with a scaled down model of the apparatus used by McDevit and Long.[5] A check determination of the solubility of benzene in pure water by this method gave a result of C_i° = 1.79 g./l. in good agreement with results reported by McDevit and Long[5] (1.78) and by Bohon and Claussen[10] (1.79).

In all cases the activity coefficients and values of k_s which are wanted are those for the *un-ionized*, molecular species. Hence for the weak acids and bases it was necessary either to repress the ionization so that the measured solubilities and distribution ratios were for the un-ionized form or to make corrections for the concentration of ionized material present. Calculations show that contributions from the ionized forms of phenol and aniline are negligible. The ionization of piperidine, benzylamine and benzoic acid was adequately repressed by using aqueous solutions which contained 0.12 *M* piperidine hydrochloride, 0.0034 *M* benzylamine hydrochloride and 0.01 *M* sodium benzoate, respectively. (For these cases the reference phase for f_i° is a dilute solution of the non-electrolyte in the respective buffer ion solution rather than in pure water.) For the acids salicylic and phthalic it was not convenient to repress the ionization since the buffer ion interfered with the spectral analysis. For these cases the desired concentration of un-ionized acid was calculated from the measured solubility using the known values for the ionization constants of the acids in pure water. A more precise calculation would entail use of ionization constants for the particular salt solution but these values are not available.

For every non-electrolyte–salt pair, solubility or distribution experiments were made for at least four salt concentrations in the range of from 0.2 to 2 normal. In all cases plots of log f_i for the molecular species *vs.* C_s were linear within experimental error (see Fig. 1 and 2 for examples). Values of the salting out parameter k_s, were obtained from the slopes of these plots with correction for self interaction in a few cases.

Salting out studies, particularly with alkali halides have been reported for several of these non-electrolytes (see Table V for references). In most cases, where the same salts were studied, agreement between the present work and the earlier studies is good. One exception, which we are unable to account for, is for the case of tetramethylammonium bromide with benzene. The value of k_s which results from our work is −0.149 whereas the data of Saylor, Whitten, Claiborne and Gross[6] at 30° lead to k_s = −0.24.

Results and Discussion

Tables III and IV give examples of data for a single salt with two of the non-electrolytes studied.[11] Table III illustrates typical data and calculations for a distribution experiment. C_{H_2O} and C_{iso} are measured concentrations of benzylamine in 0.0034 *M* benzylamine hydrochloride plus salt and in the isooctane phase, respectively. $C^\circ_{H_2O}$ is the concentration of benzylamine in a solution of 0.0034 *M* benzylamine hydrochloride alone in equilibrium with the observed value of C_{iso}; it is calculated from the known distribution coefficient for salt-free solutions. The last two columns give log $f_i \equiv$ log $C^\circ_{H_2O}/C_{H_2O}$ and the value of k_s which results from a plot of log f_i *vs.* C_s.

Table IV gives data for solubility of salicylic acid in aqueous solutions of ammonium thiocyanate and illustrates the magnitude of the corrections for the ionized species for a case where the ionization is not repressed. The calculation of C_{mol}, the concentration of un-ionized salicylic acid, from the observed

(10) R. L. Bohon and W. F. Claussen, *J. Am. Chem. Soc.*, **73**, 1571 (1951).

(11) Complete data are available in the Ph.D. thesis of R. L. Bergen, Jr., Cornell University, June, 1955. This is on file at University Microfilms, Ann Arbor, Mich.

TABLE III

SALT EFFECT OF TETRAETHYLAMMONIUM BROMIDE FOR BENZYLAMINE, 25°

C_s (equiv./l.)	C_{H_2O} (g./l.)	C_{iso} (g./l.)	$C^{\circ}_{H_2O}$ (g./l.)	log f_i	Av. k_s
0	3.41	1.08	...	...	
0.60	4.12	1.12	3.51	−0.070	
1.00	3.98	0.943	3.02	−0.120	−0.114
1.40	5.10	1.14	3.57	−0.155	
2.00	5.61	1.084	3.41	−0.217	

solubility, C_t, was made using the value $pK = 2.98$ for salicylic acid in water at 25°.

TABLE IV

SALT EFFECT OF AMMONIUM THIOCYANATE FOR SALICYLIC ACID, 25°

C_s (equiv./l.)	C_t (moles/l.)	C_{mol} (moles/l.)	log f_i	Av. k_s
0.00	0.0159	0.0123	0.0	
0.49	.0181	.0142	− .061	
0.98	.0197	.0156	− .103	−0.100
1.40	.0200	.0159	− .112	
2.00	.0240	.0194	− .197	

Figures 1 and 2 give plots of log f_i *vs.* C_s for the non-electrolytes phthalic acid and benzylamine. Experimental points are given for a few of the curves. The salts studied and the values obtained for k_s are listed in each figure. Table V summarizes the k_s values obtained for all of the systems studied. It also includes data of other investigators particularly for the alkali halides.

Two general conclusions follow from the data of Table V. The first is that large ion salts quite generally lead to salting in, the effect increasing fairly regularly with the size of the large ion of the salt. This appears to be true for both large anions and large cations. The second conclusion, which is also evident from a comparison of Fig. 1 and 2, is that there is a pronounced dependence of the extent of salting in on the acidic or basic character of the non-electrolyte.

The tendency for large ion salts to cause salting in is in accord with the theory of McDevit and Long[4] which was developed for the case of non-polar non-electrolytes. This theory led to the following expression for the limiting value of the salting out parameter in infinitely dilute solution

$$k_s = \frac{\bar{V}_i^{\circ}(V_s - \bar{V}_s^{\circ})}{2.3\beta_0 RT} \qquad (3a)$$

$$= \frac{\bar{V}_i^{\circ}}{2.3RT}\frac{dP_e}{dC_s} \qquad (3b)$$

where β_0 is the compressibility of water, $\bar{V}_i^{\circ}$ is the partial molar volume of the non-electrolyte, $\bar{V}_s^{\circ}$ is the partial molar volume of the salt and V_s is the "liquid" volume of the salt.[12] In the alternate form (3b), P_e is Gibson's "effective pressure."[13] Equation 3 predicts salting in when the partial molar volume of the salt exceeds its liquid volume. Long and McDevit[7,8] have shown that this equation gives a satisfactory prediction of the salt order for salt effects on non-polar non-electrolytes although the predicted magnitude of k_s is usually somewhat larger than the observed. For the salting in salts of the present study, V_s or dP_e/dC_s values are available only for ammonium thiocyanate, tetramethylammonium bromide and tetraethylammonium bromide. The resulting values of $(V_s - \bar{V}_s^{\circ})$ are, respectively, −0.6, −15.6 and −23.0 ml./mole. Equation 3 thus correctly predicts salting in by all three salts. In addition the over-all salt order predicted by eq. 3 agrees well with the experimental results. It is most plausible that $(V_s - \bar{V}_s^{\circ})$ for tetrapropylammonium bromide will be even more negative, in agreement with the observed larger salting in by this salt. Unfortunately no data are available for the large anion salts.

A likely explanation of the observed values of the term $(V_s - \bar{V}_s^{\circ})$ is that they depend at least partly on the interaction of the ions with the structure of the water and that the values are positive for "order-producing" solutes and negative for disorder-causing solutes.[16] In this sense salting in oc-

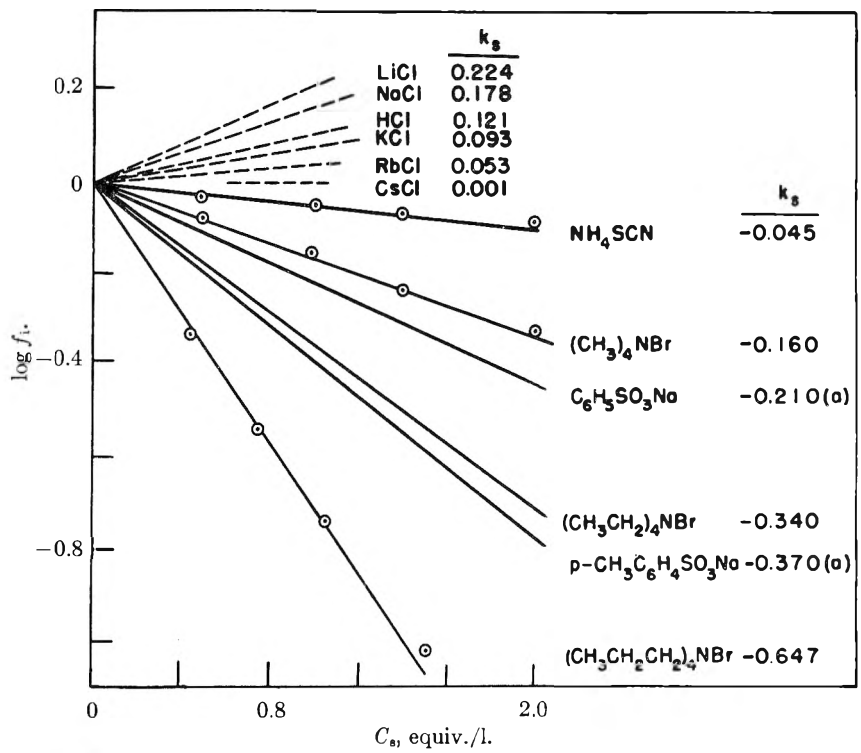

Fig. 1.—Salt effects for phthalic acid at 25°; dotted lines are data of Rivett and Rosenblum[14]; data marked (a) are from Freundlich and Slottman.[15]

(12) B. Lunden, *Z. physik. Chem.*, **192**, 345 (1943).

(13) R. E. Gibson, *Am. J. Sci.*, [5] **35A**, 49 (1938); see also H. S. Harned and B. Owen, "The Physical Chemistry of Electrolytic Solutions," Reinhold Publ. Corp., New York, N. Y., 1942, p. 271–274.

(14) A. C. D. Rivett and E. I. Rosenblum, *Trans. Faraday Soc.*, **9**, 297 (1914).

(15) H. Freundlich and G. V. Slottman, *Biochem. Z.*, **188**, 101 (1927) (at 20°).

(16) For a discussion of this aspect of ionic solutions see R. W.

TABLE V

VALUES OF k_s FOR SEVERAL NON-ELECTROLYTES AND SALTS AT 25°

Salt/Non-electrolyte	Salicylic acid	Phthalic acid	Benzoic acid	Phenol	Benzene	Aniline	Benzylamine	Piperidine
HCl	0.081[17]	0.121[14]	0.082[17]	...	0.048[1]	...	...	...
LiCl	.192[18]	.224[14]	.189[19]	0.143[21]	.141[4]	0.07[23]	0.08±	0.056
NaCl	.117[18]	.178[14]	.182[19]	.172[22]	.195[4]	.136	.112	.156
KCl	.120[18]	.093[14]	.144[19]	.122	.166[4]	.115	.140	.167
RbCl	...	.053[14]	...	...	.140[4]	.09[23]	...	.135
CsCl	...	.001[14]	...	...	.088[4]	.02[23]	...	...
NH_4SCN	− .100	− .045	− .051	− .075	− .040	− .072	...	...
$(CH_3)_4NBr$	− .199	− .160	− .140	− .186	− .149	− .185	− .065	− .095
$C_6H_5SO_3Na$	− .210[18]	− .210[15]	− .170[18,15]	− .092	− .090	− .062	− .074	.000
$C_6H_5CO_2Na$	...	...	− .218[20]	− .130	− .052	− .043	− .048	− .037
$(CH_3CH_2)_4NBr$	− .440	− .316	− .360	− .346	− .248	− .308	− .114	− .047
$(CH_3)_3C_6H_5NCl$	− .492	...	− .365	− .343	...	− .266	− .069	− .059
p-$CH_3C_6H_4SO_3Na$	− .415[18]	− .370[15]	− .355[15,18]	− .228	− .070	− .093	− .105	− .108
$(CH_3CH_2CH_2)_4NBr$	− .821	− .647	− .706	− .639	− .408	− .380	− .145	− .095

curs when a solute causes a loosening-up or disordering of the water structure and salting out occurs when the electrolyte leads to increased order.

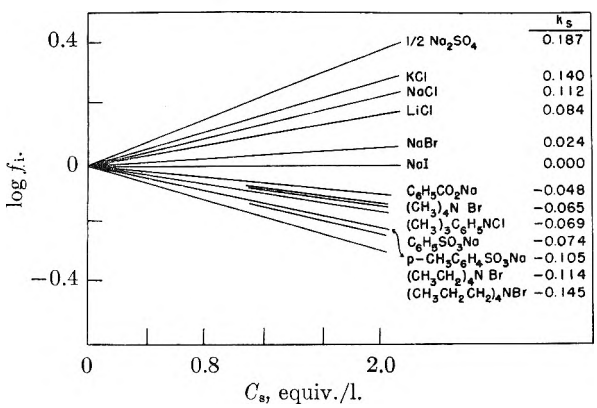

Fig. 2.—Salt effects for benzylamine at 25°.

Equation 3 should hold at least qualitatively for polar non-electrolytes also. Relative to a non-polar molecule of similar molar volume, the existence of a dipole moment should lead to more salting in of a polar molecule for any given salt. However, the general salt order might be expected to be much the same for the two. Table V shows this is in general true. In a more detailed sense there are pronounced variations both in the salt order and in the amount of salting out and salting in and it is evident that both of these variations depend on the acidic and basic character of the non-electrolyte.

Figures 3 and 4 show these trends in a more explicit fashion. These figures give plots of the quantity $(k_{KCl} - k_x)$ for the salting out parameter of each salt, *relative* to the value of k_s for the reference salt potassium chloride. The use of this relative value minimizes differences which may enter from variations in dipole moment and molar volume for the various non-electrolytes. The values of $(k_{KCl} - k_x)$ are plotted against the pK_A and pK_B values of the non-electrolyte; the latter are listed on scales which extend to 14 at the reference line. Finally, the relative salt effects for benzene are given on the reference line.

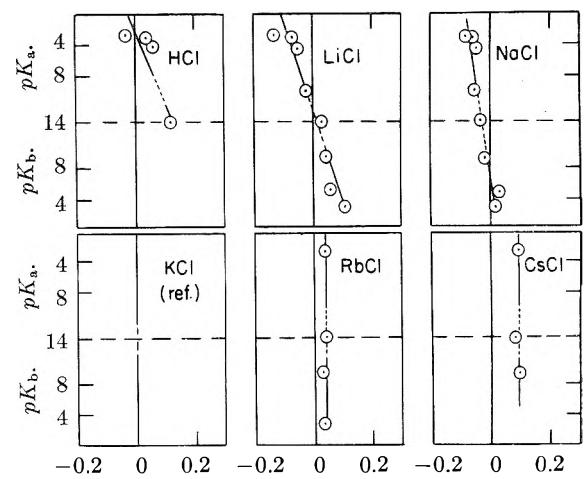

Fig. 3.—Plots of relative salting out parameter, $(k_{KCl} - k_x)$, *vs.* pK_a and pK_b for alkali chlorides with substituted benzenes.

Figure 3 for the alkali chlorides shows the general trend toward more salting in as the cation size increases. For example, rubidium and cesium chlorides give more salting in than potassium chloride for all of the non-electrolytes. This trend is in agreement with the predictions of eq. 3. Figure 3 also shows the character of the acid and base effect for the alkali cations. For the smallest ions, lithium and hydrogen, there is a distinct tendency for more salting out with acidic non-electrolytes and less salting out with basic. Qualitatively the effects increase with increasing values of pK_A and pK_B.

The data of Fig. 4 for the large ion salts show that ammonium thiocyanate and tetramethylammonium bromide continue the trend noted with rubidium and cesium chlorides, *i.e.*, an increase of salting in with ion size but no acid–base dependence. However, with tetraethylammonium bromide the acidic

Gurney, "Ionic Processes in Solution," McGraw-Hill Book Co., New York, N. Y., 1955, and also R. E. Gibson and J. F. Kincaid, *J. Am. Chem. Soc.*, **59**, 580 (1937).

(17) J. Kendall and J. Andrews, *J. Am. Chem. Soc.*, **43**, 1545 (1921).

(18) A. Osol and M. Kilpatrick, *ibid.*, **55**, 4440 (1933).

(19) I. M. Kolthoff and W. Bosch, THIS JOURNAL, **36**, 1685 (1932).

(20) E. Larsson, *Z. physik. Chem.*, **148**, 148 (1930) (at 18°).

(21) W. Herz and E. Stanner, *ibid.*, **128**, 399 (1927).

(22) K. Endo, *Bull. Chem. Soc. (Japan)*, **2**, 124 (1927).

(23) S. Glasstone, J. Bridgman and W. R. P. Hodgson, *J. Chem. Soc.*, 635 (1927).

non-electrolytes are distinctly more salted in than are the basic. This trend is even more pronounced with the larger tetrapropylammonium bromide. Quite evidently the effects depend qualitatively on the acid and base strengths of the non-electrolytes but in the opposite direction to the dependence with lithium chloride. With the large anion salts the effects are more complex. There is increased salting in of the acidic species relative to benzene and the effect increases with acid strength but with the basic species there appears to be little or no change with base strength. Conceivably, an explanation for this different behavior of the large anions could depend on the fact that they all have a decidedly asymmetric charge distribution. Actually this sort of explanation does not appear to be tenable since one of the large cations, trimethylphenylammonium ion, is decidedly asymmetric and yet its behavior is almost identical with that of tetraethylammonium ion.

It is doubtful that a single theory of salt effects will permit explanation of the different sorts of acid–base dependence which are exhibited, for example, by lithium chloride, by a large cation salt such as tetraethylammonium bromide and by a large anion salt. A tentative explanation for the first type of acid–base effect was previously given by considering the variations in hydration of the cations.[3,8] The proposal was that the water molecules which hydrate a cation will be oriented with their protons outwards and that as a result there will be a net repulsion between these protons and an acidic non-electrolyte and a net attraction between the protons and a basic non-electrolyte. (An inverse acid–base dependence would be predicted for highly hydrated anions and this is experimentally found to be true.[8]) These hydration effects should make significant contributions to the salting out parameters only for the small or highly charged cations for which hydration will be extensive. Thus the disappearance of the acid–base effect for rubidium and cesium ions is the expected result. On this basis one would predict that for either cations or anions of still larger size, there would be no dependence of salting out on the acidic or basic character of the non-electrolyte. Figure 4 shows that this prediction does not hold.

A different sort of explanation for the dependence of salt effects on the acid or base character of the non-electrolyte can be based on the notion that the effect involves changes in the water structure and that the various acidic and basic species differ in their sensitivity to such structure changes. As noted earlier it seems reasonable to suppose that the typical "salting out" electrolytes have an order-increasing effect on water and that the electrolytes which lead to salting in are disorder causing. In this sense lithium or hydrogen ion and tetrapropylammonium ion may represent two extremes. Furthermore it is not unreasonable that acidic molecules may be relatively more salted in than basic by a loosening or disordering of the water structure (due, for example, to a tendency of an acidic molecule to be attracted to the oxygen of a "depolymerized" water molecule).

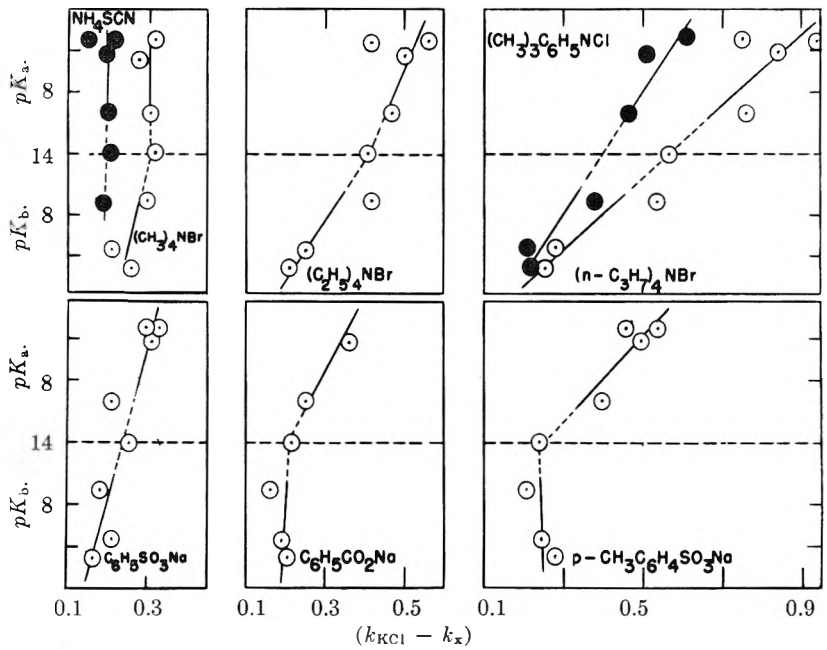

Fig. 4.—Plots of $(k_{KCl} - k_x)$ *vs.* pK_a and pK_b for large ion salts with substituted benzenes.

This explanation is pretty speculative and needs to be subjected to further study. There is however one somewhat indirect piece of evidence which supports the idea of a varying sensitivity of acidic and basic species to modification of the medium. This concerns the values of the self interaction parameter k_i for the non-electrolytes of Table II. Values of k_i can be estimated from data on the vapor pressure, boiling point elevation or freezing point depression of solutions of the non-electrolytes in water and also from combined solubility and distribution data as was done for phenol.[8] From data of this sort we have arrived at the following estimates of k_i: benzoic acid −0.9; phthalic acid −0.5; phenol −0.16; aniline −0.2; benzylamine −0.05. The larger negative values of k_i shown by the acidic species is at least consistent with the notion that these are relatively more solubilized by a loosening of the water structure.

NOTES

FREEZING POINT DIAGRAMS OF SOME SYSTEMS CONTAINING TNT. II

By Lohr A. Burkardt and Donald W. Moore

Chemistry Division, U. S. Naval Ordnance Test Station, China Lake, California

Received September 6, 1955

In the course of a study of the physical properties of 2,4,6-trinitrotoluene (TNT), data are being acquired on a number of binary systems containing TNT. Freezing point data of two of these systems TNT–2,4,6-trinitro-1,3-dimethyl-5-*t*-butylbenzene and TNT–2,4,6-trinitrobenzoic acid are presented here. These systems do not appear to have been investigated previously.

The TNT used in these studies had a vacuum melting point of 80.9°. The 2,4,6-trinitro-1,3-dimethyl-5-*t*-butylbenzene was Eastman Kodak Co. material melting at 111.5°. The trinitrobenzoic acid was Eastman Kodak Co. material melting at 227°.

The apparatus used for determining freezing points has been described elsewhere.[1] Three-gram samples were taken and temperatures were determined with 10% rhodium–platinum thermocouples. Supercooling of the melts was minimized by withdrawing small portions of the melt on a platinum ribbon, allowing the material to solidify and returning it to the melt.

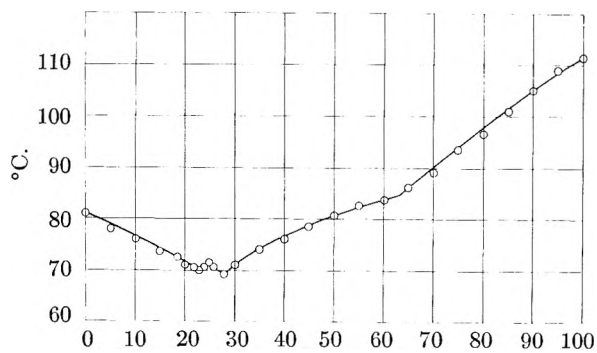

Mole % 2,4,6-trinitro-1,3-dimethyl-5-*t*-butylbenzene.

Fig. 1.

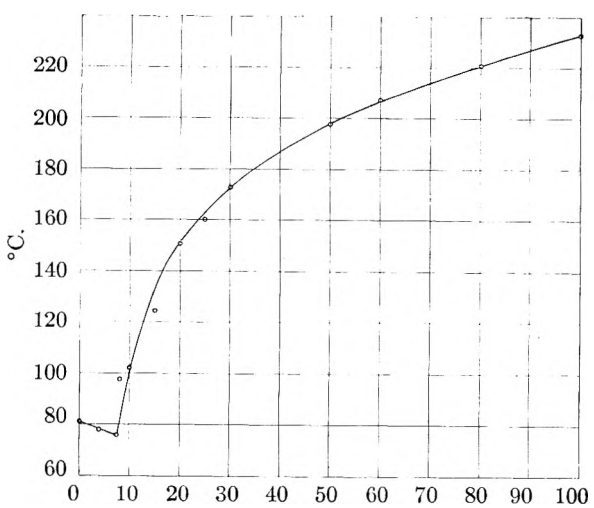

Mole % trinitrobenzoic acid.

Fig. 2.

The system TNT–2,4,6-trinitro-1,3-dimethyl-5-*t*-butylbenzene was found to form two compounds. The first compound contains one mole of 2,4,6-trinitro-1,3-dimethyl-5-*t*-butylbenzene and three moles of TNT. This compound melts at 71.5°. The second compound, which appears to contain two moles of 2,4,6-trinitro-1,3-dimethyl-5-*t*-butylbenzene, is indicated by the incongruent melting point of 83.8° found at a composition of 61.5 mole % 2,4,6-trinitro-1,3-dimethyl-5-*t*-butylbenzene. Two eutectic mixtures are formed. These occur at 23 and 28 mole % 2,4,6-trinitro-1,3-dimethyl-5-*t*-butylbenzene and melt at 70 and 69.5°, respectively. Data for this system are shown in Fig. 1.

The system TNT–2,4,6-trinitrobenzoic acid shows a eutectic mixture melting at 76° and containing 7.5 mole % 2,4,6-trinitrobenzoic acid. Compositions containing more than 20 mole % of 2,4,6-trinitrobenzoic acid show evidence of decomposition. Attempts to rerun these compositions resulted in successively lower freezing points with each remelting of the material. Data for this system are shown in Fig. 2.

(1) L. A. Burkardt, D. W. Moore and W. S. McEwan, *Rev. Sci. Inst.*, **40**, 461–2 (1953).

THE HEAT OF COMBUSTION OF TRI-*sec*-BUTYLBORANE

By E. A. Haseley, A. B. Garrett and Harry H. Sisler[1]

Contribution from the McPherson Chemical Laboratory of The Ohio State University, Columbus, Ohio

Received April 2, 1956

In conjunction with work in progress in this Laboratory the heat of combustion of tri-*sec*-butylborane has been determined. It was interesting to compare the data obtained for this compound with data obtained in a similar study of tri-*n*-butylborane by Tannenbaum and Schaeffer.[1a]

Experimental

Tri-*sec*-butylborane.—Tri-*sec*-butylborane was prepared according to the method of Johnson, Snyder and Van Campen.[2] The reaction mixture was fractionated and the fraction boiling between 85 and 86° at 9–10 mm. was used in this work. The infrared spectrum of the product was in excellent agreement with a spectrum of tri-*sec*-butylborane supplied by Beachell.[3]

Apparatus and Procedure.—The combustion measurements were carried out in a non-adiabatic Parr Calorimeter using a double valve bomb with a capacity of 360 ml. The bomb was calibrated with standard benzoic acid supplied by the Parr Instrument Company, according to the proce-

(1) S. Tannenbaum and P. S. Schaeffer, *J. Am. Chem. Soc.*, **77**, 1385 (1955).

(1a) Department of Chemistry, Univ. of Florida, Gainesville, Fla.

(2) J. R. Johnson, H. R. Snyder and M. G. Van Campen, Jr., *ibid.*, **60**, 115 (1938).

(3) H. C. Beachell, private communication.

dure outline in the Parr Manual.[4] The only modifications of this procedure in the experimental runs were that the sample was contained in glass bulbs as described by Tannenbaum, Kaye and Lewens[5] and that the usual Parr sample container was placed in a tight fitting 98% nickel sleeve to increase the depth by about 1/2 inch and thus prevent spattering of the unburned sample on the cold bomb walls. A pressure of 30 atmosphere of oxygen was used in all cases.

Analysis.—Carbon dioxide was determined by bleeding the bomb gases through a standard carbon dioxide absorption train containing carboxite (Fisher Scientific Co.) as the absorbent, and then flushing the bomb three or four times with oxygen under 10 atmospheres pressure. Boron analyses were made by determining the boric acid present in the reaction products. The determinations were made by titrating samples of the washings with sodium hydroxide, using a *p*H meter to determine the end-point.

Treatment of Data.—The total raw heat value obtained from the combustion measurement was corrected for the contributions of the fuse wire and masking tape (which was used to hold the fuse to the sample bulb) and for the sample weight to give ΔE_1 (cal./g.). To this value were added the correction factors shown in Table I which are as follows: the conversion to 1 atmosphere pressure and to a constant pressure process giving $\Delta H_1 = \Delta E_1 - 29$ cal./g.; corrections for the conversion of boric acid to B_2O_3, $\Delta H_2 =$ 13 cal./g. sample; and correction for the oxidation of unburned carbon (assumed to be amorphous) to CO_2, ΔH_3. Since it was not possible to obtain accurate boron analyses in the concentration range used in this work, it was assumed on the basis of the rough values (which ranged from 95 to 100% of the theoretical value) that the combustion of boron was 97.5% complete in all cases. In view of the low weight per cent. of boron in the sample, this approximation seems justifiable. The correction for unburned boron (assumed to be elemental) is thus constant at $\Delta H_4 = -21$ cal./g. sample. The heat of combustion (ΔH_c) is then given by $\Delta H_1 + \Delta H_2 + \Delta H_3 + \Delta H_4$.

Results and Discussion

The results of six consecutive determinations are given in Table I.

TABLE I

Sample wt., g.	CO_2, % theor.	$-\Delta H_1$, kcal./g. sample	$-\Delta H_3$, kcal./g. sample	ΔH_c, kcal./g. sample
0.5085	98.8	11.590	0.078	11.68
.3442	96.1	11.453	.248	11.71
.5318	99.4	11.665	.039	11.71
.5151	98.1	11.518	.121	11.65
.8202	99.5	11.646	.030	11.68
.5209	98.0	11.559	.131	11.70
			Av.	11.69

Since the precision of the values of ΔH_c is quite good despite variations in the degree of combustion and in the sample weight used, it appears that the corrections employed are satisfactorily self-consistent.

The value 11.69 kcal./g. for tri-*sec*-butylborane corresponds to 2130 kcal./mole in comparison with Tannenbaum and Schaeffer's value of 2110 ± 10 kcal./mole for tri-*n*-butylborane. This latter was calculated without corrections for unburned carbon and boron which averaged about 1% of the theoretical. On consideration of these corrections and of the inherent differences in the alkyl groups, these two values seem quite compatible. It is also felt that by using the corrections mentioned above, increased confidence can be placed in the results—in fact, it does not seem likely that our values should be in error by more than 0.3%. The presence in the residue of unburned boron and carbon in the elemental state has been found by other workers who have studied compounds of this type.

On the basis of the foregoing statements, the corrections applied, and the consistency of the values in Table I it may be concluded that the heat of combustion of tri-*sec*-butylborane is 2130 ± 6 kcal./mole. From this value and the following heats of formation: B_2O_3(s), −306 kcal./mole[6]; CO_2(g), −94.1 kcal./mole[7]; H_2O(l), −68.3 kcal./mole,[7] the heat of formation of this compound may be calculated to be −75 kcal./mole.

(4) "Oxygen Bomb Calorimetry and Oxygen Bomb Combustion Methods," Parr Manual No. 120, Parr Instrument Co., Moline, Ill.

(5) S. Tannenbaum, S. Kaye and G. F. Lewens, *J. Am. Chem. Soc.*, **75**, 3753 (1953).

(6) E. J. Prosen, W. H. Johnson and F. Y. Pergiel, Natl. Bur. Standards Report No. 1552, March 26, 1952.

(7) F. D. Rossini, D. D. Wagman, W. H. Evans, S. Levine and I. Jaffee, "Selected Values of Chemical Thermodynamic Properties," Circular No. 500, Natl. Bur. Standards, Feb. 1, 1952.

STUDIES OF THE RECOIL TRITIUM LABELING REACTION. II. METHANE AND ETHANE[1]

BY RICHARD WOLFGANG, JOSEPH EIGNER[2] AND F. S. ROWLAND

Received February 4, 1956

Brookhaven National Laboratory Upton, Long Island, New York
Princeton University, Princeton, New Jersey

A tritium atom produced in the $Li^6(n,\alpha)T$ nuclear reaction recoils with an initial kinetic energy of 2.7 Mev. This energy makes it potentially more reactive chemically than hydrogen atoms produced by more conventional means. About 12% of these recoil tritium atoms enter non-labile positions in the parent molecule when stopped in crystalline sugars.[3,4] It is not practical, however, to determine the chemical fate of all of the tritium reacting in sugars because of the great number of possible degradation and polymeric products which could have been formed. With the simple alkanes of the present study, these products are such that a determination of the location of almost all of the tritium is quite feasible.

The irradiation mixtures consisted of low temperature slurries of approximately 40 mg. of Li salt and 3 mg. of alkane, sealed in quartz capillaries. These tubes were irradiated for 30–60 seconds in the Brookhaven reactor at −160°. After irradiation, they were warmed to room temperature *in vacuo* and then broken mechanically. A protective brass cup prevented the resultant explosion from shattering the vacuum line.

Measured volumes of carrier ethane, propane and *n*-butane were introduced into the line, mixed with

(1) Research carried out under the auspices of the U. S. Atomic Energy Commission.

(2) Chemistry Department, Harvard University, Cambridge, Massachusetts.

(3) R. Wolfgang, F. S. Rowland and C. N. Turton, *Science*, **121**, 715 (1955).

(4) F. S. Rowland, C. N. Turton and R. Wolfgang, *J. Am. Chem. Soc.*, **78**, 2354 (1956).

the irradiated alkane, and condensed in a trap cooled with solid nitrogen, reducing the vapor pressure of methane to about 50 μ. Hydrogen gas was then admitted, and an aliquot removed and counted as described below. After pumping off the remaining hydrogen, repetition of this procedure with a second batch of carrier hydrogen always yielded a negligible activity. This, together with the reproducibility of the results, indicates a valid assay of the amount of HT produced.

Following removal of the hydrogen carrier, the alkanes were separated from each other by distillation successively from liquid nitrogen, frozen isopentane and liquid isopentane. As gas was evolved, it was removed batchwise for counting. Traces of higher alkanes were permitted to distil into the final fraction by warming the trap to room temperature. The ethane run was performed similarly, with the inclusion of methane carrier gas.

All counting was done using silver-walled glass, gas proportional counters.[5] The sample to be counted was expanded into the counter and then filled to a pressure of 70 cm. with "P-10" (90% A, 10% CH_4) counter gas.

Figure 1 shows the results of a typical run on a slurry of methane with $Li_2SO_4 \cdot H_2O$ particles. The specific activity of the successive fractions is plotted against the cumulative volume of carrier

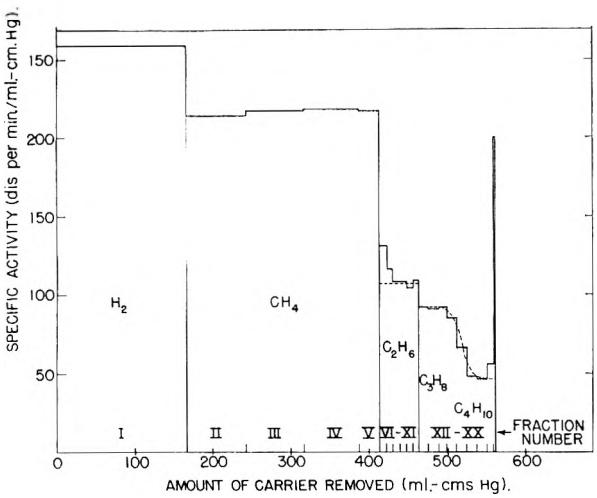

Fig. 1.—Activity spectrum from carrier distillation of tritium irradiated methane.

removed. In this plot, the areas corresponding to each carrier fraction are proportional to the per cent. of the total activity present in that carrier fraction. The hydrogen carrier was removed in one fraction, and the successive methane samples showed substantially constant specific activity. However, the distillation of the ethane carrier showed a small but steady decrease in specific activity, consistent with the preferential distillation of carrier-free radioactive ethylene in the earlier fractions. The amount of C_2H_3T is estimated from the area of the histogram above the ethane carrier asymptote. A number of other C_3 and C_4 compounds would also be removed in the propane and *n*-butane fractions, and the activity cannot be assigned to particular compounds. The rise in specific activity at the end of the distillation is attributed to still higher hydrocarbons.

Table I summarizes the data on the percentages of the total activity found in each carrier for five methane and one ethane runs. Three different lithium salts were used as the sources of the energetic tritium atoms. The Li_2CO_3 and LiF particles were 1 μ or less in diameter, while the $Li_2SO_4 \cdot H_2O$ had been sieved to select particles of diameter 53–61 μ. The reproducibility appears to be quite satisfactory and presumably indicates that the surfaces of the lithium compounds do not influence the reactions and final combination of the "hot" tritium.

Thermal hydrogen atoms do not react with gaseous methane[6] and it is reasonable to assume they would not attack the liquid at −160°. Hence the finding that recoil tritium reacts with methane, giving labeled products, confirms that recoil tritium labeling reactions do indeed proceed while the tritium still has excess kinetic energy, *i.e.*, they are "hot-atom" reactions. However, the result (Table I) that most of the tritium goes into HT and the tagged form of the alkane irradiated, is also consistent with the earlier hypothesis[6] that this excess energy has become quite small when the tritium finally reacts to enter stable combination. Probably most tritium atoms, having lost nearly all their recoil energy, are finally stopped by a collision in which they break a single bond and then combine with one of the radicals formed to yield HT, CH_3T or C_2H_5T. Walden inversion and hydrogen abstraction reactions by these "epithermal" atoms would also yield these products. (These possible alternate mechanisms are presently being studied using other systems.)

TABLE I

CHEMICAL COMBINATION OF TRITIUM FROM IRRADIATED ALKANE–LITHIUM SYSTEMS (PER CENT. OF TOTAL ACTIVITY)

	Irradiation mixture						C_2H_6
			CH_4				
Active product	Li_2CO_3	Li_2CO_3	LiF	LiF	$Li_2SO_4 \cdot H_2O$	Best values	LiF
H_2	40.3	39.1	40.6	38.2	39.3	39.1	41.7
CH_4	44.7	47.6	47.0	49.4	48.9	48.6	5.4
C_2H_6	~10	6.8	..	5.90	4.80	5.5	37.5
C_2H_4[a]			..	~0.36	~0.31	~0.3	~4.0
C_3 fraction	~4.9	6.5	..	4.14	4.27	4.2	5.3
C_4 fraction			..	1.86	2.05	2.0	5.9
$C_{>4}$ fraction[a]			..	~0.30	~0.38	~0.3	>0.3

[a] No corresponding carrier present.

The occurrence of many-carbon and unsaturated molecules among the labeled products requires a more complex reaction path. In these cases, the tritium must have sufficient energy left on arriving at the end of its track to rupture several bonds, producing radicals such as CH_2, or charged fragments, etc. The decreasing probability of finding labeled higher hydrocarbons is a measure of the decreasing probability of producing larger numbers of fragments in the immediate vicinity of the end of the range of the tritium atom.

(5) W. Bernstein and R. Ballentine, *Rev. Sci. Instr.*, **21**, 158 (1950).

(6) E. W. R. Steacie, "Atomic and Free Radical Reactions," 2nd ed., Reinhold Publ. Corp., New York, N. Y., 1954.

ACTIVITY COEFFICIENTS OF BENZOIC ACID IN SOME AQUEOUS SALT SOLUTIONS

BY JAMES N. SARMOUSAKIS AND MANFRED J. D. LOW

Wm. H. Nichols Chemical Laboratory, New York University, University Heights, New York 53, N. Y.

Received February 6, 1956

The considerable mass of data on the salting-out and salting-in of benzoic acid in aqueous solution[1] does not include any extensive contributions on the effects of thiocyanates[2] or hexafluorophosphates on the solubility of benzoic acid in water. Accordingly, an investigation of the activity coefficients of benzoic acid in aqueous solutions of sodium thiocyanate, potassium thiocyanate and potassium hexafluorophosphate has been made, and its results are now reported.

Experimental.—Solid benzoic acid was brought to equilibrium with water or the various salt solutions in Pyrex bottles turning over in a water thermostat at 25 ± 0.01°. Samples of the resulting solutions were removed by means of wide-mouth pipets equipped with filter paper tips. Measured portions were then titrated with carbonate-free sodium hydroxide solution, employing phenolphthalein as indicator, while CO_2-free air was bubbled through the solution. Empirical corrections were applied for benzoic acid taken up by the filter paper tips. In most cases attainment of equilibrium was verified by titrating samples of a given solution after widely differing times of equilibration. Titration of aqueous solutions containing known amounts of benzoic acid with large concentrations of the various salts, after long standing, yielded analytical results agreeing with the stoichiometric amounts of acid within the experimental error of the analysis. Accordingly, indicator salt error and any effects due to chemical interaction of the salts with acid or water, leading to incorrect analytical results, were taken as negligible.

The aqueous solutions were made up by weighing out the appropriate amounts of potassium hexafluorophosphate or concentrated thiocyanate solutions, standardized by the Volhard method, into calibrated volumetric flasks, adding from a pipet the amount of carbonate-free sodium hydroxide solution necessary to render the final solution 0.01109 molar in that compound, and making up to volume with CO_2-free water. The benzoic acid was Baker U.S.P. grade. The values of the acid solubility in pure water obtained with this material did not differ significantly from those determined employing the following: Baker U.S.P. benzoic acid recrystallized up to four times from water, Baker U.S.P. benzoic acid precipitated from ethanol solution with water, Bureau of Standards benzoic acid, Bureau of Standards acid once recrystallized from water, and Bureau of Standards acid precipitated from ethanol solution with water. Reagent grade sodium thiocyanate and potassium thiocyanate were recrystallized at least twice from water. Potassium hexafluorophosphate[3] was recrystallized at least once from water made alkaline with sodium hydroxide by the method of Woyski.[4]

The small corrections required to obtain the concentrations of molecular benzoic acid (molecular solubilities) from the stoichiometric solubilities were calculated from estimates of the classical dissociation constants of benzoic acid in the various salt solutions. These estimates were based on the data of Kilpatrick[5] for the classical dissociation constants and molar activity coefficients of the molecules of benzoic acid in aqueous solutions of potassium chloride and sodium chloride at 25°. It was assumed that the dissociation constants of benzoic acid at a given concentration of potassium (or sodium) salts of various univalent anions in aqueous solution would vary approximately as the molar activity coefficients of molecular benzoic acid in the solutions irrespective of the nature of the anion.

Results.—The values of the experimentally determined solubilities of benzoic acid in aqueous solutions of potassium thiocyanate, sodium thiocyanate and potassium hexafluorophosphate, all 0.01109 molar in sodium benzoate, are recorded in Table I as functions of the molar concentrations, C_s, of the salts.

TABLE I

SOLUBILITY OF BENZOIC ACID IN SALT SOLUTIONS AT 25.00°

(All solutions 0.01109 molar in sodium benzoate.)

KCNS		NaCNS		KPF_6	
Salt concn., mole/l.	Solubility, mole/l.	Salt concn., mole/l.	Solubility, mole/l.	Salt concn., mole/l.	Solubility, mole/l.
0.0739	0.02669	0.1495	0.02647	0.0540	0.02651
.1293	.02679	.1573	.02648	.1092	.02645
.2683	.02719	.3247	.02645	.1096	.02641
.3236	.02726	.3547	.02645	.1635	.02640
.4012	.02739	.5511	.02635	.2181	.02628
.4809	.02757	.6429	.02621	.2187	.02642
.4943	.02761	.7429	.02616	.2719	.02629
.6807	.02777	1.150	.02582	.3256	.02630
.7077	.02786	1.153	.02578	.3813	.02616
.989	.02824	1.995	.02450	.4425	.02609
1.361	.02847	2.324	.02351		
1.463	.02851				
1.571	.02847				
1.935	.02829				
2.892	.02739				
3.237	.02641				

An estimate, −1.5794, of the logarithm of the molecular solubility, S^0, of benzoic acid in 0.01109 molar sodium benzoate solution was obtained by graphical extrapolation to zero concentration of added salt in plots of the logarithms of the molecular solubilities, S, of the acid in the thiocyanate solutions, or by the method of least squares for the hexafluorophosphate solutions assuming a linear relation of log S to the salt concentration. The logarithms of the molar activity coefficients, f, of the molecular benzoic acid given by the relation $f = S^0/S$, as function of the concentrations, C_s, of the added salt in the solutions are represented in Fig. 1 together with the least square line for the hexafluorophosphate solutions and the visually estimated best smooth curves through the points for the thiocyanate solutions.

In dilute solution the activity coefficient of the non-electrolyte, benzoic acid, is given by the relation[1] $\log f = k_B S + k_s C_s$, where k_s is the salting-out parameter and k_B is the "self-interaction" parameter for the benzoic acid. The limiting slopes of the curves in Fig. 1 at zero concentration of salt serve as estimates of k_s, namely, 0.004, −0.037 and 0.017 for sodium thiocyanate, potassium thiocyanate and potassium hexafluorophosphate, respectively. In the case of the thiocyanates the expected additive property of the salting-out parameter[6] is exhibited since the value of k_s for sodium thiocyanate minus that for potassium thiocyanate is 0.041, to be compared with the corresponding values, 0.041 and

(1) F. A. Long and W. F. McDevit, *Chem. Revs.*, **51**, 119 (1951).

(2) H. Freundlich and A. N. Seal, *Kolloid Z.*, **11**, 257 (1912), report values of 0.02799, 0.02891 and 0.02950 *M* for the solubilities of benzoic acid in unbuffered 0.0, 0.5 and 1.0 *M* aqueous potassium thiocyanate solutions, respectively.

(3) The donation of a supply of this salt by the Ozark-Mahoning Company Tulsa, Oklahoma, is gratefully acknowledged.

(4) M. M. Woyski, "Inorganic Syntheses," Vol. III, McGraw-Hill Book Co., Inc., New York, N. Y., 1953, p. 111.

(5) M. Kilpatrick, *J. Am. Chem. Soc.*, **75**, 585 (1953).

(6) E. Larsson, *Z. physik. Chem.*, **153**, 299 (1931).

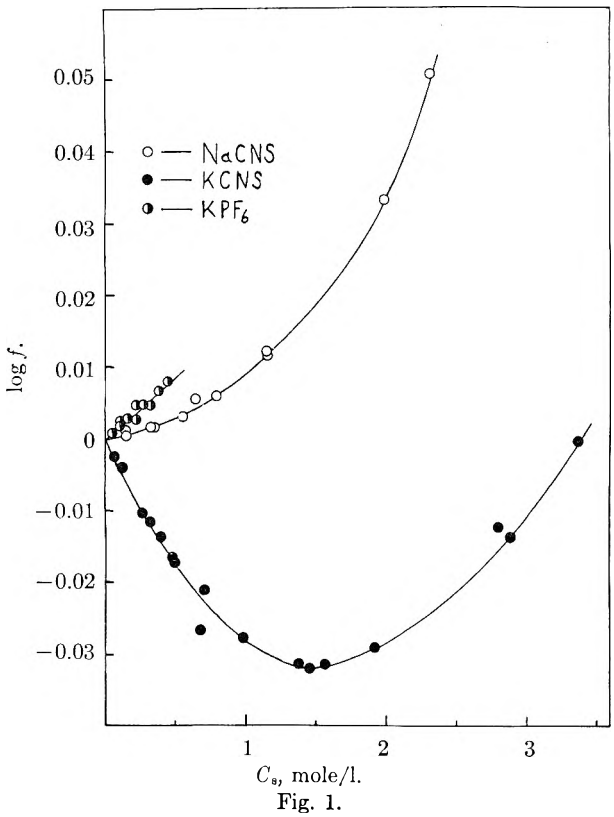

Fig. 1.

0.039, for chlorides and nitrates[7] and 0.042 for bromides.[8] The ionic salting-out constants for the thiocyanate and hexafluorophosphate ions, based on a value, 0.070,[6,7] for that of potassium ion, are −0.107 and −0.053, respectively. These numbers, when compared with corresponding data for other ions, follow reasonably well the generally recognized increasing trend of the ionic salting-out parameters with decreasing ion size.[1] Ionic salting-out parameters for the anions Cl^-, Br^-, I^-, NO_3^-, ClO_4^-, PF_6^- and CNS^-, are 0.70,[7] 0.038,[8] −0.016,[8] −0.034,[7] −0.052,[7] −0.053 and −0.107, respectively. Corresponding anion crystal radii (in Å.) are 1.81,[9] 1.95,[9] 2.16,[9] 2.6,[10] 2.9,[11] 2.9[12] and 3.1,[13] respectively. The radius given for the linear thiocyanate ion is an estimate of half the length of that ion and is to be looked upon as a maximum value. It is seen that the orders of salting-out parameters and anion radii have the expected correspondence.

Features worthy of note in Fig. 1 are the non-linearity of the curves for thiocyanates and the minimum in log f for potassium thiocyanate at about 1.5 M salt concentration. Usually the relation of log f to the molar concentration of a given salt is linear.[1] No ready explanation is at hand for the two effects mentioned. Any specific interactions of the thiocyanate ion with the non-electrolyte acid molecules might be expected to be monotonically increasing with the concentration of the salt. Further, with respect to interaction of the salt ions with water, the ratio of the total internal pressure in aqueous uni-univalent salt solutions to the square of the molar concentration of the water, has been shown by Gibson[14] in the case of potassium thiocyanate to be the same function of molal concentration of salt as in the case of the chlorides, bromides and iodides of sodium and potassium, of potassium nitrate, and cesium chloride. This last correlation leads to the presumption that the answer to the problem of explaining the form of the curves for thiocyanates does not lie in an unusual specific interaction of the thiocyanate involving the variables dealt with by Gibson.

The authors wish to express their thanks to Dr. Martin Kilpatrick of the Illinois Institute of Technology for having suggested the study of the thiocyanates.

(7) I. M. Kolthoff and W. Bosch, THIS JOURNAL, **36**, 1685 (1932). The values of k_s for chlorides and nitrates were computed by applying least squares to the data of these authors.

(8) G. M. Goeller and A. Osol, *J. Am. Chem. Soc.*, **59**, 2132 (1937).

(9) L. Pauling, "The Nature of the Chemical Bond," Cornell University Press, Ithaca, N. Y., Second Edition, 1940, p. 346.

(10) An estimate obtained by adding to the N–O bond distance, 1.21 Å., in sodium nitrate (M. Elliott, *J. Am. Chem. Soc.*, **59**, 1380 (1937)) the van der Waals radius for oxygen, 1.40 Å. (ref. 9, p. 189).

(11) An estimate obtained by adding to the Cl–O bond distance, 1.50 Å., the van der Waals radius for oxygen. The Cl–O bond distance used here is an average of values obtained by C. Gottfried and C. Schusterius (*Z. Krist.*, **84**, 65 (1933)) for potassium and ammonium perchlorates, and a value of W. H. Zachariasen, (*Z. Krist.*, **73**, 141 (1930)) for sodium perchlorate.

(12) An estimate obtained by adding to the P–F bond distance, 1.58 Å., in potassium hexafluorophosphate (H. Bode and H. Clausen, *Z. anorg. allgem. Chem.*, **265**, 229 (1951)) the van der Waals radius of fluorine, 1.35 Å., (ref. 9, p. 189).

(13) This value is obtained by adding to the N–C and C–S bond distances in potassium thiocyanate, 1.24 and 1.58 Å., respectively (A. P. Klug, *Z. Krist.*, **85**, 214 (1933)) the van der Waals radii of nitrogen and sulfur, 1.5 and 1.85 Å., respectively (ref. 9, p. 189).

(14) R. E. Gibson, *Sci. Monthly*, **46**, 103 (1938).

THE ORDER-DISORDER PROBLEM FOR ICE

BY KENNETH S. PITZER AND JAN POLISSAR

Department of Chemistry and Chemical Engineering, University of California, Berkeley, California

Received February 10, 1956

In 1935 Pauling[1] proposed a structure for ice which provided for hydrogen bonds throughout the crystal but involved a disordered pattern of proton locations. The proton was assumed to be unsymmetrically located in each hydrogen bond and about each oxygen atom two protons were assumed to be nearby, comprising a water molecule, and two farther away. This disorder involves an entropy of $R \ln 3/2 = 0.81$ cal./degree mole, which is in excellent agreement with the residual entropy at 0°K., found by Giauque and Stout[2] to be 0.82 ± 0.05 for H_2O and by Long and Kemp[3] to be 0.77 ± 0.1 for D_2O.

Although the agreement in entropy of disorder is excellent and the neutron diffraction results of Wollan, Davidson and Shull[4] are consistent with the Pauling structure, it is also desirable to estimate the interaction energies which would tend to remove the disorder. Bjerrum[5] initiated this sort of study and obtained approximate results, which in-

(1) L. Pauling, *J. Am. Chem. Soc.*, **57**, 2680 (1935).

(2) W. F. Giauque and J. W. Stout, *ibid.*, **58**, 1144 (1936).

(3) E. A. Long and J. D. Kemp, *ibid.*, **58**, 1829 (1936).

(4) E. A. Wollan, W. L. Davidson and C. G. Shull, *Phys. Rev.*, **75**, 1348 (1949).

(5) N. Bjerrum, *Kgl. Danske Videnskab. Selskab, Math-fys. Medd.*, **27**, 1 (1951); *Science*, **115**, 385 (1952).

dicated that ice would not have a disordered state even at its melting point. Several authors[6] have discussed other possible structures which, however, are not acceptable for reasons to be mentioned below.

The dielectric constant measurements on ice[7] yield high values below the freezing point which are roughly an extension of the values for the liquid. At lower temperatures the time required for polarization increases and the apparent dielectric constant for high frequencies drops to a value of 3.1. If ice had an ordered array of dipolar water molecules it would necessarily show one or the other of two effects.

If the crystal pattern was such as to cancel all dipole moments, then the dielectric constant would be small. The other possible alternative for an ordered structure is that with net parallel dipole moment along some axis; this situation yields a ferroelectric such as Rochelle salt or KH_2PO_4. The dielectric properties of ice are clearly of neither of these types, but are those characteristic of a disordered structure with molecules free to reorient themselves in response to the field.

Let us now review Bjerrum's model and the approximations in his calculations. The water molecule in ice is assumed to be a tetrahedron with center to vertex distance of 0.99 Å. and a charge of $0.171e$ at each vertex. Two of these charges are positive, corresponding to the hydrogen atoms, and the other two negative, corresponding to the unshared electron pairs. This magnitude of charge yields the correct dipole moment for the water molecule. The ice structure involves tetrahedral orientations of oxygen atoms about a given central oxygen with an O–O distance of 2.76 Å. Thus the hydrogen bond in this model has opposite charges of $0.171e$ spaced 0.78 Å. apart.

The ice crystal has hexagonal symmetry. Bjerrum showed very clearly the possible orientation of pairs of water molecules. One fourth of the hydrogen bonds are parallel to the hexagonal axis, and for these the two H_2O tetrahedra are mirror symmetric. But when signs of charge are considered the orientation may be inverse mirror (*i.e.*, all + charges reflect to − charges) or oblique mirror (which differs by $\pm 120°$ rotation). All other hydrogen bonds have their pairs of tetrahedra rotated by 60° so that they have a center of symmetry and again when charge signs are considered the orientation may be either inverse center or oblique center symmetric. The Pauling structure requires random distributions between the inverse and oblique orientation for each type of bond.

In his first approximation Bjerrum included only the electrostatic interactions between the charges of a pair of water molecules. In a second approximation he included all interactions between two water molecules hydrogen bonded to an intermediate molecule. Bjerrum remarked that it would be an extremely difficult task to include all interactions between pairs of water molecules separated by two other water molecules. However, reference to Fig. 1 will show that one such interaction is very important. In Fig. 1 we show just a sequence of three hydrogen bonds. The interaction marked *a* is included in Bjerrum's first approximation while his second approximation includes the two terms marked *b*. However, the interaction marked c is of nearly the same magnitude but is omitted in Bjerrum's calculation. Since this term will be opposite in sign to the *b* terms it will tend to reduce the net energy markedly.

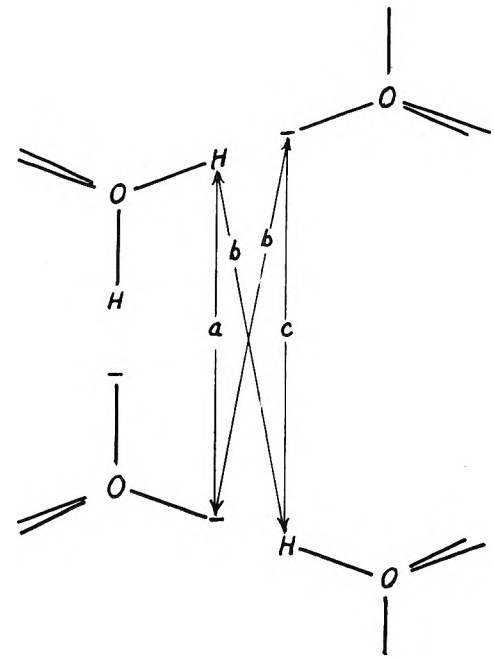

Fig. 1.—Three successive hydrogen bonds in an ice crystal.

By making the calculation in terms of hydrogen bonds instead of water molecules we believe we have obtained a reasonably good approximation without excessive effort. We followed Bjerrum's model exactly, and included all hydrogen bonds adjacent to a given bond. Thus there are three hydrogen bonds adjacent to each end of the central bond, and we included both the positive and the negative charge associated with each of the seven hydrogen bonds. All interactions between this array of 14 charges were considered.

In Table I we present our results together with those of Bjerrum's first approximation. His second approximation yields intermediate values but these are complicated by the orientations about additional hydrogen bonds. The dielectric constant is unity in these calculations; its proper value will be discussed later.

TABLE I

ENERGY DIFFERENCES IN ICE FOR $\epsilon = 1$

	Bjerrum (1st approx.)	This research
Oblique mirror–inverse mirror	7.48×10^{-14}	1.67×10^{-14} erg
Inverse center–oblique center	6.75×10^{-14}	0.95×10^{-14}

We see that the inclusion of the interactions of the *c* type in Fig. 1 has a profound effect and greatly reduces the energy differences.

(6) R. E. Rundle, *J. Chem. Phys*, **21**, 1311 (1953); **22**, 344 (1954); THIS JOURNAL, **59**, 680 (1955); W. N. Lipscomb, *J. Chem. Phys.*, **22**, 344 (1954); P. G. Owston, *J. chim. phys.*, **50**, C13 (1953).

(7) C. P. Smyth, "Dielectric Behavior and Structure," Chap. V, McGraw–Hill Book Co., Inc., New York, N. Y., 1955, and references there cited.

We must now consider the effective dielectric constant for these electrostatic interactions. Since all molecular orientations are specified in our model, the contribution of molecular orientation to ϵ must be excluded. Our model assumes an electron cloud distribution for a single molecule but makes no allowance for its readjustment under the influence of neighboring molecules. Consequently these electron cloud readjustments should be introduced through a dielectric constant. We have noted above that the high-frequency value for ice is 3.1. We shall adopt the value 3, not with any pretense that it is precisely correct for the calculation at hand, but merely that the value should be near 3 rather than 1 or 80.

The transition from disordered ice to ordered ice, if it occurred at a detectable rate, would undoubtedly be a coöperative phenomenon. There would be a lambda or Curie type of transition with high heat capacity just below the Curie temperature and almost complete disorder above that temperature. We may estimate the approximate Curie temperature by dividing the energy change from complete order to disorder by the corresponding entropy change. The ordered state would have all mirror symmetric bonds in the inverse orientation and all center symmetric bonds oblique. There are $^1/_3$ inverse and $^2/_3$ oblique of each type for disorder. Per water molecule there is $^1/_2$ mirror symmetric bond and $^3/_2$ center symmetric bond. Consequently

$$\Delta E = \frac{1}{\epsilon}\left(\frac{1.67}{3} + \frac{0.95}{2}\right) \times 10^{-14}\ \text{erg}$$
$$= \frac{149}{\epsilon}\ \text{cal./mole}$$
$$T_c \cong \frac{149}{0.81\epsilon} = \frac{184^\circ\text{K}}{\epsilon}$$

If ϵ is taken as 3, we have $T_c \cong 60^\circ$K., which is a reasonable value. Giauque and Stout observed that ice reaches thermal equilibrium sluggishly in the range 85–100°K. If this phenomenon is associated with a slight shift toward an ordered structure, the Curie temperature cannot be greatly lower. Nevertheless, it must be appreciably lower because Giauque and Stout were unable to obtain actual transition to the ordered state even on very slow cooling. In other words, for the sluggish equilibrium at 85–100°K. the relaxation time is of the order of an hour but at the Curie point it must exceed a day.

Bjerrum was able to show that, with dielectric constant unity, his model gave a total binding energy in reasonable agreement with the observed heat of sublimation of ice. The introduction of a dielectric constant of three would, of course, spoil this agreement. However, the binding energy arises chiefly from the adjacent charge pairs which constitute the hydrogen bonds themselves. The important phenomenon is then distortion of the electron cloud comprising the unshared pair on the water molecule right next to the bonding hydrogen. For this problem the use of a dielectric constant would be a poor approximation. Indeed this distortion could easily be of a type to increase rather than decrease the bond energy. The interactions which are important for the order-disorder problem are the more distant ones shown in Fig. 1. For these the use of a dielectric constant seems an appropriate method.

For complete disorder one calculates that a cubic ice, analogous to the diamond structure, would have the same energy as actual hexagonal ice. A metastable cubic ice has been reported by König[8] to form from the vapor at −80°. Even the slightest amount of ordering about the mirror symmetric bonds in the hexagonal crystal makes the hexagonal structure more stable. Hence there is no difficulty in understanding the structure which ice actually takes. Near the melting point one might expect another type of disorder, however, in which a large group of normally mirror symmetric bonds in a plane perpendicular to the hexagonal axis are of the center symmetric type instead. This sort of irregularity is observed in silicon carbide.[9] Possibly the disorder X-ray scattering[10] which occurs near the melting point but disappears at low temperatures arises from irregularities of this type.

In conclusion we may remark that all of our evidence is consistent with the Pauling structure and the thermal properties observed by Giauque and Stout.

(8) H. König, *Z. Krist.*, **105**, 279 (1944); *Nature*, **157**, 449 (1946).
(9) A. W. Hull, *Phys. Rev.*, **15**, 545 (1920); see also *Z. Krist, Strukturbericht*, **1**, 144 (1931).
(10) P. G. Owston and K. Lonsdale, *J. Glaciology*, **1**, 118 (1951).

THE KINETICS OF THE REACTION OF ETHYL ALCOHOL WITH *p*-NITROBENZOYL CHLORIDE IN NITROBENZENE AT 7.38°

By W. R. Gilkerson

Contribution from the Department of Chemistry, University of South Carolina, Columbia, South Carolina

Received February 13, 1956

The kinetics of the alcoholysis of acyl halides have been studied previously in ether[1] and in 60–40 ether–ethyl alcohol mixture.[2] Ashdown, using a titration method, found that within one run, the rates for several alcohols with *p*-nitrobenzoyl chloride were first order with respect to the acid chloride and second with respect to the alcohol. However, the experiments were conducted at only two initial concentrations of the reactants. The third-order specific rate constants so obtained at the two different concentrations were not equal to each other. The effect of both products of the reaction on the rate in *n*-butyl alcohol was found to be negligible. The ester alone had no effect on the rate in ethyl alcohol. Hydrogen chloride was not tested in this case. Ashdown concluded the variation of rate with initial concentration was due to the changing activity coefficient of alcohol with concentration. In excess ethanol Branch and Nixon (ref. 2) found the rate to be first order in the acid chloride. They observed that, initially, the rate was some ten per cent. slower than the final rate. They also showed that, in the presence of added hydrogen chloride, the initial rate decreased, but the final rate remained essentially constant.

(1) A. A. Ashdown, *J. Am. Chem. Soc.*, **52**, 268 (1930).
(2) G. E. K. Branch and A. C. Nixon, *ibid.*, **58**, 2499 (1936).

In view of the foregoing, it would be of interest to determine more conclusively the order of the reaction with respect to ethyl alcohol, and to attempt to detect any lower order reaction present initially. The order of the reaction with respect to the alcohol may be determined definitely from a study of the variation of initial rate with alcohol concentration. That Ashdown observed second-order dependence within a run may be due to complicating factors associated with the appearance of appreciable concentrations of the products of the reaction. Following the discussion of Branch and Nixon (ref. 2), any contribution to the over-all rate due to ionization of the acid chloride would be reduced considerably as the reaction proceeds and the concentration of HCl is built up. Thus, the most favorable time for detection of any ionic reaction would be at the beginning of a run. It was therefore decided to study the initial rate of the reaction between ethyl alcohol and *p*-nitrobenzoyl chloride in which the concentrations of both reactants were of the same order of magnitude (*ca.* 0.05 *M*) and were varied over a range. Such a study is reported here. Nitrobenzene was used as a solvent since hydrogen chloride in ethyl ether had too small a conductance. The reaction was followed by observing the change of conductance with time. Several runs were followed by titrating the hydrogen chloride. This served as a check on the conductance calibrations.

Experimental.—The nitrobenzene (Coleman and Bell, C.P.) was prepared by first passing it through an alumina column, then distilling at 10 mm. of mercury, and taking a middle cut of the distillate, which boiled within 0.1°. The specific conductance of this solvent was less than 10^{-7} ohms^{-1} cm.$^{-1}$. Ethanol was allowed to stand over fresh lime for a week, with intermittent shaking, and then distilled from fresh lime. A middle cut, boiling within 0.1° was taken. The *p*-nitrobenzoyl chloride was freshly prepared from *p*-nitrobenzoic acid and PCl_5. It was recrystallized twice from carbon tetrachloride; m.p. 71.6°.

The calibration of the conductance of hydrogen chloride in nitrobenzene was carried out by using stock solutions of ethyl *p*-nitrobenzoate and hydrogen chloride in nitrobenzene (prepared by mixing equal quantities of the acid chloride and alcohol in nitrobenzene, and thermostatting at 65° for one week). The stock solutions were diluted to the desired concentrations and conductance measurements were made on these as well as with added amounts of ethanol and the acid chloride. The latter had no detectable effect on the conductance. The conductance bridge used was a Leeds and Northrup model 1554 A-2. Two cells were used. Their constants were not determined, only the ratio between the two was necessary for the purpose of this work.

The bath, containing transformer oil, was maintained at 7.39 ± 0.005°.

In a batch reaction, a weighed sample was diluted with 15 ml. of acetic acid, and titrated potentiometrically using sodium acetate in glacial acetic acid as base.

The initial rates were determined from the slopes of the curves drawn through the experimental points.

Results.—The form of the rate expression was obtained by trial and error. The initial rates, S_0, were divided by various powers of the initial concentrations (molality) *a*, of acid chloride, and *b*, of ethanol, until the quotients remained constant for the series of runs. It was found that the initial rate was first order in the acid chloride, and second order in ethanol. The data and third-order rate constants are tabulated in Table I.

A typical run, no. 2, is shown in Fig. 1. It may be seen that the rate increases slightly to a maximum and then falls off. This behavior was noticed in all the runs. It is not possible to decide from these data whether or not the increase is real. The estimated error in determining the initial rate from the conductance data and calibration curves is ±12%. The maximum rate in no. 2 is 18.0 × 10^{-8} *m* sec.$^{-1}$. The actual deviation of the maximum and the initial rate is ±13%. This is almost equal to the estimated error. The conductance results were checked (runs 8, 9 and 10) using a titration method. The initial rates determined by the two methods are in agreement, although the experimental error at low HCl concentrations was greater in the latter.

TABLE I

Run no.	$a \times 10^2$, *m*	$b \times 10^2$, *m*	$S_0 \times 10^8$, *m* sec.$^{-1}$	$k_3 \times 10^4$, m^{-2} sec.$^{-1}$
1	10.07	2.42	1.48	2.52
2	11.10	6.24	14.2	3.30
3	11.00	4.55	6.31	2.77
4	3.26	14.75	23.6	3.30
5	6.15	3.93	2.33	2.45
6	6.24	8.76	5.45	2.63
7	10.30	6.24	11.6	2.89
8[a]	5.23	4.80	3.02	2.51
9[a]	4.22	6.59	3.94	2.15
10[a]	4.28	8.25	3.89	3.30

[a] Determined by titration method.

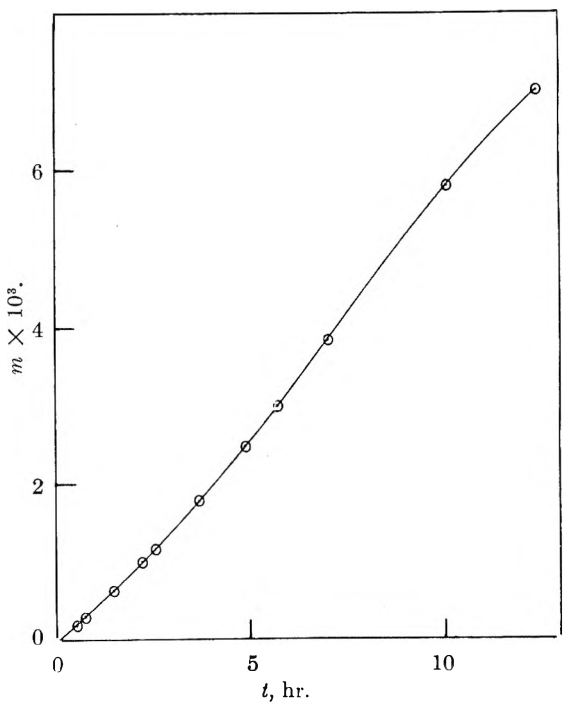

Fig. 1.—Plot of the molal concentration, *m*, of hydrogen chloride *versus* time, *t*, for run no. 2.

The rate law found for this reaction in nitrobenzene is the same deduced by Ashdown from his data for ether. The evidence, however, is more positive since the range of initial concentrations is greater and the range of the ratio of alcohol to acid chloride is greater. No indication of the contribution by an ionic reaction, postulated by Branch and Nixon (ref. 2), was found. Their initial concentrations were lower (10^{-4} *M*) than those in this

study, and it is not impossible that an investigation at such a low concentration would indicate some ionic contribution.

There are various interpretations which might be placed upon the second-order dependence of the rate on ethanol. The "push-pull" mechanism of Swain[3] could be invoked. The implication would be that the two alcohol molecules attack simultaneously, and from different directions. Another approach would be similar to that proposed by Bartlett and Nebel[4] for the kinetics of the methanolysis of *p*-methoxybenzhydryl chloride in nitrobenzene. They found that the rate obeyed the equation

$$\text{Rate} = k_2[\text{RCl}][\text{MeOH}] + k_3[\text{RCl}][\text{MeOH}]^2$$

The rate-determining step was considered to be the solvation of the incipient chloride ion by the alcohol, acting as a molecule or in clusters of two or more alcohol molecules (hydrogen-bonded). The latter view doesn't seem applicable in this case since no first-order dependence was observed. The concentrations of ethanol here are comparable to those of methanol used by Bartlett and Nebel. An explanation that differs only a little from the "push-pull" viewpoint is that a stepwise process is involved in which one alcohol molecule complexes with the acid chloride in a rapid step. Another alcohol molecule subsequently attacks to pull off a molecule of hydrogen chloride. If, as assumed, the first step is much faster than the second, there exists no detectable kinetic difference between this scheme and the Swain viewpoint. However, it is kinetically simpler, involving as it does only bimolecular steps, rather than a termolecular one.

Conclusion.—The kinetics of the reaction of ethanol with *p*-nitrobenzoyl chloride have been investigated in nitrobenzene at 7.38°. The rate is second order in the alcohol and first order in the acid chloride. These results confirm the conclusions drawn by Ashdown (ref. 1), but eliminate the discrepancies between his results at two different concentrations. Ionic contributions to the reaction were undetectable. The results have been interpreted as indicating an initial rapid formation of a complex by one ethyl alcohol molecule and a molecule of acid chloride with a subsequent slow attack on this complex by a second alcohol molecule, splitting off a hydrogen chloride–alcohol complex and leaving the ester.

Acknowledgment.—The author wishes to thank the Research Corporation and the University of South Carolina Research Fund for grants in support of this research.

(3) C. G. Swain, *J. Am. Chem. Soc.*, **70**, 1119 (1948).
(4) P. D. Bartlett and R. W. Nebel, *ibid.*, **62**, 1345 (1940).

THE Ni K ABSORPTION EDGES OF OXIDES OF NICKEL

BY H. P. HANSON AND W. O. MILLIGAN

Department of Physics, The University of Texas, Austin, Texas, and Department of Chemistry, The Rice Institute, Houston, Texas

Received February 14, 1956

It has been observed that finely-divided nickelous oxide prepared by heat-treatment of nickelous hydroxide exhibits a remarkable enhancement in its room temperature magnetic susceptibility, the susceptibility increasing regularly as the temperature of heat treatment is decreased.[1] More recently,[2] it has been found that these nickel oxide samples exhibit maxima in susceptibility–temperature plots. The temperatures, T_c, at which the maxima appear, decrease regularly and the amplitudes of the maxima increase regularly, with decreasing crystal size. In the range of crystal size studied (80–2000 Å.), linear plots are obtained for T_c as a function of f, the ratio of the average number of next nearest magnetic neighbors per nickel atom to the number of next nearest magnetic neighbors in an infinite crystal, as computed from observed crystal sizes. A complete explanation of this magnetic behavior requires a consideration of the state of oxidation of the nickel ions in the crystals, inasmuch as the finely-divided nickel oxide contains small amounts of "active" oxygen (Bunsen test).

The existence of trivalent nickel has long been in dispute, although it is recognized that the anodic, bromine or chlorine oxidation of $Ni(OH)_2$ or nickelous salts yields a black precipitate exhibiting a characteristic X-radiogram distinct from that of NiO or $Ni(OH)_2$. This black form of nickel has been variously considered to be Ni_2O_3, $Ni(OH)_3$,[3] $Ni_2O_3\ 1.5H_2O$,[4] $Ni_2O_3 \cdot 2H_2O$,[5] NiOOH,[6] etc. The preparation of the higher oxides of nickel has been discussed recently by Briggs, Jones and Wynne-Jones.[7] One of the important experiments purportedly demonstrating the existence of trivalent or higher oxides of nickel is the measurements by Cairns and Ott[5] of a displacement of the Ni K X-ray absorption edge toward higher energies than that corresponding to the edge in NiO. The observed values for the shift ranged from about 2 to 5 volts depending on the sample. Cauchois[8] has commented on these measurements and expressed some disagreement. The results of Cairns and Ott were obtained photographically and with a spectrometer of low resolving power. Techniques and instruments are now available which are better suited to investigating this type of problem. Furthermore it is now known that the absorption edge has a complex structure, and that the concept of the shift of the edge is somewhat ambiguous. Consequently a study of the Ni K edge in certain nickel oxides has been undertaken, employing a two-crystal spectrometer.

The six samples examined were (A) a sample of commercial nickel oxide considered to be essentially NiO; (B) a commercial oxide designated by the manufacturer as "Ni_2O_3"; (C) a black oxide prepared by the addition of a solution of bromine in

(1) W. O. Milligan and J. T. Richardson, THIS JOURNAL, **59**, 831 (1955).
(2) J. T. Richardson and W. O. Milligan, unpublished results.
(3) J. Zedner, *Z. Elektrochem.*, **12**, 463 (1906).
(4) F. Foerster, *ibid.*, **13**, 414 (1907); **14**, 17 (1908).
(5) R. W. Cairns and E. Ott, *J. Am. Chem. Soc.*, **55**, 534 (1933); **56**, 1904 (1934).
(6) O. Glemser and J. Einerhand, *Z. anorg. allgem. Chem.*, **261**, 26, 42 (1950); *Z. Elektrochem.*, **54**, 302 (1950).
(7) G. W. D. Briggs, E. Jones and W. F. K. Wynne-Jones, *Trans. Faraday Soc.*, **51**, 1433 (1955).
(8) Y. Cauchois, *J. chim. phys.*, **46**, 307 (1949).

sodium hydroxide to nickelous chloride solution, followed by washing by decantation until the black gel was free of chloride ions; (D) nickel oxide prepared by heat-treatment of $Ni(OH)_2$ at 1100° in a current of nitrogen for 2 hours ("active" oxygen content *ca.* 0.02% and crystal size about 1500 Å.); (E) nickel oxide as in (D) except for heat treatment at 300° ("active" oxygen content 0.37%, crystal size 104 Å.); and (F) $Ni(OH)_2$ prepared by precipitation from nickelous nitrate solution, followed by washing by decantation until the green gel was free of nitrate ions, and drying at room temperature.

Presumably the significant characteristic of the edge is the location of the first principal peak, since this is thought to be the result of 1s-4p transitions. In Fe and Mn this feature of the trivalent oxides is displaced some 3 or 4 volts toward higher energies than in the respective divalent oxides. Figure 1 shows the K edge structure for various nickel oxides. The zero shown is taken as the top of the Fermi band in pure nickel.[9] The six curves are labeled as indicated in the previous paragraph. Curves A and B are very similar, there being no significant difference between them with regard to position or shape. Curves C to F are likewise very much alike, but there are small, yet significant, differences which deserve comment. The principal peak for samples A, D and E occurs at the same position. Our measurements place the peak for sample C at about 0.75 volt higher, whereas sample F [$Ni(OH)_2$] peaks about 0.75 volt lower. Inasmuch as these data are obtained by simultaneous runs, the shifts are real and are considered to be precise to about 0.25 volt. However, the shifts are far smaller than one finds in the corresponding Fe and Mn compounds. It is noteworthy that there is a virtual absence of low energy absorption in sample C. The oxides of all of the previously examined elements of the first transition series show such an absorption, and hence the results for the black nickel oxide (sample C) represent an anomaly. It may be more than coincidental that samples D and E, containing small amounts of active oxygen, likewise exhibit a comparatively small low energy absorption, and are black in color as is sample C. It is this lack of low energy absorption which apparently accounts for the results of Cairns and Ott. Since they measured the shift in the edge by photographic methods, thick samples of nickel oxide would give considerable absorption before the principal peak was reached.

Although it is shown that the Cairns–Ott measurements are not definitive, the present results do not constitute proof that higher nickel oxides do not exist, but suggest that if the trivalent or other higher oxides of nickel exist, their K edge structure does not bear the same relation to the edges of the divalent oxides as do the edges in the corresponding oxides of iron and manganese which have been measured. This is a likely possibility inasmuch as lattice symmetry and the homopolar character of the bonding may be involved in determining the exact edge structure.

(9) W. W. Beeman and H. Friedman, *Phys. Rev.*, **46**, 392 (1939).

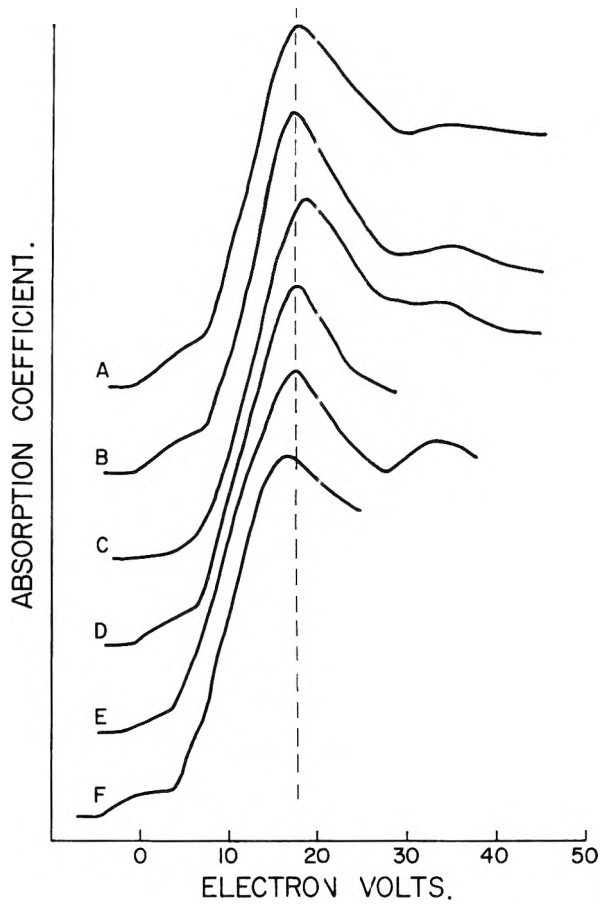

Fig. 1.—K absorption edges of various oxides of nickel. The zero is chosen as the top of the Fermi band in pure nickel.

One of us (H. P. H.) gratefully acknowledges financial assistance from The Robert A. Welch Foundation.

THE SOLUBILITIES OF SOME METAL NITRATE SALTS IN TRI-*n*-BUTYL PHOSPHATE

BY WESLEY W. WENDLANDT AND JOHN M. BRYANT

Department of Chemistry and Chemical Engineering, Texas Technological College, Lubbock, Texas

Received February 20, 1956

The use of tri-*n*-butyl phosphate (TBP) as a solvent in the liquid–liquid extraction of metal ions from aqueous solutions is well known. The rare earths,[1] thorium,[2] uranium[3] and plutonium[4] have all been extracted from aqueous solutions using

(1) D. F. Peppard, J. P. Faris, P. R. Gray and G. W. Mason, THIS JOURNAL, **57**, 294 (1953); B. Weaver, F. A. Kappelmann and A. C. Topp, *J. Am. Chem. Soc.*, **75**, 3942 (1953); A. C. Topp and B. Weaver, U. S. Atomic Energy Commission, Rept. ORNL-1811, Oct. 15, 1954; J. G. Cuninghame, P. Scargill and H. H. Willis, Atomic Energy Research Establishment, Harwell, Rept. AERE-C/M-215, Aug. 13, 1954; J. C. Warf, *J. Am. Chem. Soc.*, **71**, 3257 (1949).

(2) M. W. Lerner and G. J. Petretic, *Anal. Chem.*, **28**, 227 (1956); M. R. Anderson, U. S. Atomic Energy Commission, Rept. ISC-116, Dec., 1953.

(3) H. T. Hahn, ref. 2, HW-32626, July 20, 1954.

(4) B. Goldschmidt, P. Regnaut and T. Prevot, *Rapp. cent. et. nucl. Saclay*, number 397, 1955.

this solvent under various conditions of acidity and foreign electrolyte concentrations. Analytical determinations have been developed for the separation of uranium,[5] copper,[6] iron[7] and aluminum[8] from aqueous solutions using TBP. To investigate other possible metal ions which may be separated by liquid–liquid extraction, a systematic study of the solubilities of a series of metal nitrate salts was made in the pure solvent.

Experimental Procedure

Chemicals.—Tri-*n*-butyl phosphate was obtained from Eastman Organic Chemicals, Inc., Rochester 3, N. Y., and used without further purification. All the other chemicals were of reagent grade quality.

The procedure for the solubility determinations consisted of adding about 25 g. of the solid salt to 20 ml. of TBP contained in a 50-ml. screw cap bottle, sealing the bottle, and equilibrating the contents on a mechanical "wrist action" shaker for 48 to 72 hr. at room temperature, 25 to 27°. It was found that this time was sufficient for equilibrium conditions to be established. At the end of this time, three phases were present in the bottles: a solid hydrated salt phase, an aqueous phase containing a saturated solution of the metal nitrate salt and an organic phase containing the dissolved metal salt. The organic phase was separated, centrifuged and analyzed for the metal salt content.

The analysis consisted of weighing out 1 to 4 g. duplicate samples of the centrifuged organic phase into 125-ml. separatory funnels containing 25 ml. of benzene and 50 ml. of water. After an equilibration time of two minutes, the aqueous phase was removed, 50 ml. of water added and the equilibration repeated. Two such extractions were sufficient to remove the metal salt from the organic benzene phase.

The metal ion contents in the extracted aqueous phases were determined by standard procedures.[9]

Results

The solubilities of the metal nitrates are given in order of decreasing solubility in Table I. The most soluble salts are those of uranium(VI) and thorium. Thus, it can be seen why liquid–liquid extraction procedures are so effective with these two metal salts from nitric acid solutions.

The solubility of the metal nitrates is due to the formation of molecular addition complexes between the salt and the TBP. This complex for uranium (VI) nitrate has the formula $[UO_2(TBP)_2(NO_3)_2]$.[10] Cerium(IV) nitrate also forms such an addition complex but having the composition $[Ce(TBP)_2(NO_3)_4]$.[5] The extraction of the other metal nitrates obviously forms molecular addition complexes but as yet they have not been investigated.

The solubility of lanthanum nitrate is very similar to the transition metal nitrates. The fairly great solubility of this representative of the rare earth group explains why separation procedures have been so successful using TBP.

The solubilities of metal nitrates in any one group decrease with increasing atomic weight. However, with the alkaline earth group, an anomaly occurs in that magnesium nitrate is less soluble than calcium nitrate. The order of solubilities of the remaining alkaline earth nitrates decreases sharply.

TABLE I

THE SOLUBILITIES OF METAL NITRATE SALTS IN TRI-*n*-BUTYL PHOSPHATE

Salt	Solubility[a] g./100 g. soln.	
$UO_2(NO_3)_2 \cdot 6H_2O$	43.6	43.4
$Th(NO_3)_4 \cdot 4H_2O$	42.6	42.4
$Fe(NO_3)_3 \cdot 9H_2O$	34.8	33.9
$Bi(NO_3)_3 \cdot 5H_2O$	28.6	28.6
$La(NO_3)_3 \cdot 6H_2O$	28.5	28.3
$Cu(NO_3)_2 \cdot 6H_2O$	21.5	21.3
$Cd(NO_3)_2 \cdot 4H_2O$	21.5	21.4
$Zn(NO_3)_2 \cdot 6H_2O$	20.6	20.6
$Hg(NO_3)_2$	18.5	19.0
$Ca(NO_3)_2 \cdot 6H_2O$	17.0	17.0
$Co(NO_3)_2 \cdot 6H_2O$	13.5	13.4
$LiNO_3 \cdot 3H_2O$	12.0	11.9
$Mg(NO_3)_2 \cdot 6H_2O$	11.6	11.4
$Ni(NO_3)_3 \cdot 6H_2O$	10.4	10.5
$Al(NO_3)_3 \cdot 9H_2O$	9.37	9.45
$AgNO_3$	2.59	2.59
$Sr(NO_3)_2$	0.81	0.81
$Pb(NO_3)_2$	0.39	0.38
$Ba(NO_3)_2$	0.00	0.00

[a] Solubilities expressed in g. of anhydrous salt per 100 g. of solution.

The possibility of extracting other metal ions from solution by liquid–liquid procedures with TBP seems to be quite favorable. Under certain conditions, it should be possible to extract about the first 15 metal salts in the table. Further work is being conducted on these separation possibilities.

(5) W. B. Wright, U. S. Atomic Energy Commission. Rept. Y-884, Oct. 18, 1954; R. J. Guest, Dept. of Mines and Technical Surveys, Canada, Rept. NP-5763, May 30, 1955.

(6) L. M. Melnick and H. Freiser, *Anal. Chem.*, **27**, 462 (1955).

(7) L. M. Melnick and H. Freiser, *ibid.*, **25**, 856 (1953).

(8) M. Aven and H. Freiser, *Anal. Chim. Acta*, **6**, 412 (1952).

(9) W. W. Scott, "Standard Methods of Chemical Analysis," Vol. I, edited by N. H. Furman, D. Van Nostrand Co., Inc., New York, N. Y., 5th edition, 1946; G. E. F. Lundell, H. A. Bright and J. I. Hoffman, "Applied Inorganic Chemistry," John Wiley and Sons, Inc., New York, N. Y., 2nd edition, 1953.

(10) R. L. Moore, U. S. Atomic Energy Commission, Rept. AECD-3196, July 10, 1951.

ACETONITRILE–WATER LIQUID–VAPOR EQUILIBRIUM

BY F. D. MASLAN AND E. A. STODDARD, JR.

Petrochemicals Department, National Research Corporation, Cambridge, Mass.

Received February 20, 1956

In the course of a research project at this Laboratory, the distillation of acetonitrile–water mixtures has received attention. A preliminary experiment indicated a difference from the azeotrope at 760 mm. as published by Othmer and Josefowitz.[1] Further examination of the literature indicated an uncertainty as to the composition and boiling points of the azeotrope. Othmer, *et al.*, give 72.60 mole % acetonitrile at the azeotrope, while an industrial source gives 69.2.[2] Our preliminary results indicated a figure closer to the latter.

In order to clear up this matter, the liquid–vapor equilibrium for acetonitrile–water at 1 atmosphere was determined.

Materials.—The acetonitrile for this work was purified as follows. Eastman research grade acetonitrile was distilled in a 20-plate, 1-inch diameter, perforated plate column. A reflux ratio of 10 to 1 was used. The middle cut, boiling at 82°, was retained. Carbide and Carbon reports 81.8°

(1) D. F. Othmer and S. Josefowitz, *Ind. Eng. Chem.*, **39**, 1175 (1947).

(2) Carbide and Carbon Chemicals Co., "Acetonitrile," February, 1955.

as the boiling point.[3] This cut had a refractive index of 1.3413 at 25° as compared with 1.34163 given in the literature.[4] The specific gravity was 0.7756 25/25 compared with 0.7839 20/20 given by Carbide and Carbon.[3]

An Abbe refractometer and a Westphal balance were used for the refractive index and specific gravity measurements, respectively.

As a further test for the purity of the acetonitrile, the infrared spectrum for this cut was compared with that of Eastman spectrograde acetonitrile on a Baird infrared spectrometer. The spectra were almost identical. The indications were that the cut was, if anything, slightly more pure than the Eastman spectrograde material.

Experimental and Discussion

A standard Othmer still supplied by the Emil Greiner Company was used for the determination. The insulated still was operated until 4 checking samples, taken 15 minutes apart, were obtained. This took 2 to 6 hours. The compositions of the liquid and vapor samples were determined by specific gravity using the Westphal balance. Values of specific gravity at various compositions are given in Table I.

TABLE I

SPECIFIC GRAVITY 25/25 OF ACETONITRILE–WATER SOLUTIONS

Acetonitrile wt. %	Sp. gr. 25/25	Acetonitrile, wt. %	Sp. gr. 25/25
4.75	0.9902	59.96	0.8678
9.62	.9816	78.77	.8242
14.53	.9737	87.02	.8037
18.72	.9636	92.43	.7921
19.63	.9622	95.86	.7848
29.70	.9395	100.00	.7765
39.15	.9170		

The results of these determinations are shown in Table II and Fig. 1. These data were obtained at a total pressure of 760 mm. with a possible variation of ±15 mm. According to Othmer and Josefowitz, a pressure variation of ±15 mm. at this total pressure would cause a deviation of about ±0.2 wt. % acetonitrile in the azeotrope composition range.

TABLE II

ACETONITRILE–WATER LIQUID–VAPOR EQUILIBRIUM EXPERIMENTAL DATA

(Pressure 760 ± 15 mm.)

B.p., °C.	Liquid composition % Acetonitrile Wt.	Mole	Vapor conen. % Acetonitrile Wt.	Mole
90.3	6.8	3.1	48.5	28.5
84.2	11.8	5.4	65.9	45.8
80.9	20.7	10.3	73.5	54.9
80.7	21.7	10.5	73.9	55.4
78.0	35.2	19.2	77.3	59.8
77.2	64.5	44.3	78.0	60.9
...	65.4	45.3	80.9	65.0
76.8	79.0	62.2	82.4	67.2
77.2	56.5	36.3	79.4	68.4
77.0	83.2	68.5	81.2	69.1
76.8	85.8	72.5	84.0	69.7
77.0	90.2	80.2	86.3	73.3
78.1	95.5	90.3	91.5	82.5
79.4	98.4	96.4	95.5	90.3

The azeotrope boiling point and composition are given in Table III compared with those quoted by Carbide and Carbon and Othmer.[1] The azeotrope boiling point and composition were determined by graphical interpolation of the bracketing data presented in Table I. The comparison of the data of this work with those of Carbide and Carbon is quite good. On the other hand, the composition

(3) Carbide and Carbon Chemicals Co., private communication, Dec. 28, 1955.

(4) The Dow Chemical Co., "Physical Properties of Chemical Substances," Serial No. 20.1, 4-23-52.

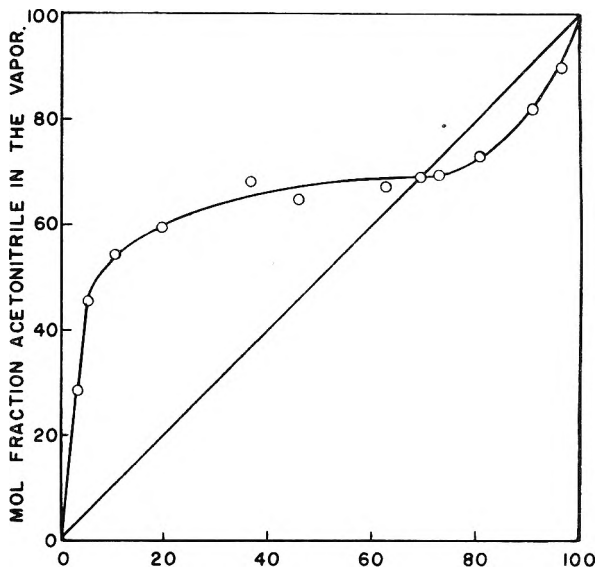

Fig. 1.—Acetonitrile–water liquid–vapor equilibrium; 760 mm.

shown by Othmer is high by approximately 2.3 wt. %. It is believed that the Carbide and Carbon data and the data determined in this work are correct. As has been pointed out,[3] the specific gravity of the pure acetonitrile used by Othmer indicates their sample may have contained about 2.5 wt. % water instead of being 100% acetonitrile. When this is allowed for, the Othmer azeotrope composition fits the others very closely.

TABLE III

ACETONITRILE–WATER AZEOTROPE AT 760 MM.

	B.p., °C.	Acetonitrile Wt. %	Mole %
This work	76.8	83.5	69.0
Carbide and Carbon Chemicals Co.	76.5	83.7	69.2
Othmer and Josefowitz	76.0	85.8	72.6

The equilibrium curve was calculated from the azeotrope using the Van Laar equations in order to test their applicability to this system. The calculated curve was quite close to the experimental one. For mole fraction acetonitrile from 0 to 0.4, the deviation of the calculated curve was about 10% low. For the remainder of the range, 0.4 to 1.0, the calculated curve was within ±5%.

The experimental curve, Fig. 1, shows it is relatively easy to separate acetonitrile from water in concentrations up to the azeotrope.

Acknowledgment.—The authors wish to thank C. Cenerizio, E. Kupski and E. Miley for making the measurements in this work.

A DETERMINATION OF THERMODYNAMIC PROPERTIES OF LIQUID 3-METHYLTHIOPHENE BY THE ULTRASONIC METHOD

BY GEORGE M. CAMPBELL

Contribution from the Department of Physics and Astronomy, Vanderbilt University, Nashville, Tennessee

Received February 20, 1956

Sound velocity and density values have been determined in 3-methylthiophene at five degree intervals over the temperature range −10 to 50°.

These values were combined with the specific heat at constant pressure (C_p) data of the American Petroleum Institute[1] and several other important thermodynamic values calculated. The 3-methylthiophene sample was purchased from the American Petroleum Institute, Carnegie Institute of Technology, to insure a high degree of purity. It was of 99.97 ± 0.03 mole % purity.

Experimental Work

The sound velocity measurements were made by the interferometer method. The interferometer used was the same as the one used by Gilbert and Lagemann[2] with one significant modification. Instead of using a conducting foil to maintain electrical contact to the top of the quartz crystal, the bottom of the polytetrafluoroethylene reservoir was coated with silver conducting paint. A conducting wire attached to a copper ring around the reservoir and touching the paint, completed the circuit to the interferometer housing.

The frequency of the oscillator was adjusted to that of the National Bureau of Standards Station WWV at 500 kc./sec. Sound velocity measurements were repeated on methyl alcohol as a check on the over-all apparatus. The interferometer was immersed in a thermostated water-bath and the temperature measured by a thermometer calibrated by the National Bureau of Standards.

The density measurements were made using a pycnometer similar to the one described by M. R. Lipkin, *et al.*,[3] with a volume of three milliliters. The procedure also was that followed by Lipkin. At temperatures where the density had been previously determined[1,4] the agreement was very good.

Results

The sound velocity data in this temperature range were found to be quite linear with the temperature. Although there was some difficulty in reaching complete temperature equilibrium between the sample and the bath, the data are believed to be accurate to approximately ±0.1%.

The same mathematical relationships used by Gilbert[2] were used to calculate the values for the isothermal compressibility (B_{is}), the adiabatic compressibility (B_{ad}), the coefficient of expansion and the specific heat at constant volume (C_v). The measured and calculated values of the various properties are listed in Tables I and II.

TABLE I

THERMODYNAMIC PROPERTIES OF LIQUID 3-METHYLTHIOPHENE

Temp., °C.	Ultrasonic velocity, m./sec.	Density, g./cc.	Coefficient of expansion (°C.)$^{-1}$ × 10^3	C_p,[a] cal./g. °C.
50	1191.3	0.9895	1.071	0.3508
45	1207.4	0.9955	1.065	.3529
40	1226.8	1.0004	1.059	.3550
35	1245.1	1.0058	1.054	.3573
30	1264.0	1.0111	1.049	.3596
25	1282.1	1.0164	1.043	.3619
20	1303.8	1.0216	1.037	.3643
15	1320.7	1.0268	1.032	.3667
10	1336.0	1.0320	1.027	.3692
5	1357.5	1.0371	1.023	.3717
0	1379.2	1.0426	1.017	.3742
−5	1396.6	1.0480	1.011	.3767
−10	1415[b]	1.0526	1.007	.3796

[a] From a curve constructed from data given by McCullough, *et al.*[1] [b] Extrapolated from −9.3°.

TABLE II

THERMODYNAMIC PROPERTIES OF LIQUID 3-METHYLTHIOPHENE

Temp., °C.	B_{ad}, cm.^{2} dyne^{-1} 10^{12}	B_{is}, cm.^{2} dyne^{-1} × 10^{12}	C_p/C_v	C_v, cal./g. °C.
50	71.25	94.83	1.331	0.2636
45	68.95	91.94	1.333	.2647
40	66.50	88.92	1.337	.2655
35	64.14	86.02	1.341	.2664
30	61.90	83.26	1.345	.2674
25	59.86	80.65	1.347	.2687
20	57.57	77.81	1.352	.2695
15	55.81	75.54	1.354	.2708
10	54.29	73.52	1.356	.2723
5	52.36	71.13	1.358	.2737
0	50.44	68.68	1.362	.2747
−5	48.89	66.60	1.362	.2766
−10	47.45	64.72	1.364	.2783

(1) J. P. McCullough, S. Sunner, H. L. Finke, W. N. Hubbard, M. E. Gross, R. E. Pennington, J. F. Messerly, W. D. Good and Guy Waddington, *J. Am. Chem. Soc.*, **75**, 5075 (1953).

(2) J. W. Gilbert and R. T. Lagemann, THIS JOURNAL, **60**, 804 (1956).

(3) M. R. Lipkin, J. A. Davison, W. T. Harvey and S. S. Kurtz, Jr., *Ind. Eng. Chem.*, **16**, 55 (1944).

(4) F. S. Fawcett, *J. Am. Chem. Soc.*, **68**, 1420 (1946).

"β-TUNGSTEN" AS A PRODUCT OF OXIDE REDUCTION

BY G. MANNELLA[1] AND J. O. HOUGEN

Department of Chemical Engineering, Rensselaer Polytechnic Institute, Troy, N. Y.

Received February 22, 1956

The phase known as β-tungsten was originally reported by Hartman, *et al.*[2] This material was later found by Charlton[3] in his work on the reduction of WO_3 with hydrogen. Recently, Hägg and Schönberg[4] have suggested that β-W is a low oxide of the metal, with a maximum oxide content corresponding to an over-all stoichiometric ratio of W_3O. In his latest work, Charlton[5] has corroborated the W_3O theory.

A kinetics study has been carried on at Rensselaer Polytechnic Institute which has been concerned with the reduction of pelletized tungsten oxides with hydrogen. Kinetic data from this research program have appeared in another publication.[6] In this research, β-tungsten had been identified on the surface of pellets when they were partially reduced at low temperatures. By the continued reduction of a pellet at a temperature sufficiently below 600° to preclude the formation of any α-tungsten, it was proposed to produce a pellet of the pure β-material. Since the amount of oxide removed during the reduction may be determined gravimetrically, the composition of the final material could be established, and the oxide content could be determined.

(1) Research Fellow, Chemical Engineering Department.

(2) H. Hartman, F. Ebert and O. Bretschneider, *Z. anorg. Chem.*, **116**, 198 (1931).

(3) M. G. Charlton, *Nature*, **169**, 109 (1952); Charlton, M. G., **174**, 703 (1954).

(4) G. Hägg and N. Schönberg, *Acta Cryst.*, **1**, 351 (1954).

(5) M. G. Charlton, *Nature* **175**, 131 (1955).

(6) J. O. Hougen, R. R. Reeves and G. Mannella, *Ind. Eng. Chem.*, **48**, 318 (1956).

Experimental Apparatus and Procedure.—The apparatus used in the experimentation was developed to procure data on the rate of reduction of pelletized tungsten oxides with hydrogen. This apparatus has been described in detail in several theses and a publication.[6-8]

The reduction took place in a 1 inch schedule 40 Inconel tube 58″ long. Heating was accomplished by electric resistances, which surrounded the tube and provided two zones in the reactor. The pellets were right circular cylinders of height equal to diameter. Several sizes, ranging in diameter from $^1/_8$ to $^5/_{16}$ inches, were available.

Nitrogen was used as an inert medium while thermal equilibrium was being established in the reaction zone. The flow of gases into or by-passing the reactor was controlled by solenoid valves. Since the reaction was very sensitive to water vapor,[7,8] both the nitrogen and hydrogen streams were dried by passage through Dry Ice–trichloroethylene traps. A back pressure regulator was used to maintain the reactor at 5 p.s.i.g.

The procedure for a run was to bring the empty reactor to approximately the temperature desired under a nitrogen atmosphere. A pellet in its holder was then inserted into the reaction zone of the reactor. When the desired temperature was attained, the nitrogen was by-passed and the hydrogen admitted to the reactor. After the desired reduction time, the hydrogen was by-passed and the reactor flushed with nitrogen. The pellet was then removed from the reaction zone and cooled in a stream of nitrogen. Since the material was pyrophoric, especially following reduction at low temperatures, great care was taken to exclude oxygen during the cooling step. The extent of reduction was found by determining the loss of weight.

The reactor was also used to produce pellets of WO_2. This was done by saturating the hydrogen with water vapor and reducing WO_3 with this mixture at an appropriate temperature. The identity of this material was established by its X-ray spectrum.

Results and Discussion.—The results of experiments made in an effort to produce β-W are given in Table I. The column "Phases Present" lists the number and identity of phases identifiable in the reduced pellet. The reduction of tungsten trioxide to tungsten proceeds through the formation of several intermediate oxides, which are identifiable by their characteristic color. A partially reduced pellet has several phases present such that when it is split along its longitudinal axis, one might observe an outer layer of grey-black tungsten and an inner core of purple or brown intermediate oxide.

TABLE I

TABULATED DATA ON RUNS TO PRODUCE β-TUNGSTEN

Starting composition of pellet 463 was WO_2. All other runs made with WO_3.

Run	Pellet size, in.	Temp., °C.	Time of reduction, sec.	% Reduced[a]	Phases present
460	$^3/_{16}$	520	20,029	83.1	β-W + WO_2
461	$^3/_{16}$	520	20,044	85.0	
462	$^3/_{16}$	575	9,414	85.0	β-W + WO_2
463	$^3/_{16}$	520	3,000	14.4	β-W + WO_2
468	$^1/_8$	500	24,500	82.0	β-W
470	$^5/_{16}$	500	30,000	78.3	
468A	$^1/_8$	570	32,300	87.9	β-W + WO_2
746	$^1/_8$	500	29,000	94.7	β-W
747	$^1/_8$	475	43,500	94.7	β-W
748	$^1/_8$	475	43,500	92.1	β-W
746A	$^1/_8$	475	43,500	102.1[b]	β-W
747A	$^1/_8$	475	36,000	99.3[b]	β-W
748A	$^1/_8$	475	21,600	103.6[b]	β-W

[a] Calculated on the basis that any weight beyond that of the tungsten metal is combined oxygen not removed in the reduction process. [b] Helium used as an inert instead of nitrogen. Weighing bottles sealed with Apiezon M grease.

The presence of WO_2 in many of the pellets following these relatively long periods of reduction is difficult to explain since Reeves[8] reports that a $^3/_{16}$″ pellet of WO_3 is 80% reduced after 8000 sec. at 520°. Runs 460, 461 and 462 indicate the rate of reduction beyond 80% must be extremely slow. Since the rate varies inversely with pellet size, the latter portion of the work was carried out with $^1/_8$″ pellets.

Normally, pellets were kept in ground-glass weighing bottles in a nitrogen atmosphere from the time they were removed from the reactor until they were weighed. It was discovered that under these conditions the pellets gained in weight over a period of 96 hours. Hence, the true weight of the pellet at the end of the reduction period could not be determined by this procedure. To circumvent this difficulty, runs 746A, 747A and 748A were made with a modification in procedure.

This modification consisted of using helium as an inert medium and sealing the weighing bottles with Apiezon M stopcock grease. The use of helium decreased the possibility of the hot pellet adsorbing or reacting with the inert gas while cooling in the reactor. Sealing the weighing bottle eliminated the possibility of surface oxidation or adsorption of oxygen by "breathing" of the bottle. The material produced below 600° was extremely pyrophoric and oxidized upon contact with air even after several weeks at room temperature in a helium atmosphere.

The pellets from runs 746A, 747A and 748A were homogeneous and gave the β-W spectrum when X-rayed. Gravimetric analyses on these pellets gave 102.1, 99.3 and 103.6% reduced, respectively. The use of helium apparently solved the problem of keeping the pellets from adsorbing or reacting with any gases prior to their final weighing and X-ray analysis. These last three runs are significant in that they indicate that the spectrum identified with β-W is that of a crystalline form of tungsten metal. Any oxide present probably acts as an impurity. Hence β-W appears to be a low temperature form of tungsten metal.

Acknowledgments.—Grants by the National Science Foundation and the Trustees' Research Fund at Rensselaer Polytechnic Institute are gratefully acknowledged. Contributions of high purity gases, tungsten powder and equipment by the Lamp Division of the General Electric Company are also appreciated. The X-ray work by Joseph Fisher and the valuable counsel of Dr. Robert Reeves contributed immeasurably to the progress of this work. The assistance of Dr. Arthur Newkirk of the General Electric Research Laboratory was indispensable.

(7) G. Mannella, M.Ch.E. Thesis, Dept. of Chem. Eng., R.P.I., Troy, New York.

(8) R. R. Reeves, Ph.D. Thesis, Dept. of Chem. Eng., R.P.I., Troy, New York.

THE DECARBOXYLATION OF MALONIC ACID IN TRIETHYL PHOSPHATE

BY LOUIS WATTS CLARK

Contribution from the Department of Chemistry, Saint Joseph College, Emmitsburg, Maryland

Received February 27, 1956

Kinetic studies on the thermal decarboxylation of malonic acid alone and in various solvents have been reported frequently in the literature.[1-4] Hall[2] has shown that the decomposition of malonic acid in aqueous solution can be explained by assuming two different mechanisms operating simultaneously: (1) decomposition of the unionized malonic acid, and (2) decomposition of the acid malonate ion. Reaction (1) is considerably faster than reaction (2).

Despite the large amount of work done heretofore on this problem a great need still exists for more data, since every additional experiment throws further light on the reaction and aids kinetic theory.

Preliminary experiments in this Laboratory revealed that malonic acid was smoothly decarboxylated in triethyl phosphate. The kinetics of the reaction were carefully investigated between 128–150° and results are reported herein.

Experimental

Reagents.—Analytical reagent grade malonic acid was used. The triethyl phosphate (product of Tennessee Eastman Corporation) showed on the label the following analysis: specific gravity, 20°/4°, 1.065–1.070; chlorides, less than 5 p.p.m.; sulfates, none; acidity, not more than 0.03% calculated as H_3PO_4; ester content, 97% minimum; boiling point, 216°, refractive index, $n^{25}D$ 1.404.

Apparatus and Technique.—Considerable development in the apparatus and technique has occurred since the inception of these experiments.[5] For this reason a brief, general description at this time appears warranted.

The experiments are conducted in a well insulated, electrically heated, efficiently stirred constant temperature oil-bath of 10-liters capacity. The temperature of the reaction is maintained through the use of an oil-bath thermostat regulated to ±0.1°. The reaction is carried out in a 200-ml. round-bottom Pyrex brand 2-neck (standard-taper) flask. Through the center neck is inserted an electrically driven, mercury seal stirrer controlled by a variac. In the other neck is inserted a reflux condenser. A short piece of glass tubing leads from the top of the condenser to the top of a 50-ml. water jacketed buret provided with a leveling bulb and an entraining liquid (20% by weight aqueous solution of sodium sulfate, 5% by volume sulfuric acid, plus a few drops of methyl orange). Tap water circulates through the water jacket and condenser. Between the condenser and the buret is a small T tube, one end of which is sealed with a rubber policeman. A fine nichrome wire pierces the tip of the rubber policeman, forming a hermetic seal, and extends down the condenser tube. The lower end of the wire, near the lower neck of the condenser, terminates in a small loop bent at right angles to its length. The upper end of the wire extends several inches beyond the tip of the rubber policeman.

In running an experiment the oil-bath is brought to the desired temperature, the solvent is added to the thoroughly dried flask, the tap water is turned on, and a stream of dry carbon dioxide gas is bubbled through the solvent for several minutes to ensure saturation. A suitable size sample of the compound being studied is weighed quantitatively into a thin glass capsule blown from 6 mm. soft glass tubing and weighing approximately 0.2 g. The capsule is lodged on the loop inside the neck of the condenser and the condenser is fitted to the flask. The stirrer is started, and the tube leading from the top of the condenser is connected to the top of the buret through a short piece of rubber tubing, the entraining liquid in the leveling bulb and buret being set at zero volume. When the system reaches equilibrium, as shown by a steady state of the colored solution inside the buret, all variables—barometric pressure, water jacket temperature, volume, etc.—are recorded and the external end of the nichrome wire is twisted slightly to dislodge the capsule which falls into the rapidly stirred solvent initiating the reaction. The operator moves the leveling bulb by hand to maintain the inside and outside pressures equal at all times, and records the volume, time and other variables at frequent intervals. That the experiments are carried out with a high degree of accuracy and precision is demonstrated by the fact that invariably the stoichiometric volume of carbon dioxide is collected from every quantitative sample undergoing decarboxylation.

Used in each experiment in the present study were 100 ml. of triethyl phosphate and a sample of malonic acid weighing 0.1856 g. (the amount required to furnish exactly 40.0 ml. of carbon dioxide at STP on complete reaction). The reaction was carried out at seven different temperatures between 128–150°. The experiment was often repeated two or three times at the same temperature. A total of fifteen experiments were performed with excellent reproducibility.

Results and Discussion

The experimental data were converted to standard conditions and milliliters of evolved gas was plotted against time for each temperature. Values of x corresponding to different values of t were obtained from the resulting isotherms. Log $(a - x)$ was then plotted against t (a is the theoretical stoichiometric volume of carbon dioxide, 40.0 ml.). The points thus obtained for the middle 80% of the reaction fell on perfectly straight lines in every experiment. This fact indicates that the decomposition of malonic acid in triethyl phosphate is a first-order reaction.

From the slopes of the lines thus obtained the specific reaction velocity constants for the decomposition of malonic acid in triethyl phosphate were calculated for the various temperatures on the basis of the equation for a first-order reaction.

The temperatures studied, as well as the corresponding specific reaction velocity constants in sec.$^{-1}$, were as follows: 128.3°, 0.00203; 133.3°, 0.00317; 139.1°, 0.00506; 142.5°, 0.0062; 144.6°, 0.00816; 145.8°, 0.00867; 149.4°, 0.0107.

When log k was plotted against $1/T$ according to the Arrhenius equation a straight line was produced. The energy of activation and the frequency factor, calculated from the slope of the line, are 26,900 cal. and 1.0×10^{12}, respectively. The temperature coefficient for the reaction is 2.5.

Based on the Eyring equation, the enthalpy of activation is 26,100 cal.; the entropy of activation is −6.2 e.u.; the free energy of activation at 140° is 28,600 cal. The specific reaction velocity constant at 140° is 0.0052 sec.$^{-1}$.

Some interesting conclusions can be drawn by comparing this reaction with data for the decomposition of molten malonic acid. According to the data of Hinshelwood,[1] the energy of activation for the thermal decomposition of molten malonic acid is 34,500 cal., the frequency factor is 1.8×10^{14}, the temperature coefficient is 2.72, the enthalpy of activation is 33,000 cal., the entropy of activation is +2.5 e.u.; the free energy of activa-

(1) C. N. Hinshelwood, *J. Chem. Soc.*, **117**, 156 (1920).
(2) G. A. Hall, Jr., *J. Am. Chem. Soc.*, **71**, 2691 (1949).
(3) P. E. Yankwich and R. Linn Belford, *ibid.*, **75**, 4178 (1953).
(4) L. W. Clark, THIS JOURNAL, **60**, 825 (1956).
(5) H. N. Barham and L. W. Clark, *J. Am. Chem. Soc.*, **73**, 4638 (1951).

tion at 140° is 32,000 cal., and the rate constant at 140° is 0.00024 sec.$^{-1}$. Studies in this Laboratory are in good agreement with Hinshelwood's results.[4]

It is thus seen that at 140° malonic acid decomposes in triethyl phosphate twenty-two times as fast as it does alone. We see that triethyl phosphate brings about a decrease in the entropy of activation, decreasing the probability of the formation of the activated state.[6] However, this effect is compensated for by the lowering of the enthalpy of activation, so that less energy is required to bring about activation. The over-all effect is the lowering of the free energy of activation at 140° from 32,000 to 28,600 cal., resulting in an increase in the rate of reaction.

(6) S. Glasstone, K. J. Laidler and H. Eyring, "The Theory of Rate Processes," McGraw-Hill Book Co., New York, N. Y., 1941, p. 24.

POLAROGRAPHIC THIOUREA–FORMALDEHYDE KINETIC STUDIES

By Martin G. Chasanov and Cecil C. Lynch

Department of Chemistry, University of Delaware, Newark, Del.

Received February 29, 1956

The initial condensation of thiourea and formaldehyde in alkaline media was followed by polarographic analysis for formaldehyde. The reaction was found to be second order with respect to formaldehyde and thiourea. Values of the rate constant for the reaction were determined at 5, 15 and 25°. The value for the activation energy for this reaction, determined from these rate constants, is 23.4 kcal./mole.

Experimental

The polarographic determinations were made with an E. H. Sargent and Company Model XII Polarograph. Electrodes of the original Heyrovsky-Shikata type[1] were employed. For the determination of the half-wave potential of formaldehyde *versus* the saturated calomel electrode (SCE) the H-cell of Lingane and Laitinen[2] was used.

The formaldehyde employed was Merck and Company neutral reagent grade; analysis by the hydroxylamine method[3] showed the formaldehyde content to be 36.5%; the solution was diluted to prepare a stock solution of molarity 0.01246 for use in the polarographic measurements. The half-wave potential of the formaldehyde *versus* the mercury pool was −1.56 v.; *versus* the SCE, −1.66 v. The limiting current, i_k, due to the formaldehyde was proportional to the formaldehyde concentration over the range studied.

The thiourea was Eastman Kodak White Label. The thiourea crystals were dried at 120° for two hours; volatile material was less than 1/2 of 1%. The dried crystals were dissolved in water to make up a stock solution of molarity 0.02588. The supporting electrolyte was 0.05 *M* sodium hydroxide (Baker C.P.). The drop mass for the capillary was 1.48 mg./sec.; the drop time was 4.74 sec.; the mercury head was 34.6 cm.

For kinetic determinations solutions were prepared and thermostated prior to use. Formaldehyde and the supporting electrolyte were mixed first; the thiourea was then added. When half of the thiourea had been added the timer was started; the reaction mixture was agitated for 30 seconds, and then it was placed in the polarographic cell. The limiting current was measured as the difference between the upper and lower plateaus of the formaldehyde wave.

(1) I. M. Kolthoff and J. J. Lingane, "Polarography," Interscience Publishers, New York, N. Y., 1941.

(2) J. J. Lingane and H. A. Laitinen, *Ind. Eng. Chem., Anal. Ed.*, **11**, 504 (1939).

(3) L. E. Smythe, This Journal, **51**, 369 (1947).

The results of the kinetic determinations are shown in Table I. The data fitted a second-order rate plot for thiourea and formaldehyde. The values shown are the averages of three determinations for each concentration. The activation energy may be estimated from the Arrhenius relation

$$\frac{\mathrm{d} \ln k}{\mathrm{d}(1/T)} = = \frac{\Delta E_A}{R}$$

Table I

Rate Constant for the Reaction of Formaldehyde with Thiourea in Strongly Alkaline Media at 5, 15 and 25°

Temp., °C.	Initial CH_2O concn., *M*	Initial thiourea concn., *M*	k(mole^{-1} sec.$^{-1}$)
25	415×10^{-5}	431×10^{-5}	2.03
25	208	132	2.00
15	312	205	0.44
15	208	273	0.42
5	415	547	0.119
5	375	656	0.124

Discussion

Good yields of mono- and dimethylolthiourea have been produced by the reaction of thiourea and formaldehyde at temperatures less than 50°.[4] Studies have shown that isomeric forms of the above exists. Pollak[4] postulated the isomers of monomethylolthiourea as

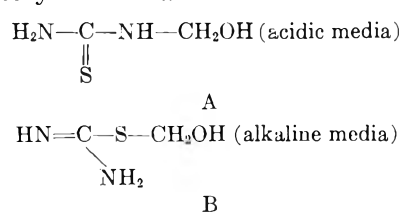

A

B

In alkaline media thiourea reacts to produce mercaptans, sulfur, and often H_2S. The reaction to form B may be postulated as

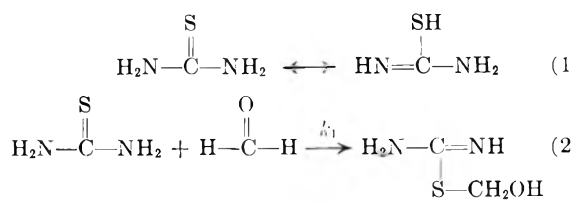

(1)

(2)

(3)

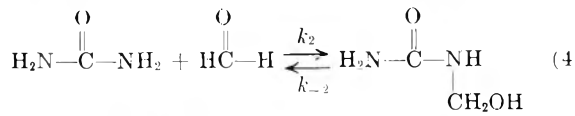

(4)

$$-\frac{\mathrm{d}C_F}{\mathrm{d}t} = k_1 C_F C_T + k_2 C_F C_U - k_{-2} C_P \qquad (a)$$

where

C_F is the formaldehyde concn.
C_T is the thiourea concn.
C_U is the urea concn.
C_P is the concn. of monomethylolurea

Crowe and Lynch[5] have found at 25° that k_2 is 2.97×10^{-2} mole^{-1} sec.$^{-1}$ and k_{-2} is 1.45×10^{-3}

(4) F. Pollak, *Modern Plastics*, **16** No. 10, 45 (1939).

(5) G. Crowe and C. C. Lynch, *J. Am. Chem. Soc.*, **70**, 3795 (1948).

sec.$^{-1}$. For $C_U << C_T$ and $k_1 >> k_2$ equation a becomes

$$-\frac{dC_F}{dt} = k_1 C_F C_T \qquad (b)$$

The experimental data fit (b) quite well. The activation energy, ΔE_A, was found to be 23.4 kcal./mole.

CRYSTALLOGRAPHIC EVIDENCE FOR THE TRIHYDRATE OF ALUMINUM FLUORIDE[1]

By Robert D. Freeman[2]

Technical Division, Goodyear Atomic Corporation, Portsmouth, Ohio

Received April 9, 1956

The existence of a hydrate of aluminum fluoride which contains either 3.0 or 3.5 moles of H_2O per mole of AlF_3 has been well established. Whether there are two distinct hydrates has been open to question. Ehret and Frere[3] have pointed out the discrepancies in the literature regarding these hydrates and have reported evidence for the existence of two forms (α and β) of $AlF_3 \cdot 3H_2O$. They also have listed X-ray diffraction data (d values and relative intensities) for their stable (β) form of $AlF_3 \cdot 3H_2O$. It has been of interest to correlate similar data with a unit cell for possible crystallographic confirmation of their chemical evidence for $AlF_3 \cdot 3H_2O$.

X-Ray powder diffraction patterns of "Reagent" grade hydrated aluminum fluoride (exptl.: 19.61% Al, 39.7% loss on heating at 500° *in vacuo;* theoretical for $AlF_3 \cdot 3H_2O$: 19.54% Al, 39.14% H_2O) were obtained with a Norelco diffractometer using nickel-filtered copper radiation (λ of Cu $K\alpha_1$ = 1.5405 Å.). Samples were passed through a 400-mesh sieve and prepared for the diffractometer as suggested by Klug and Alexander.[4]

Interplanar distances, d, and relative intensities obtained for these samples are in good agreement with the data given for β-$AlF_3 \cdot 3H_2O$ by Ehret and Frere.[3] The following table shows the planar indices, observed and calculated values of $\sin^2\theta$ (using a tetragonal unit cell with a = 7.734 Å. and c = 7.330 Å.), and relative intensities. The agreement between the observed and the calculated values of $\sin^2\theta$ listed in the table and the agreement between the observed and the calculated values of $\sin^2\theta$ above 0.3 (which are not listed) is also good. From the pycnometric density, the volume, and the tetragonal symmetry of the unit cell, it is readily deduced that, whether the correct formula is $AlF_3 \cdot 3H_2O$ or $AlF_3 \cdot 3.5H_2O$, there must be four formula units per unit cell. Using water as the pycnometric liquid and making no correction for solubility (0.41% by weight[3]), the density of the samples was found to be 2.03 g./cc. Calculated density, assuming $AlF_3 \cdot 3H_2O$, is 2.09 g./cc.; assuming $AlF_3 \cdot 3.5H_2O$, it is 2.23 g./cc. Obviously, the value for $AlF_3 \cdot 3H_2O$ is in better agreement with the observed value.

Crystallographic Data

hkl	$\sin^2\theta \times 10^4$ Obsd.	$\sin^2\theta \times 10^4$ Calcd.	I/I_o
110	200	199	100
200	397	398	62
002	445	444	5
102	535	544	17
112	644	643	14
220	794	796	30
202	842	842	9
212	942	941	12
310	993	995	56
222	1239	1240	5
302	1337	1339	2
312	1440	1439	12
400	1590	1592	13
322	1736	1738	8
004, 330	1786	1776, 1791	7
104	1877	1876	8
420	1991	1990	42
412	2132	2135	5
332	2233	2235	2
214	2273	2273	2
422	2433	2434	2
510	2579	2587	5

Examination of the indices for systematic absences reveals that the special reflections $hk0$ are present only when $h + k = 2n$; $0kl$, only when $l = 2n$; and hhl, only when $2h + l = 2n$. The only tetragonal space group which requires these particular conditions for possible reflections is P4/ncc — D_{4h}^5. In this space group, equivalent positions may occur only in sets of 4, 8 and/or 16. This restriction on the number of equivalent positions presents no problem if there are assumed to be 4 units of $AlF_3 \cdot 3H_2O$ per unit cell; both O and F atoms may be arranged in 3 sets of 4 equivalent positions each, or in two sets, one with 4, and one with 8, equivalent positions. However, the restriction is incompatible with the assignment of 4 units of $AlF_3 \cdot 3.5H_2O$ per unit cell; the fourteen O atoms cannot be divided into sets of equivalent positions comprised of 4 and/or 8 positions each.

(1) This work performed under Contract-AT-(33-2)-1, United States Atomic Energy Commission.

(2) Dept. of Chemistry, Oklahoma A and M College, Stillwater, Okla.

(3) W. F. Ehret and F. J. Frere, *J. Am. Chem. Soc.*, **67**, 64 (1945).

(4) H. P. Klug and L. E. Alexander, "X-Ray Diffraction Procedures," John Wiley and Sons, Inc., New York, N. Y., 1954, p. 300.

ORDER THESE SPECIAL PUBLICATIONS FOR YOUR PERMANENT RECORDS

Selected For Reprinting Solely On The Basis Of Their Importance To You

UNIT OPERATIONS REVIEWS

1st Annual Review	$0.50
2nd Annual Review	0.50
4th Annual Review	0.50
5th Annual Review	0.50
6th Annual Review	0.50
7th Annual Review	0.75
8th Annual Review	0.75
9th Annual Review	0.75

FUNDAMENTALS REVIEWS

1st Annual Review	0.75
2nd Annual Review	0.75

UNIT PROCESSES REVIEWS

1st Annual Review	0.50
5th Annual Review	0.75
7th Annual Review	1.50

MATERIALS OF CONSTRUCTION REVIEWS

3rd Annual Review	0.50
4th Annual Review	0.75
5th Annual Review	0.75
6th Annual Review	0.75
7th Annual Review	0.75
8th Annual Review	1.50

ANALYTICAL CHEMISTRY REVIEWS

2nd Annual Review	1.50
3rd Annual Review	1.50
5th Annual Review	0.75
7th Annual Review	1.50

INDUSTRIAL & ENGINEERING CHEMISTRY REVIEWS

March 1955 edition includes: 3rd Fundamentals Review 10th Unit Operations Review	2.00
September 1955 edition includes: 9th Annual Materials of Construction Review 8th Unit Processes Review	2.00

RESOURCES SYMPOSIA

Southwest	0.50
Far West	0.50
New England	0.75
Mid Atlantic	0.75
Rocky Mountain—Part 1	0.75
East North Central States	0.75
West North Central States	0.75
South Atlantic States	0.75

MISCELLANEOUS REPRINTS

Raman Spectra	0.35
Corrosion Testing in Pilot Plants	0.25
Atmospheric Contamination and Purification Symposium	0.75
Titanium Symposium	0.50
Adsorption Symposium	0.50
Careers in Chemistry & Chemical Engineering	1.50
Information Please Symposium	0.50
Dispersion in Gases	0.50
Statistical Methods in Chemical Production	0.50
Liquid Industrial Wastes Symposium	0.75
Nucleation Phenomena	0.75
Chemical Facts and Figures—1952	1.00
Corrosion Data Charts	0.75
Synthetic Fibers	1.00
Chemical Progress in 1952	0.75
Chemical Facts and Figures 1954	1.50
Process Kinetics Symposium	0.75
X-Ray Symposium	0.75
Emulsion Paints	0.75
Industrial Process Water Symposium	0.75
Symposium on Pilot Plants	0.75
Symposium on Boiler Water Chemistry	0.75
Flow through Porous Media	0.75
Process Instrumentation Symposium	0.75
First Air Pollution Review	0.50
Jet Fuels Symposium	0.75
Symposium on Application of Silicones	0.75
Pulsatory and Vibrational Phenomena	1.25
Plastics as Materials of Construction	1.75

ADVANCES IN CHEMISTRY SERIES

No. 4, Searching the Chemical Literature	2.00
No. 5, Progress in Petroleum Technology	4.00
No. 6, Azeotropic Data	4.00
No. 7, Agricultural Applications of Petroleum Products	1.50
No. 8, Chemical Nomenclature	2.50
No. 9, Fire Retardant Paints	2.50
No. 10, Literature Resources for Chemical Process Industries	6.50
No. 11, Natural Plant Hydrocolloids	2.50
No. 12, Use of Sugars and other Carbohydrates in the Food Industry	3.00
No. 13, Pesticides in Tropical Agriculture	2.50
No. 14, Nomenclature for Terpene Hydrocarbons	3.00
No. 15, Physical Properties of Chemical Compounds	5.85

MISCELLANEOUS

Seventy-Five Eventful Years (History of the ACS)	5.00
Chemistry—Key to Better Living	4.00
Combination of Seventy-Five Eventful Years and Chemistry—Key to Better Living	7.50
List of Periodicals Abstracted by Chem. Abs.	3.00
10 Years Numerical Patent Index (1937–1946)	6.50
27 Year Collective Formula Index	80.00
2nd Decennial Index to Chemical Abstracts	100.00
3rd Decennial Index to Chemical Abstracts	150.60
4th Decennial Index to Chemical Abstracts	120.60
Directory of Chemical and Chemical Processing Plants in the South Atlantic States	1.00

Supply of the above items is limited, and each will be sold only until present stock is exhausted.

Order from: Special Publications Department, American Chemical Society
1155 Sixteenth Street, N.W., Washington 6, D. C.